REPORT NO.
UCB/SEMM-89/23

STRUCTURAL ENGINEERING
MECHANICS AND MATERIALS

SIMPLIFIED EARTHQUAKE ANALYSIS OF BUILDINGS INCLUDING SITE EFFECTS

BY

J. D. HART

AND

E. L. WILSON

DECEMBER 1989

DEPARTMENT OF CIVIL ENGINEERING
UNIVERSITY OF CALIFORNIA
BERKELEY, CALIFORNIA

Simplified Earthquake Analysis of Buildings Including Site Effects

by

James D. Hart

and

Edward L. Wilson

December, 1989

Report No. UCB/SEMM-89/23
Structural Engineering and Mechanics of Materials
Department of Civil Engineering
University of California, Berkeley

"Simplified Earthquake Analysis of Buildings Including Site Effects"

By

James D. Hart and Edward L. Wilson

Abstract

The September 19, 1985 Mexico City earthquake clearly illustrated the potentially dangerous modifying effect that soft soil profiles can have on the earthquake motions as they propagate from the bedrock level to the ground surface, and the importance of considering this phenomenon in the seismic analysis of building systems. The use of simple methods for the earthquake analysis of buildings founded on soft soil sites is investigated.

The topic of site response analysis is addressed including the development and implementation of efficient time domain numerical procedures which are incorporated into a one-dimensional site response analysis computer program, WAVES. A soft clay site in downtown Mexico City is modeled and analyzed with WAVES for various base input records and the computed results are compared to data recorded during the September 1985 earthquake.

An overview of conventional building response analysis procedures is followed by a discussion of the use of simple harmonic earthquake motions to represent the "near harmonic" motions frequently recorded at the surface of soft soil profiles. A study comparing the analytical response of a multi-degree-of-freedom representation of a two-dimensional frame system with that of an equivalent single-degree-of-freedom representation for harmonic earthquake loading is presented and the extension of single-degree-of-freedom analysis to general two and three-dimensional systems is discussed.

A brief discussion of various soil-structure interaction analysis methods is followed by a presentation of the free-field formulation of the equations of motion for soil-structure systems. Simplified procedures which include the effects of site amplification and foundation flexibility, are suggested and applied in the investigation of a simple soil-structure system.

ACKNOWLEDGEMENT

The research leading to this report was a joint research effort between the University of California and ULTRA Engineering Services in Mexico City. The research was funded by the National Science Foundation under grant CES-8611071 entitled "Earthquake Analysis of Buildings Including Site Properties". This financial support is gratefully acknowledged.

I wish to express my sincere thanks to Professor E. L. Wilson for the advice, guidance and encouragement he provided during the rewarding years I spent doing research under his supervision. I also wish to express my gratitude to Professors J. P. Moehle and O. H. Hald for their advice and comments regarding this report. Sincere thanks are due Dr. A. S. Whittaker for his enthusiastic encouragement and support and for the time and effort he spent in carefully reviewing this report. Dr. R. Sause and J. P. Conte are also thanked for their cooperation and helpful advice.

Table of Contents

List of Tables

List of Figures

CHAPTER 1

INTRODUCTION

The September 19, 1985 Mexico City earthquake, which had a Richter magnitude of 8.1 and a Modified Mercalli Intensity of IX, was one of the most devastating ground motions ever recorded. The acceleration record from the SCT station, which is located on a soft soil site in downtown Mexico City, had a peak ground acceleration of 0.17g and a duration of 180 seconds. The SCT ground motions were dominated by near harmonic vibration at a period of approximately 2.0 seconds with maximum acceleration amplitudes three to five times larger than the maximum accelerations recorded at nearby "rock" sites. Structures damaged in the downtown area included structures with vibration periods equal to or less then the 2.0 second site period. Structures with vibration periods near 2.0 seconds were damaged due to resonant response while structures with periods less than approximately 0.5 seconds were damaged because they did not have sufficient strength to withstand the sequence of relatively long period acceleration pulses. The devastation caused by the 1985 Mexico City earthquake clearly illustrates the influence of site effects on the seismic response of buildings.

1.1. Research Objectives

In order to design earthquake resistant buildings, engineers and designers require detailed information related to the magnitude and distribution of seismic forces and deformations induced by earthquake loading. Almost all building codes offer the static method of analysis wherein the dynamic lateral forces generated by earthquake ground motions are replaced by equivalent static forces. When a more accurate evaluation of seismic loading and structural response is required, modal analysis techniques or time history analyses for hypothetical earthquakes can be implemented. Nonlinear analysis methods can also be utilized, but are usually reserved for very important, expensive or complicated structures.

The first step in conventional earthquake analysis of structures, which is common to all analysis methods, is the discretization of the real structure to an equivalent mathematical model. Typically, the beams, columns and walls of the building are idealized by line elements with equivalent mechanical properties and the mass of the building is lumped at the story levels where horizontal dynamic degrees-of-freedom (DOF's) are defined. The resulting structural model can then be analyzed as a dynamic force resisting system, and the response of the model in terms of displacements and stresses can be used to evaluate a structural design. The fundamental oversight in this procedure is that the earthquake motions effect not only the structure, but also the site upon which the structure is founded. In other words, the structure and the site form a combined dynamic system which responds to the earthquake motions.

It is common to neglect the effect of foundation flexibility for very stiff sites, but softer (more flexible) sites introduce foundation flexibility which can increase the effective natural period of the building and significantly modify the lateral force requirements. Additionally, neglecting the seismic energy dissipated by the site can give rise to larger lateral forces, base shears and overturning moments resulting in overly conservative seismic designs. Neglecting site effects is not always conservative; many of the most significant earthquakes have demonstrated that the amplification of seismic waves through a soil profile can have disastrous effects on buildings. In any case, it is clear that earthquake analysis procedures which can include site effects, even in an approximate sense, can lead to more realistic and safer design of building structures with a very small increase in computational effort.

The evolution of advanced structural analysis software and the increased availability of mini and micro computers has greatly enhanced the ability of structural design firms to accurately determine the magnitude and distribution of forces and deformations induced by ground motions and hence, produce more efficient and robust earthquake resistant designs. Sophisticated linear structural analysis programs [14,54,73,77] are routinely imple-

mented to produce designs of even irregular, three-dimensional structures which satisfy building code requirements. Sophisticated nonlinear analysis programs [1,17,19,45] which can be used to model the distribution of damage in structures under extreme earthquake loadings, are also available as a means to evaluate seismic designs.

Design offices must often attempt to strike a balance between the importance, size and complexity of the structure and the level of sophistication and cost of the analysis for seismic forces and deformations. The lack of modern technology transfer and easy-to-use nonlinear analysis computer programs has resulted in an extremely limited application of nonlinear procedures in conventional building design practice. However, conventional linear procedures are of no use in estimating the member ductility demands and the distribution of damage throughout the structure as a result of severe earthquake ground motions. Thus, there is an immediate requirement, at least for practical design purposes, to adopt simple and approximate nonlinear analysis methods which permit rapid earthquake response analysis of even complex structures with reasonable accuracy. Simplified nonlinear analysis procedures, which could provide a means to efficiently evaluate the earthquake resistance of various structural designs, would prove to be a valuable tool for earthquake engineers and designers. Moreover, the availability of such simple procedures could provide an important step toward a better understanding and wider use of nonlinear analysis.

The work presented in this report was undertaken in consideration of these observations regarding the effect of the site on the earthquake response of structures and the need for simplified analysis procedures for evaluating the seismic design of buildings. The primary objectives of this report are to:

1) Present simple, efficient and easy-to-use procedures for evaluating the earthquake response of horizontally layered soil profiles.

2) Present simplified procedures for evaluating the seismic response and performance of building structures.

3) Review various methods of soil-structure interaction analysis and present simplified procedures for analyzing the earthquake response of building structures including site effects.

The emphasis of the work presented herein is on the use of simple, physical modeling procedures which can capture the essential features of the response of soil profiles, building structures and interacting soil-structure systems.

1.1.1. Site Response Analysis

Investigations of major destructive earthquakes (Caracus 1967, Managua 1972, Mexico City 1985) indicate that perhaps the single most important aspect of the response of soil-structure systems is the amplifying effect that the soil profile can have on the bedrock motions [9,16,33,60,61,63]. In cases where the predominant period of the bedrock motion roughly matches the fundamental site period, severe amplification of the earthquake waves between the bedrock and the ground surface can be expected. If, in addition, the fundamental structural period matches the fundamental site period, potentially devastating resonant motions can occur.

Extensive research has been conducted regarding the earthquake response of soil profiles. Several computer programs for evaluating the effect of local soil conditions on the ground surface response are presently available. LAYER [53] is a finite element program for linear convolution and deconvolution analysis of one-dimensional soil deposits. SHAKE [59] is a widely used program which implements frequency domain analysis and equivalent linear techniques to compute the one-dimensional earthquake response of soil profiles. QUAD4 [26] evaluates the two-dimensional seismic response of soil deposits using a variable damping finite element procedure and equivalent linear iterative analysis. LUSH2 [39] is a two-dimensional finite element program which utilizes frequency domain analysis and equivalent linear iteration to compute the earthquake response of soil systems. CHARSOIL [65] implements hysteretic soil elements and applies the method of characteristics for computing one-dimensional site response. MASH [42] utilizes hysteretic finite

elements and time domain integration to compute the earthquake response of one-dimensional soil profiles.

These programs are all based on the assumption that the response of a soil deposit is dominated by the upward propagation of shear waves from the underlying bedrock. Analytical procedures based on shear wave propagation which account for the nonlinear behavior of soils have been shown to yield results in reasonable agreement with field observations in many cases.

1.1.2. Building Response Analysis

The first step in the earthquake analysis of building structures consists of discretizing the real structure to an equivalent multi-degree-of-freedom (MDOF) mathematical model, which in the most general case is a three-dimensional model, but may consist of one or more two-dimensional representations. The result of the discretization is an MDOF building model which must be analyzed for seismic forces and deformations, using either static or dynamic analysis methods. Over the past 20 years, extensive research has been conducted regarding the analytical response of structural systems to static and dynamic loadings. Numerous structural analysis programs have been developed and are routinely implemented in structural design practice. SAP90 [54], DRAIN-2DX [1], FACTS [17] and ANSR [45] are a few examples of general purpose structural analysis programs which are presently available.

For practical design purposes, it is often prudent to employ approximate analysis methods which can efficiently evaluate structural response to earthquake ground motions with reasonable accuracy. ETABS [14,77] is a computer program for the simplified linear analysis of three-dimensional frame and shear wall buildings subjected to equivalent static or dynamic earthquake loads. The building is idealized by a system of independent frame and shear wall substructures interconnected by rigid floor diaphragms. The program is an efficient tool based on physically reasonable simplifications that can model the essential behavior of three-dimensional structural systems. ETABS provides an excellent example of

a simplified structural analysis procedure which produces a good estimate of the distributions of force and deformation in complex three-dimensional buildings.

Because earthquake ground motions tend to strongly excite only the lowest modes of structural vibration, reasonable approximations of the linear earthquake response of MDOF structures can be obtained by carrying out the analysis for only one or a few modal coordinates [11]. The use of load dependent Ritz vectors for coordinate reduction can yield more accurate results than the use of the same number of exact mode shapes, with a fraction of the computational effort [37]. In any case, formal coordinate reduction methods using either the exact mode shapes or derived Ritz vectors can lead to very efficient and accurate approximations of the earthquake response of linear MDOF structures.

Procedures for coordinate reduction of MDOF systems to equivalent single-degree-of-freedom (SDOF) approximations for use in nonlinear response analysis have also been developed [8]. A good deal of research related to SDOF representations of regular structures [56,58], irregular structures [55], and torsionally coupled structural systems [35,57] for nonlinear response analysis has been conducted. The essential features of MDOF to SDOF reduction for nonlinear analysis are the assumptions that the vibrational response of the MDOF system is dominated by one vibration shape and that the nonlinear resistance of the MDOF system can be represented by a simple hysteretic resistance function. Time history earthquake response of the resulting SDOF system can be used to estimate the MDOF response or alternately, inelastic response spectrum analysis can be implemented to estimate the response maxima.

The use of simplified procedures to predict the linear or nonlinear earthquake response analysis of MDOF systems could provide a useful means of evaluating various preliminary seismic designs. However, in order to be of use to engineers and designers, simplified procedures must be improved and their correlation with the results of MDOF response analysis must be evaluated.

1.1.3. Soil-Structure Interaction Analysis

Soil-structure interaction (SSI) is one of the most widely studied phenomena in earthquake engineering. It is important because the vibrational behavior of structures during earthquakes can be influenced significantly by the properties of the soil profile upon which they are founded and the feedback mechanisms that exist between the soil and the structure.

Extensive reviews of various SSI analysis methods are presented in [6] and [41]. SSI analysis methods have been developed to account for rocking behavior [67,70], torsional effects [4,69], different support motions [11], nonlinear behavior [6] and many other complex phenomena. Various substructure methods [21], hybrid methods [20], and volume methods [40] have been implemented for one, two and three-dimensional analysis using finite element and continuum based procedures.

SSI solution procedures are commonly carried out in the frequency domain. The primary reason for the use of frequency domain analysis is that it permits the use of frequency dependent impedance coefficients and frequency dependent radiation boundaries at the terminus of the soil model. As an example, the program SASSI [40] implements a system of SSI analysis in the frequency domain following the flexible volume formulation. It uses frequency dependent radiation boundaries and complex stiffness coefficients to account for element damping. LUSH [39] and FLUSH [38] are other examples of SSI programs which utilize frequency domain analysis.

The primary disadvantages of frequency domain analysis are that it cannot solve true nonlinear soil and structure problems and it is computationally inefficient for the solution of three-dimensional problems. Efficient time domain procedures for SSI analysis have been developed [6]. These procedures can be utilized for the solution of nonlinear vibration problems and are especially applicable for problems with local nonlinearities at the foundation level such as structural uplift or soil nonlinearity near the soil-structure interface.

Even though numerous methods are available for SSI analysis, they are typically only implemented for very important structures such as dams or nuclear power plants. The complex nature of the modeling and formulation of SSI analysis problems and the prohibitive costs associated with such analyses are the primary reasons why SSI analyses are not routinely implemented in seismic analysis for design of typical building structures. However, simplified procedures, such as those presented in ATC-03-06 [3], which reflect the essential characteristics of the response of the soil-structure system, can easily be implemented in practice.

1.2. Organization of Text

The text of this report is divided into five chapters. The contents of the various chapters are outlined below.

Chapter 1 serves as an introduction and outlines the research objectives of this work. A brief introduction and literature review on the topics of site amplification analysis, simplified building analysis, and soil-structure interaction are also presented in this chapter.

Chapter 2 deals with the topic of site amplification analysis. Frequency domain procedures are reviewed and various time domain procedures are developed and implemented in various examples.

In Chapter 3, the topic of simplified building analysis is presented. Linear analysis methods are discussed and nonlinear analysis methods for MDOF and SDOF systems are presented. A comparison of the response of a MDOF frame system and an equivalent SDOF representation subjected to harmonic base motion is conducted. The extension of simplified SDOF analysis procedures to other two and three-dimensional systems is also presented. Methods of design evaluation based on structural response to earthquakes represented as harmonic motion are also discussed.

Chapter 4 reviews various methods of soil-structure interaction analysis. Simplified soil-structure interaction analysis procedures, which account for the most important interaction effects, are discussed and demonstrated for a simple soil-structure system.

Chapter 5 provides a summary of the results from previous chapters and presents conclusions and recommendations based on these results.

CHAPTER 2

SITE RESPONSE ANALYSIS

As discussed in Chapter 1, earthquake analyses of building structures which include site effects, even in an approximate sense, can lead to more realistic, efficient and safer earthquake resistant designs. Perhaps the most important consideration is the amplifying effect that the site can have on the earthquake motions. This consideration is reflected in many building codes which modify the lateral design forces based on a knowledge of the fundamental period of the site. Site effects can be investigated more thoroughly by implementing site response analysis procedures. The basic idea behind site response analysis is outlined as follows;

1) Determine the dynamic properties (mass, stiffness and damping) of the soil deposit. Site boring logs and the results of geophysical tests together with empirical relationships [22,28,62] developed for various soil types can be used to determine the mass properties and the strain dependent shear moduli and damping ratios of the soil layers. Ambient site vibration tests can also be used to determine the natural vibration frequencies of a site.

2) Based on variables such as distance from causative faults and expected earthquake magnitudes, determine the characteristics of the design motions likely to develop in the base rock underlying the site. Important base motion characteristics are the earthquake magnitude, duration, effective peak acceleration and frequency content. Once these (and other) characteristics are established, design motions can be selected from previously recorded earthquake accelerograms or from artificial earthquakes which are compatible with a given target spectrum.

3) The analytical response of the soil deposit to various base rock motions can then be computed using any of the various site response analysis methods.

In this chapter, frequency domain procedures for site response analysis are reviewed and

simplified time domain methods are introduced and applied to the analysis of an example soil profile.

2.1. Review of Frequency Domain Analysis

The basic object of site response analysis is to obtain an estimate of the motions at or near the surface of a soil profile resulting from a given base rock motion. Regardless of the analysis procedure implemented, one of the most important considerations is the discretization of the site into an appropriate mathematical model. The most general site model is a three-dimensional representation. However, simpler two-dimensional or even one-dimensional models can often be utilized to approximate the subsurface conditions.

Frequency domain procedures obtain the response of the site model by assuming that the input and output motions are the summation of harmonic motions which are related through a frequency domain transfer function. Details regarding the development and implementation of complex analysis are presented in [39], [59] and [78]. Only a qualitative discussion will be presented herein.

In the most basic form, the method of complex analysis assumes that the earthquake loading, expressed here as a vector $\mathbf{R}(t)$, is a harmonic function of frequency ω;

$$\mathbf{R}(t) = \bar{\mathbf{R}}(\omega)\, e^{(i\omega t)} \tag{2.1}$$

where the amplitude vector $\bar{\mathbf{R}}(\omega)$ may be complex. This assumption implies that the response (which may be a vector) is also harmonic;

$$\mathbf{U}(t) = \bar{\mathbf{U}}(\omega)\, e^{(i\omega t)} \tag{2.2}$$

where the response amplitude vector $\bar{\mathbf{U}}(\omega)$ is also, in general, complex. The amplitudes of the harmonic input and output are related through the frequency domain equations of motion;

$$\bar{\mathbf{I}}(\omega)\, \bar{\mathbf{U}}(\omega) = \bar{\mathbf{R}}(\omega) \tag{2.3}$$

where $\bar{\mathbf{I}}(\omega)$ is the complex stiffness or impedance matrix of the finite element model, which includes the resistance due to inertial, viscous and static forces. The response amplitude

$\bar{U}(\omega)$ can be obtained as a function of ω using the complex frequency response function $\bar{H}(\omega)$;

$$\bar{U}(\omega) = \bar{H}(\omega)\,\bar{R}(\omega) \tag{2.4}$$

The complex frequency response function is also called the compliance matrix or the complex flexibility matrix and is equal to the inverse of the complex stiffness matrix;

$$\bar{H}(\omega) = [\bar{I}(\omega)]^{-1} \tag{2.5}$$

Once the vector of response amplitudes is determined, it can be used to generate the time history of the response vector $\mathbf{U}(t)$.

Frequency domain analysis relies on the use of Fourier transformation and inverse Fourier transformation to move from the time domain to the frequency domain and back. The essential operations of response analysis in the frequency domain are outlined as follows:

1) Obtain the Fourier transform of the earthquake load vector:

$$\bar{R}(\omega) = \int_{-\infty}^{\infty} R(t) e^{(-i\omega t)} dt \tag{2.6}$$

2) Based on the mass, stiffness and damping matrices of the site model, obtain the impedance matrix of the system, $\bar{I}(\omega)$.

3) Obtain the compliance matrix of the system:

$$\bar{H}(\omega) = [\bar{I}(\omega)]^{-1} \tag{2.5}$$

4) Obtain the vector of response amplitudes from the Fourier transform of the earthquake load vector and the compliance matrix:

$$\bar{U}(\omega) = \bar{H}(\omega)\,\bar{R}(\omega) \tag{2.4}$$

5) Transform the response amplitude vector to the time domain using the inverse Fourier transform:

$$U(t) = \int_{-\infty}^{\infty} \bar{U}(\omega) e^{(i\omega t)} d\omega \tag{2.7}$$

Numerical implementation of frequency domain analysis requires the use of discrete rather than continuous Fourier analysis and is usually accomplished using efficient Fast Fourier Transform (FFT) algorithms [12].

2.2. Time Domain Procedures

As mentioned in previous sections, the ground motions developed near the surface of a soil deposit during an earthquake can be attributed primarily to the upward propagation of shear waves from an underlying rock formation. If it is assumed that the soil profile consists of horizontal layers, then the lateral extent of the soil layers has no influence on the shear wave propagation and the soil deposit may be considered as a one-dimensional shear beam system. Clearly, the use of a one-dimensional site model is not applicable for sites with two or three-dimensional subsurface geometries, but for practical engineering analysis, one-dimensional site models can provide reasonable results which reflect the essential character of the site response. Moreover, the use of even the simplest site idealization to estimate the earthquake response is an improvement over completely neglecting site effects.

This section presents various time domain numerical procedures for the earthquake response analysis of soil deposits modeled as one-dimensional shear beam finite element systems. All of the procedures presented herein have been developed as Fortran subroutines and are available in the site response analysis program, WAVES. The primary advantages of WAVES over previously developed site response analysis programs are; 1) the free-field input format is very easy-to-use, 2) it is extremely computationally efficient, 3) it combines linear, equivalent linear and nonlinear analysis options in one package, 4) it performs energy balance computations as a means to investigate the distribution of earthquake energy in the soil profile, and 5) it can be used in direct conjunction with structural analysis programs. The user manual for the WAVES program can be found in Appendix C.

In order to model a horizontally layered soil deposit, it must first be discretized into an equivalent shear beam finite element system. Figure 2.1 shows a horizontally stratified soil deposit, the corresponding finite element discretization and a physically analogous lumped mass, spring system. Before the details of the numerical procedures are discussed, the dynamic property matrices and the equilibrium equations of the finite element system (which are common to all of the analysis methods) must be developed.

Element Shape Functions: Utilizing a finite element formulation, each layer or sublayer of the soil profile is replaced by an element of unit cross sectional area (Figure 2.2) for which the shape functions N(z) are assumed to be linear for unit values of the nodal displacements u_i and u_j:

$$u_i = 1 \, , \, u_j = 0 \; : \; N_i(z) = (1 - \frac{z}{H})$$

$$u_i = 0 \, , \, u_j = 1 \; : \; N_j(z) = (\frac{z}{H})$$

where z is the element coordinate and H is the element thickness. This displacement pattern corresponds to pure (constant) shear deformation. Once the element shape functions have been established, the displacement within an element can be interpolated based on the nodal displacements:

$$u(z) = \begin{bmatrix} (1-\frac{z}{H}) & (\frac{z}{H}) \end{bmatrix} \begin{bmatrix} u_i \\ u_j \end{bmatrix} = \mathbf{N}\,\mathbf{u} \tag{2.8}$$

The shear strain within each element can likewise be established from the nodal displacements:

$$\gamma = \frac{du(z)}{dz} = \begin{bmatrix} (\frac{-1}{H}) & (\frac{1}{H}) \end{bmatrix} \begin{bmatrix} u_i \\ u_j \end{bmatrix} = \frac{dN}{dz}\,\mathbf{u} = \mathbf{B}\,\mathbf{u} \tag{2.9}$$

where **B** is the strain-displacement transformation matrix.

Element and Global Stiffness Matrices: Application of the virtual displacements principal leads to the relationship between nodal forces and nodal displacements, i.e. the layer element stiffness matrix, $\mathbf{k}_l$:

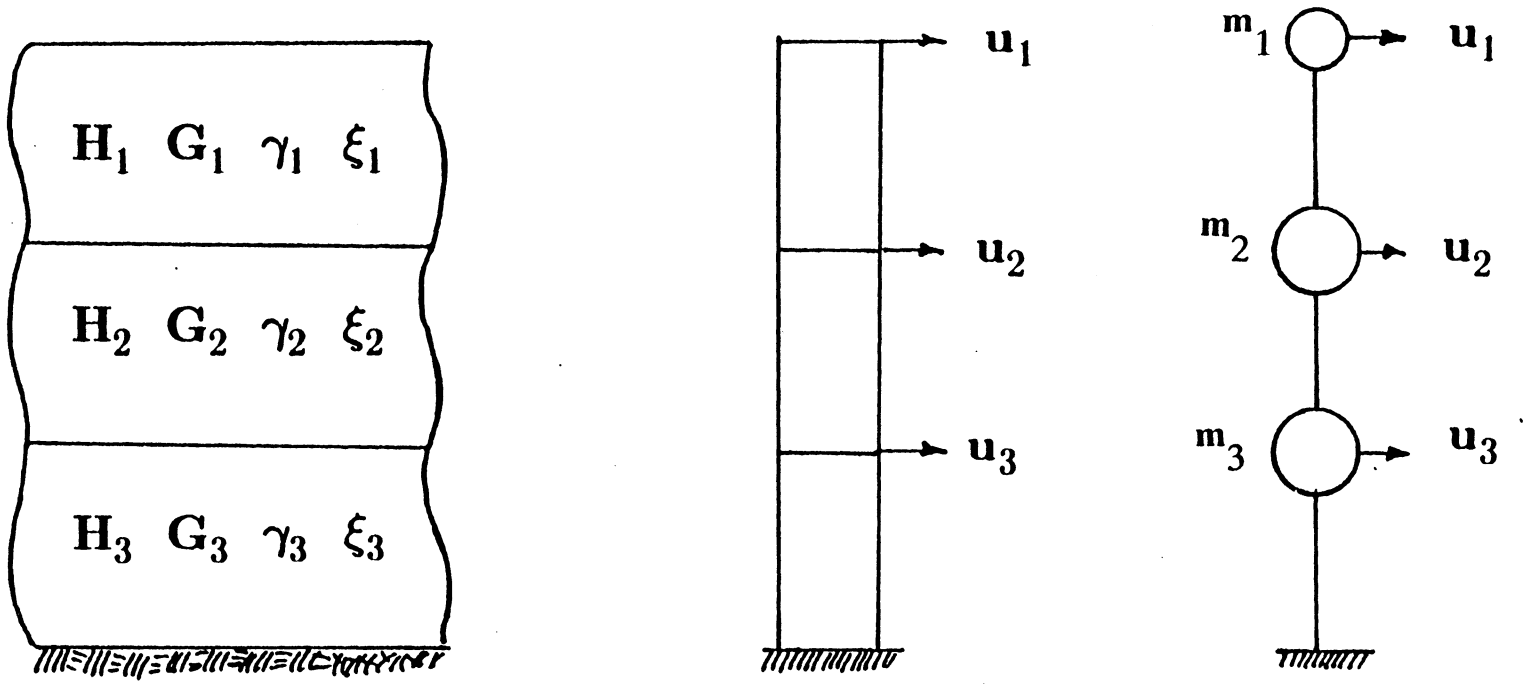

Figure 2.1 Soil Profile Model

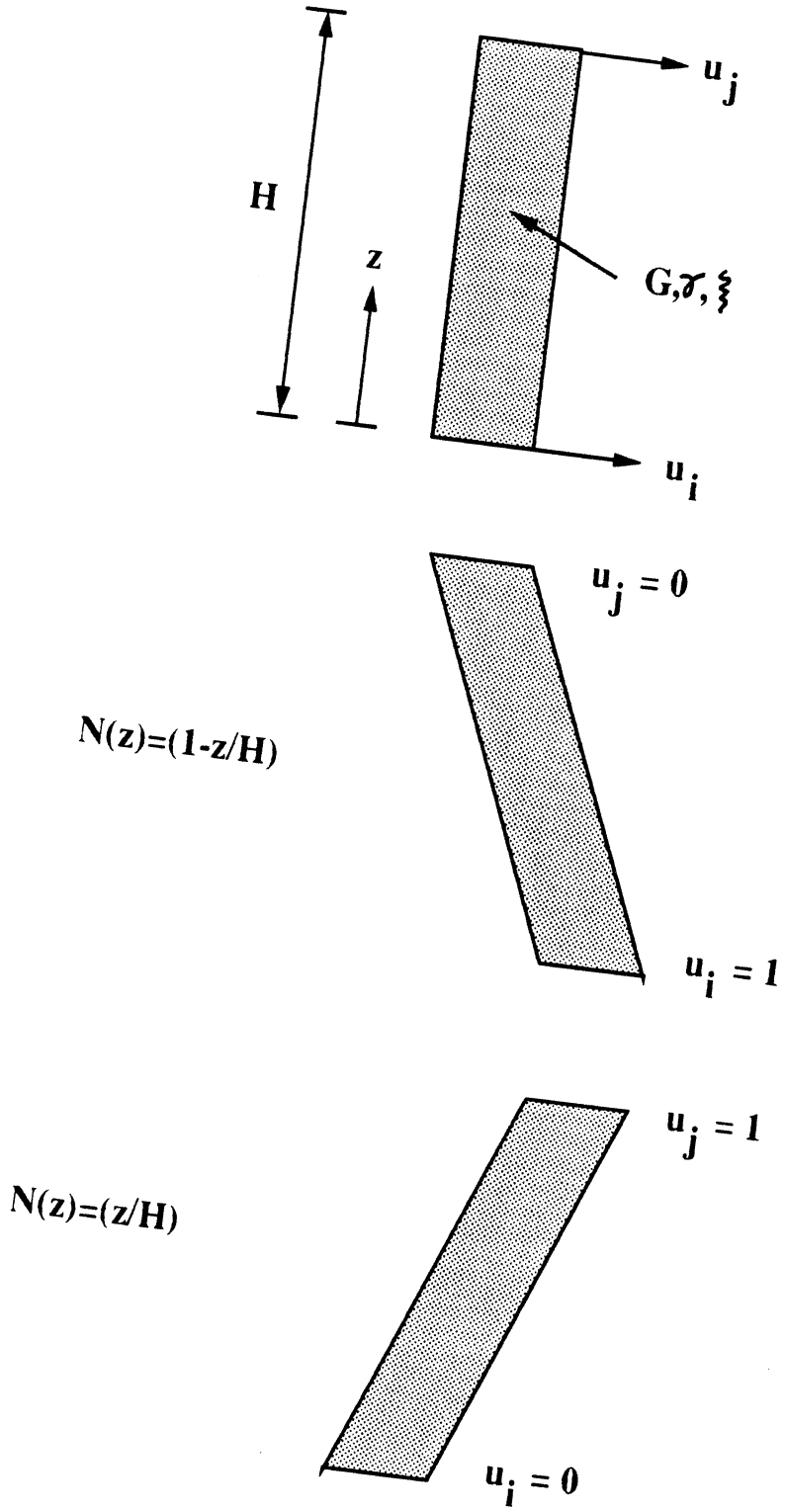

Figure 2.2 Soil Layer Element Shape Functions

$$\mathbf{k}_l = \int_0^H \mathbf{B}^T \, G \, \mathbf{B} \, dz = \frac{G}{H} \begin{bmatrix} 1 & -1 \\ -1 & 1 \end{bmatrix} \tag{2.10}$$

where G is the element shear modulus. Using direct stiffness assembly the layer element stiffness matrices are added into the global stiffness matrix:

$$\mathbf{K} = \sum_{l=1}^{\#layers} \mathbf{k}_l \tag{2.11}$$

where Σ is an assembly operator. It should be noted that $\mathbf{K}$ is a tri-diagonal matrix with a half-bandwidth of two which enables the use of an extremely efficient numerical solution scheme.

Element and Global Mass Matrices: It is possible to formally develop the layer element mass matrix using the principal of virtual displacements. However, such an approach would result in a matrix with the same coupling properties as the stiffness matrix. If a physical lumped mass approximation is used, the element mass matrix is diagonal resulting in a slight reduction in accuracy and a considerable savings in computer storage and time. In this formulation, one-half of the element mass is lumped at each node to obtain:

$$\mathbf{m}_l = \frac{\rho H}{2} \begin{bmatrix} 1 & 0 \\ 0 & 1 \end{bmatrix} \tag{2.12}$$

where ρ is the mass density of the layer element. The global mass matrix of the system is generated by assembling the mass matrices of each layer element:

$$\mathbf{M} = \sum_{l=1}^{\#layers} \mathbf{m}_l \tag{2.13}$$

Element and Global Damping Matrices: Since the exact nature of damping forces on an underdamped physical system is not well understood, and since the effect of these forces on the transient response is generally small, a simplifying assumption regarding the nature of these forces is justified. For most structural engineering applications, it is common to assume that the damping matrix is proportional to both the mass and stiffness matrices (proportional damping). Application of this assumption at the element level results in the following form of the layer element damping matrix:

$$c_l = \alpha_l m_l + \beta_l k_l \tag{2.14}$$

Because most of the experimental information regarding damping has been related to the frequencies and mode shapes of the vibrating system, it is natural to determine the constants α and β for each element based on a knowledge of the element damping ratio ξ, and the frequencies of the system. Two approaches for determining the constants α and β will be presented herein; the first uses a single control frequency and the second uses two control frequencies.

The determination of α and β based on a knowledge of the damping ratio ξ and a single vibration frequency ω is termed equivalent modal damping [72]. It can be shown that the modal damping ratio ξ_i for mode number i is given in terms of the constants α and β by:

$$\xi_i = \frac{\alpha}{2\omega_i} + \frac{\beta\omega_i}{2} \tag{2.15}$$

where ω_i is the frequency of mode i. For given values of α and β, the frequency ω^* which yields a minimum value of damping ratio ξ^* is given by :

$$\omega^* = \left(\frac{\alpha}{\beta}\right)^{1/2} \tag{2.16}$$

If the minimum damping ratio ξ^* and the frequency ω^* are given, the damping coefficients α and β are calculated from the following equations:

$$\alpha = \xi^*\omega^* \tag{2.17}$$

$$\beta = \frac{\xi^*}{\omega^*} \tag{2.18}$$

The modal damping expression can now be rewritten as:

$$\xi_i = \left(\frac{\omega^*}{\omega_i} + \frac{\omega_i}{\omega^*}\right)\frac{\xi^*}{2} \tag{2.19}$$

or in terms of period as:

$$\xi_i = \left(\frac{T_i}{T^*} + \frac{T^*}{T_i}\right)\frac{\xi^*}{2} \tag{2.20}$$

which is represented graphically in Figure 2.3. It is most common to select α and β based on the fundamental frequency of the system, which insures that all of the higher frequencies are more heavily damped than the fundamental frequency.

Determination of α and β based on a knowledge of a damping ratio ξ^* and two frequencies is termed damping with two mode control. Assuming the damping ratio is the same in modes i and j yields the following expressions for α and β :

$$\alpha = \frac{2\,\xi^*\,\omega_i\omega_j}{(\omega_i+\omega_j)} \tag{2.21}$$

$$\beta = \frac{2\,\xi^*}{(\omega_i+\omega_j)} \tag{2.22}$$

This relationship between damping ratio and frequency is shown in Figure 2.4. It is observed that for frequencies between ω_i and ω_j, the damping ratio is less than ξ^* while for frequencies outside of this range, larger damping ratios are obtained.

Once the element damping matrices have been determined, the global damping matrix can be assembled:

$$\mathbf{C} = \sum_{l=1}^{\#layers} \mathbf{c}_l \tag{2.23}$$

Note that **C** is also a tri-diagonal matrix with a half-bandwidth of two. It is important to note that because each soil layer element in the finite element mesh can have a different damping ratio, the global damping matrix assembled from the proportional element damping matrices is, in general, nonproportional.

Dynamic Equilibrium Equations: Using the finite element formulation, the soil profile is first discretized into layer elements, each of which is completely defined by a thickness H, shear modulus G, mass density ρ and damping ratio ξ. The element property matrices are then assembled into the global property matrices, which can be used in the dynamic equilibrium equations for the site model:

$$\mathbf{M}\,\ddot{\mathbf{U}}(t) + \mathbf{C}\,\dot{\mathbf{U}}(t) + \mathbf{K}\,\mathbf{U}(t) = \mathbf{R}(t) \tag{2.24}$$

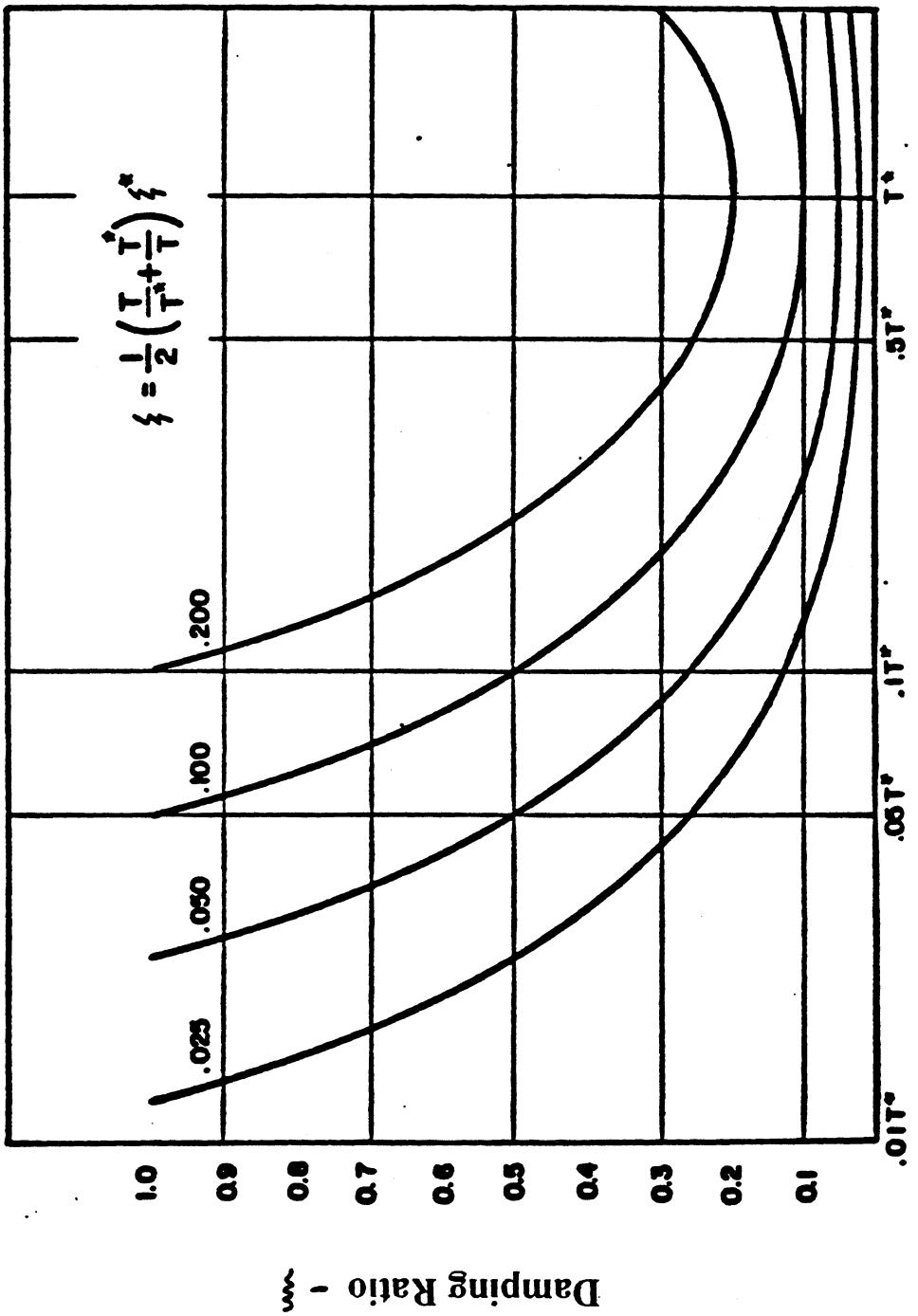

Figure 2.3 Equivalent Modal Damping

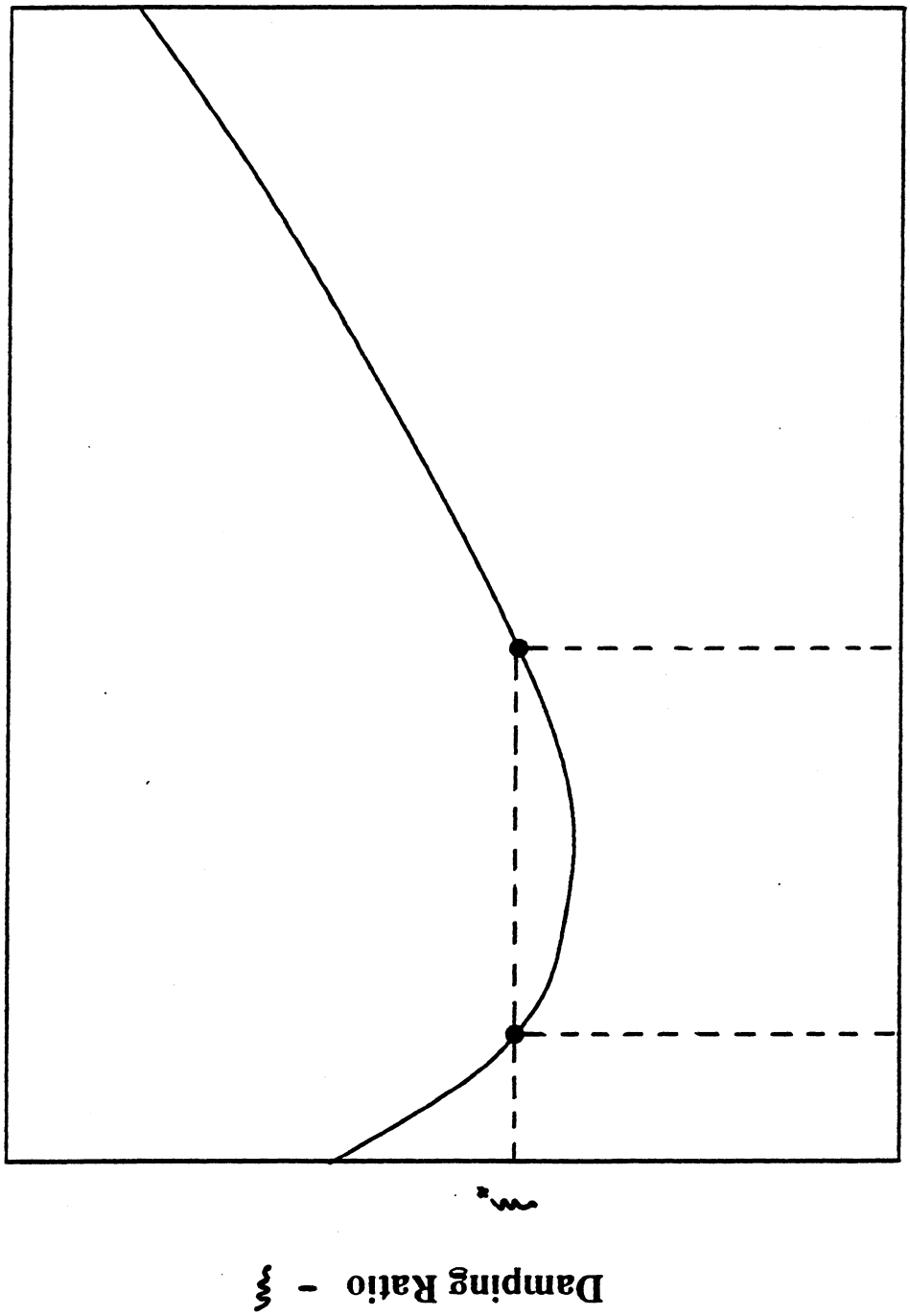

Figure 2.4 Damping with Two Mode Control

where :

$\ddot{U}(t)$ = vector of relative nodal accelerations

$\dot{U}(t)$ = vector of relative nodal velocities

$U(t)$ = vector of relative nodal displacements

M = global mass matrix

C = global damping matrix

K = global stiffness matrix

$R(t)$ = earthquake load vector = $- M1\ddot{u}_g(t)$

1 = unity vector

$\ddot{u}_g(t)$ = base acceleration

The primary advantage of this discrete formulation is that the dynamic equilibrium of the soil profile is expressed as a set of ordinary differential equations rather than the partial differential equation required to describe the continuous profile model. The dynamic equilibrium equations can be solved numerically by discretizing them in the time domain with the exact solution $U(t)$, $\dot{U}(t)$ and $\ddot{U}(t)$ approximated by U_t, $\dot{U}_t$ and $\ddot{U}_t$, respectively.

2.2.1. Linear Analysis

For linear systems, the solution of the dynamic equilibrium equations can be obtained in two ways; the mode superposition method or by direct integration procedures. Because the standard mode superposition method is applicable only to proportionally damped systems, the discussion herein focuses on direct integration techniques.

The basic idea behind direct integration is to begin with the known initial conditions of motion and to march forward in time computing solution states at discrete time intervals (hence the term step-by-step integration). References [2], [5], and [24] discuss the accuracy and stability of various numerical integration schemes.

The integration method employed herein is the Newmark β method [47] with modifications by Wilson [5]. In this scheme, three integration parameters, γ, β and θ can be

selected to provide the desired accuracy and stability. As developed in [2], the Newmark method is based on the following equations:

$$\mathbf{M}\ddot{\mathbf{U}}_{t+\Delta t} + \mathbf{C}\dot{\mathbf{U}}_{t+\Delta t} + \mathbf{K}\mathbf{U}_{t+\Delta t} = \mathbf{R}_{t+\Delta t} \tag{2.25}$$

$$\mathbf{U}_{t+\Delta t} = \mathbf{U}_t + \Delta t\dot{\mathbf{U}}_t + \Delta t^2\left(\frac{1}{2} - \beta\right)\ddot{\mathbf{U}}_t + \Delta t^2\beta\ddot{\mathbf{U}}_{t+\Delta t} \tag{2.26}$$

$$\dot{\mathbf{U}}_{t+\Delta t} = \dot{\mathbf{U}}_t + \Delta t(1-\gamma)\ddot{\mathbf{U}}_t + \Delta t\gamma\ddot{\mathbf{U}}_{t+\Delta t} \tag{2.27}$$

These equations constitute three vector equations for determining three vector unknowns; $\mathbf{U}_{t+\Delta t}$, $\dot{\mathbf{U}}_{t+\Delta t}$ and $\ddot{\mathbf{U}}_{t+\Delta t}$. Values of $\gamma < 1/2$ will introduce positive numerical damping in the solution while values of $\gamma > 1/2$ will introduce negative numerical damping (which in effect adds spurious energy to the system). For $\gamma = 1/2$, no numerical damping is introduced to the solution. These observations, coupled with the fact that second order accuracy is achieved if and only if $\gamma = 1/2$, essentially force the selection of $\gamma = 1/2$. The β parameter controls the assumed "shape function" of the nodal accelerations across the time interval Δt. The most popular selections of γ and β are:

1) $\gamma = 1/2$, $\beta = 1/4$: This is the constant average acceleration (CAA) method which assumes a constant acceleration vector with a value of ½ ($\ddot{\mathbf{U}}_t + \ddot{\mathbf{U}}_{t+\Delta t}$) over the time step. This assumption results in a linear variation in velocity and a quadratic variation in displacement over the time step (Figure 2.5a).

2) $\gamma = 1/2$, $\beta = 1/6$: This is the linear acceleration method which assumes a linear variation of acceleration vector between $\ddot{\mathbf{U}}_t$ and $\ddot{\mathbf{U}}_{t+\Delta t}$ over the time step. This assumption results in a quadratic variation of velocity and a cubic variation in displacement over the time step (Figure 2.5b).

The Wilson θ method [5] is a modification of the linear acceleration method. The technique includes satisfying equilibrium at a time $t+\theta\Delta t$ then interpolating (based on linear acceleration) to calculate the state of motion at time $t+\Delta t$ for use as initial conditions for the next time step. An unconditionally stable method with large damping in the higher modes is produced with $\theta = 1.4$.

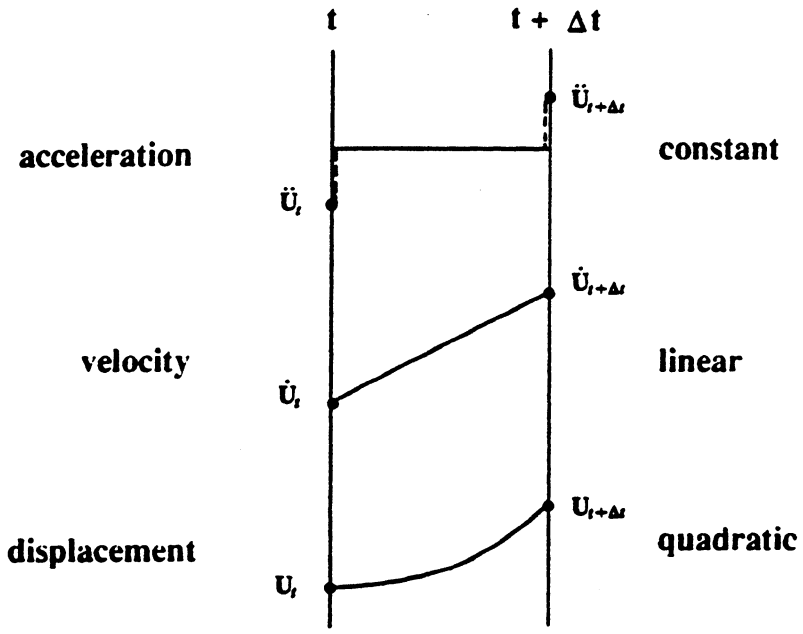

Figure 2.5a Time Domain Shape Functions for CAA Method

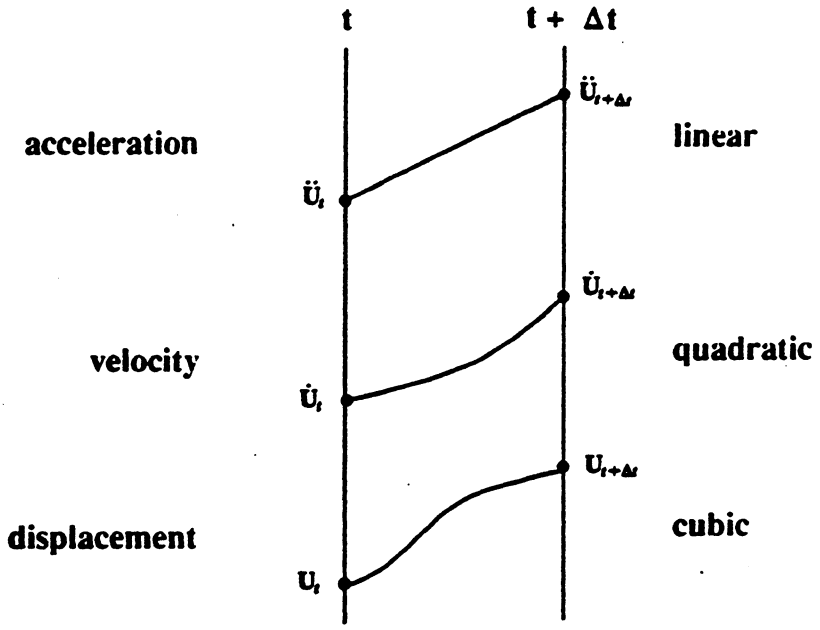

Figure 2.5b Time Domain Shape Functions for Linear Acceleration Method

A Fortran subroutine, TSTEPS has been developed to integrate the dynamic equilibrium equations for a tri-diagonal system implementing the Newmark-Wilson scheme for use in linear earthquake response analysis of soil profiles. The algorithm is outlined in Table 2.1.

2.2.2 Equivalent Linear Analysis

Because it is known that soils can exhibit nonlinear behavior, even at small strain amplitudes, it is important to appropriately account for the effects of nonlinearity on the earthquake response of the soil profile. In many cases, the use of an equivalent linear site model has been found to provide a satisfactory means of evaluating the nonlinear seismic response characteristics of soil profiles [59]. The idea is to perform linear analysis using strain-compatible dynamic stiffness and damping properties selected to qualitatively represent the effects of nonlinear behavior in each layer.

For a single hysteretic strain cycle in a given layer, equivalent linear dynamic properties can be determined graphically as shown in Figure 2.6. The equivalent shear modulus, G_{eq}, is the slope of the line connecting the two unloading points while the equivalent viscous damping ratio, ξ_{eq}, is established by equating the energy dissipated by the hysteretic layer to that dissipated in the viscous layer over the cycle [31]. For multiple hysteresis cycles in a given layer, the equivalent linear properties can be obtained by using the average of the properties for each cycle, or equivalently by using the graphical approach on the hysteretic cycle corresponding to the average or effective strain developed during the cycling. Empirical observations indicate that for cyclic shear strain histories, the ratio of effective strain to maximum strain is between 0.5 and 0.7 [59]. Relationships between equivalent linear dynamic properties and effective strains have been established for various soil types [22,28,62]. The trends observed in typical soil types are that the shear modulus and damping ratio decrease and increase, respectively, with increasing effective strain values (Figure 2.7).

TABLE 2.1 TSTEPS – ALGORITHM SUMMARY

Linear Earthquake Response Analysis

a. Assemble global stiffness matrix **K**, mass matrix **M**, and damping matrix **C**.

b. Set initial conditions; $U_0, \dot{U}_0, \ddot{U}_0$

c. Specify integration parameters; γ, β, θ

1. Compute integration constants :

$$\tau = \theta\Delta t \qquad a_0 = \frac{1}{(\beta\tau^2)} \qquad a_1 = \frac{\gamma}{(\beta\tau)} \qquad a_2 = \frac{1}{(\beta\tau)}$$

$$a_3 = \frac{1}{2\beta} - 1 \quad a_4 = \frac{\gamma}{\beta} - 1 \qquad a_5 = \frac{\tau}{2}\left(\frac{\gamma}{\beta} - 2\right) \qquad a_6 = \Delta t(1-\gamma)$$

$$a_7 = \Delta t\gamma \qquad a_8 = \Delta t^2\left(\frac{1}{2} - \beta\right) \quad a_9 = \Delta t^2\beta$$

2. Form and triangularize dynamic stiffness :

$$\mathbf{K}^* = \mathbf{K} + a_0\mathbf{M} + a_1\mathbf{C}$$
$$\mathbf{K}^* = \mathbf{L}\mathbf{D}\mathbf{L}^T$$

3. Compute effective load vector at time $t+\tau$:

$$\mathbf{R}^* = \mathbf{R}_{t+\tau} + \mathbf{M}\,(a_0\mathbf{U}_t + a_2\dot{\mathbf{U}}_t + a_3\ddot{\mathbf{U}}_t) + \mathbf{C}\,(a_1\mathbf{U}_t + a_4\dot{\mathbf{U}}_t + a_5\ddot{\mathbf{U}}_t)$$

4. Solve for displacement at time $t+\tau$:

$$\mathbf{L}\mathbf{D}\mathbf{L}^T\,\mathbf{U}_{t+\tau} = \mathbf{R}^*$$

5. Compute state of motion at time $t+\Delta t$:

$$\ddot{\mathbf{U}}_{t+\tau} = a_0(\mathbf{U}_{t+\tau} - \mathbf{U}_t) - a_2\dot{\mathbf{U}}_t - a_3\ddot{\mathbf{U}}_t$$
$$\ddot{\mathbf{U}}_{t+\Delta t} = \ddot{\mathbf{U}}_t + \frac{1}{\theta}(\ddot{\mathbf{U}}_{t+\tau} - \ddot{\mathbf{U}}_t)$$
$$\dot{\mathbf{U}}_{t+\Delta t} = \dot{\mathbf{U}}_t + a_6\ddot{\mathbf{U}}_t + a_7\ddot{\mathbf{U}}_{t+\Delta t}$$
$$\mathbf{U}_{t+\Delta t} = \mathbf{U}_t + \Delta t\dot{\mathbf{U}}_t + a_8\ddot{\mathbf{U}}_t + a_9\ddot{\mathbf{U}}_{t+\Delta t}$$

6. Perform energy balance calculations if required.

7. Update maxima

8. If t < duration, go to step 3.

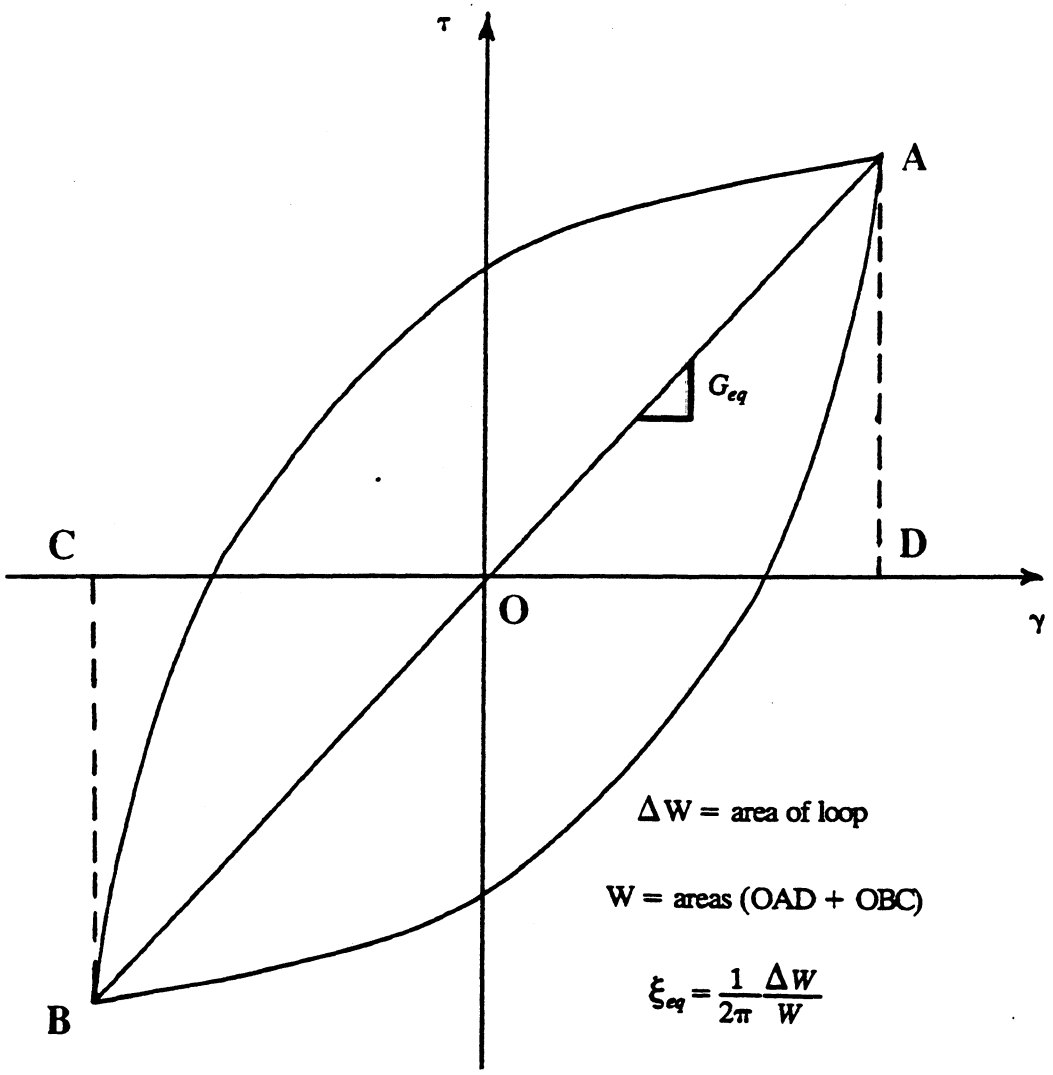

Figure 2.6 Definition of Equivalent Shear Modulus and Equivalent Damping Ratio for a Single Hysteretic Cycle

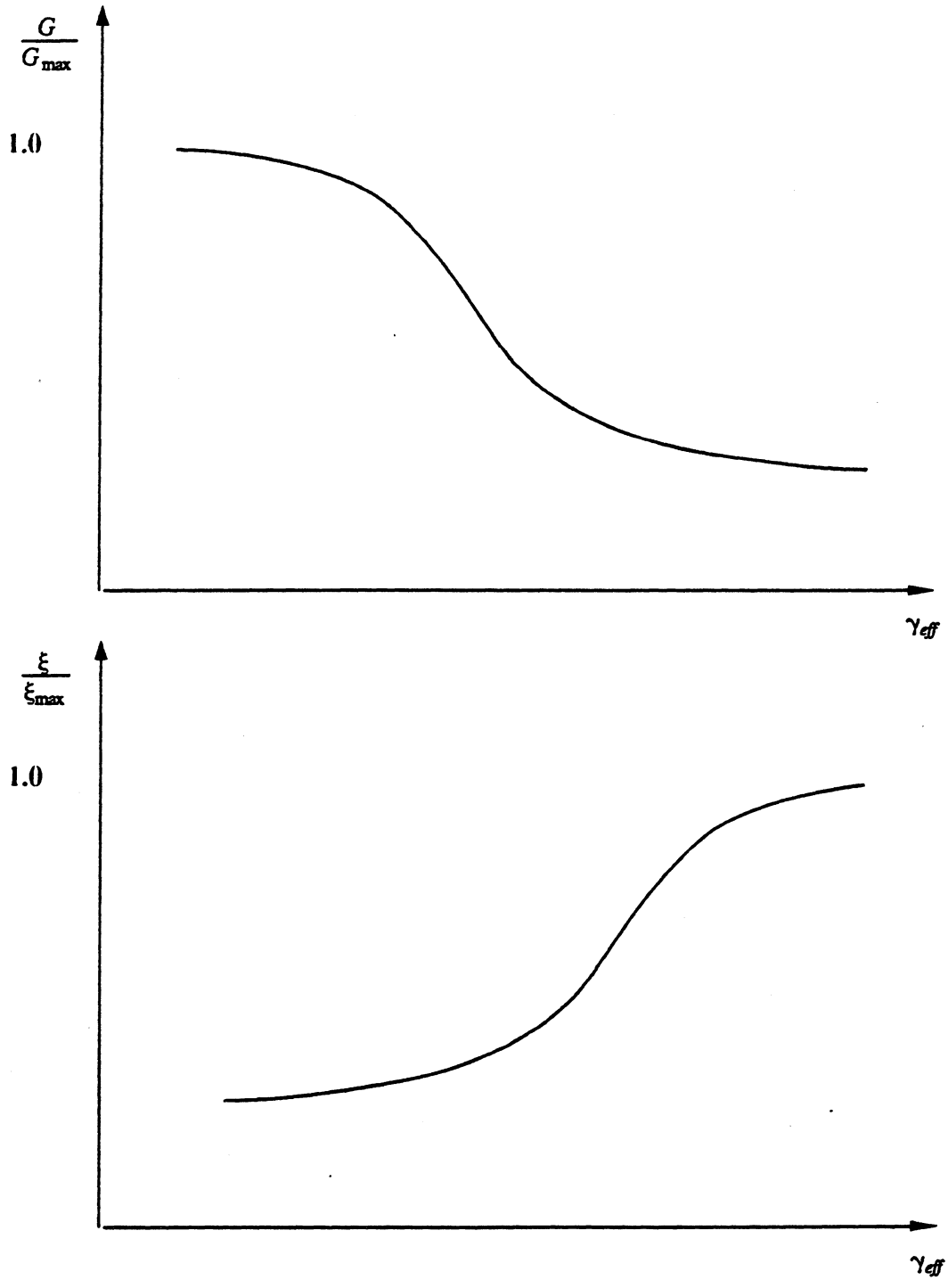

Figure 2.7 Strain Dependent Dynamic Properties for Soil

The fundamental idea behind the application of equivalent linear analysis to the earthquake response of soil profiles is that after some iteration to obtain strain compatible dynamic properties, a qualitative representation of the true nonlinear response of the profile can be obtained. The steps involved in the analysis are outlined as follows:

1) Perform linear earthquake response analysis based on the current layer properties monitoring the layer strain histories for maxima. The dynamic equilibrium equations can be integrated using the linear techniques discussed in Section 2.2.1.

2) Calculate effective strains in each layer; $\gamma_{eff} = \lambda \gamma_{max}$ where λ is usually assumed to be between 0.55 and 0.65 [59] with the larger value appropriate for giving more uniform strain histories.

3) Using the effective strains, update the shear modulus and damping ratio for each layer using the strain dependent curves (Figure 2.7).

Steps 1, 2, and 3 are repeated until the difference between the modulus and damping used and the strain compatible modulus and damping ratio are less than some acceptable difference for each layer. A Fortran subroutine, ITERAT has been developed for use in equivalent linear iterative response analysis of soil profiles. The algorithm is summarized in Table 2.2.

2.2.3. Nonlinear Analysis

During cyclic loading, the stress-strain behavior of soils is nonlinear and hysteretic, hence the earthquake response of soil profiles may be influenced significantly by nonlinear effects. The discrete finite element site model can be used to approximate the nonlinear response of soil profiles by implementing soil layer elements whose nonlinear hysteretic properties are representative of soil behavior. Appendix A discusses the Ramberg-Osgood hysteresis model which is used herein to represent the constitutive relationships of the soil layer elements. This section discusses the extension of the discrete finite element site model to the nonlinear earthquake analysis of soil profiles.

TABLE 2.2 ITERAT -- ALGORITHM SUMMARY

Iterative Equivalent Linear Earthquake Response Analysis

1. Form global mass matrix, **M**.

2. Set vector of maximum layer strains to zero:

$$\gamma_{max} = 0$$

3. Form global stiffness matrix based on current layer shear moduli, **G** :

$$\mathbf{K} = \mathbf{K}(\mathbf{G})$$

4. Form global damping matrix based on current layer damping ratios, ξ :

$$\mathbf{C} = \mathbf{C}(\xi)$$

5. Call TSTEPS integration subroutine, save maximum layer strains, γ_{max}.

6. Compute vector of effective strains, γ_{eff} :

$$\gamma_{eff} = \lambda\ \gamma_{max}$$

7. Calculate strain compatible layer shear moduli, **G** :

$$\mathbf{G} = \mathbf{G}(\gamma_{eff})$$

8. Calculate strain compatible layer damping ratios, ξ :

$$\xi = \xi(\gamma_{eff})$$

9. If strain compatible dynamic properties have converged, repeat steps 3, 4 and 5.

10. If strain compatible dynamic properties have not converged, go to step 2.

The instantaneous dynamic equilibrium equations of the finite element site model can be expressed in vector form as:

$$\mathbf{R_I} + \mathbf{R_D} + \mathbf{R_S} = \mathbf{R_E} \tag{2.28}$$

where:

$\mathbf{R_I}$ = vector of inertial resisting forces

$\mathbf{R_D}$ = vector of damping resisting forces

$\mathbf{R_S}$ = vector of stiffness or static resisting forces

$\mathbf{R_E}$ = earthquake load vector

When the property matrices af the system remain constant with time, the resisting force vectors $\mathbf{R_I}$, $\mathbf{R_D}$ and $\mathbf{R_S}$ are explicit functions of the nodal accelerations, velocities and displacements, respectively:

$$\mathbf{R_I} = \mathbf{M}\,\ddot{\mathbf{U}} \tag{2.29}$$

$$\mathbf{R_D} = \mathbf{C}\,\dot{\mathbf{U}} \tag{2.30}$$

$$\mathbf{R_S} = \mathbf{K}\,\mathbf{U} \tag{2.31}$$

For linear systems, equilibrium can be satisfied at discrete time intervals using step-by-step integration (Section 2.2.1). In the analysis of systems whose elements have nonlinear stress-strain behavior, the global stiffness matrix becomes a function of the time varying nodal displacements and the element constitutive relationships, i.e., $\mathbf{K} = \mathbf{K}(\mathbf{U})$. In such systems, the static resisting force vector can no longer be determined as above, rather it must be determined indirectly from the nodal displacements using the element constitutive relationships:

$$\mathbf{R_S} = \mathbf{R_S}(\mathbf{U}) \tag{2.32}$$

In general, the application of step-by-step integration to systems with nonlinear stiffness properties results in a loss of equilibrium at the end of each time step. The instantaneous unbalance can be expressed as:

$$\mathbf{R_U} = \mathbf{R_E} - \mathbf{R_I} - \mathbf{R_D} - \mathbf{R_S}(\mathbf{U}) \tag{2.33}$$

If the unbalanced forces are allowed to accumulate over successive time steps, substantial errors can be introduced into the solution. Hence it is apparent that the step-by-step solution strategy must be appropriately modified to account for equilibrium errors in order to generate accurate solutions. Several methods have been developed to deal with the loss of equilibrium at a time step for nonlinear dynamic analysis [2,18,19] but the choice of solution strategy is largely problem dependent and must be selected with judgement. Because the Ramberg-Osgood hysteresis model (see Figure A.1) provides a continuous relationship between stresses and strains for a given branch of the hysteresis loop but is discontinuous between branches (at unloadings), a solution strategy which implements tangent stiffness iteration within a branch and an event-to-event scheme between branches will be employed herein.

Iteration Strategy: The primary reasons for selecting a Newton type iteration scheme to correct equilibrium errors at the end of a time step are that reformation and solution of the tri-diagonal global stiffness matrix is relatively inexpensive and the element constitutive model (Ramberg-Osgood) provides a continuous relationship between stress and strain on a given branch of the hysteresis loop. Within a branch, the Ramberg-Osgood function is well behaved and the tangent stiffness is continuously defined; these conditions are critical for convergence with the Newton method [15]. The essential features of iteration to satisfy equilibrium can be investigated by considering the relationships between dynamic load and displacement for a SDOF system. Figure 2.8 shows the dynamic load vs. displacement in the **R**–**U** plane. The steps corresponding to Figure 2.8 are summarized as follows:

1) An equilibrium state has been obtained at time t. The state is defined by the instantaneous displacement, velocity, acceleration, static resisting force and tangent dynamic stiffness ($\mathbf{U}$, $\dot{\mathbf{U}}$, $\ddot{\mathbf{U}}$, $\mathbf{R}_S$ and $\mathbf{K}^*$).

2) The solution is advanced by assuming the dynamic stiffness remains constant over the time step and solving the pseudo-static equation for the incremental displacement ($\Delta\mathbf{U}$) :

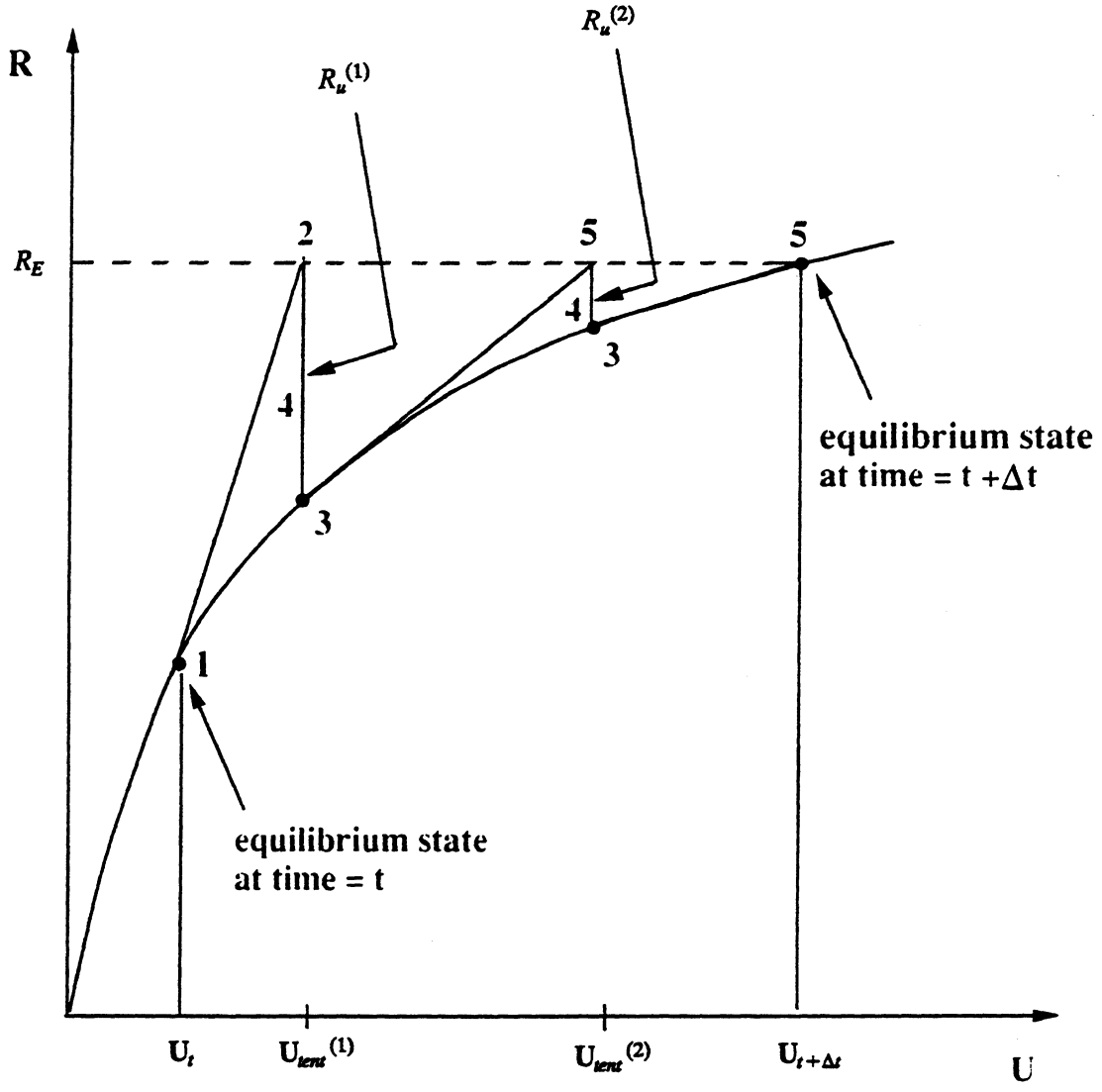

Figure 2.8 Schematic of Newton Iteration

$$\mathbf{R}^* = \mathbf{K}^* \Delta \mathbf{U} \tag{2.34}$$

then calculating the tentative acceleration, velocity and displacement based on the numerical integration scheme.

3) The static resisting force and the tangent stiffness corresponding to the tentative displacement ($\mathbf{U}_{tent}$) are obtained from the element constitutive relationship:

$$\mathbf{R}_S = \mathbf{R}_S (\mathbf{U}_{tent}) \tag{2.35}$$

$$\mathbf{K}^* = \mathbf{K}^* (\mathbf{U}_{tent}) \tag{2.36}$$

4) The unbalance between the dynamic load $\mathbf{R}_E$ and the tentative internal resisting forces at time $t+\Delta t$ is then obtained:

$$\mathbf{R}_U = \mathbf{R}_E - \mathbf{M}\, \ddot{\mathbf{U}}_{tent} - \mathbf{C}\, \dot{\mathbf{U}}_{tent} - \mathbf{R}_S (\mathbf{U}_{tent}) \tag{2.37}$$

5) If the unbalance is unacceptably large, the solution is advanced to a new tentative state by solving the following pseudo static equation for the incremental displacement:

$$\mathbf{R}_U = \mathbf{K}^* \Delta \mathbf{U} \tag{2.38}$$

6) Steps 3, 4 and 5 are then continued until the unbalanced force is smaller than the acceptable level, at which point the tentative state becomes the equilibrium state at time $t+\Delta t$.

This iteration strategy is directly applicable to MDOF systems, but because of the vector states in the MDOF problem, the graphic representation of the iteration occurs in the **R**–**U** space rather than the **R**–**U** plane. Hence, the MDOF iteration strategy is more difficult to interpret physically.

The number of iterations within a given time step depends on the degree of nonlinearity and the step size, but for earthquake analysis of moderately nonlinear soil profiles, only a few iterations should provide acceptable accuracy. Details regarding the convergence rate of Newton iteration can be found in [15].

Event-to-Event Strategy: Because the slope of the Ramberg-Osgood function is discontinu-

ous between branches of the hysteresis loops (Figure A.1) Newton iteration is not applicable when unloading occurs. A solution strategy which captures unloading events will insure that the equilibrium paths or branches are properly linked. Herein, the linking of equilibrium paths is accomplished with an event-to-event scheme.

The Ramberg-Osgood model satisfies the Masing criterion [29] which dictates that the unloading and reloading branches of the hysteresis loop are the same backbone curve with both the stress and strain scales expanded by a factor of two and the origin translated. One consequence of this stipulation is that the unloading stiffness is equal to the initial stiffness. Physically, element unloading occurs when the element strain rate has a zero crossing, or in discrete time, when two subsequent strain increments are of opposite sign. The method used to capture unloading events within the step-by-step integration scheme is outlined as follows:

1) At the beginning of a time step, the incremental shear strains are determined from the incremental displacements using the strain-displacement transformation:

$$\Delta\gamma = \mathbf{B}\,\Delta\mathbf{U} \tag{2.39}$$

2) The strain increment of each layer element is compared to the corresponding strain increment from the previous time step. If the strain increments are of opposite sign, then unloading has occurred in the selected layer element during the time step. The shear modulus of each unloading element is set to the unloading shear modulus.

3) If unloading occurred, the global stiffness matrix is reformed based on the updated shear moduli and the time step is restarted.

This type of event-to-event scheme was developed in [18]. It is important to note that this procedure is not exact because it assumes that unloading occurs at time t when in reality, unloading occurs somewhere between times t and $t+\Delta t$. However, for the small time steps used in earthquake response analysis, the errors generated by this method are not expected to be significant.

A Fortran subroutine WALK has been developed to perform linear or nonlinear earthquake response analysis of soil profiles implementing the combination iteration and event-to-event strategy with the CAA integration method. The algorithm is presented in Table 2.3.

Automatic Time Step Control: The idea behind most step-by-step integration techniques is to satisfy the dynamic equilibrium equations of the finite element system at discrete time intervals. It is important to note that within a given time step, the equilibrium equations are not satisfied, otherwise the numerical solution would be the same as the exact solution. As the integration time step is reduced, the discretization errors tend to zero and the numerical solution approaches the exact solution. It is obvious that the appropriate selection of the integration time step is critical for generating accurate numerical solutions. It is very common for the analyst to select an integration time step based on various rules of thumb, perform the dynamic analysis, then rerun the analysis with a smaller time step until only small differences exist between subsequent solutions. Although this technique does insure the numerical solution will not change with further decreases in the time step, it wastes a tremendous amount of computational effort. Therefore, a more efficient procedure is desirable. This section discusses a procedure in which the accuracy of the numerical solution is controlled by increasing or decreasing the integration time step as the analysis progresses based on a measure of the mean equilibrium error over a time step. The technique presented herein is based in part on work presented in [2] and represents an attempt to balance the tradeoff between solution accuracy and computational efficiency for the earthquake response analysis of soil profiles.

Within a given time step, if the vectors of inertia forces, damping forces, static forces and external loads varied linearly with time, the equilibrium errors would be zero at all times. If the CAA method is applied to a linear system, the variation of the dynamic force vectors over the time step is shown in Figure 2.9. By considering the time average of the difference between the assumed force variations and a linear variation over the time step, a

TABLE 2.3 WALK – ALGORITHM SUMMARY

Nonlinear Earthquake Response Analysis (Constant Time Step)

a. Form stiffness matrix **K**, mass matrix **M**, and damping matrix **C**.

b. Set initial conditions; $U_0, \dot{U}_0, \ddot{U}_0$

1. Compute integration constants (CAA method) :

$$a_1 = \frac{4}{\Delta t^2} \qquad a_2 = \frac{4}{\Delta t} \qquad a_3 = 2 \qquad a_4 = \frac{2}{\Delta t} \qquad a_5 = 2$$

2. Compute dynamic portion of dynamic stiffness matrix, **D** :

$$\mathbf{D} = a_1\mathbf{M} + a_4\mathbf{C}$$

3. Compute effective load vector at time $t+\Delta t$:

$$\mathbf{R}^* = \mathbf{R}_{t+\Delta t} + \mathbf{M}\,(a_2\dot{U}_t + a_3\ddot{U}_t) + \mathbf{C}\,(a_5\dot{U}_t)$$

4. Form dynamic stiffness, $\mathbf{K}^*$:

$$\mathbf{K}^* = \mathbf{K} + \mathbf{D}$$

5. Solve for incremental displacement vector, $\Delta\mathbf{U}$:

$$\mathbf{K}^*\Delta\mathbf{U} = \mathbf{R}^*$$

6. Compute layer strain increments, $\Delta\gamma$:

$$\Delta\gamma = \mathbf{B}\,\Delta\mathbf{U}$$

7. Check for unloading event :

if unloading occurred :

reform **K** based on unloading shear moduli; $\mathbf{K} = \mathbf{K}(\mathbf{G})$

go to step 4

8. Update tentative state of motion :

if iter = 0 :

$$\ddot{U}_{tent} = \ddot{U}_t + a_1\Delta\mathbf{U} - a_2\dot{U}_t - a_3\ddot{U}_t$$
$$\dot{U}_{tent} = \dot{U}_t + a_4\Delta\mathbf{U} - a_5\dot{U}_t$$
$$\mathbf{U}_{tent} = \mathbf{U}_t + \Delta\mathbf{U}$$

TABLE 2.3 WALK -- ALGORITHM SUMMARY (CONTINUED)

if iter = 1 :

$$\ddot{U}_{tent} = \ddot{U}_{tent} + a_1 \Delta U$$
$$\dot{U}_{tent} = \dot{U}_{tent} + a_4 \Delta U$$
$$U_{tent} = U_{tent} + \Delta U$$

9. Calculate resisting force vector, R_s and updated shear moduli, G :

$$R_s = R_s (U_{tent})$$
$$G = G (\gamma_{tent})$$

10. Calculate unbalance force vector, R_u :

$$R_u = R_{t+\Delta t} - M \ddot{U}_{tent} - C \dot{U}_{tent} - R_s$$

11. Reform stiffness based on current shear moduli, G :

$$K = K (G)$$

12. Check equilibrium error :

if ($\| R_u \|$ > tolerance) :

set iteration flag, iter = 1

go to step 4

13. Set state at time t+Δt equal to tentative state :

$$\ddot{U}_{t+\Delta t} = \ddot{U}_{tent}$$
$$\dot{U}_{t+\Delta t} = \dot{U}_{tent}$$
$$U_{t+\Delta t} = U_{tent}$$

14. Perform energy balance calculations if required.

15. Update maxima

16. If t < duration, go to step 3.

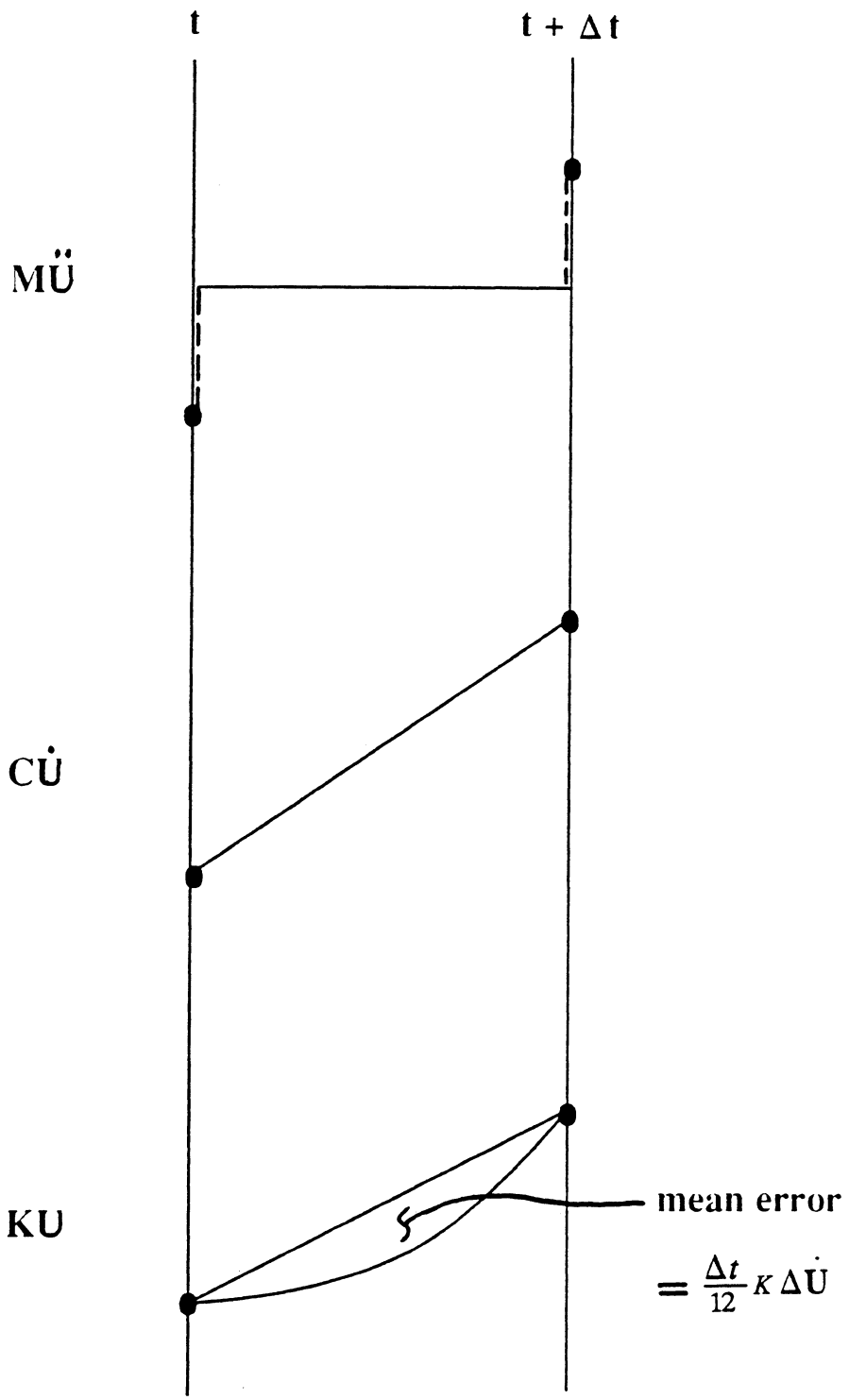

Figure 2.9 Variation of Internal Forces for a Linear System using CAA Method

measure of the mean equilibrium error over the step can be computed. Because the inertial and damping forces are constant and linear, respectively, over the time step, the time average of the difference between these distributions and a linear distribution integrates to zero (see Figure 2.9). However, the error due to static forces varies quadratically and has a nonzero mean value given by:

$$\mathbf{E}_m = \frac{\Delta t}{12} \mathbf{K} \Delta \dot{\mathbf{U}} \tag{2.40}$$

For nonlinear systems which utilize an iteration strategy, the stiffness matrix **K** may vary over the time step and this equation for mean static error is no longer valid. However, by using an effective stiffness matrix, $\mathbf{K}_{eff}$ based on the element states at the beginning and end of the time step (see Figure 2.10), the mean equilibrium error of the system can be approximated by replacing **K** with $\mathbf{K}_{eff}$.

In order to perform earthquake response analysis with automatic step size control, a tolerance for the mean equilibrium error over the time step is specified. If the norm of the mean equilibrium error vector exceeds the tolerance then the time step is halved and the step is repeated with the new time step. If the error norm is less than the tolerance for a user specified number of time steps (implying that Δt is unnecessarily small) then the time step is doubled and the step is repeated. It should be noted that the maximum time step cannot exceed the time step of the input earthquake acceleration if the loading is to be properly discretized. Methods for determining appropriate tolerances on the mean equilibrium error are developed in [2] or may be developed with experience and by comparison with the results of constant time step analyses.

A Fortran subroutine AUTO has been developed to perform linear or nonlinear earthquake response analysis of soil profiles implementing the iteration and event-to-event strategy (similar to WALK) including automatic time step control. The algorithm is presented in Table 2.4.

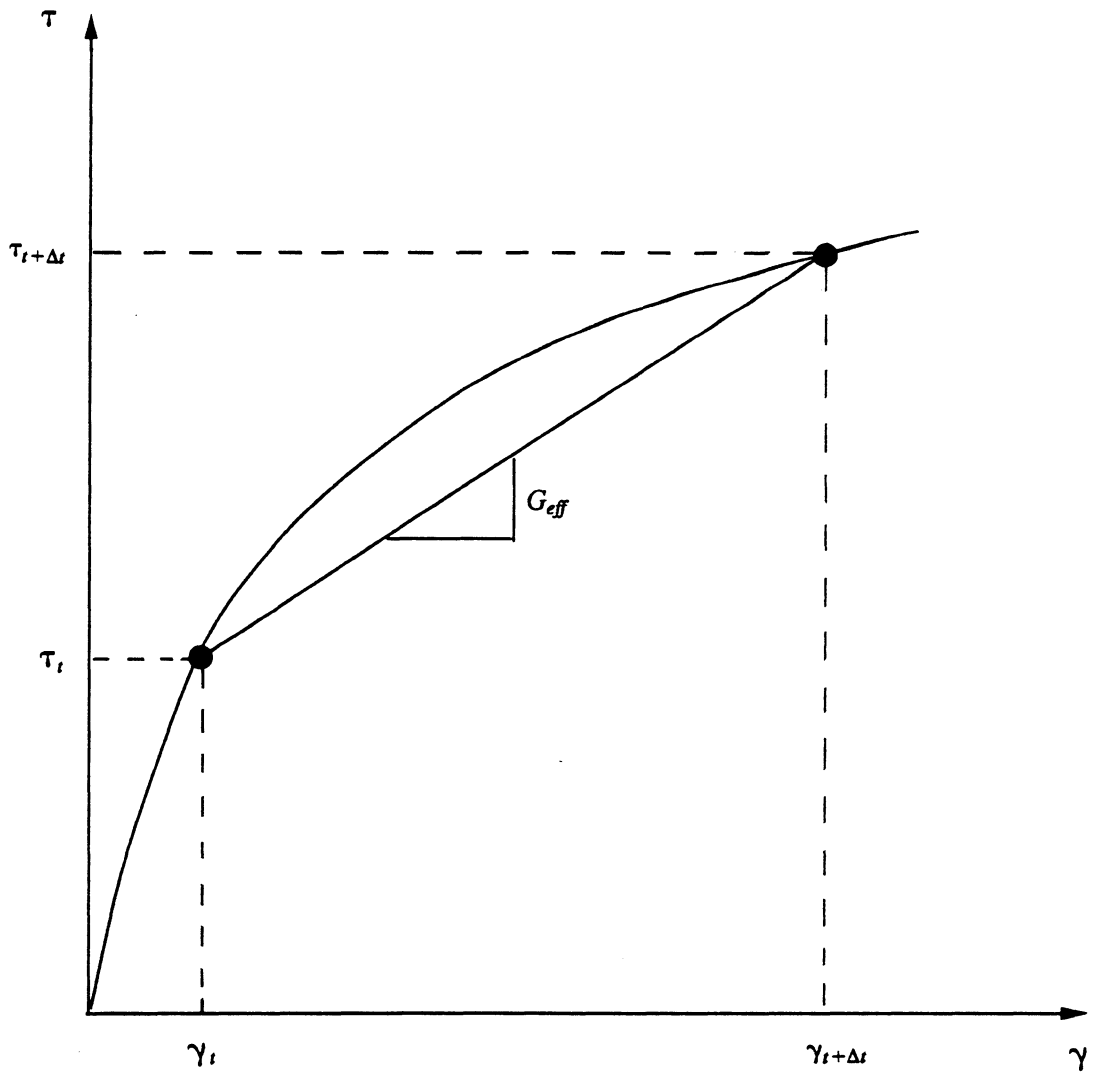

Figure 2.10 Schematic for Determining Effective Shear Stiffness over Time Step

TABLE 2.4 AUTO -- ALGORITHM SUMMARY

Nonlinear Earthquake Response Analysis (Variable Time Step)

a. Form stiffness matrix **K**, mass matrix **M**, and damping matrix **C**.

b. Set initial conditions; $\mathbf{U}_0, \dot{\mathbf{U}}_0, \ddot{\mathbf{U}}_0$

1. Compute integration constants (CAA method) :

$$a_1 = \frac{4}{\Delta t^2} \qquad a_2 = \frac{4}{\Delta t} \qquad a_3 = 2 \qquad a_4 = \frac{2}{\Delta t} \qquad a_5 = 2$$

2. Compute dynamic portion of dynamic stiffness matrix, **D** :

$$\mathbf{D} = a_1\mathbf{M} + a_4\mathbf{C}$$

3. Compute effective load vector at time $t+\Delta t$:

$$\mathbf{R}^* = \mathbf{R}_{t+\Delta t} + \mathbf{M}\,(a_2\dot{\mathbf{U}}_t + a_3\ddot{\mathbf{U}}_t) + \mathbf{C}\,(a_5\dot{\mathbf{U}}_t)$$

4. Form dynamic stiffness, $\mathbf{K}^*$:

$$\mathbf{K}^* = \mathbf{K} + \mathbf{D}$$

5. Solve for incremental displacement vector, $\Delta\mathbf{U}$:

$$\mathbf{K}^*\Delta\mathbf{U} = \mathbf{R}^*$$

6. Compute layer strain increments, $\Delta\gamma$:

$$\Delta\gamma = \mathbf{B}\,\Delta\mathbf{U}$$

7. Check for unloading event :

if unloading occurred :

reform **K** based on unloading shear moduli; **K** = **K** (**G**)

go to step 4

8. Update tentative state of motion :

if iter = 0 :

$$\ddot{\mathbf{U}}_{tent} = \ddot{\mathbf{U}}_t + a_1\Delta\mathbf{U} - a_2\dot{\mathbf{U}}_t - a_3\ddot{\mathbf{U}}_t$$
$$\dot{\mathbf{U}}_{tent} = \dot{\mathbf{U}}_t + a_4\Delta\mathbf{U} - a_5\dot{\mathbf{U}}_t$$
$$\mathbf{U}_{tent} = \mathbf{U}_t + \Delta\mathbf{U}$$

TABLE 2.4 AUTO -- ALGORITHM SUMMARY (CONTINUED)

if iter = 1 :

$$\ddot{\mathbf{U}}_{tent} = \ddot{\mathbf{U}}_{tent} + a_1 \Delta \mathbf{U}$$

$$\dot{\mathbf{U}}_{tent} = \dot{\mathbf{U}}_{tent} + a_4 \Delta \mathbf{U}$$

$$\mathbf{U}_{tent} = \mathbf{U}_{tent} + \Delta \mathbf{U}$$

9. Calculate resisting force vector, $\mathbf{R}_s$ and updated shear moduli, $\mathbf{G}$:

$$\mathbf{R}_s = \mathbf{R}_s (\mathbf{U}_{tent})$$

$$\mathbf{G} = \mathbf{G} (\gamma_{tent})$$

10. Calculate unbalance force vector, $\mathbf{R}_u$:

$$\mathbf{R}_u = \mathbf{R}_{t+\Delta t} - \mathbf{M}\, \ddot{\mathbf{U}}_{tent} - \mathbf{C}\, \dot{\mathbf{U}}_{tent} - \mathbf{R}_s$$

11. Reform stiffness based on current shear moduli, $\mathbf{G}$:

$$\mathbf{K} = \mathbf{K} (\mathbf{G})$$

12. Check equilibrium error :

if ($\| \mathbf{R}_u \|$ > tolerance) :

set iteration flag, iter = 1

go to step 4

13. Form effective stiffness for time step control :

$$\mathbf{K}_{eff} = \mathbf{K}_{eff} (\mathbf{G}_{eff})$$

14. Calculate mean equilibrium error vector over time step :

$$\mathbf{E} = \frac{\Delta t}{12} \mathbf{K}_{eff}\, \Delta \dot{\mathbf{U}}$$

TABLE 2.4 AUTO -- ALGORITHM SUMMARY (CONTINUED)

15. Check accuracy, change time step if required :

    if ($\| E \| >$ tolerance) :

        reduce time step : $\Delta t = \Delta t/2$

        set change flag, ichange = 1

        start step counter, icount = 1

    if ($\| E \| \leq$ tolerance AND icount = nmax) :

        increase time step : $\Delta t = 2\Delta t$

        set change flag, ichange = 1

        start step counter, icount = 1

    if ($\| E \| \leq$ tolerance AND icount < nmax) :

        unset change flag, ichange = 0

        increment step counter, icount = icount + 1

16. If time step has been changed (ichange = 1) :

        restore previous state

        go to step 1

17. Set state at time $t+\Delta t$ equal to tentative state :

$$\ddot{U}_{t+\Delta t} = \ddot{U}_{tent}$$
$$\dot{U}_{t+\Delta t} = \dot{U}_{tent}$$
$$U_{t+\Delta t} = U_{tent}$$

18. Perform energy balance calculations if required.

19. Update maxima

20. If t < duration, go to step 3.

2.3. Application of Time Domain Procedures

As a demonstration of time domain site response analysis procedures, the WAVES computer program is utilized to investigate the seismic response of a horizontally layered soil profile. In this section, the soil profile and the corresponding finite element discretization are discussed and some of the analysis results are presented.

The soil profile selected for analysis (shown in Figure 2.11) represents the subsurface conditions at the SCT site in downtown Mexico City. The most important feature of the site conditions in downtown Mexico City is the thick deposit of soft clay extending horizontally across a wide area, which was once a lake bed. Detailed investigations of the seismic response of this site and other sites at acceleration recording stations around Mexico City have been conducted and the analytical results are in reasonable agreement with measured results [63]. However, it is extremely important to note that the discretization of the SCT site used in [63] was based on an "interpreted soil profile" which was obtained by selecting (or "tuning") the average shear wave velocity of the site to yield the same fundamental site period observed in the recorded motions. It should also be noted that the average shear wave velocity of the clay layer in the "interpreted soil profile" (75 m/s or 246 ft/s) is significantly larger than the corresponding range of values measured in field investigations (40 to 60 m/s or 131 to 197 ft/s). Clearly, this "interpretive" procedure is only applicable when site specific strong motion or ambient vibration records are available. Rather than attempting to duplicate the results obtained using the "interpreted soil profile", the discretization used in this investigation was based on direct field measurements of shear wave velocity and soil unit weight obtained using P-S suspension logging techniques and boring and sampling procedures, respectively. The discretization shown in Figure 2.11, which is hereafter referred to as the "measured soil profile", was obtained using the following general procedure:

1) Plot the variation of measured shear wave velocity (V_s) with depth (as provided in [63] for the SCT site).

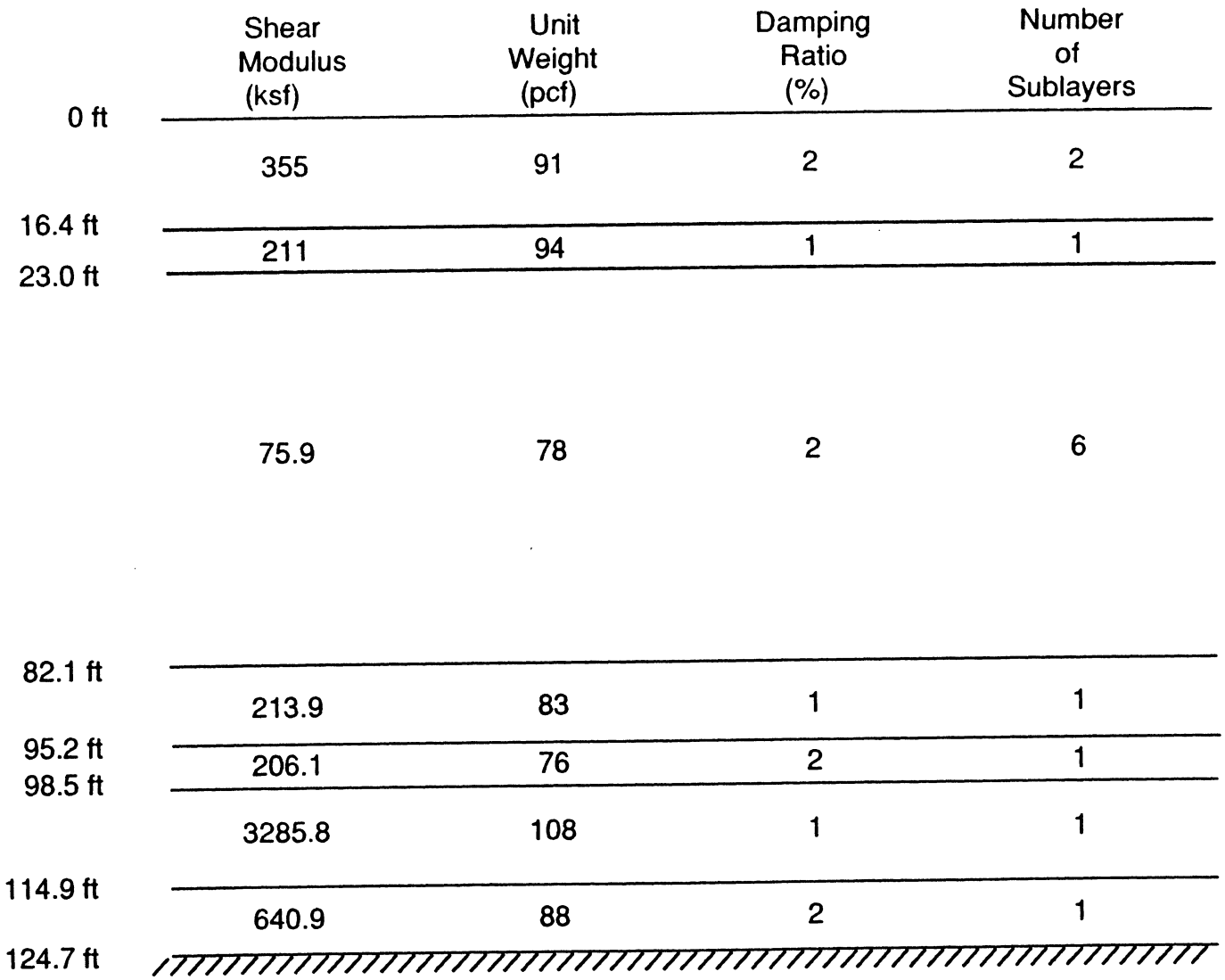

Figure 2.11 SCT Soil Profile

2) Plot the variation of soil unit weight (γ) or density (ρ) with depth (as provided in [30] for the SCT site).

3) Compare the plots obtained in steps 1) and 2) to obtain an indication of the important subsurface features as a guide for selecting individual soil layer elements which represent a stratum with constant shear modulus ($G=\rho V_s^2$) and unit weight (γ).

4) Subdivide layer elements as required to insure spatial convergence (i.e., to insure that further mesh subdivision will not effect the solution). A general rule of thumb is to select the maximum layer thickness such that 8 elements fit within the wave length of the important seismic waves propagating vertically through the site; effectively approximating a full sine wave with 8 equal length, straight line segments. For example, if the average shear wave velocity of a site is assumed to be 50 m/s (164 ft/s) and the fundamental site period is 2.0 seconds, the corresponding harmonic wavelength is 100 m (328 ft), resulting in a maximum layer thickness of 100/8 = 12.5 m (41 ft). Similarly, the harmonic wave length corresponding to the second site period (0.66 seconds) is 33.3 m (110 ft) resulting in a maximum layer thickness of 33.3/8 = 4.2 m (13.8 ft).

As discussed in [63], numerous accelerogram stations located around Mexico City recorded ground motions during the September 19, 1985 earthquake. The pseudo-acceleration response spectra (5% damping) computed from the EW and NS components of the surface acceleration recorded at the SCT site are shown along with the average spectrum in Figure 2.12. These spectra can serve as the basis for comparison with analytical results computed using WAVES. For the purposes of site response analysis, it is necessary to select input motions which can be considered as representative of the motions developed at the base rock level of the SCT site. Typically, base input motions are obtained by scaling the amplitude and/or the frequency of previously recorded earthquake accelerograms to reflect site variables such as distance from causative fault and earthquake magnitude [59]. Fortunately, many of the Mexico City accelerogram stations are located on rock or hard

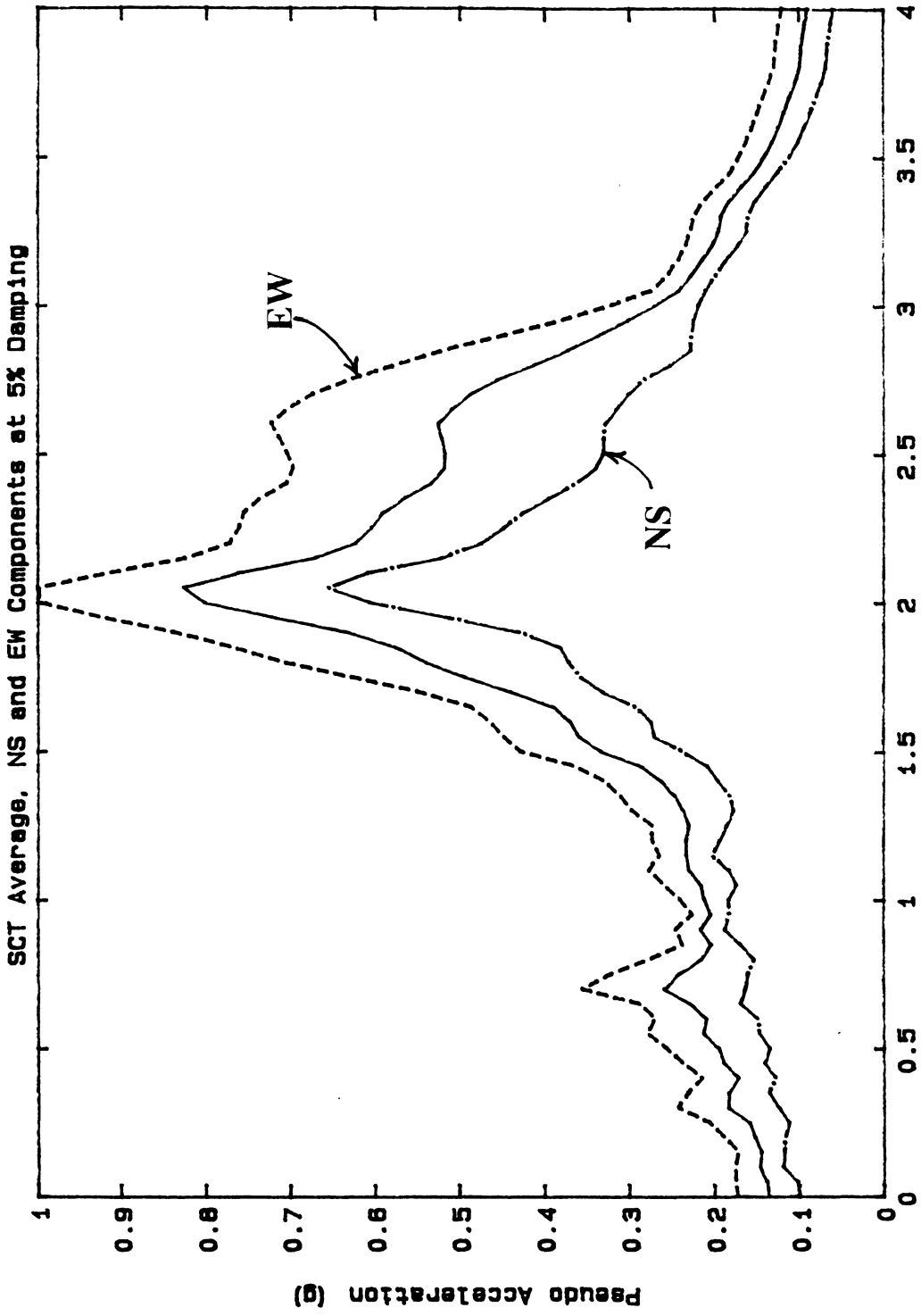

Figure 2.12 Response Spectra from Measured SCT Motions

soil formations located near the SCT site and hence the acceleration signals recorded at these stations can be used directly as input motions for the SCT site. In this study, motions recorded at two "rock" locations, namely, 1) the CUMV station and 2) the Tacubaya station were assumed to be representative of the SCT base rock input motions. Pseudo-acceleration response spectra (5% damping) computed from the EW and NS components of the surface acceleration recorded at the CUMV and Tacubaya stations are shown along with their average spectra in Figures 2.13 and 2.14, respectively.

The first step in this investigation was to determine the elastic vibration periods and mode shapes of the SCT site. The first and second mode shapes of the site, which correspond to vibration periods of 2.09 and 0.66 seconds, respectively, are shown in Figure 2.15.

Because the Mexico City clays are known to exhibit nearly linear behavior over a large strain range [63], linear earthquake response analysis of the site based on the initial dynamic soil properties was conducted. Figures 2.16 through 2.20 provide comparisons of the response spectra of the computed and measured surface motions. In general, the correlation of the computed results with the measured results is good for periods less than approximately 2.0 seconds while for periods above approximately 2.0 seconds, the spectral ordinates of the measured motion are somewhat larger than the corresponding computed values. The lack of correlation at vibration periods greater than about 2.0 seconds may be the manifestation of two-dimensional behavior in the measured results. In all cases, both the measured and computed spectra indicate that the response of the SCT site was dominated by vibration in the fundamental mode at a period of approximately 2.0 seconds.

The next step in the study was to conduct equivalent linear site response analysis as a means of estimating the dynamic response of the site including, in an approximate sense, nonlinear soil effects. As presented in [63], the results of equivalent linear analyses conducted on the site model corresponding to the "interpreted soil profile" show a correlation similar to that obtained using linear analyses of the "measured soil profile" model (Figures

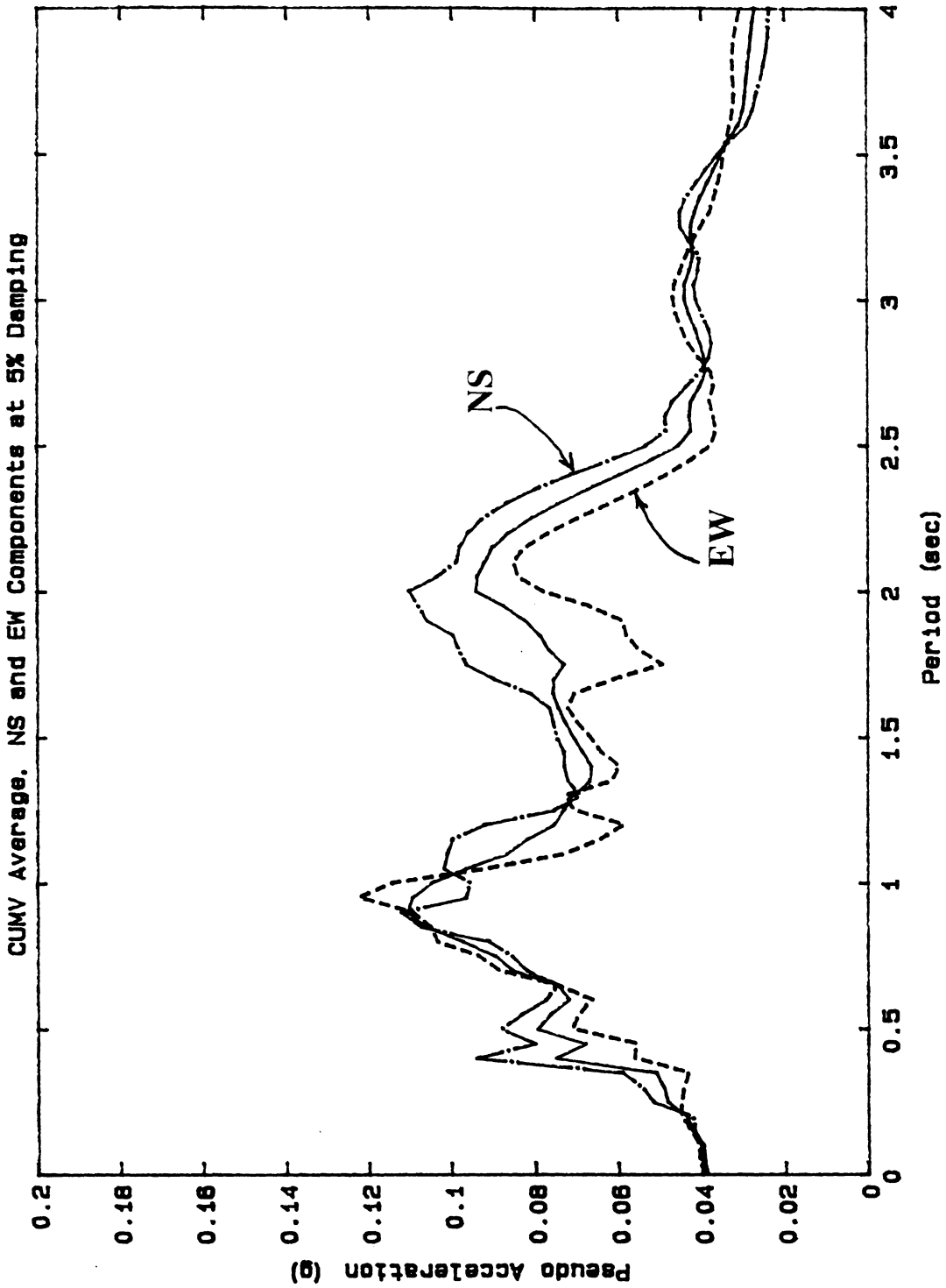

Figure 2.13 Response Spectra from Measured CUMV Motions

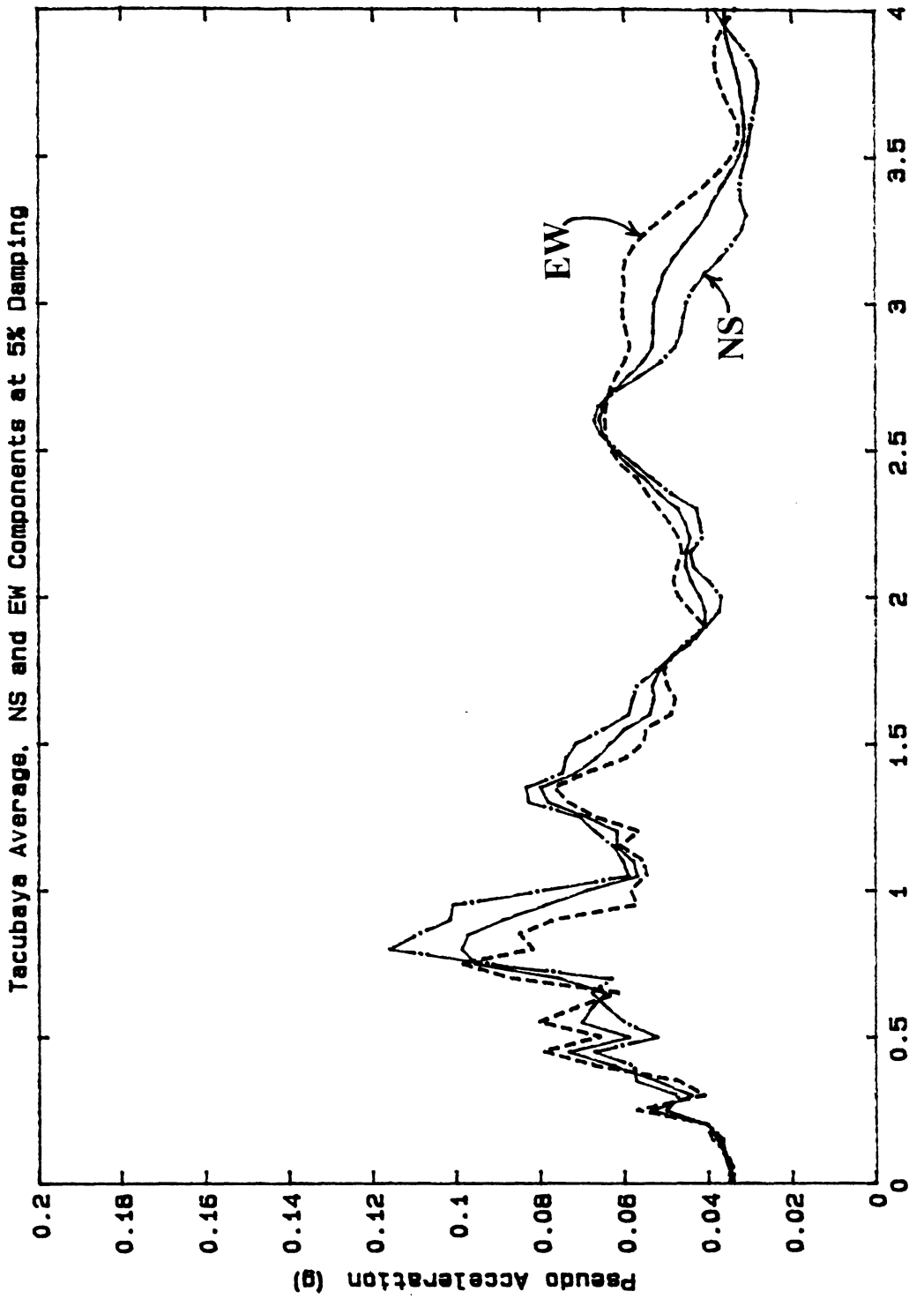

Figure 2.14 Response Spectra from Measured Tacubaya Motions

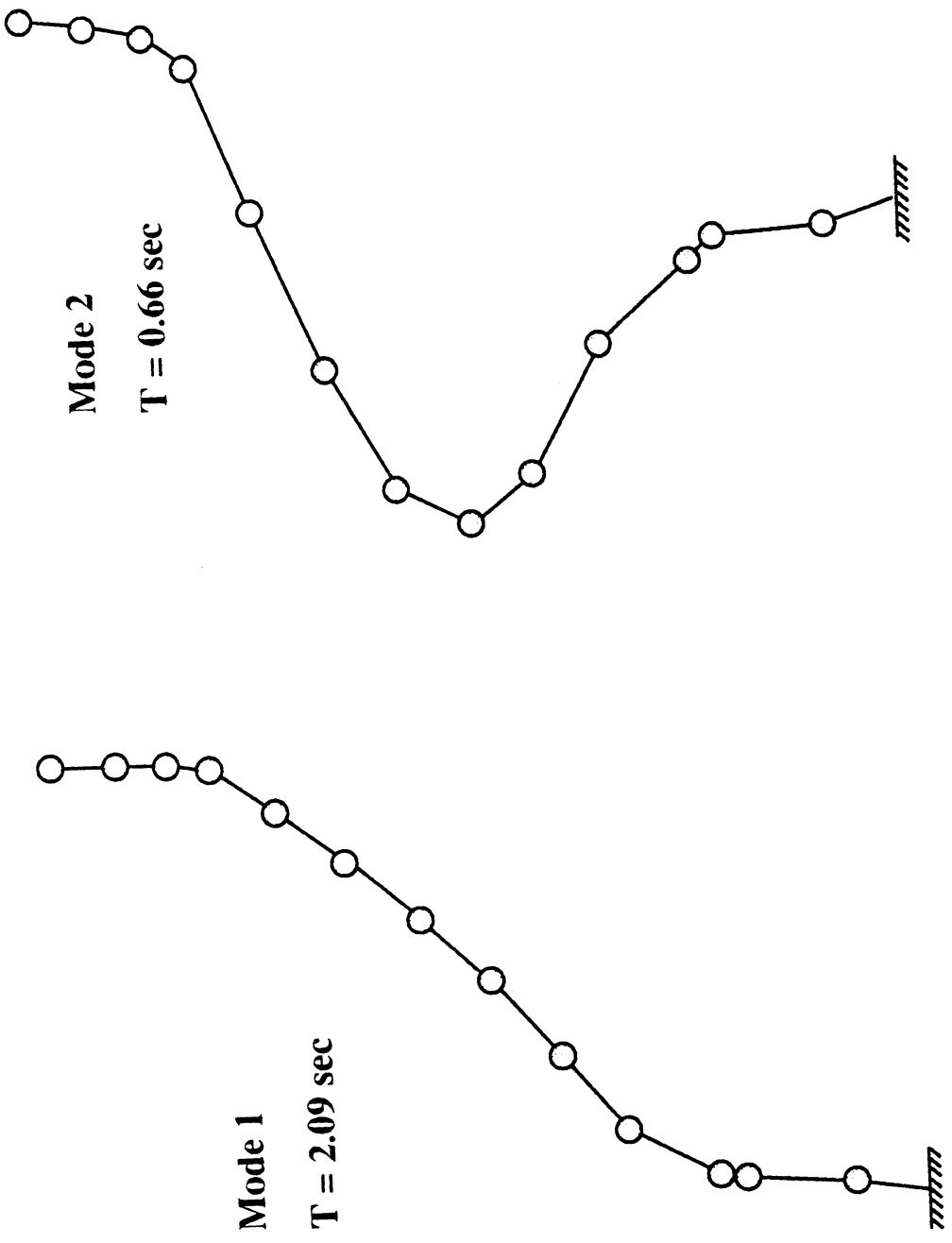

Figure 2.15 SCT Soil Profile - Modes 1 and 2

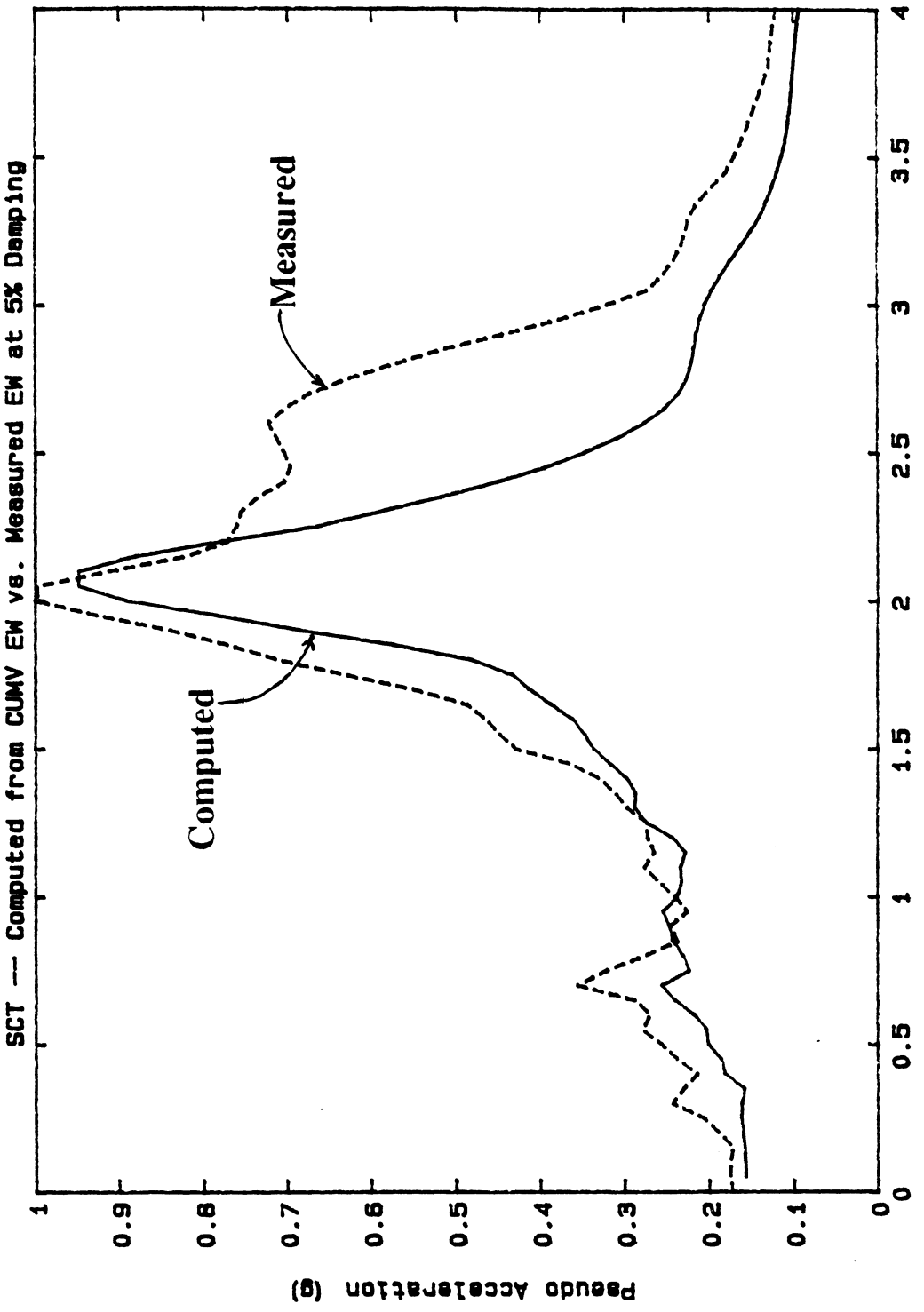

Figure 2.16 Response Spectrum from Linear Analysis vs. Measured

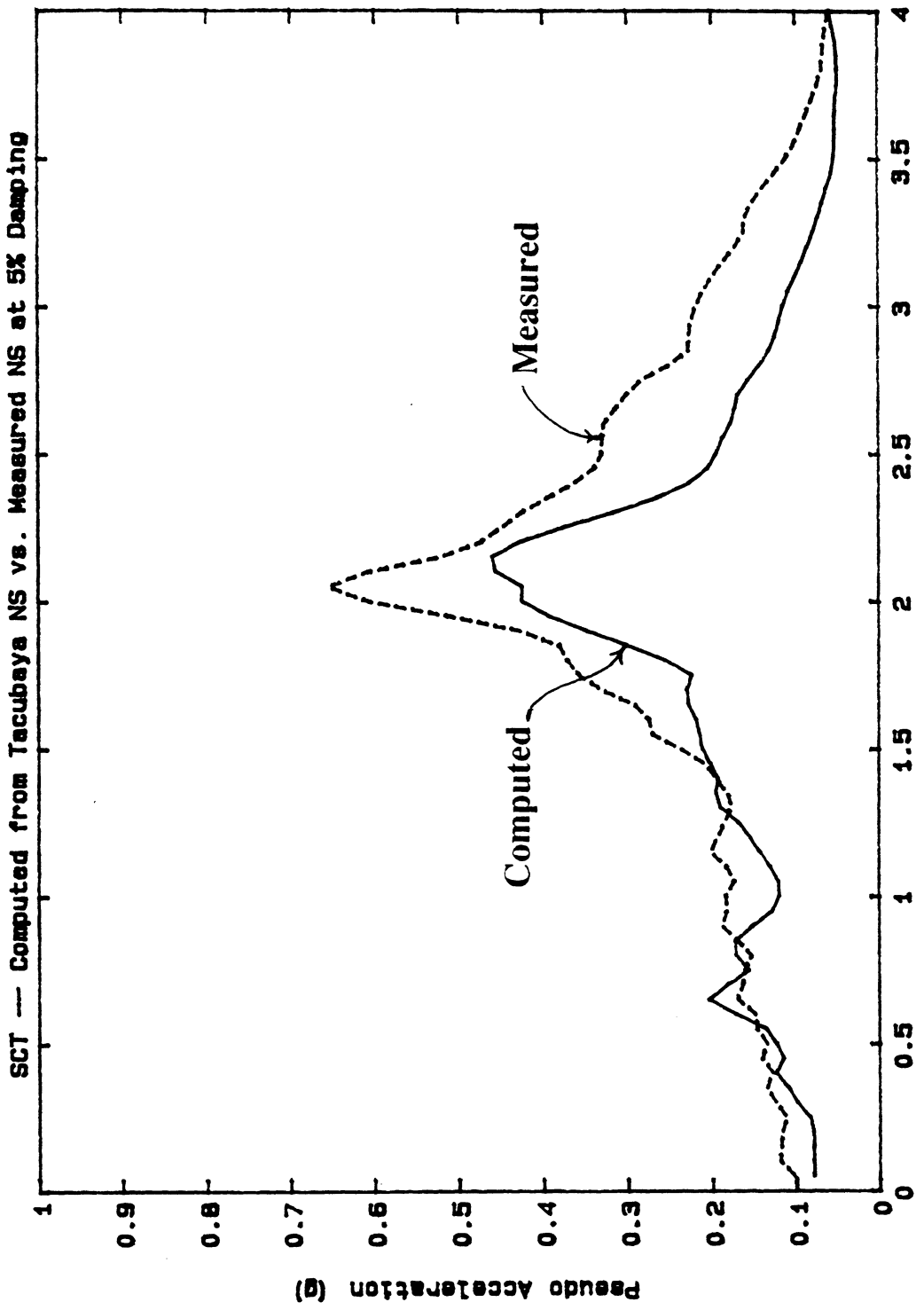

Figure 2.17 Response Spectrum from Linear Analysis vs. Measured

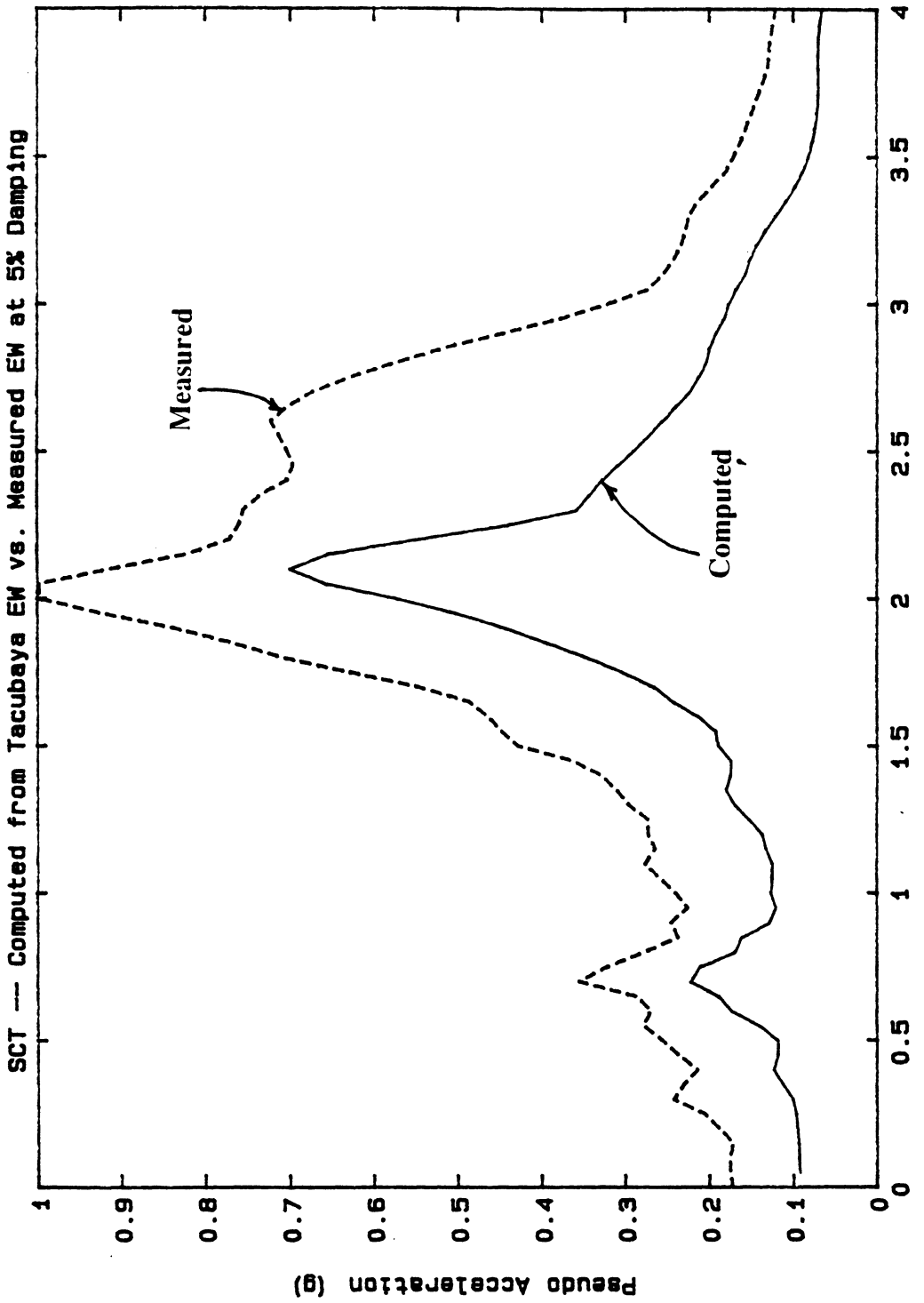

Figure 2.18 Response Spectrum from Linear Analysis vs. Measured

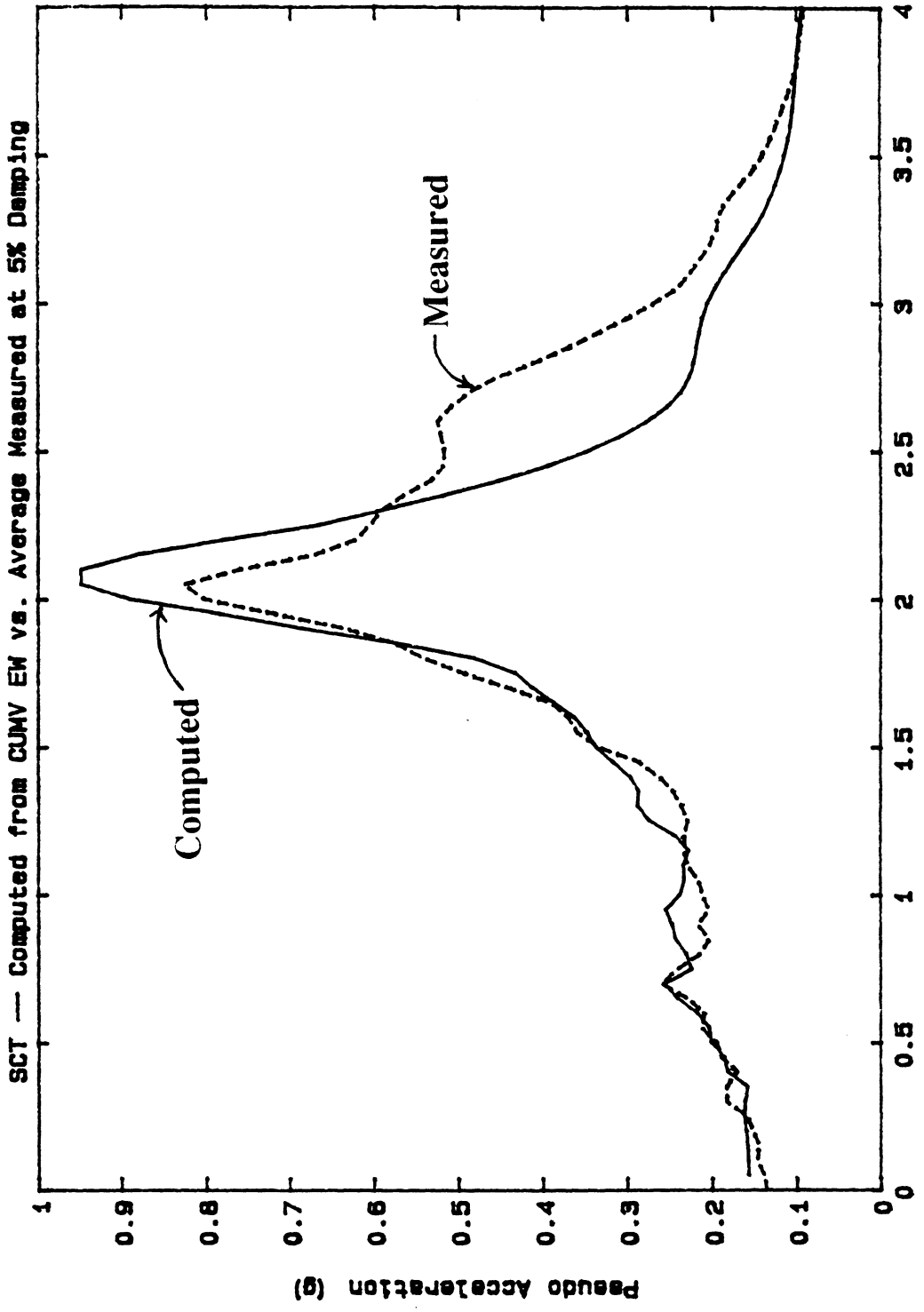

Figure 2.19 Response Spectrum from Linear Analysis vs. Measured

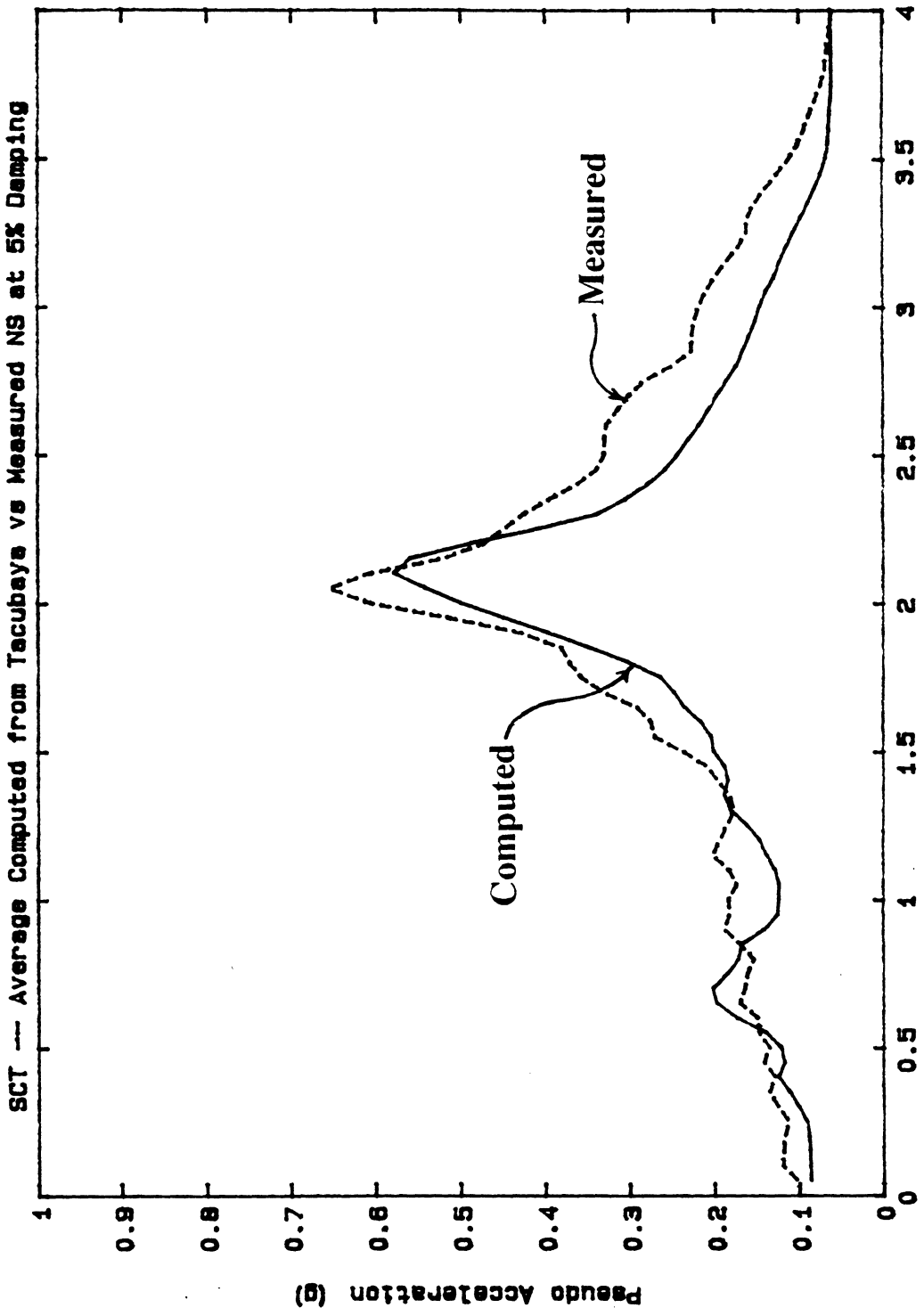

Figure 2.20 Response Spectrum from Linear Analysis vs. Measured

2.16 through 2.20). However, it is important to note that the results obtained using equivalent linear analysis of the "measured soil profile" displayed poor correlation with the measured results. The poor correlation can be readily explained by the results of a sensitivity study presented in [63], which indicated that a minor change in the shear wave velocity (-15 m/s or -49 ft/s) over a portion of the clay layer at the SCT site drastically changes the dynamic response of the site, effectively eliminating the spectral peak near 2.0 seconds. Because the shear wave velocity in the clay layer of the "measured soil profile" was roughly 20 m/s (66 ft/s) less than that of the "interpreted soil profile", the softening effect of equivalent linear analysis can be expected to decrease the correlation of the "measured soil profile" and actually improve the correlation of the "interpreted soil profile" model. No attempt was made to duplicate the results presented in [63] by performing equivalent linear analyses on the "interpreted soil profile" model.

As a final demonstration of time domain analysis, the SCT site was analyzed using true nonlinear site response analysis. The Ramberg-Osgood parameters (α and γ) which control the hysteretic properties of the soil layer elements, were selected to reflect the near linear characteristics of the Mexico City clay. The properties used for the analyses were $\alpha = 0.5$ and $\gamma = 1.4$, which resulted in effective shear stiffness values close to those used in the linear analyses. It should be noted that no attempts were made to "tune" the Ramberg-Osgood parameters to provide a better correlation with the measured results. Figures 2.21 through 2.23 provide comparisons of the response spectra of various computed and measured surface motions, Figure 2.24 shows the surface acceleration history computed from the CUMV EW input motion and Figure 2.25 displays an example of the near linear stress-strain response computed in a typical clay layer. The correlation obtained with nonlinear analysis is quite similar to that obtained using linear analysis, which was expected since the nonlinear properties were selected to reflect near linear response. It should be noted that better correlation between the nonlinear analysis results and the measured results may have been obtained by adjusting the Ramberg-Osgood parameters to better fit the measured data. However, this adjustment was not pursued.

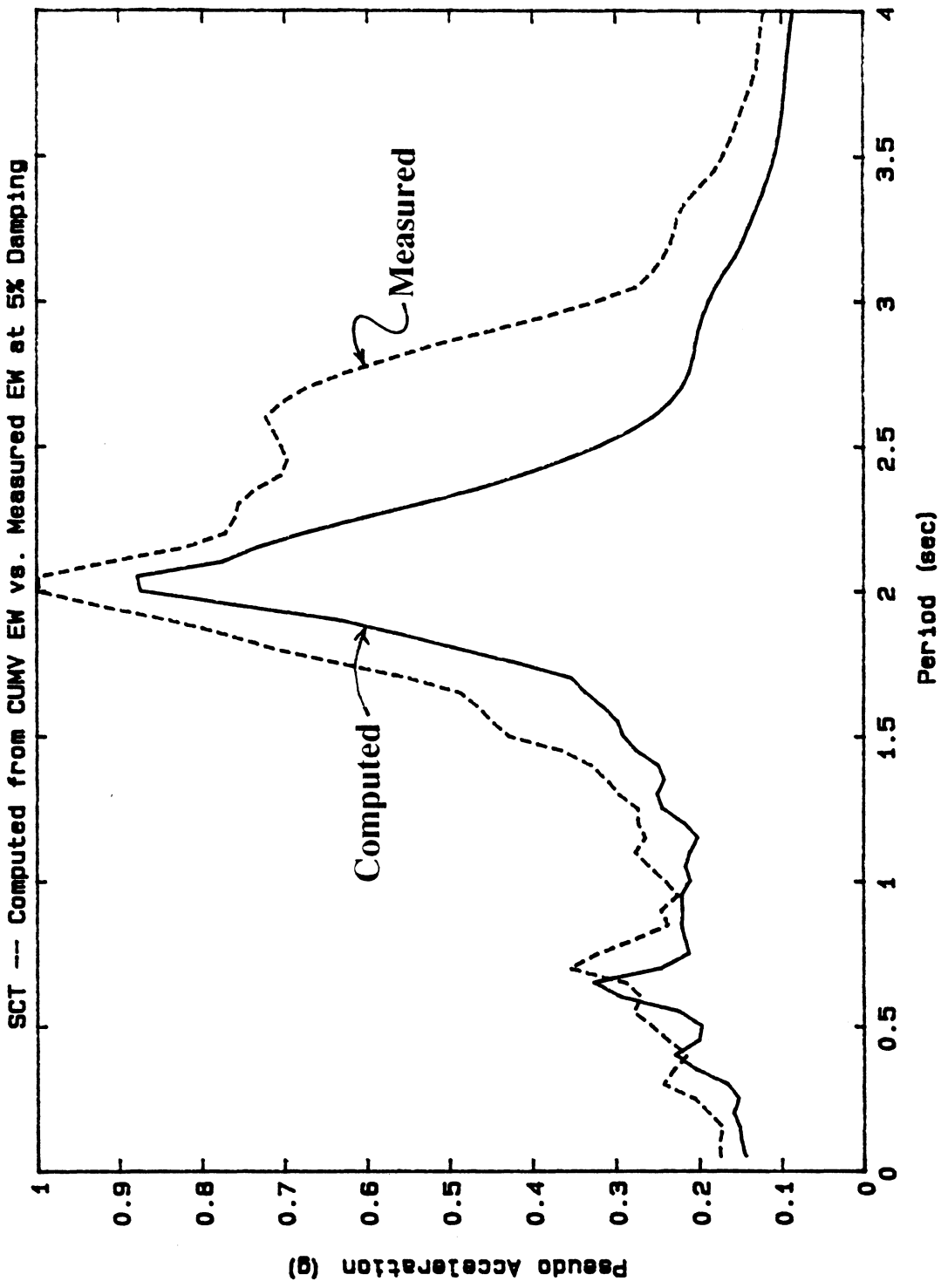

Figure 2.21 Response Spectrum from Nonlinear Analysis vs. Measured

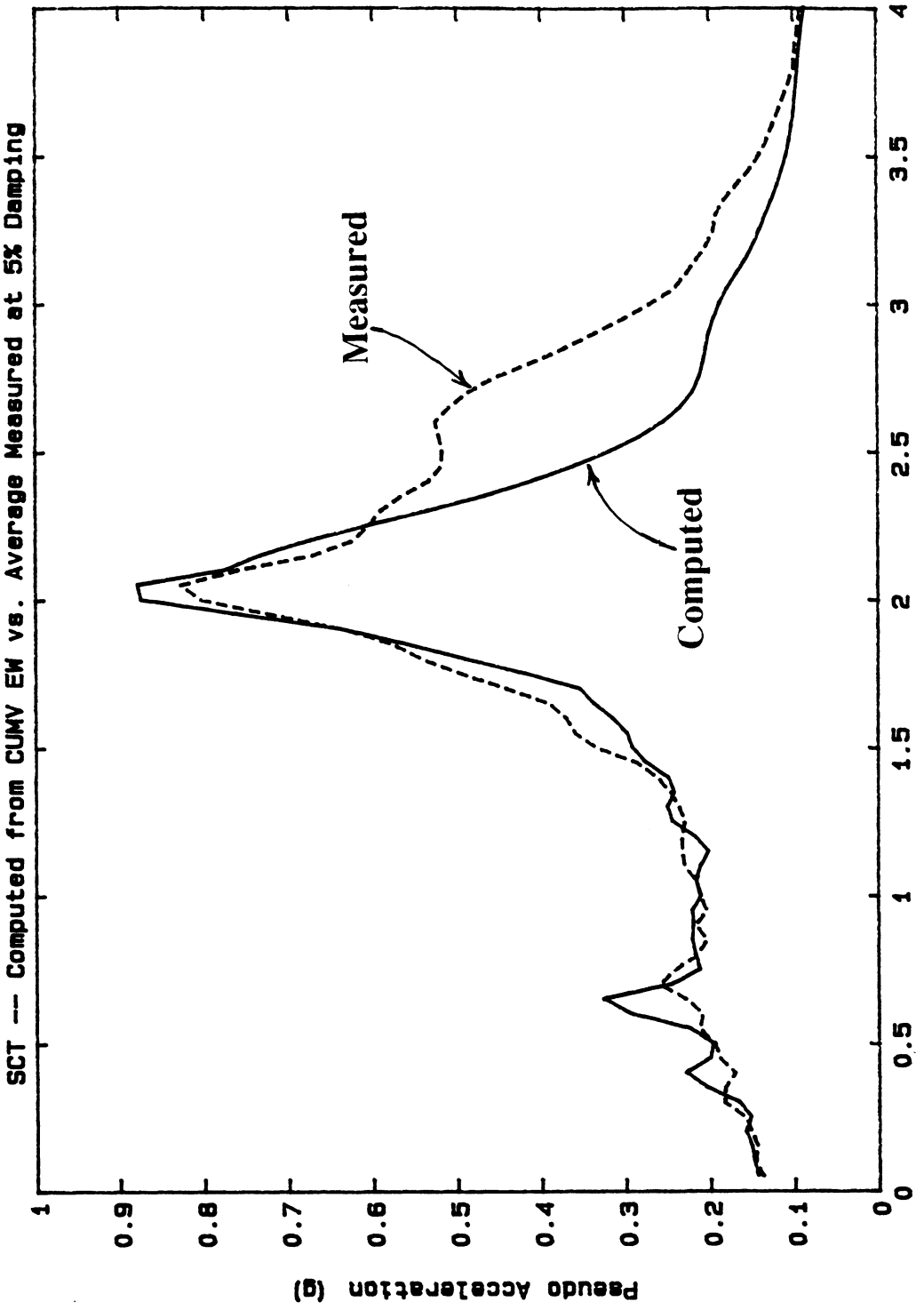

Figure 2.22 Response Spectrum from Nonlinear Analysis vs. Measured

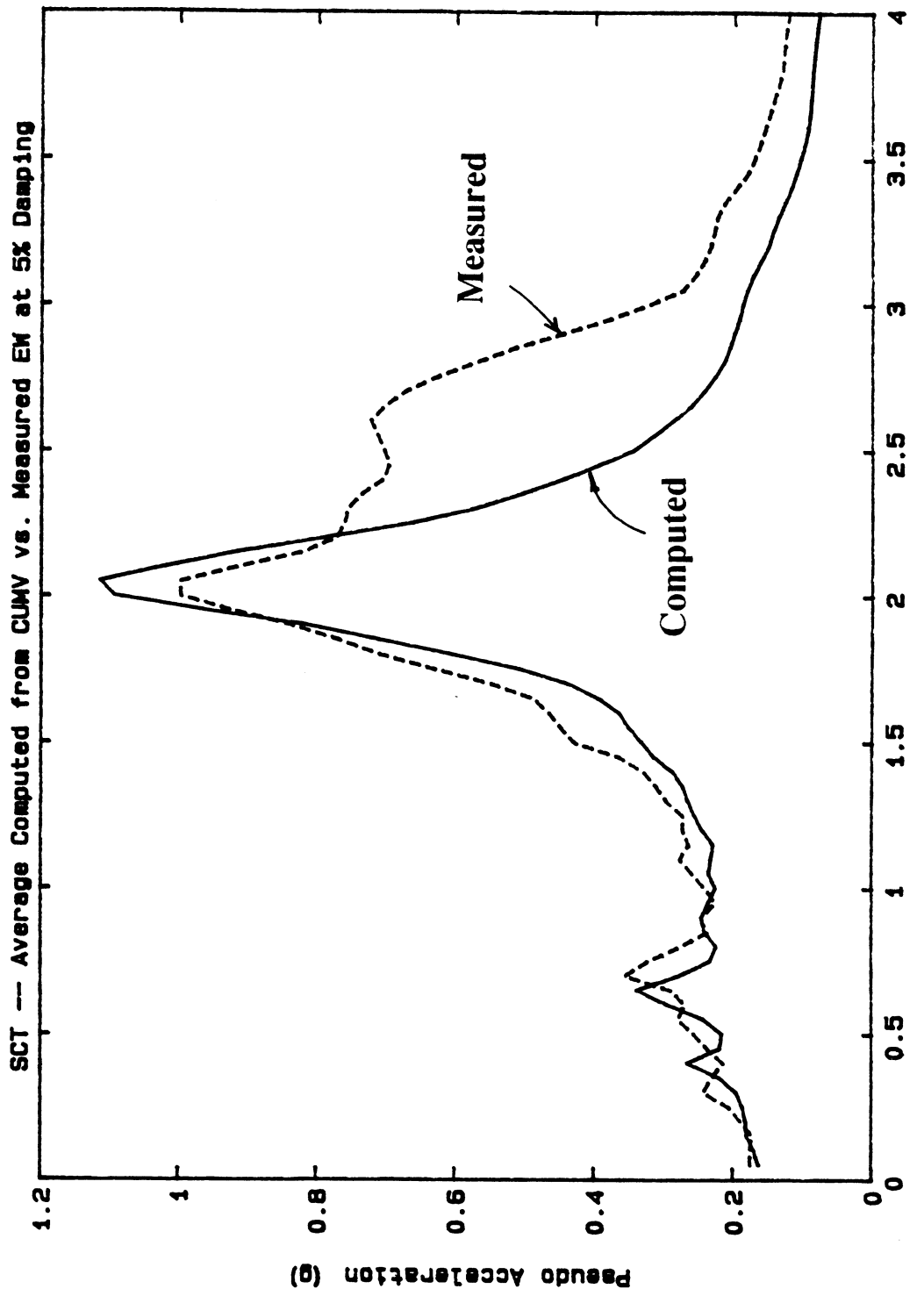

Figure 2.23 Response Spectrum from Nonlinear Analysis vs. Measured

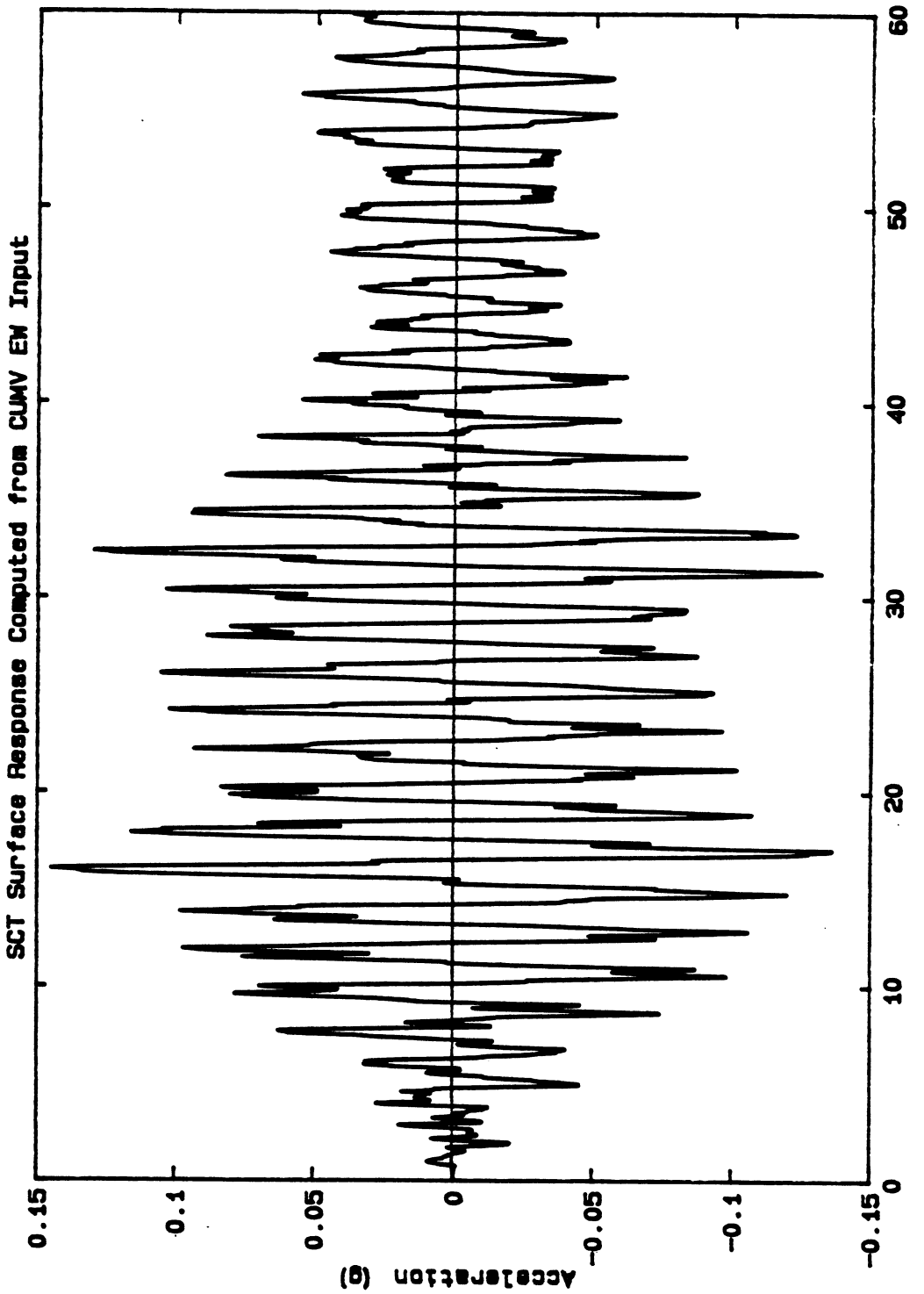

Figure 2.24 Surface Response Computed from Nonlinear Analysis

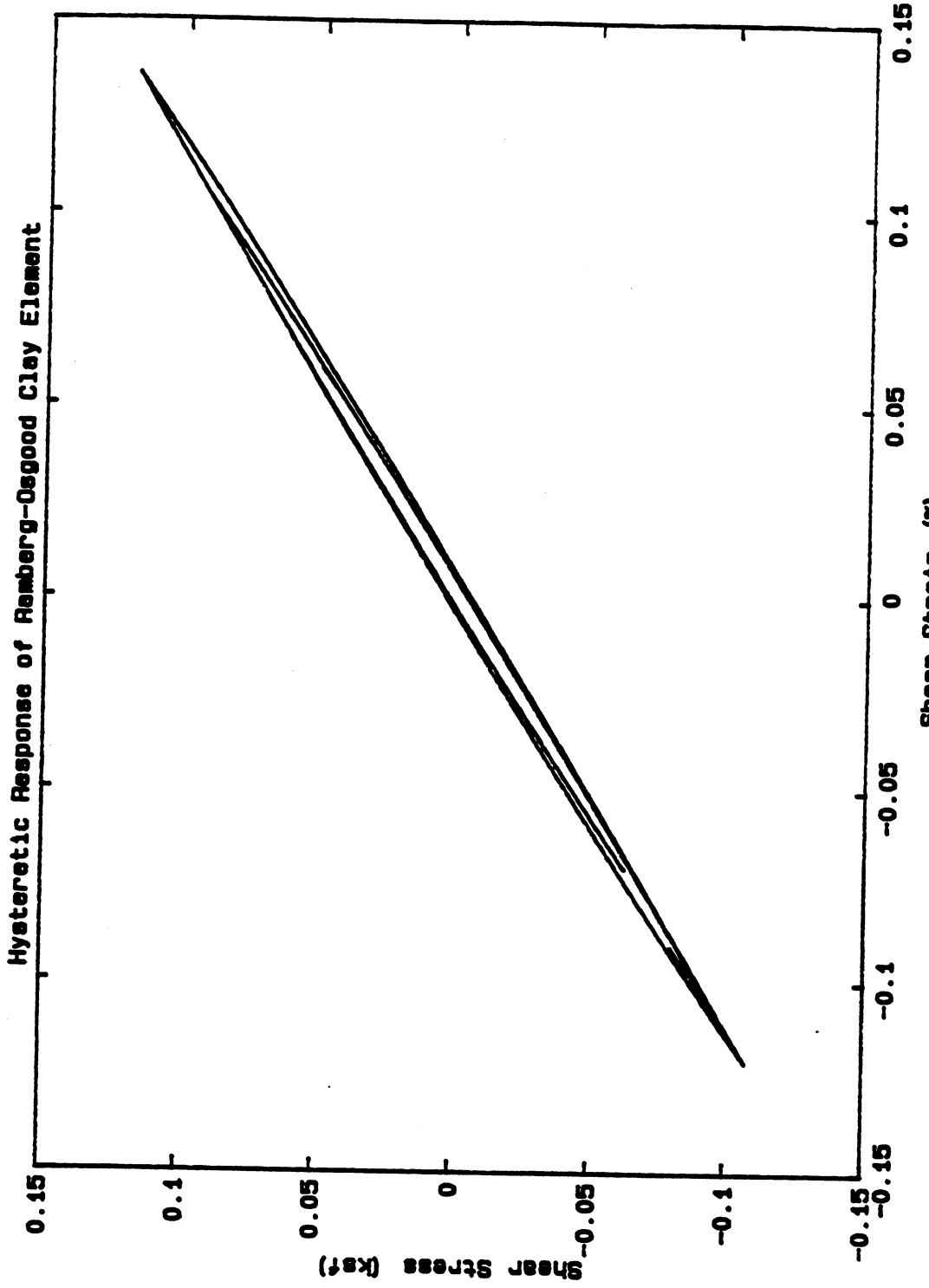

Figure 2.25 Response of Typical Clay Layer from Nonlinear Analysis

CHAPTER 3

BUILDING RESPONSE ANALYSIS

The analysis of structural behavior under seismic loading using rigorous modeling and analysis procedures is an important step in reliable and economical earthquake resistant designs. It is rational, however, from an engineering viewpoint, to carry out an analysis appropriate for the structural system, configuration, size and importance as well as other relevant characteristics of the structure under consideration. One of the keys to effective earthquake resistant design of structures is the use of representative structural models from which the distribution of seismic forces and deformations can be determined. The most general seismic response analysis procedure would consider a three-dimensional representation of the structure subjected to three-dimensional seismic forces. Simpler three-dimensional models which approximate floor systems as rigid diaphragms have been shown to be acceptable for most buildings [14]. For buildings of regular geometry, where no stiffness and mass discontinuities exist, results from the analyses of two-dimensional planar representations can be combined for seismic design. In any case, the result of the structural discretization is a MDOF lumped mass building model which must be analyzed for seismic forces, using either static or dynamic analysis methods. The major advantage of using the forces and deformations obtained from dynamic analysis as a basis for structural design is that their distributions can be significantly different than the distributions obtained from an equivalent static load analysis.

In conventional earthquake response analysis of building structures, it is most common to assume that the building responds as a linear elastic system. The concepts involved with the linear earthquake response analysis of two and three-dimensional structures are well established and well understood and analysis and design procedures based on the assumption of linear response are routinely implemented. The primary disadvantage of linear earthquake response analysis is that it cannot provide any information related to ductility demands and the distribution of damage throughout the structure in the event of

severe earthquake ground motions. In such situations, the response of buildings is influenced, if not dominated by nonlinear behavior. Code designs based on linear response spectra require detailing which will ensure reasonable ductility, essentially providing for damage tolerant structures in the event of strong earthquake ground motions. This reflects the underlying philosophy that codes rely on nonlinear structural behavior as a means to reduce the required elastic strength and to increase the seismic energy dissipation of structural systems. Although sophisticated procedures for the nonlinear earthquake analysis of building structures are available, their application in conventional design practice is somewhat limited and usually implemented only for very important, expensive or complicated structures. The primary reasons for the limited use of nonlinear earthquake response analysis are; 1) it is not required by most building codes, 2) it is more difficult to develop a nonlinear mathematical model than a linear model, 3) it generally requires significantly more computational effort than linear analysis and hence is more expensive, and 4) the results of nonlinear analysis are more difficult to understand and must be carefully interpreted.

Two extremely important considerations in establishing the level of sophistication of the modeling and analysis procedures used for seismic design are; 1) the uncertainties associated with the seismic loading, and 2) the sensitivity of the structural response to variations in the seismic loading. Ideally, structural designs should be evaluated for a wide variety of seismic events, consistent with site-specific seismic hazards. Investigating the sensitivity of the analytical structural response to variations in the seismic input is a critical step in effective earthquake resistant design.

Selecting the appropriate seismic analysis procedure is a difficult task which must consider issues such as the type of structural system and configuration, the cost and importance of the structure, the time involved in developing and analyzing a representative structural model as well as the uncertainties associated with the seismic loading and their effects on the structural response. As a starting point, it is often prudent to a adopt simplified

modeling and analysis procedures which idealize the structure and the dynamic loading to some degree. Simplified procedures which permit rapid and inexpensive analysis of structures with reasonable accuracy can be used to evaluate structural response to a wide variety of earthquake loadings. The simplified evaluation of preliminary designs can serve as a basis for more refined designs, which can then be evaluated using more refined modeling and analysis procedures.

It is clear that an important first step toward the wider use and better understanding of nonlinear dynamic analysis is the implementation of simplified modeling and analysis methodologies which reflect the essential nature of the structural response. In this chapter, a brief overview of conventional linear and nonlinear dynamic analysis procedures is presented. A comparison of the nonlinear response of various MDOF building systems with the nonlinear response of equivalent SDOF representations is then presented for earthquake motions which are idealized as harmonic motions. Finally, methods for evaluating seismic designs based on simplified nonlinear analysis for harmonic ground motions are presented.

3.1. Overview of Conventional Methods

3.1.1. Linear Analysis

The most general form of the equations of motion of a linear, lumped mass, MDOF structural model subjected to earthquake loading is:

$$\mathbf{M}\,\ddot{\mathbf{U}}(t) + \mathbf{C}\,\dot{\mathbf{U}}(t) + \mathbf{K}\,\mathbf{U}(t) = \mathbf{R}(t) \qquad (3.1)$$

where the terms on the left hand side are the finite element property matrices and state vectors of the structural model similar to those defined in Chapter 2 for soil profile models. The finite element property matrices, which are developed using direct stiffness assembly procedures, are often reduced in size using static condensation procedures [5] so that only the essential dynamic DOF's are considered in the dynamic equilibrium equations. Typically, the three-dimensional dynamic properties of a building can be accurately represented

by models with two horizontal translational DOF and a rotational DOF about the vertical axis for each story level. The right hand side of the equation represents the earthquake load vector which, in general, may include three components of base translation as well as the effects of different ground motions at different supports [11]. For typical building systems, the effects of multiple support excitation can usually be neglected and the earthquake load vector can be expressed as:

$$\mathbf{R}(t) = -\mathbf{M} \begin{bmatrix} r_x & r_y & r_z \end{bmatrix} \begin{bmatrix} \ddot{u}_{gx}(t) \\ \ddot{u}_{gy}(t) \\ \ddot{u}_{gz}(t) \end{bmatrix} \tag{3.2}$$

or

$$\mathbf{R}(t) = -\mathbf{M}\, \mathbf{r}\, \ddot{u}_g(t) \tag{3.3}$$

where :

$\mathbf{M}$ = lumped mass matrix of the MDOF system

r_x = static displacement influence vector for the x direction

r_y = static displacement influence vector for the y direction

r_z = static displacement influence vector for the z direction

$\ddot{u}_{gx}(t)$ = base acceleration in the x direction

$\ddot{u}_{gy}(t)$ = base acceleration in the y direction

$\ddot{u}_{gz}(t)$ = base acceleration in the z direction

$$\mathbf{r} = \begin{bmatrix} r_x & r_y & r_z \end{bmatrix}$$

$$\ddot{u}_g(t) = \begin{bmatrix} \ddot{u}_{gx}(t) \\ \ddot{u}_{gy}(t) \\ \ddot{u}_{gz}(t) \end{bmatrix}$$

As developed in [11], the static displacement influence vectors represent the structural displacements resulting from unit support displacements in the x, y and z directions.

The solution of this system of ordinary differential equations can be obtained by direct integration to obtain a response history. The time history of the structural response

can also be obtained using mode superposition analysis. If only the response maxima are required, response spectrum modal analysis can be implemented. The following sections review direct integration, mode superposition and response spectrum analysis procedures.

3.1.1.1. Direct Integration of MDOF Equations of Motion

The dynamic equilibrium equations of the linear MDOF structural model can be integrated numerically using standard procedures to obtain the response history of the system. The response histories of structural displacement, velocity and acceleration as well as base shear, overturning moment and member forces can be used to evaluate the seismic design. One of the most versatile numerical integration schemes is the Newmark β method [47] with modifications by Wilson [5]. The details of this step-by-step algorithm are presented in [74]. The only difference between the direct integration of the equilibrium equations of MDOF structural models and the one-dimensional soil profile models (presented in detail in Chapter 2) is the need for an equation solution algorithm which allows for a general banded system of equations.

3.1.1.2. Mode Superposition and Response Spectrum Analysis

The mode superposition method of dynamic analysis is based on formal coordinate transformations which serve to change the set of N coupled equations of motion of a MDOF system into a system of N uncoupled SDOF equations. The transformation is typically accomplished using the exact mode shapes of the structural system but more efficient transformations using Ritz vectors [37] can also be implemented. Details regarding coordinate transformations using vibration mode shapes or derived Ritz vectors can be found in many references [6,25,37] and are not presented here.

The geometric coordinates of the finite element system $\mathbf{U}$ are related to the modal coordinates $\mathbf{Y}$ through the transformation matrix Φ as follows:

$$\mathbf{U} = \Phi \mathbf{Y} \tag{3.4}$$

The result of the transformation is a system of N uncoupled SDOF equilibrium equations:

$$M_n\ddot{Y}_n(t) + C_n\dot{Y}_n(t) + K_nY_n(t) = P_n(t) \tag{3.5}$$

where M_n, C_n, and K_n are the generalized mass, damping and stiffness of the nth mode, $\ddot{Y}_n(t)$, $\dot{Y}_n(t)$ and $Y_n(t)$ are the modal acceleration, velocity and displacement of the nth mode and $P_n(t)$ is the generalized load for the nth mode:

$$P_n(t) = \Phi_n^T \mathbf{R}(t) \tag{3.6}$$

These N independent equations of motion can be solved by any suitable method. Once the response for each mode $Y_n(t)$ has been computed, the displacement in the original coordinates is obtained by superposition:

$$\mathbf{U}(t) = \Phi\, \mathbf{Y}(t) \tag{3.7}$$

$$\mathbf{U}(t) = \Phi_1 Y_1(t) + \ldots. + \Phi_N Y_N(t) \tag{3.8}$$

The primary advantage of using mode superposition analysis to calculate the earthquake response of structures is that the ground motions tend to strongly excite only the lower modes of structural vibration. Hence, reasonable approximations of the response of MDOF systems can be obtained by only carrying out the analysis for modes which significantly participate in the response. As developed in [11], the earthquake excitation factor L_n provides a measure of the relative participation of each mode Φ_n in the earthquake response:

$$L_n = \Phi_n^T \mathbf{M}\, \mathbf{r} \tag{3.9}$$

In most design applications, only the extreme values of the structural response are required. In such cases, earthquake response spectrum analysis is an attractive procedure for determining the magnitude and distribution of seismic forces. Each point of an earthquake response spectrum represents a response maximum from a complete time history analysis for a given structural vibration frequency and damping ratio. Hence, the earthquake response maxima for each vibration mode can be determined directly from the response spectrum. However, because all modal maxima do not occur simultaneously, they are typically combined using SRSS or CQC [75] modal combination procedures. In this fashion, the magnitude and distribution of maximum seismic forces and deformations can

be estimated for elastic seismic design.

3.1.2. Nonlinear Analysis

Under severe earthquake ground motions, the response of buildings may be influenced, if not dominated by nonlinear behavior. Thus, to estimate the dynamic response of a structure subjected to a severe earthquake, a nonlinear dynamic response analysis is necessary. The dynamic equilibrium equation for a nonlinear, lumped mass, MDOF structural model subjected to earthquake loading is:

$$\mathbf{M}\,\ddot{\mathbf{U}}(t) + \mathbf{C}\,\dot{\mathbf{U}}(t) + \mathbf{R_S}(\mathbf{U}) = \mathbf{R}(t) \tag{3.10}$$

The only difference between this equation and the equation for linear systems is in the third term on the left hand side. For finite element systems whose elements can have nonlinear force-deformation relationships, the stiffness matrix becomes a function of the time varying nodal displacements and the element force-deformation relationships, i.e. $\mathbf{K}=\mathbf{K}(\mathbf{U})$. Hence, for nonlinear systems, the vector of static resisting forces must be determined indirectly from the nodal displacements and the element force-deformation relationships:

$$\mathbf{R_S} = \mathbf{R_S}(\mathbf{U}) \tag{3.11}$$

The solution of the system of ordinary differential equations for nonlinear systems is typically obtained using direct integration methods which account for nonlinear behavior. Approximate solutions can be obtained by transforming the MDOF nonlinear system to an equivalent SDOF system and implementing numerical integration or nonlinear response spectrum methods. The following sections review procedures for direct numerical integration of the nonlinear equations of motion and procedures for obtaining approximate solutions by transforming the MDOF system to an equivalent SDOF system.

3.1.2.1. Direct Integration of MDOF Equations of Motion

The dynamic equilibrium equations of the nonlinear MDOF structural system can be integrated using various numerical solution strategies. The nonlinear solution strategies

presented for one-dimensional soil profile models in Chapter 2 can be applied to MDOF structural models by utilizing a general banded equation solver. Various nonlinear analysis programs [1,17,19,45] perform direct numerical integration of the equilibrium equations of two-dimensional and three-dimensional structural models using various numerical solution strategies. Techniques such as Newton iteration [64] or event-to-event methods [18] have been developed to deal with the loss of equilibrium which may develop as a result of structural state changes during the numerical integration of the dynamic equilibrium equations. Methods which implement a variable integration time step size have also been developed and implemented in [2], which also provides an excellent overview of numerical integration schemes for nonlinear dynamic response analysis.

3.1.2.2. MDOF to SDOF Reduction Methods

Although the concepts of coordinate reduction from MDOF to SDOF systems are usually applied to linear elastic systems, a good deal of research has been conducted on SDOF representations of MDOF systems for use in nonlinear response analysis [8,35,55,56,57,58]. The essential feature of coordinate reduction techniques using either the exact mode shapes or load dependent Ritz vectors, is that the vibration of the MDOF system is dominated by a few vibration shapes, and in most cases, sufficient accuracy can be obtained using only one vibration shape. Under large amplitude dynamic loading, yielding of the structure and subsequent stiffness changes make it intuitively obvious that the vibration shape of the structure is not constant throughout the duration of the excitation. However, results from the static nonlinear analysis of structures designed with the strong column - weak beam philosophy indicate that variations of the deflected shape at deformation levels beyond some effective yield of the structure are not significant. Based on this observation, it is plausible to employ an average effective shape which can capture the essential nature of the nonlinear response of building structures.

Procedures for MDOF to SDOF reductions for use in nonlinear analysis have been developed [8] and implemented for the earthquake response analysis of building structures

[35,55,56,57,58]. Several procedures for obtaining the vibration shape for SDOF nonlinear earthquake response analysis of buildings are presented in Appendix D.

Once the vibration shape is established, the equations of dynamic equilibrium for the MDOF system can be transformed to a single equilibrium equation. Consider the equilibrium of the undamped linear MDOF system:

$$\mathbf{M}\,\ddot{\mathbf{U}}(t) + \mathbf{K}\,\mathbf{U}(t) = \mathbf{R}(t) \tag{3.12}$$

Making the substitution $\mathbf{U} = \Phi\,\mathbf{x}$ and premultiplying the equations by $\Phi^{\mathbf{T}}$ leads to the following SDOF equation:

$$\Phi^{\mathbf{T}}\mathbf{M}\,\Phi\,\ddot{\mathbf{x}}(t) + \Phi^{\mathbf{T}}\mathbf{K}\,\Phi\,\mathbf{x}(t) = \Phi^{\mathbf{T}}\mathbf{R}(t) \tag{3.13}$$

The SDOF analogy corresponding to this transformation is shown in Figure 3.1. This SDOF system can be interpreted as a "macro element" used to model the displacement response of the structure. It is most convenient to select the SDOF system such that the deflection x, of the equivalent mass $\Phi^{\mathbf{T}}\mathbf{M}\Phi$, is the same as that of some significant point (for example, the roof level) of the MDOF system. The significant point is hereafter termed the control point. The equilibrium equation of the SDOF system can be presented as follows [56]:

$$\alpha_m\, m_t\, \ddot{x}(t) + \alpha_l k\, x(t) = \alpha_l r_t(t) \tag{3.14}$$

where;

$$m_t = \sum_{i=1}^{\#DOF} m_i \tag{3.15}$$

$$r_t = \sum_{i=1}^{\#DOF} r_i \tag{3.16}$$

$$\alpha_m = \frac{(\Phi^{\mathbf{T}}\mathbf{M}\Phi)}{m_t} \tag{3.17}$$

$$\alpha_l = \frac{(\Phi^{\mathbf{T}}\mathbf{R})}{r_t} \tag{3.18}$$

The terms m_i and r_i are the mass and external load associated with DOF "i" and hence the term m_t is the total mass of the MDOF system and r_t is the total external load acting on the MDOF system. The terms α_m and α_l are the mass and load factors, respectively. The

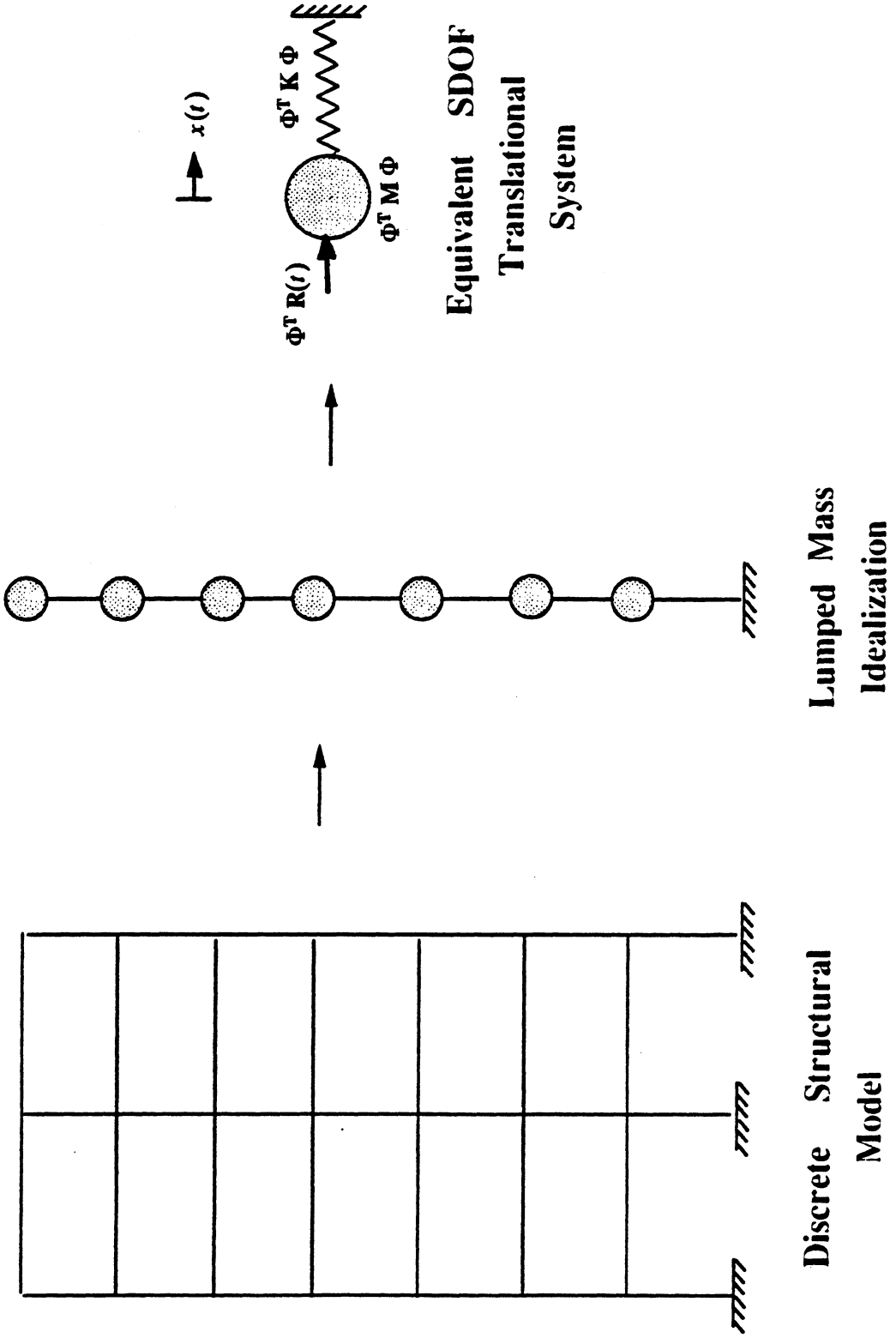

Figure 3.1 Structural Representations

scalar stiffness k, is numerically equal to the total load from a given static load distribution which would cause a unit deflection at the control point of the MDOF system, ie;

$$k\,1 \equiv r_t \tag{3.19}$$

The equation is verified by observing that:

$$\Phi^T M \Phi = \alpha_m m_t \tag{3.20}$$

$$\Phi^T R = \alpha_1 r_t \tag{3.21}$$

$$\Phi^T K \Phi = \alpha_1 k \tag{3.22}$$

$$= \Phi^T R \frac{k}{r_t}$$

$$= \Phi^T R$$

The equation can be rearranged to the following form:

$$m_e \ddot{x}(t) + kx(t) = r_t(t) \tag{3.23}$$

where $m_e = (\frac{\alpha_m}{\alpha_1})\, m_t$, is the equivalent mass of the system. It is important to observe that for earthquake loading, the external force term is defined as:

$$r_t(t) = -m_t \ddot{u}_g(t) \tag{3.24}$$

where $\ddot{u}_g(t)$ is the base acceleration.

In order to use a more physical SDOF analogy than the one shown in Figure 3.1, it is desirable to transform to the inverted pendulum oscillator shown in Figure 3.2. The equivalent height of the pendulum oscillator h_e (the height of control point of the MDOF system) is obtained by simultaneously considering the equilibrium of the MDOF and equivalent SDOF systems under free-vibration conditions. If the amplitude of the vibration shape Φ, at the location h_e is denoted Φ_e, the SDOF and MDOF expressions for base shear due to inertial forces are proportional to the following expressions:

$$m_e \Phi_e = \sum_{i=1}^{\#DOF} m_i \Phi_i \tag{3.25}$$

The base moments due to inertia forces for the SDOF and MDOF systems must also be equal and proportional to the following expressions:

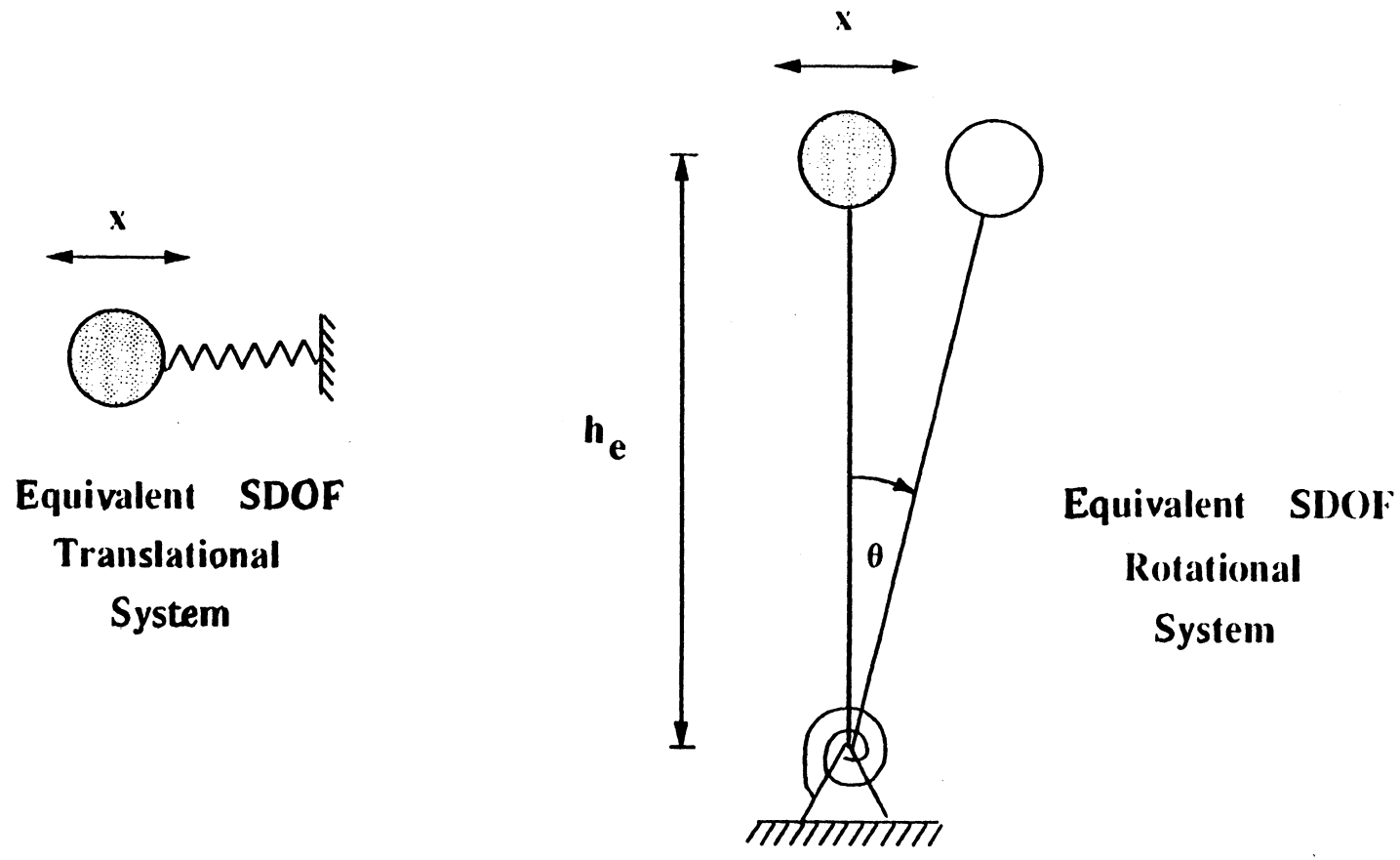

Figure 3.2 Equivalent Translational and Rotational SDOF Representations

$$m_e \Phi_e h_e = \sum_{i=1}^{\#DOF} m_i \Phi_i h_i \tag{3.26}$$

where h_i is the height of story level i. Combining these equilibrium expressions leads to the following expression for the equivalent height:

$$h_e = \frac{\left(\sum_{i=1}^{\#DOF} m_i \Phi_i h_i \right)}{(m_e \Phi_e)}$$

$$= \frac{\left(\sum_{i=1}^{\#DOF} m_i \Phi_i h_i \right)}{\left(\sum_{i=1}^{\#DOF} m_i \Phi_i \right)} \tag{3.27}$$

Transformation from a translational system in x to a rotational system in θ is accomplished by substituting $x = \theta\, h_e$ and summing moments about the base, resulting in:

$$(m_e h_e^2)\, \ddot{\theta}(t) + (k h_e^2)\, \theta(t) = r_t(t)\, h_e \tag{3.28}$$

which, for convenience, can be rewritten as:

$$M\ddot{\theta}(t) + K\theta(t) = R(t) \tag{3.29}$$

In this expression, the term $K\theta(t)$ represents the structural resistance in terms of base moment versus rotation. For nonlinear systems, this term is replaced by a static resistance term $R_S(\theta)$ which represents the restoring force of the oscillator in terms of base moment.

The simplest model for representing the nonlinear base moment resistance of the system is a bilinear spring. A bilinear approximation to a base moment verses lateral deflection curve (similar to those obtained using the procedures in Appendix D) is illustrated in Figure 3.3. This figure indicates the displacement levels (x_1, x_2 and x_4) at which structural elements 1, 2 and 4 yield as well as the yielding displacement (x_y) assumed for the bilinear resistance approximation. The ductility of the SDOF oscillator system ($\mu_{SDOF} = x_{max} / x_y$) can be related to the element ductilities ($\mu_{element\ i} = x_{max} / x_i$) using the following ductility transformation:

$$\mu_{element\ i} = \rho_i\, \mu_{SDOF} \tag{3.30}$$

where $\rho_i = x_y / x_i$. Thus, the ductilities of specified elements in the model can be estimated

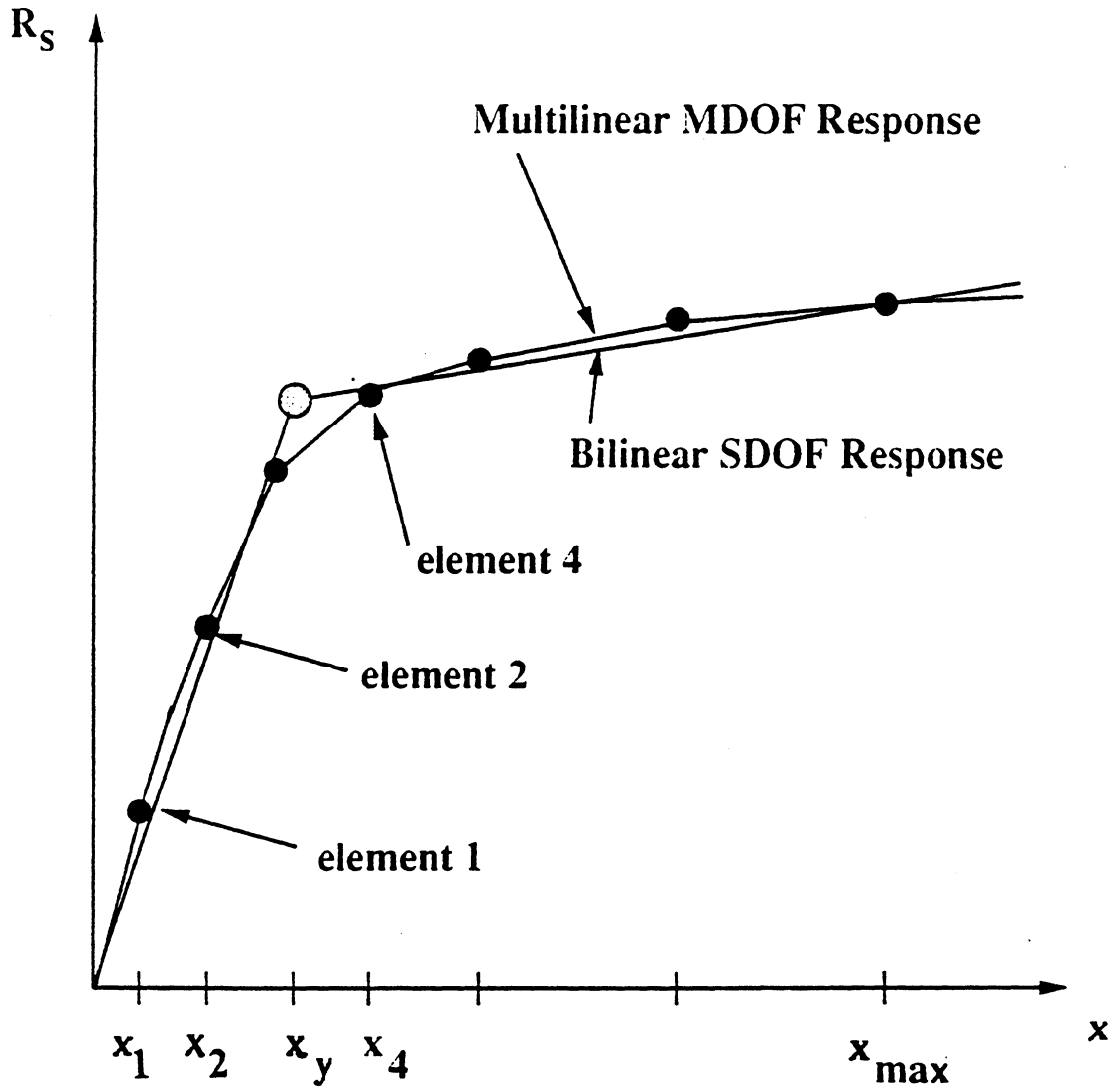

Figure 3.3 Schematic of MDOF and SDOF Base Moment Response

from the SDOF ductility through the following matrix transformation:

$$\mu_{elements} = \rho\, \mu_{SDOF} \tag{3.31}$$

It should be noted that damping can be included in the equivalent SDOF nonlinear system by adding a rotational viscous damper which resists the angular velocity of the inverted pendulum system. The rotational equilibrium of the damped oscillator can now be expressed as:

$$M\ddot{\theta}(t) + C\dot{\theta}(t) + R_S(\theta) = R(t) \tag{3.32}$$

3.1.2.3. Integration of SDOF Equation

The equilibrium equation for a viscously damped SDOF nonlinear system can be expressed in the general form:

$$M\ddot{x}(t) + C\dot{x}(t) + R_S(x) = R(t) \tag{3.33}$$

where M is the mass of the system, C is the system's damping coefficient, R_S is its restoring force, R(t) is the external dynamic load and x(t) is the system displacement coordinate.

The response history can be obtained by numerically integrating the equation of motion using small time steps. In general, any of the standard numerical integration strategies that satisfy equilibrium at discrete time intervals and account for changes in the stiffness within the time steps can provide an accurate solution. Newton and quasi-Newton [64] or event-to-event strategies [18] have been developed to correct for the loss of equilibrium which may result during each time step. Chapter 2 presents nonlinear solution strategies developed for the CAA method (Newmark method with $\beta = 1/4$) which can be applied to the solution of the SDOF equilibrium equation. NONSPEC [44] is a computer program which obtains the solution for the nonlinear SDOF system subjected to arbitrary loading using the Linear Acceleration Method (Newmark method with $\beta = 1/6$) and provides for time step repetition and/or equilibrium correction to account for nonlinearity.

Once the response x(t) of the SDOF system is obtained, the approximate response of the MDOF system can be obtained by the following transformation:

$$U(t) = \Phi\, x(t) \tag{3.34}$$

The response U(t) of the MDOF system obtained in such a fashion is subject to the assumptions involved in the transformation from a MDOF system to an equivalent SDOF system and thus, must be interpreted carefully.

3.1.2.4. Nonlinear Response Spectra

When it is feasible to represent MDOF structures as equivalent SDOF systems, nonlinear response spectrum analysis procedures can provide useful guidance in selecting the overall stiffness and strength characteristics of the system. Moreover, a variety of nonlinear response spectra can easily be investigated and used to assess the sensitivity of the overall response of a proposed structure to different excitations.

As discussed in [43], nonlinear response spectra are constructed by either; a) directly computing a sequence of response histories of nonlinear SDOF systems of varying elastic period subjected to a given excitation and extracting the maximum response values, b) implementing random vibration theory to estimate the inelastic response in probabilistic terms, or c) modifying smoothed linear elastic response spectra developed for a site. Method a) provides the most accurate assessment of inelastic response maxima and is attractive since it can be implemented for various hysteretic systems [44]. However, it should be noted that methods a) and b) require significant computational effort, while method c) is relatively simple. Because of the technical and practical difficulties associated with methods a) and b), method c) is the most widely used method for obtaining inelastic response spectra.

Procedures have been developed to obtain approximate seismic design forces for multi-story structures based on elastic SRSS modal superposition techniques using the elastic dynamic characteristics of the structure and an inelastic response spectrum. Typically however, inelastic earthquake response spectra are used in conjunction with the elastic fundamental vibration frequency of the structure to obtain estimates of ductility demands for the purposes of evaluating or developing preliminary designs.

3.2. Response of MDOF and SDOF Systems to Harmonic Ground Motions

3.2.1. General Considerations and Objectives

The complex, random nature of earthquake ground motions represents a major source of uncertainty in the analysis and design of structures for seismic loading. The lack of a specific "design earthquake" for response analysis often results in the use of ensemble of design earthquakes compatible with a site specific response spectrum. As presented in [50], the computed inelastic response of buildings subjected to an ensemble of similar earthquake ground motions can vary greatly from one motion to the next. Clearly, the use of deterministic seismic analysis to investigate the effects of probabilistic earthquake loading is a complex task requiring significant experience and engineering judgement.

For preliminary design purposes, it may be possible to employ some simplifying assumptions regarding the nature of the seismic loading. In qualitative terms, real earthquake ground motions can be classified somewhere between "impulsive type" motions consisting of one or a few strong acceleration pulses and "harmonic type" motions consisting of several cycles of similar acceleration pulses. "Harmonic type" ground motions are characteristic of soft soil sites where the response to bedrock motions tends to be dominated by the fundamental vibration mode of the soil profile. A portion of the acceleration history recorded at the SCT site (a soft clay site in downtown Mexico City) during the 1985 earthquake (Figure 3.4) provides an excellent example of essentially harmonic site response. For buildings founded on such soft soil sites, it can be argued that a pure harmonic seismic loading can be used to obtain upper bounds on the cyclic response demands placed on the structure during "harmonic type" site response. Assuming that the earthquake ground motions are harmonic is clearly a very simplistic approach which neglects the complex evolutionary character of the amplitude and frequency observed in typical earthquake histories. However, it is an attractive simplification since it allows an earthquake loading to be completely defined by only two parameters; the acceleration amplitude A_g, and the vibration period T_g;

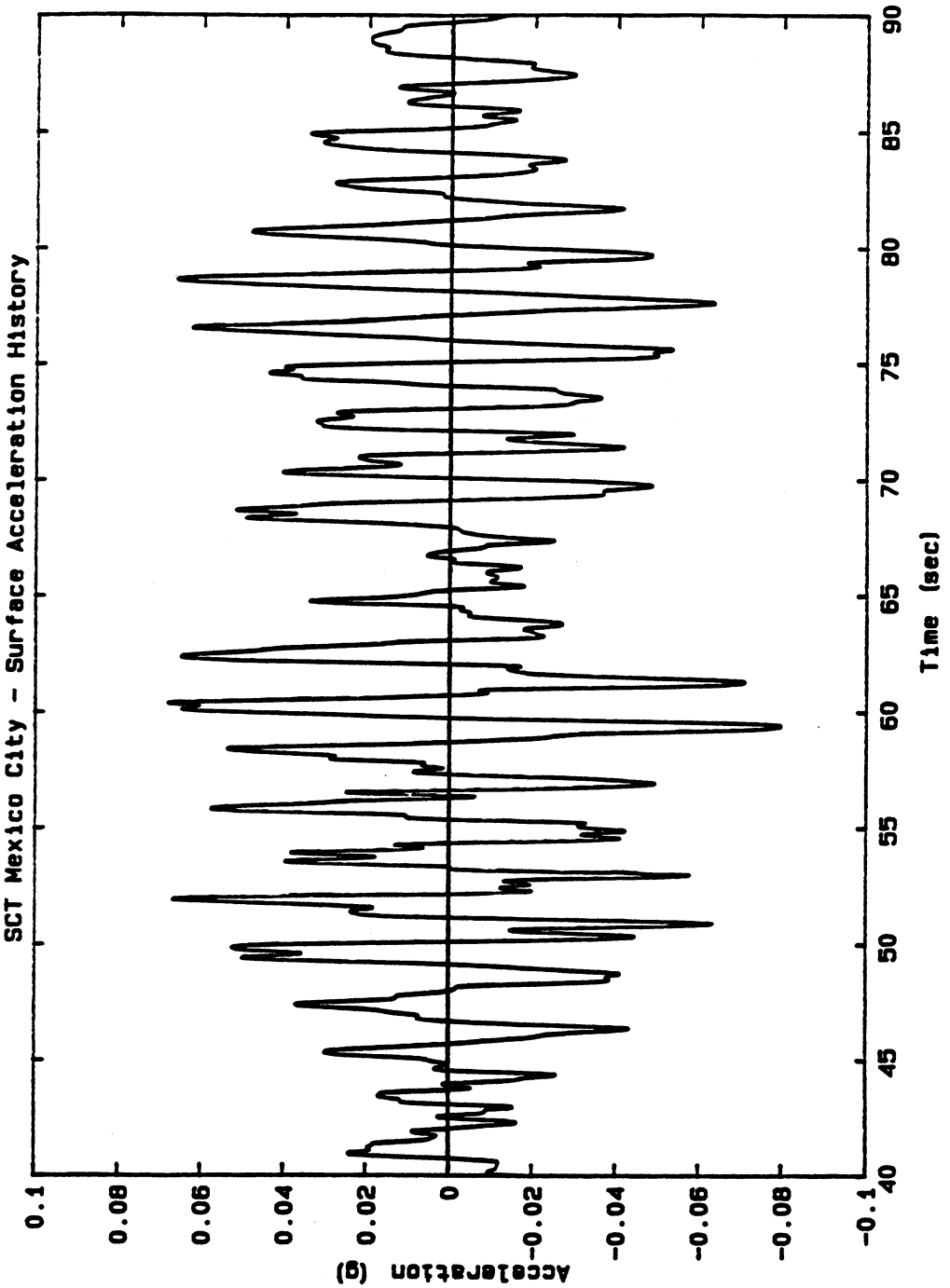

Figure 3.4 Near Harmonic Site Response

$$\mathbf{R}(t) = -\mathbf{M}\,\mathbf{r}\,\ddot{u}_g(t) = -\mathbf{M}\,\mathbf{r}\,A_g \sin\left(\frac{2\pi}{T_g}\,t\right) \tag{3.35}$$

For linear structural systems or for non-degrading nonlinear structural systems, the response obtained from harmonic earthquake input eventually reaches a steady-state with a vibration period equal to the ground motion period [11,32]. This implies that the response of the MDOF structural representation (including the phase angle, the displacement response, the energy dissipation response and the base shear and overturning moment responses) is entirely contained in a single steady-state cycle of structural response.

The elementary nature of the harmonic earthquake loading and the existence of a steady-state response imply that approximate analysis methods may be applied to obtain more efficient solutions. By applying formal coordinate reduction procedures, the MDOF structural model can be represented by an equivalent SDOF system which can be analyzed for harmonic earthquake loading with a fraction of the computations required for the MDOF system. SDOF procedures permit rapid and inexpensive analysis and re-analysis of a sequence of preliminary designs subjected to a wide range of ground motion amplitudes and frequencies. The results of these analyses can serve as the basis for more refined designs to be evaluated using more refined modeling and analysis procedures.

In this section, the response of MDOF and SDOF structural systems subjected to harmonic earthquake loading is investigated. The procedures are applicable to the analysis for preliminary design of buildings founded on soft soil sites for which the ground surface motions are essentially harmonic. The correlation between the steady-state response of MDOF structural models and their equivalent SDOF representations can be used to reduce the number of MDOF dynamic analyses required to assess the sensitivity of the structure to a range of harmonic ground motions. For the special case of harmonic loading, it may be possible to replace MDOF dynamic analysis with MDOF static and SDOF dynamic analyses.

3.2.2. Application to Two-Dimensional Frame System

In order to examine the applicability of equivalent SDOF structural models for representing the steady-state response of MDOF structural models, a very simple two-dimensional moment resisting frame system was investigated. As shown in Figure 3.5, the system considered was a ten story, one bay steel frame.

It was assumed that the frame, which has a fundamental elastic vibration period T_s = 1.25 sec, was located on a soft soil site with a nearly coincident natural site period (T_g) representing worst case, resonant vibration conditions between the site and the structure. Harmonic ground motion periods of 0.75, 1.25 and 1.75 seconds, corresponding to a frequency ratio ($\beta = \omega_g/\omega_s = T_s/T_g$) range from roughly 0.72 to 1.67, were considered. The frequency ratio β is commonly used to examine the steady-state response of systems subjected to harmonic loading. Harmonic acceleration amplitudes (A_g) of 0.02g, 0.11g and 0.20g were considered. This range of harmonic ground motion parameters can be displayed in the $T_g - A_g$ plane as shown in Figure 3.6. Each point in this plane defines a harmonic ground motion, and a series or "sweep" of harmonic earthquake analyses, performed at a grid of these points can be used to assess the sensitivity of the structure to harmonic ground motions. It should be noted that the maxima of various structural response parameters can be plotted above the grid points in the $T_g - A_g$ plane resulting in a three-dimensional spectral surface.

The instantaneous application of large amplitude harmonic ground motions to an inelastic structural model can result in a bias in the steady-state displacement response of the system. The bias is caused by plastic deformations in structural elements producing a tilt in the frame as a result of the sudden application of the load with initial vibration conditions which do not correspond to the steady-state conditions. In order to eliminate the bias from the computed steady state displacement response, the harmonic ground acceleration was increased gradually over the first several vibration cycles to the maximum amplitude, A_g. Analyses conducted at each of the grid points generally indicated that the use of five

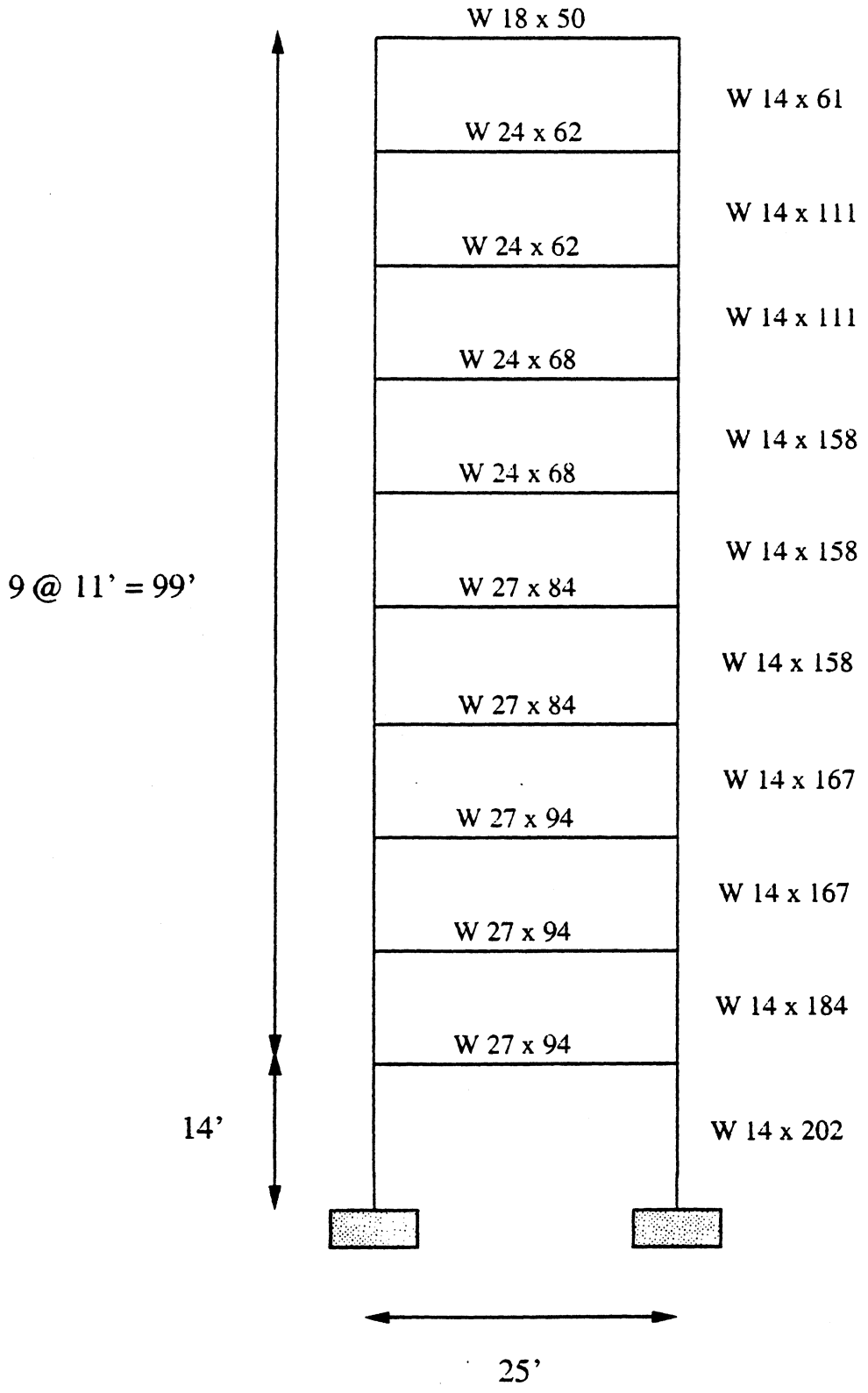

Figure 3.5 Two-Dimensional Frame System

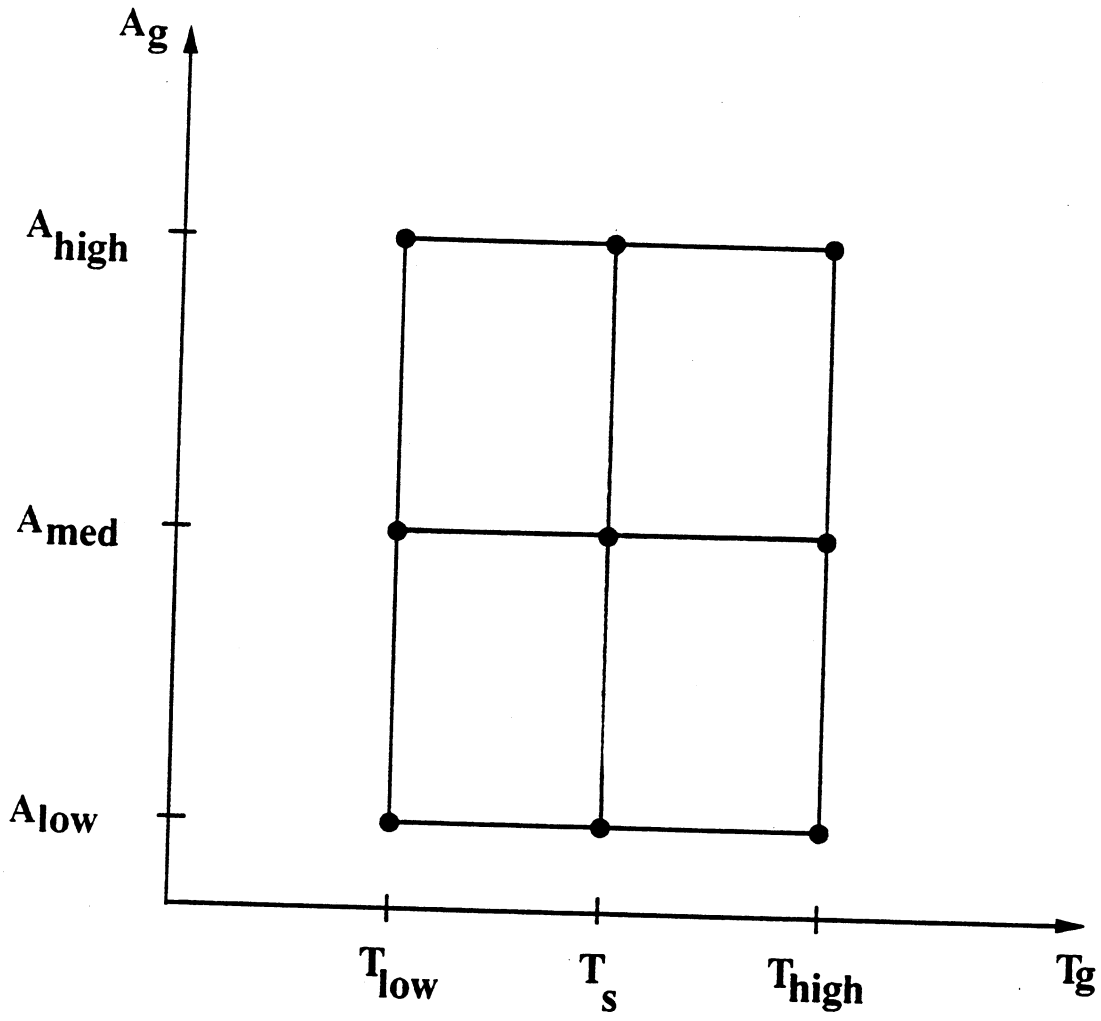

Figure 3.6 The T_g - A_g Plane

or six build-up cycles was sufficient to eliminate the bias tendencies. A build-up harmonic wave form used in the analyses is illustrated in Figure 3.7.

A steady-state is obtained when the response of the system for one vibration cycle becomes essentially indistinguishable from that of the previous cycle. The analyses indicated that in general, a stable steady-state response is obtained after only a few vibration cycles at the maximum load amplitude.

3.2.2.1. MDOF Response

Inelastic dynamic analyses were conducted on the ten story frame utilizing the program DRAIN-2DX [1]. Equilibrium was maintained in the MDOF structural model by implementing an event-to-event analysis procedure [2]. The following assumptions were employed in the analyses:

a) The structure was idealized as an assemblage of two-dimensional beam-column elements, capable of yielding only at plastic hinges at the element ends.

b) Beam axial deformations and all shear deformations were neglected.

c) Axial force - bending moment interaction was considered in all column members.

d) 50 kip story weights and a 30 kip roof weight were assumed.

e) P-Δ effects were accounted for by using the geometric stiffness associated with a two-dimensional truss element.

f) 1.0 % strain hardening in steel was assumed (E=30000 ksi).

g) 5.0 % of critical damping was assumed for dynamic response analysis.

h) Lumped static gravity loads were applied to the frame to simulate the initial state of stress in the column elements prior to the application of dynamic or static lateral loads.

The inelastic dynamic analyses conducted to obtain the steady-state response of the frame subjected to a range of harmonic ground motions were organized as follows:

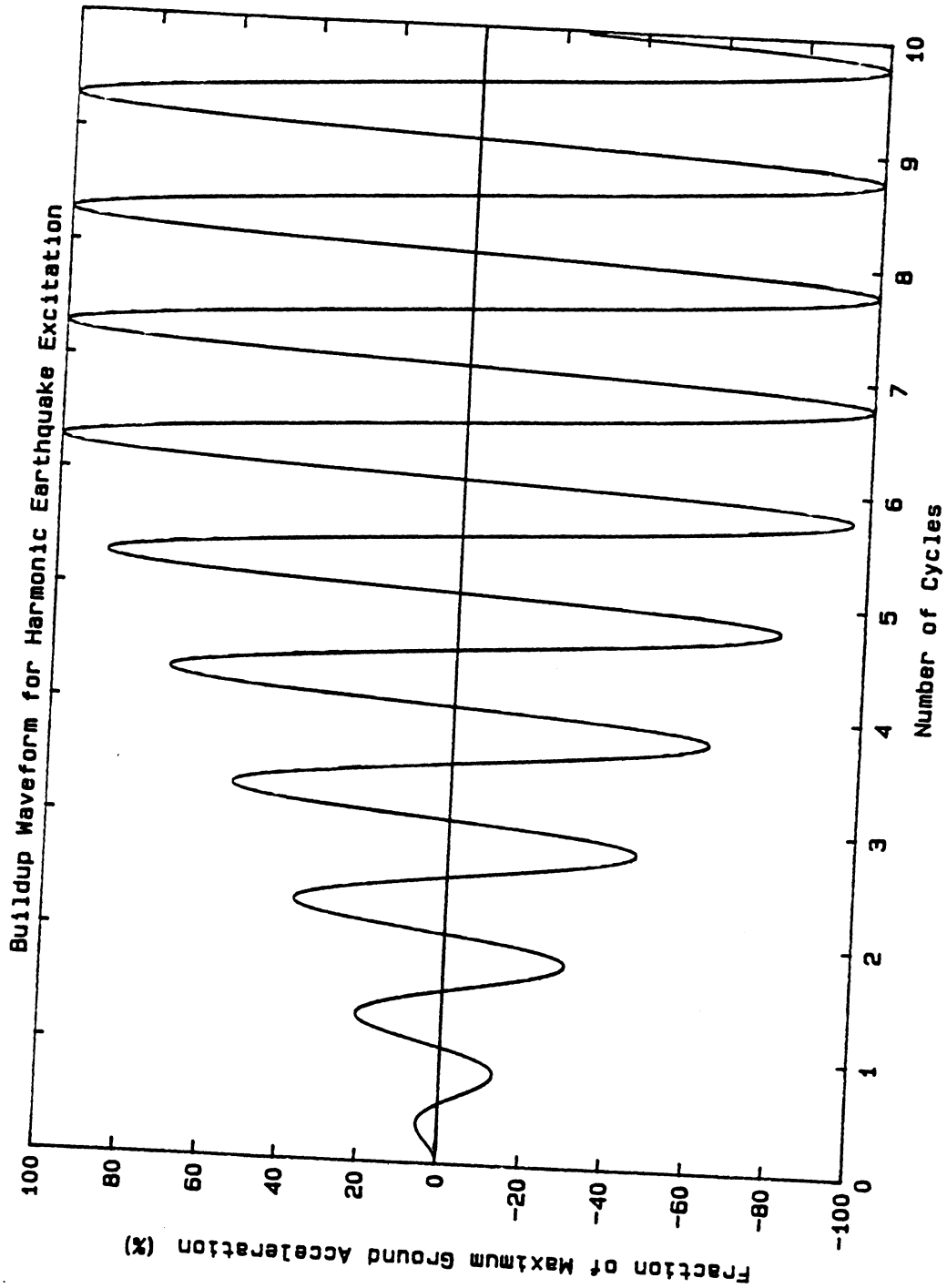

Figure 3.7 Buildup Harmonic Waveform

1) Select the harmonic ground motion parameters A_g and T_g.

2) Perform harmonic earthquake response analysis to obtain the steady-state response of the MDOF system.

3) From the steady-state response, obtain the displacement response, the base shear response and the vibration shapes.

3.2.2.2. SDOF Response

Several inelastic static analyses were conducted on the frame utilizing DRAIN-2DX [1]. The applicable assumptions from the dynamic analyses were also implemented for the static analyses. The static analyses were applications of the iterative shape improvement method (Appendix D) to obtain the vibration shape for the SDOF system. The converged static analysis results are presented in Figure 3.8. Once the approximate vibration shape and base moment resistance characteristics were established, the transformations presented in Section 3.1.2.2 were implemented to relate the MDOF system to an equivalent SDOF system represented dynamically by an inverted pendulum oscillator (as shown in Figure 3.2). The properties of the equivalent SDOF oscillator are shown in Table 3.1.

The steady-state response of the bilinear SDOF oscillator subjected to harmonic earthquake loading can be obtained using various procedures [29,31,32,34,44]. In this investigation, the response was obtained by considering the rotational equilibrium of the oscillator subjected to harmonic base motion;

$$M\ddot{\theta}(t) + C\dot{\theta}(t) + R_S(\theta) = R \sin\left(\frac{2\pi}{T_g} t\right)$$

The base moment resistance term $R_S(\theta)$ of a bilinear system is shown in Figure 3.9. The instantaneous base resisting moment can always be expressed as a linear function of the rotation θ;

$$R_S(\theta) = K_i \theta + R_i$$

where K_i is the instantaneous stiffness and R_i is the corresponding moment intercept (see Figure 3.9) Making this substitution results in the following equilibrium equation;

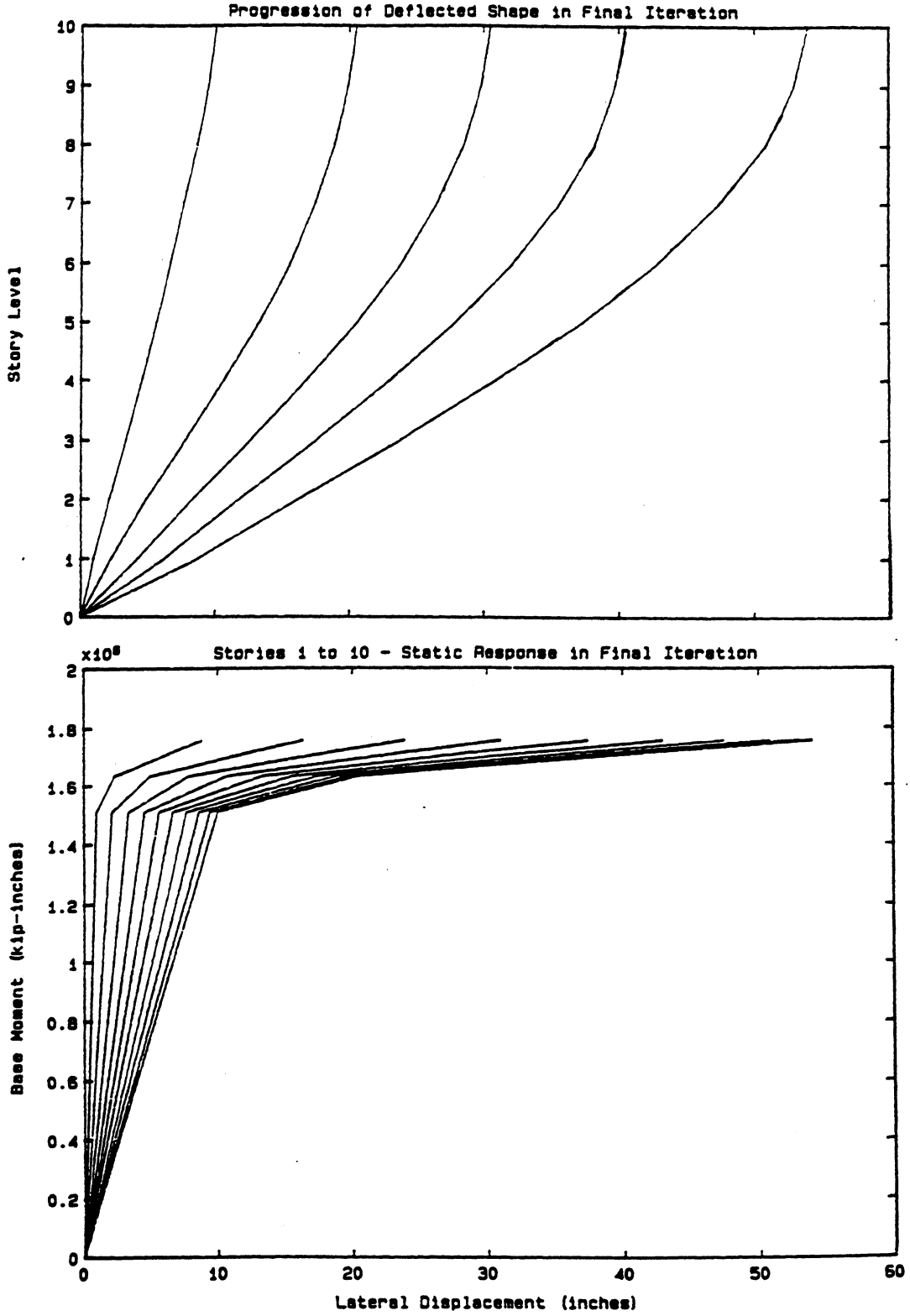

Figure 3.8 Iterative Shape Improvement Results for 2-D Frame

TABLE 3.1 EQUIVALENT SDOF PROPERTIES FOR 2-D FRAME

Property	Value	Units
K_1	19,016,040	kip-inch/rad
K_2	0.04 x K_1	kip-inch/rad
M_y	150,870	kip-inch
x_y	7.1	inches
ξ	5.0	(%)
w_e	375.0	kips
h_e	888.6	inches

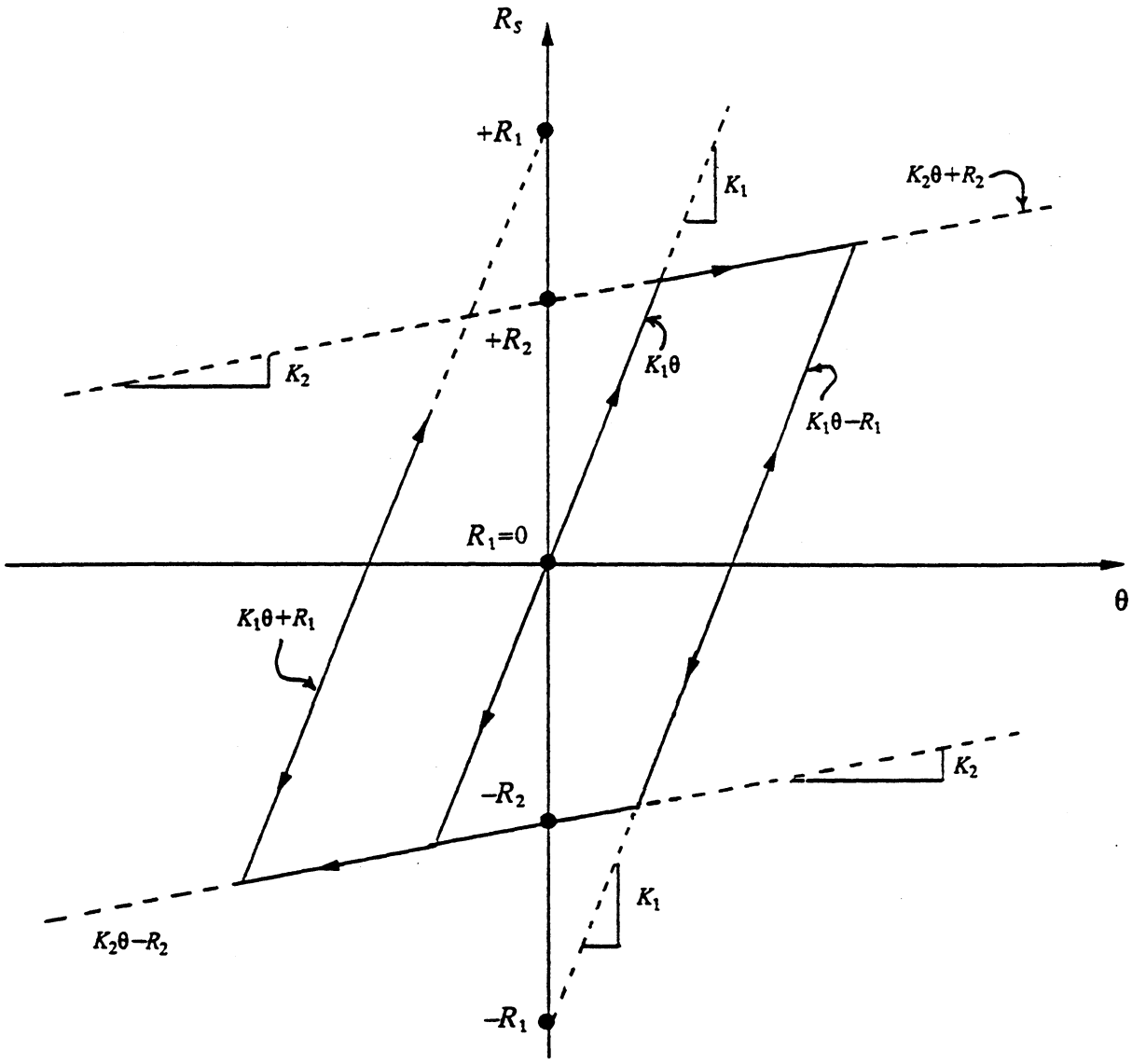

Figure 3.9 Bilinear Base Moment vs. Rotation Relationship

$$M\ddot{\theta}(t) + C\dot{\theta}(t) + K_i\,\theta(t) + R_i = R \sin\left(\frac{2\pi}{T_g}\,t\right)$$

A general closed form solution to this second order differential equation can be obtained using conventional methods [79]. An algorithm which monitored the progression of the closed form solution at discrete time intervals was used to obtain the steady-state response of the oscillator. An event-to-event strategy was used to detect state changes (yielding and unloading) during time steps. Equilibrium was maintained by updating the stiffness and moment intercept at each state change. The vibration conditions that exist at the time of each state change are used as the initial conditions for the next phase of the solution. In this fashion, the evolution of the response is obtained by properly linking a series of exact solutions resulting in a pseudo-exact numerical solution procedure. It should be noted that the solution can also be obtained using various numerical integration procedures [5,47]. The SDOF analyses were organized as follows:

1) Obtain the approximate bilinear moment resistance relationship and the approximate vibration shape for the SDOF oscillator.

2) Select the harmonic ground motion parameters A_g and T_g.

3) Perform harmonic earthquake response analysis to obtain the steady-state response of the equivalent SDOF system.

4) Transform the SDOF results to obtain the displacement response and the base shear response.

3.2.2.3. Correlation of MDOF and SDOF Response

The correlation of the results from the harmonic analyses of MDOF structural representations and their equivalent SDOF representations can be used to assess the accuracy of SDOF procedures and to determine the range of harmonic ground motion parameters over which such simple representations are applicable. Figures 3.10 through 3.18 present comparisons of steady-state roof displacement response computed with the MDOF and SDOF models at each of the grid points in the T_g - A_g plane. The steady-state base

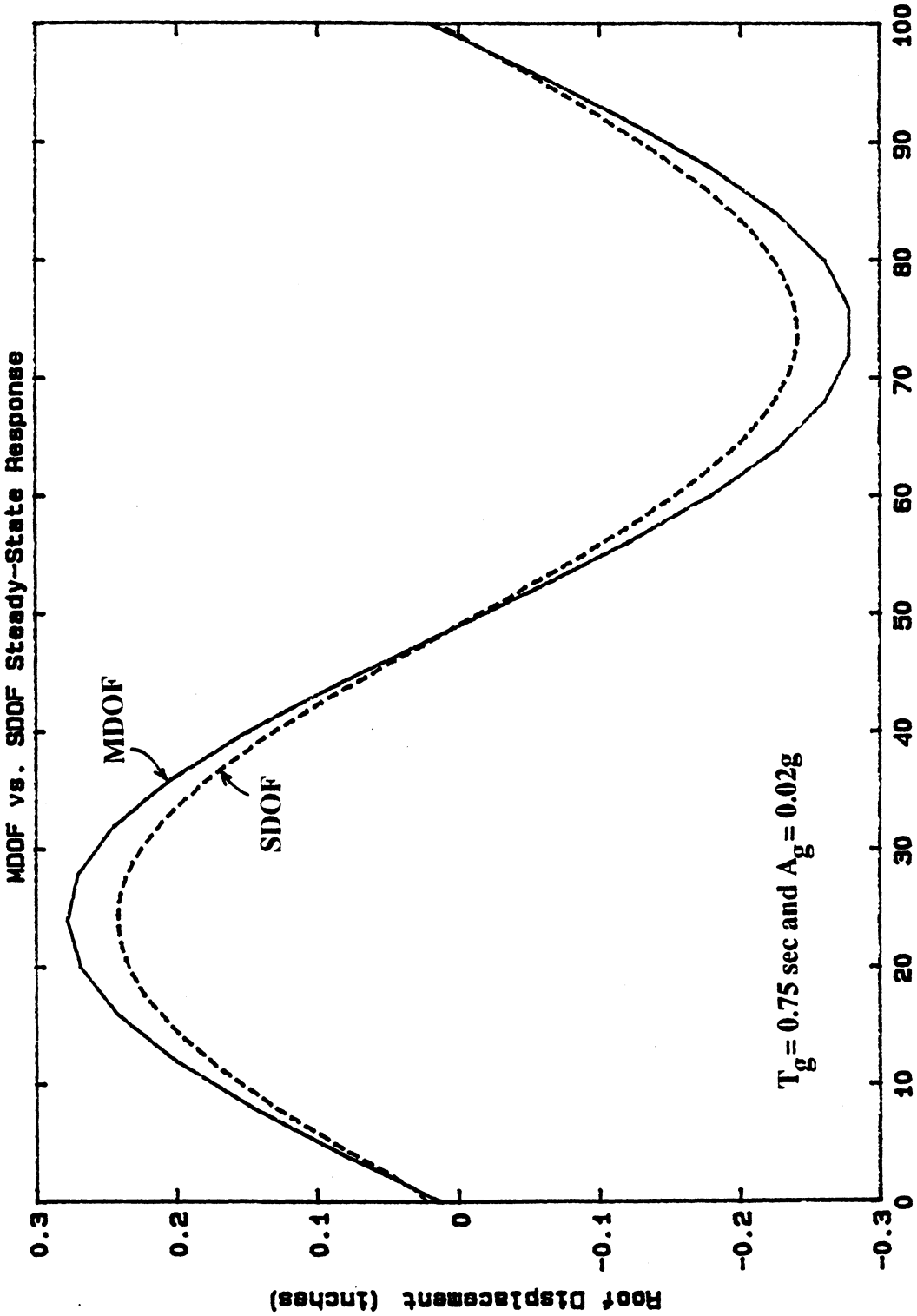

Figure 3.10 Response to Harmonic Earthquake

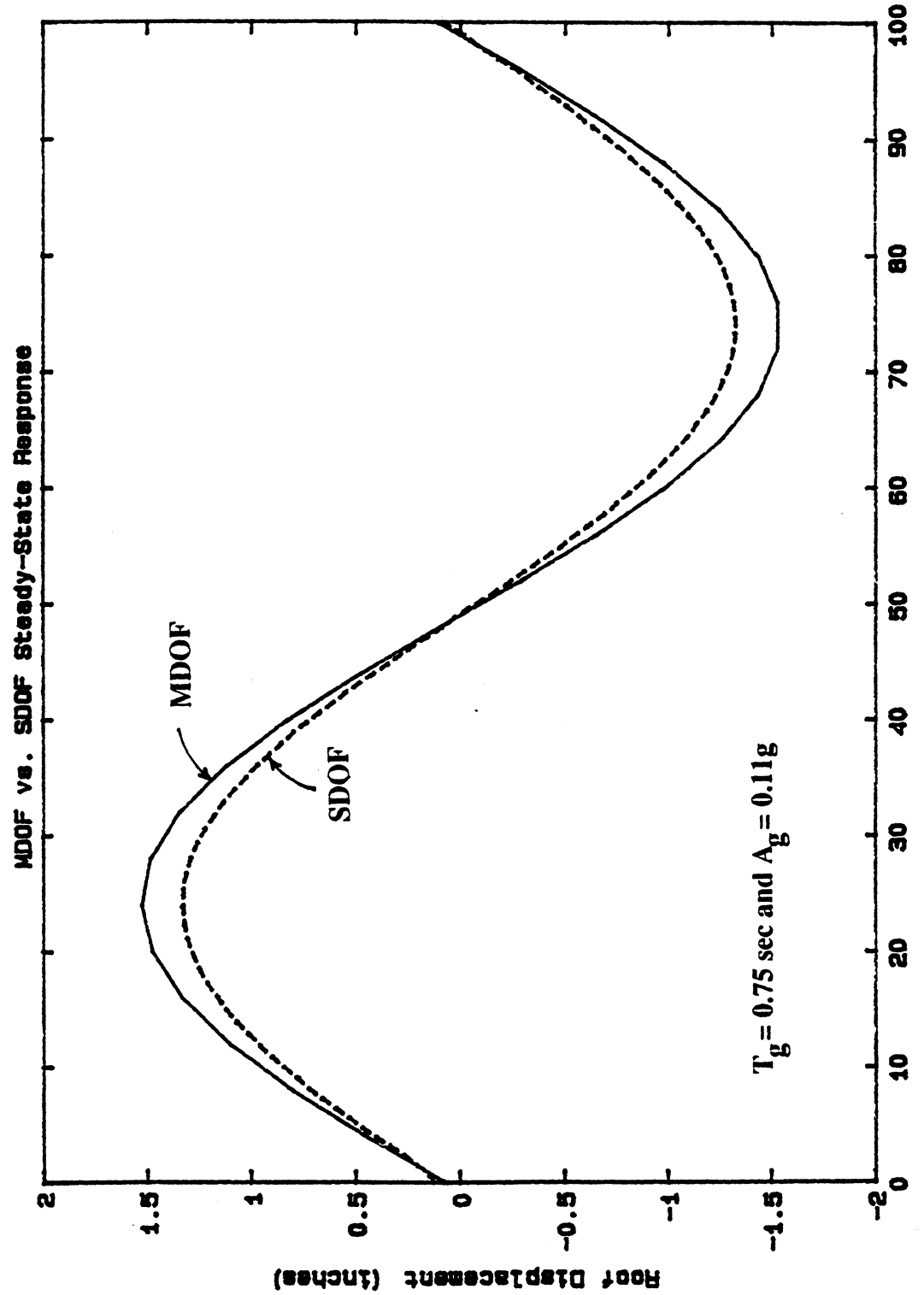

Figure 3.11 Response to Harmonic Earthquake

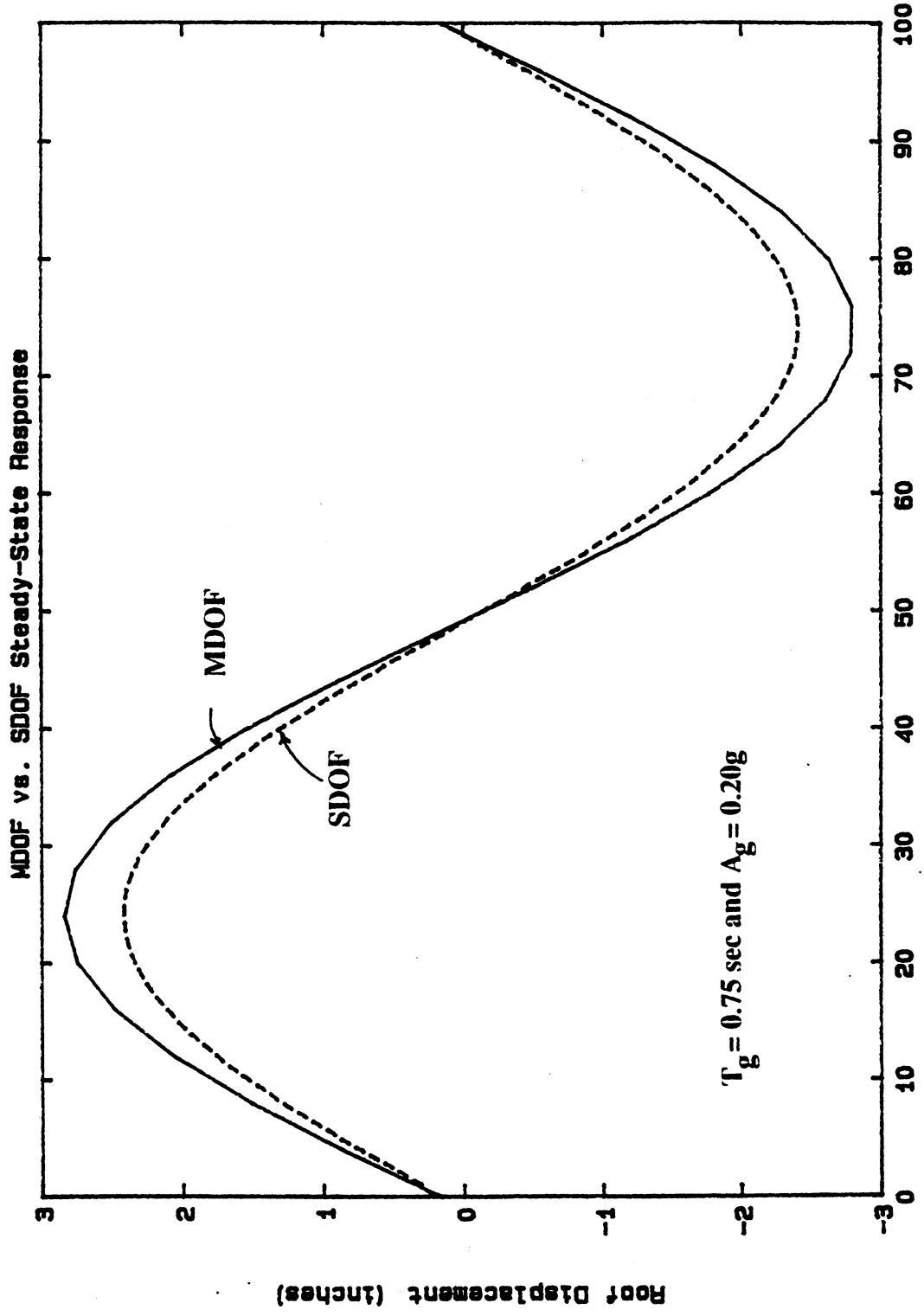

Figure 3.12 Response to Harmonic Earthquake

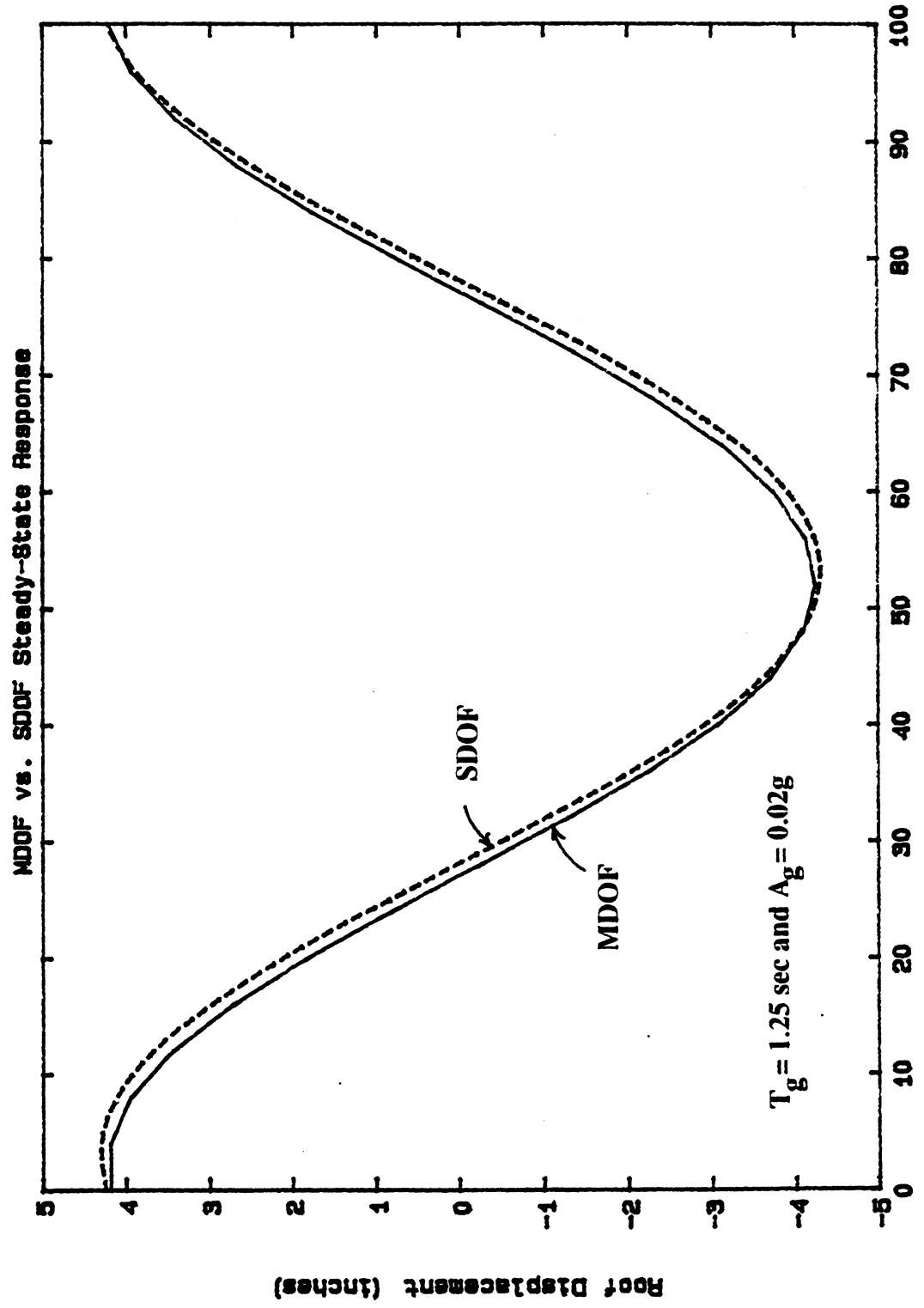

Figure 3.13 Response to Harmonic Earthquake

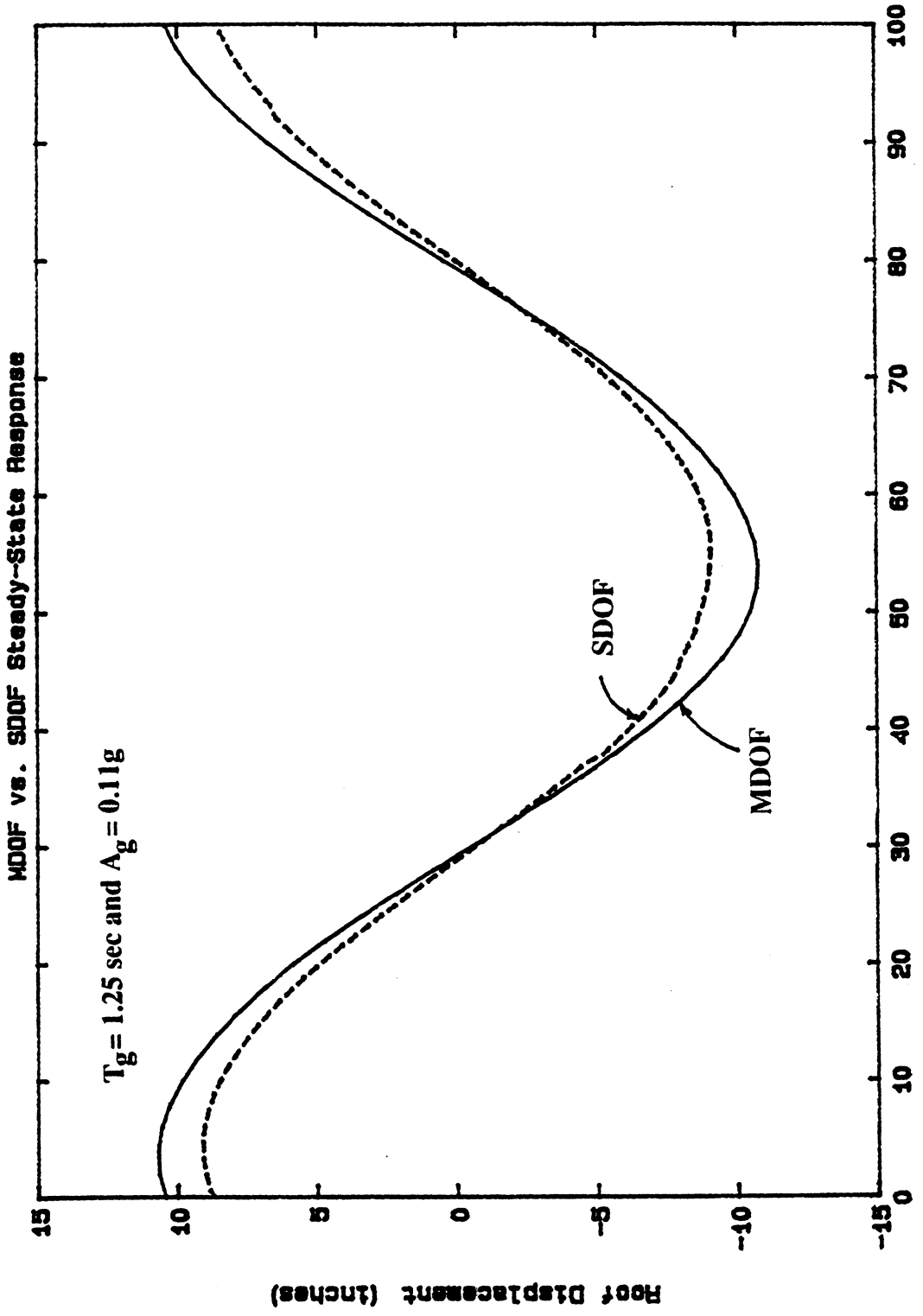

Figure 3.14 Response to Harmonic Earthquake

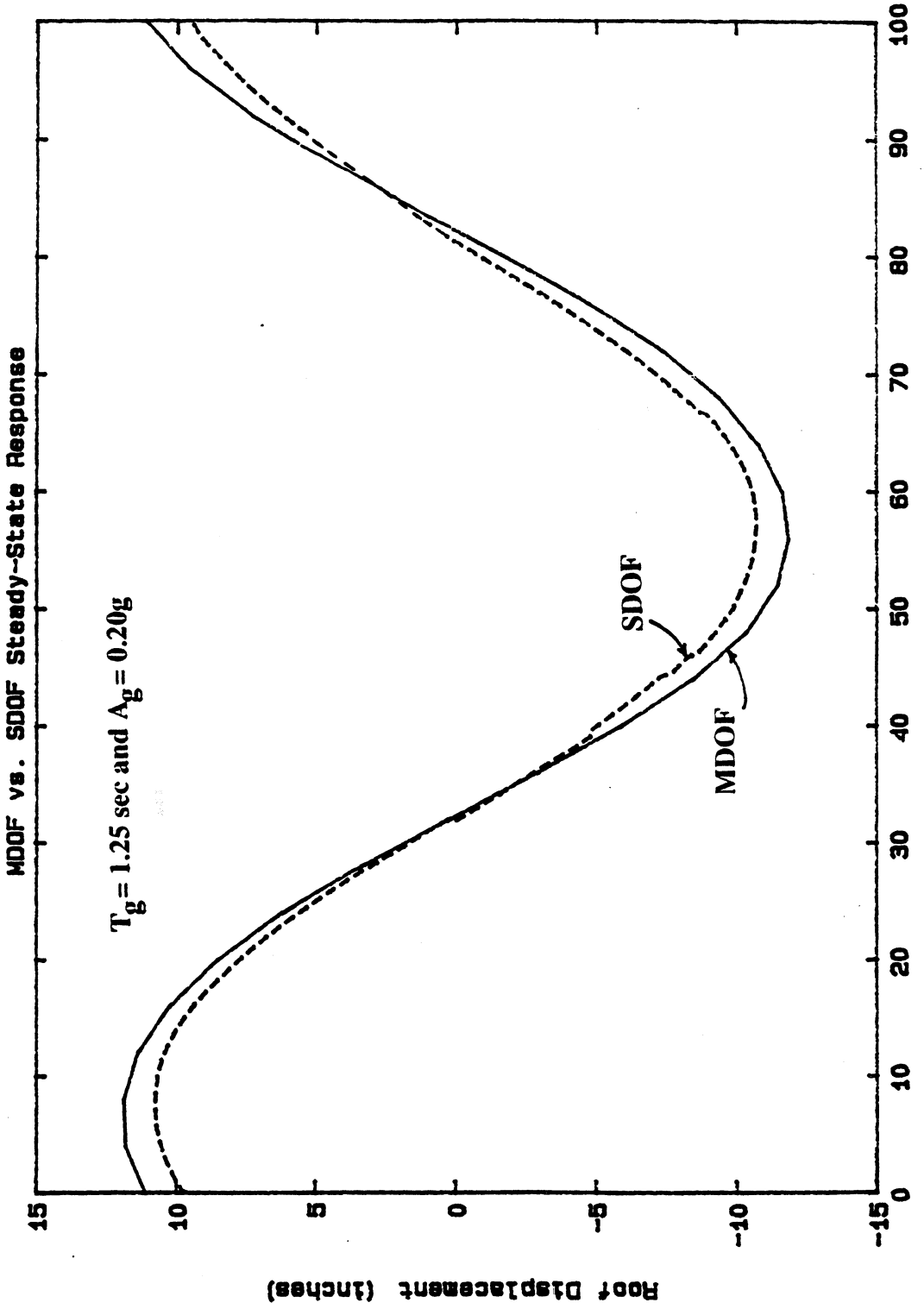

Figure 3.15 Response to Harmonic Earthquake

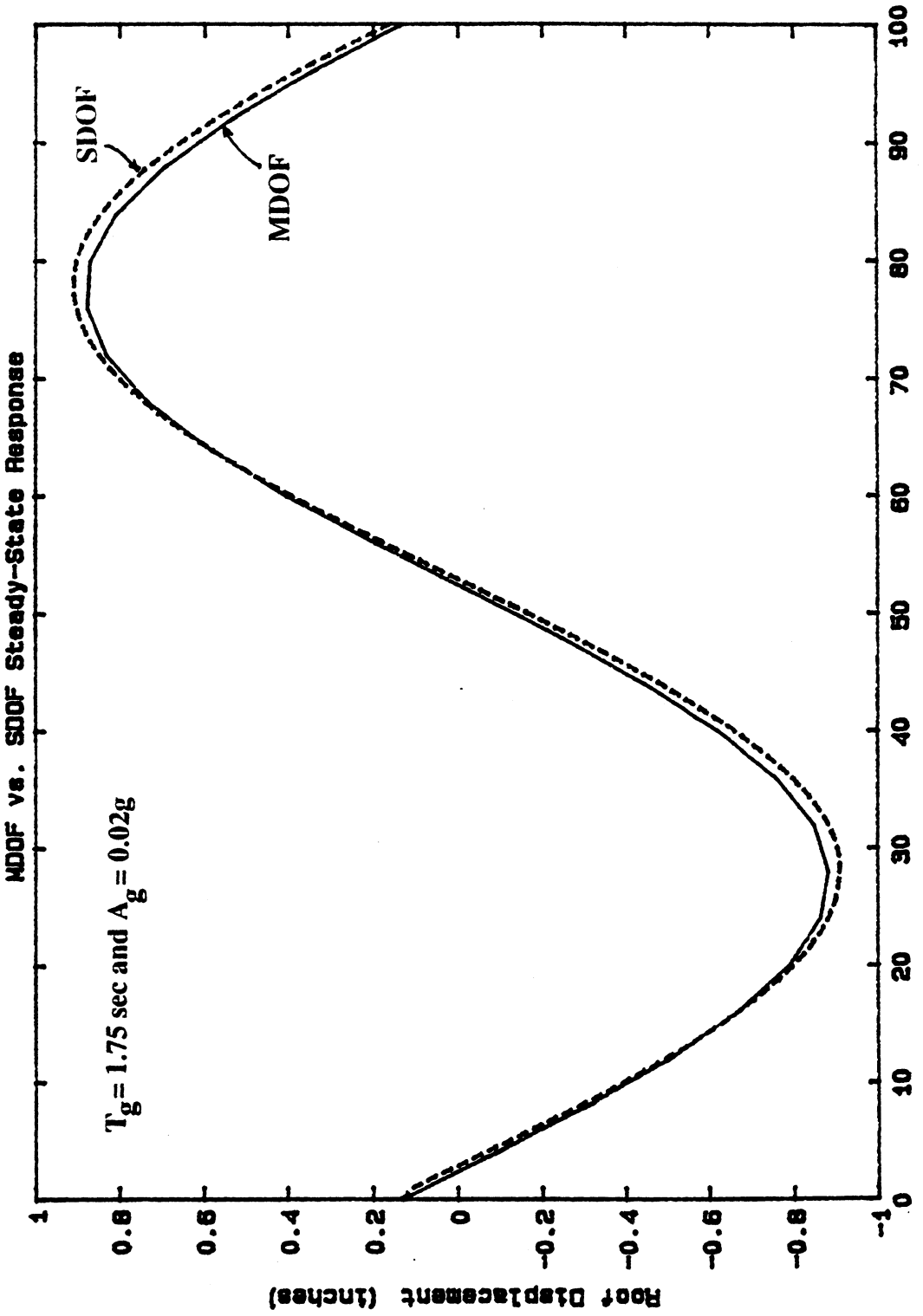

Figure 3.16 Response to Harmonic Earthquake

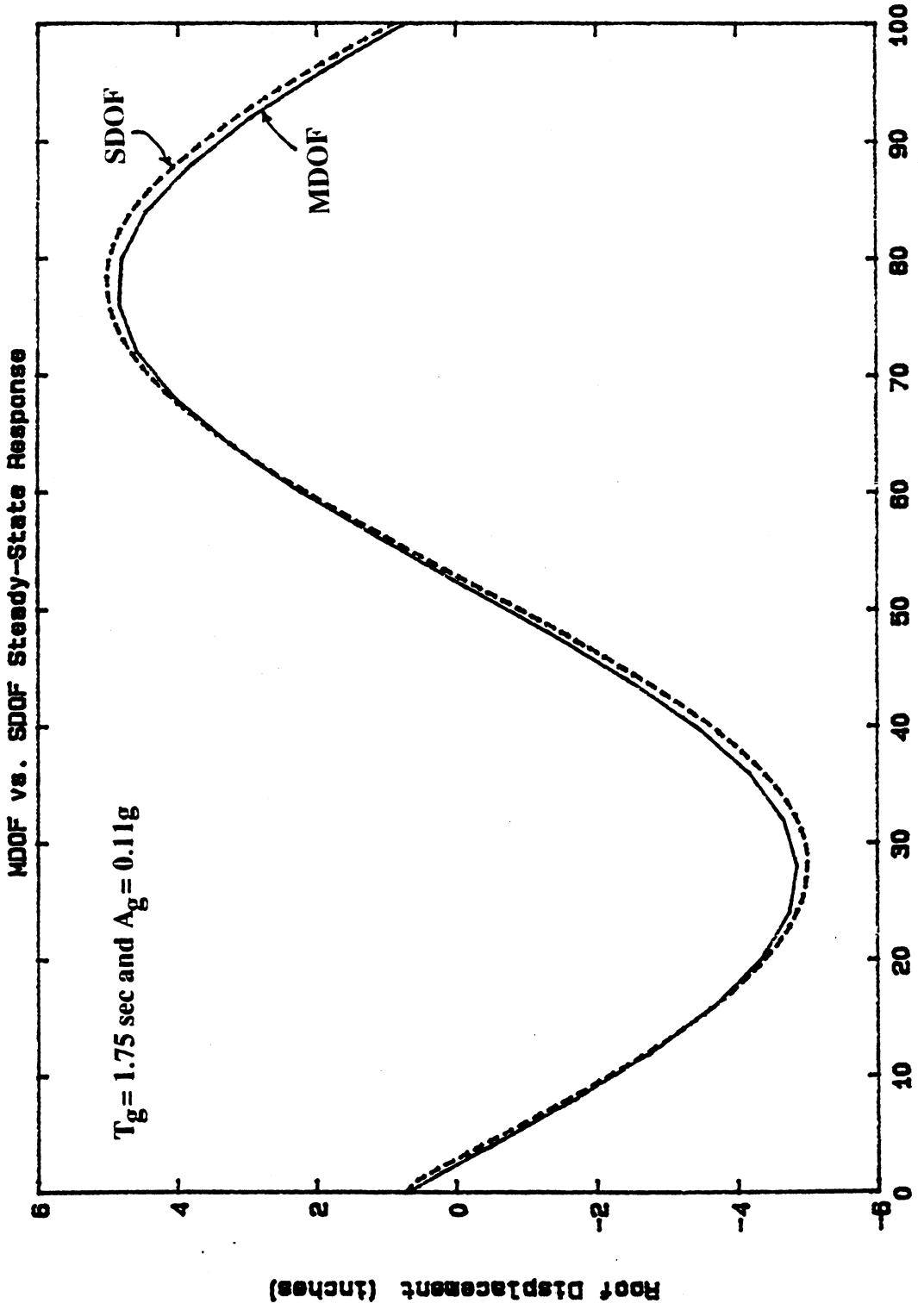

Figure 3.17 Response to Harmonic Earthquake

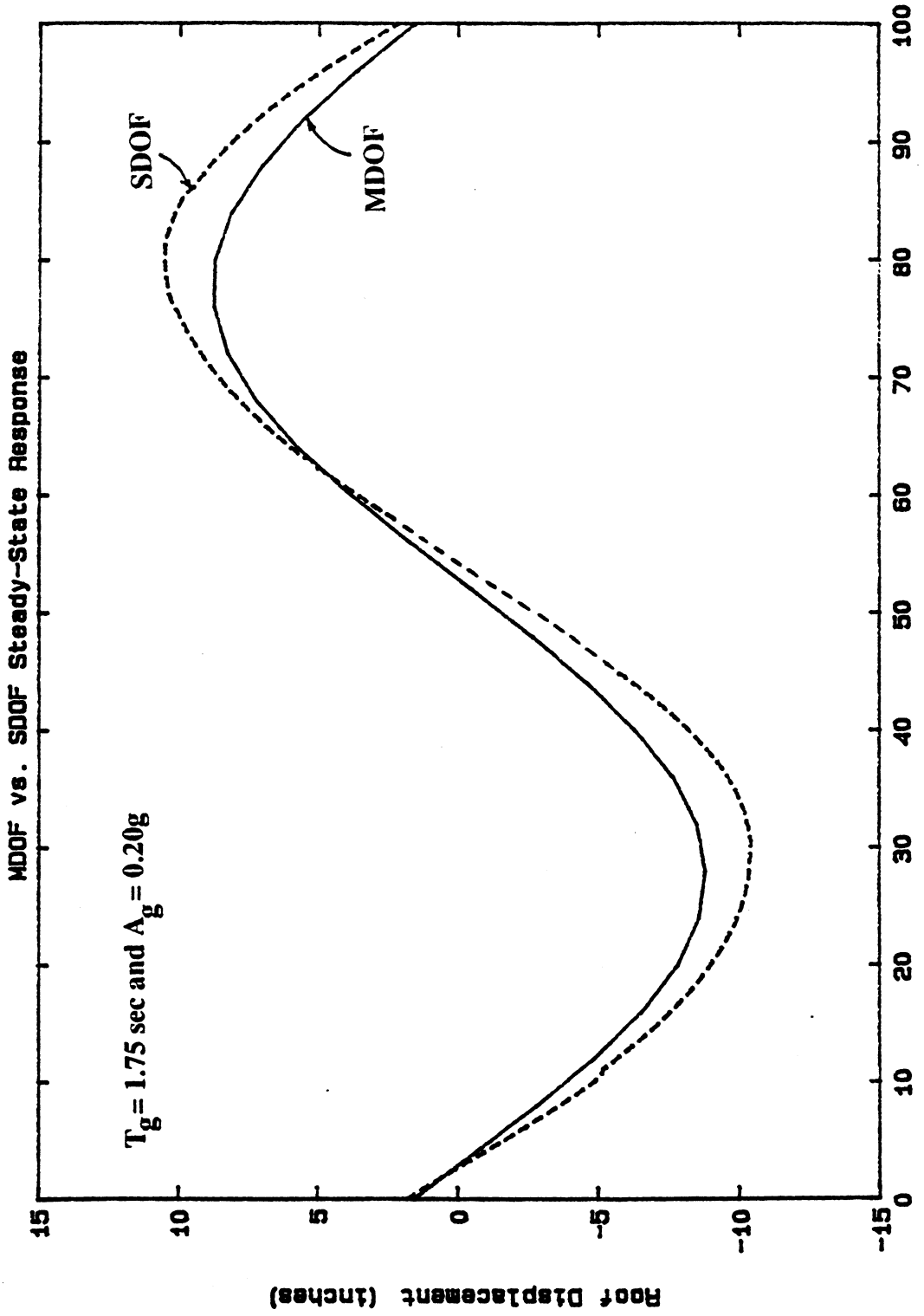

Figure 3.18 Response to Harmonic Earthquake

shear response is compared in Figures 3.19 through 3.27. The following observations can be made regarding the steady-state response of the MDOF and SDOF systems;

1) The MDOF and SDOF steady-state displacement response is in relatively good agreement at all points in the T_g - A_g plane.

2) The MDOF and SDOF base shear response is in good agreement for all points in the T_g - A_g plane for which $T_g \geq T_s$. The correlation of maximum base shear response is particularly good for T_g - A_g combinations which induced nonlinear behavior (T_g = 1.25 seconds, A_g = 0.11g; T_g = 1.25 seconds, A_g = 0.20g, and T_g = 1.75 seconds, A_g = 0.20g)

3) The base shear response of was over estimated by a factor of approximately four for all of the analyses in which T_g = 0.75 second. It should be noted that in all of these cases, the response of both the MDOF and SDOF systems was linear.

The poor correlation of the base shear response computed for the MDOF and SDOF systems at T_g = 0.75 second is a result of the participation of the second mode (which has a vibration period of T_2 = 0.46 seconds). The steady-state base shear response computed using superposition of the first and second elastic mode shapes of the system is indistinguishable from the response computed for the MDOF system. For this structure, harmonic earthquake loading at T_g =0.75 second represents dynamic loading at a period approximately midway between T_1 = 1.25 seconds and T_2 = 0.46 seconds, and hence, both modes can be expected to participate in the response. For this combination of T_g, T_1 and T_2 (β_1 = 1.67 and β_2 = 0.617), the amplitude of the dynamic base shear (which is proportional to the square of the vibration frequency) from the second mode is roughly 20% larger than that of the first mode, and because β_1 and β_2 straddle the resonance point and the corresponding phase transition near β = 1.0, the response of the second mode is roughly 180 degrees out-of-phase with that of the first mode. The superposition of the response of the two modes results in significant cancellation of the steady-state base shear, explaining why the SDOF system provides a poor representation of the base shear response

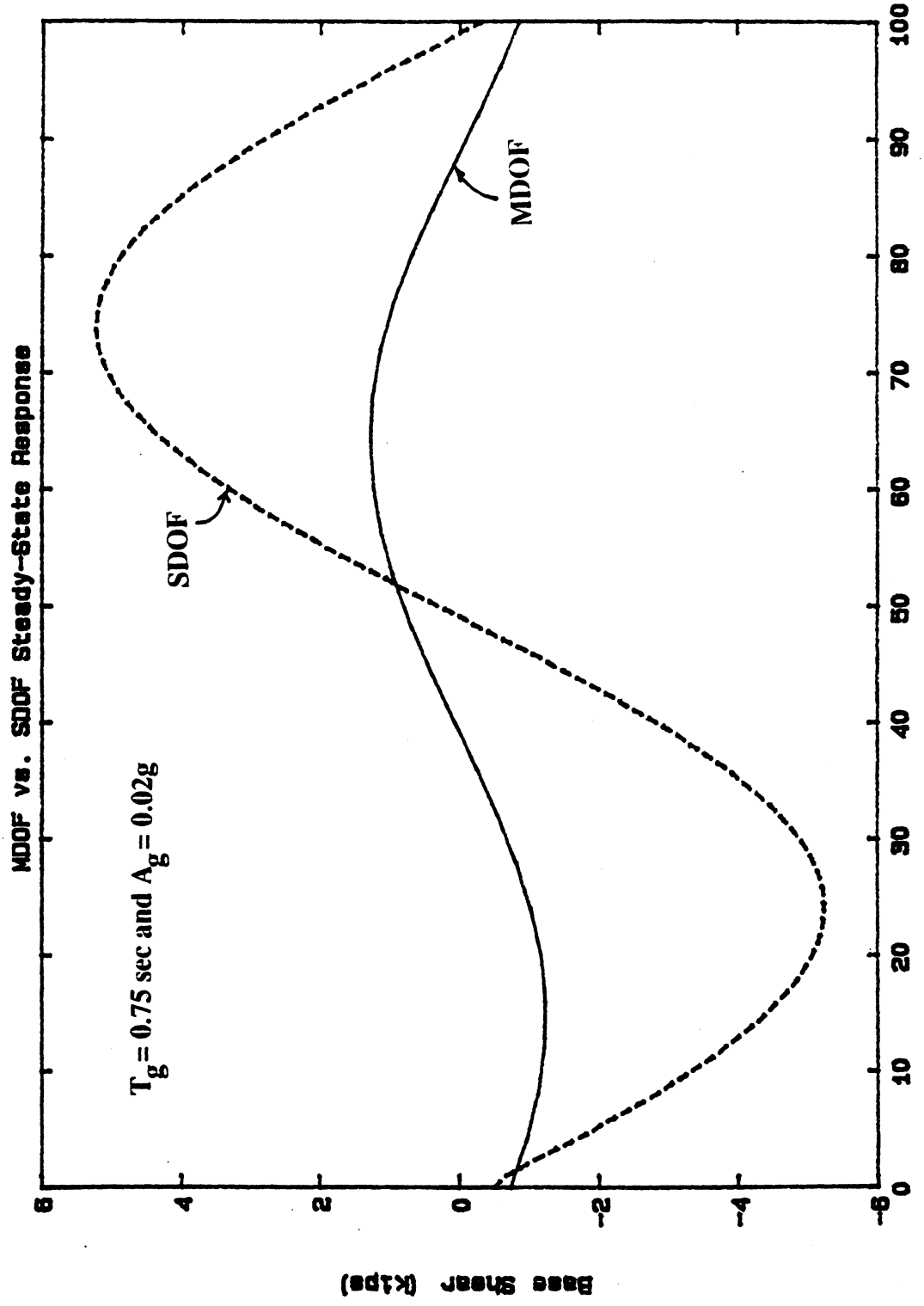

Figure 3.19 Response to Harmonic Earthquake

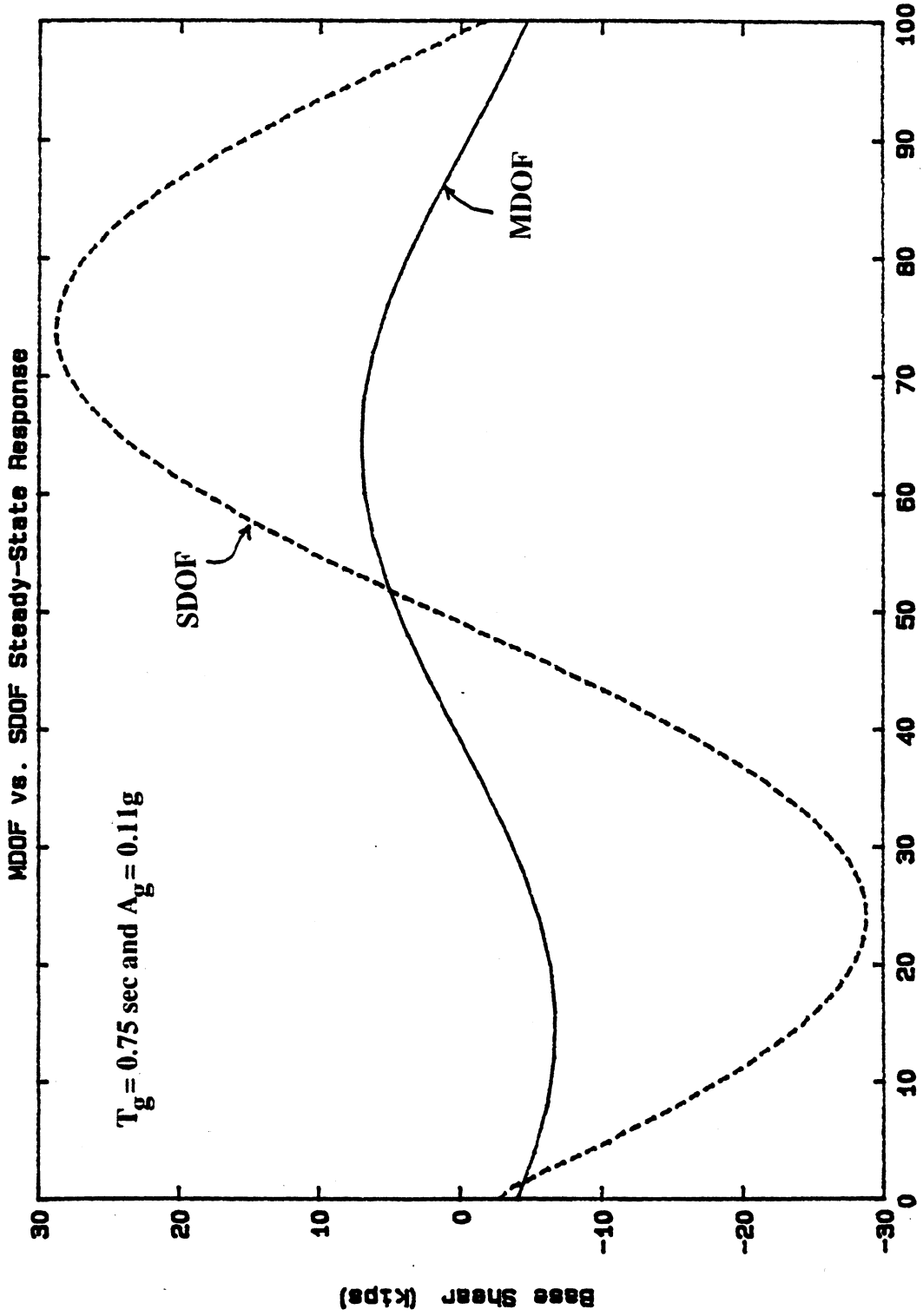

Figure 3.20 Response to Harmonic Earthquake

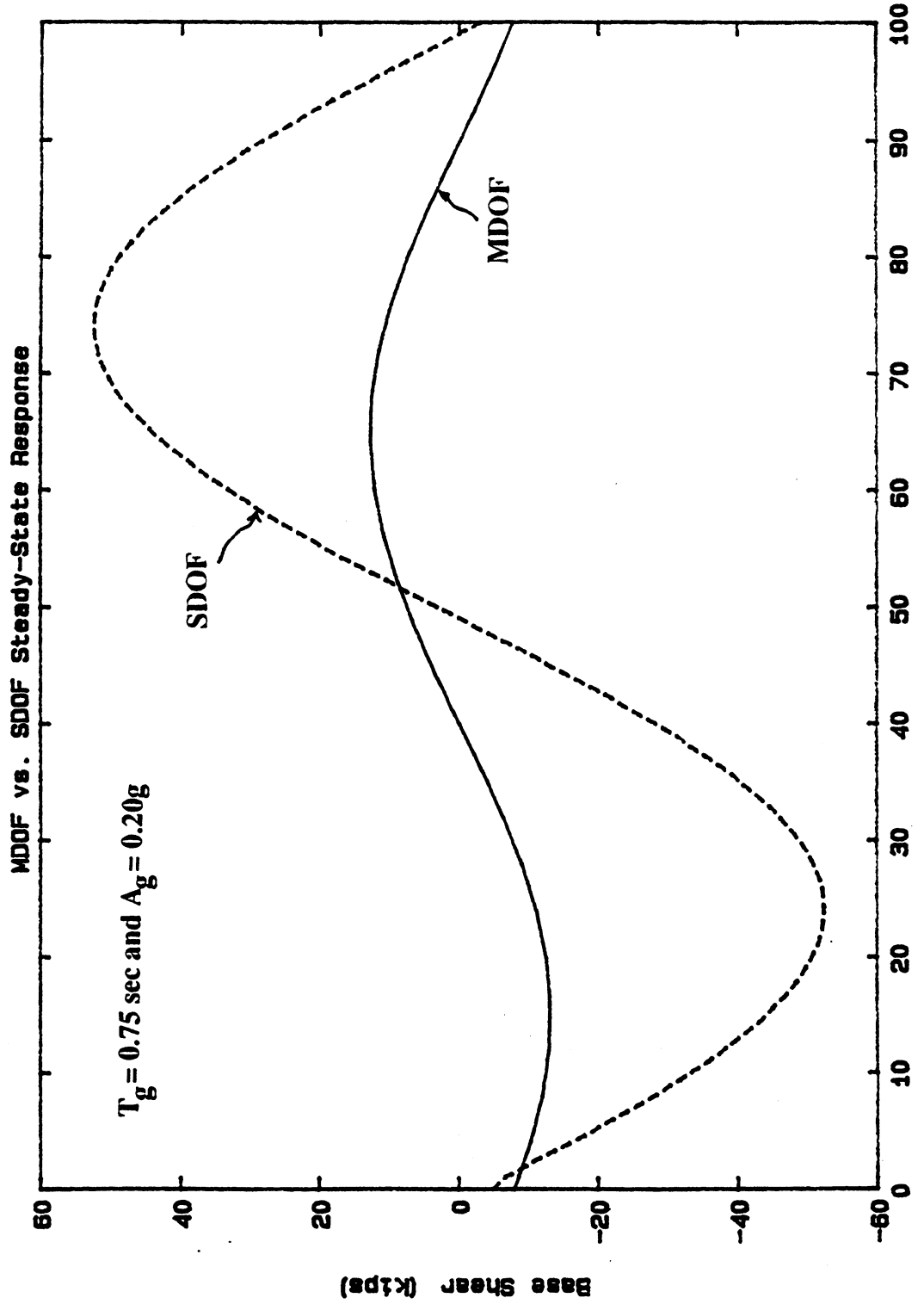

Figure 3.21 Response to Harmonic Earthquake

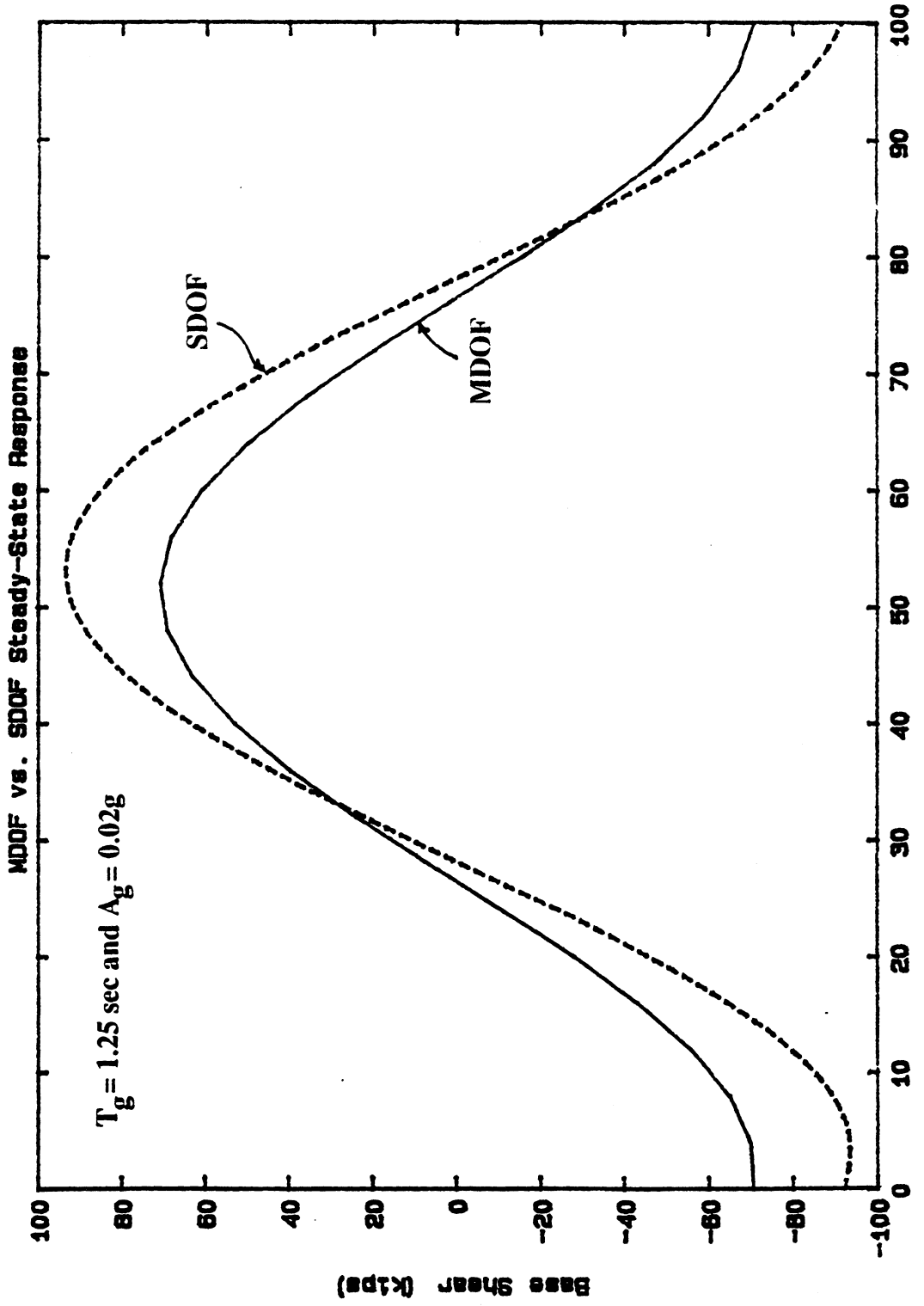

Figure 3.22 Response to Harmonic Earthquake

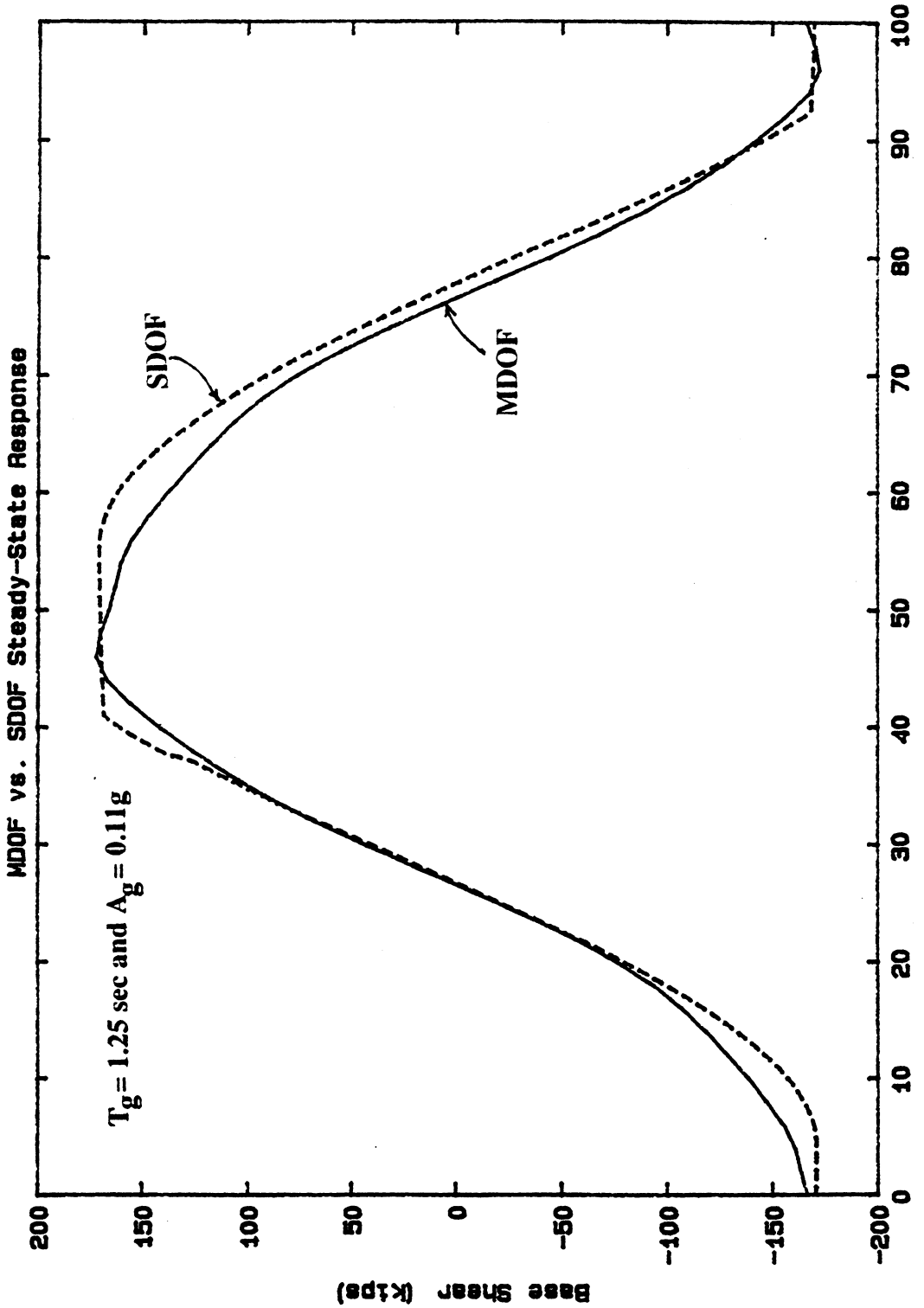

Figure 3.23 Response to Harmonic Earthquake

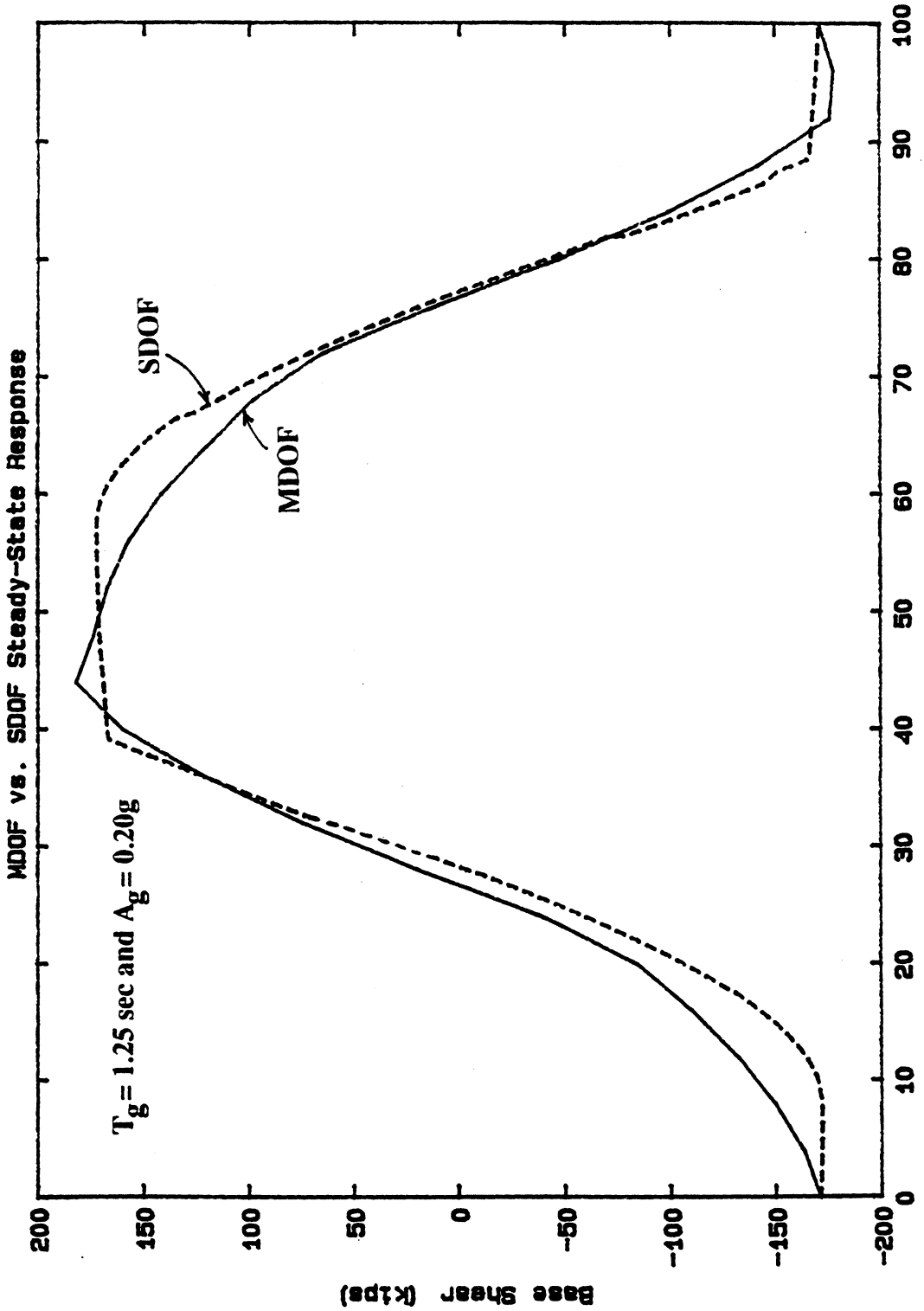

Figure 3.24 Response to Harmonic Earthquake

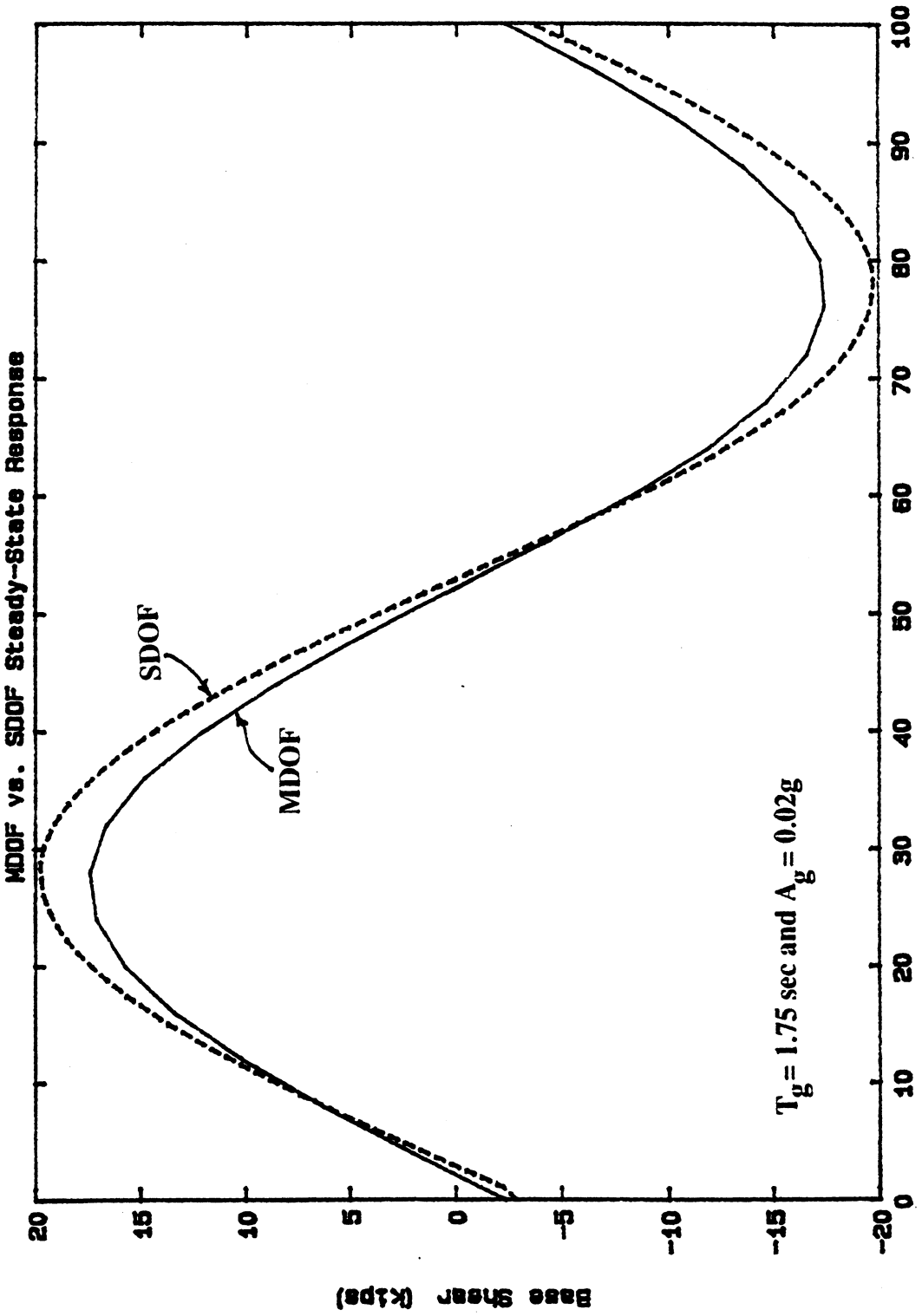

Figure 3.25 Response to Harmonic Earthquake

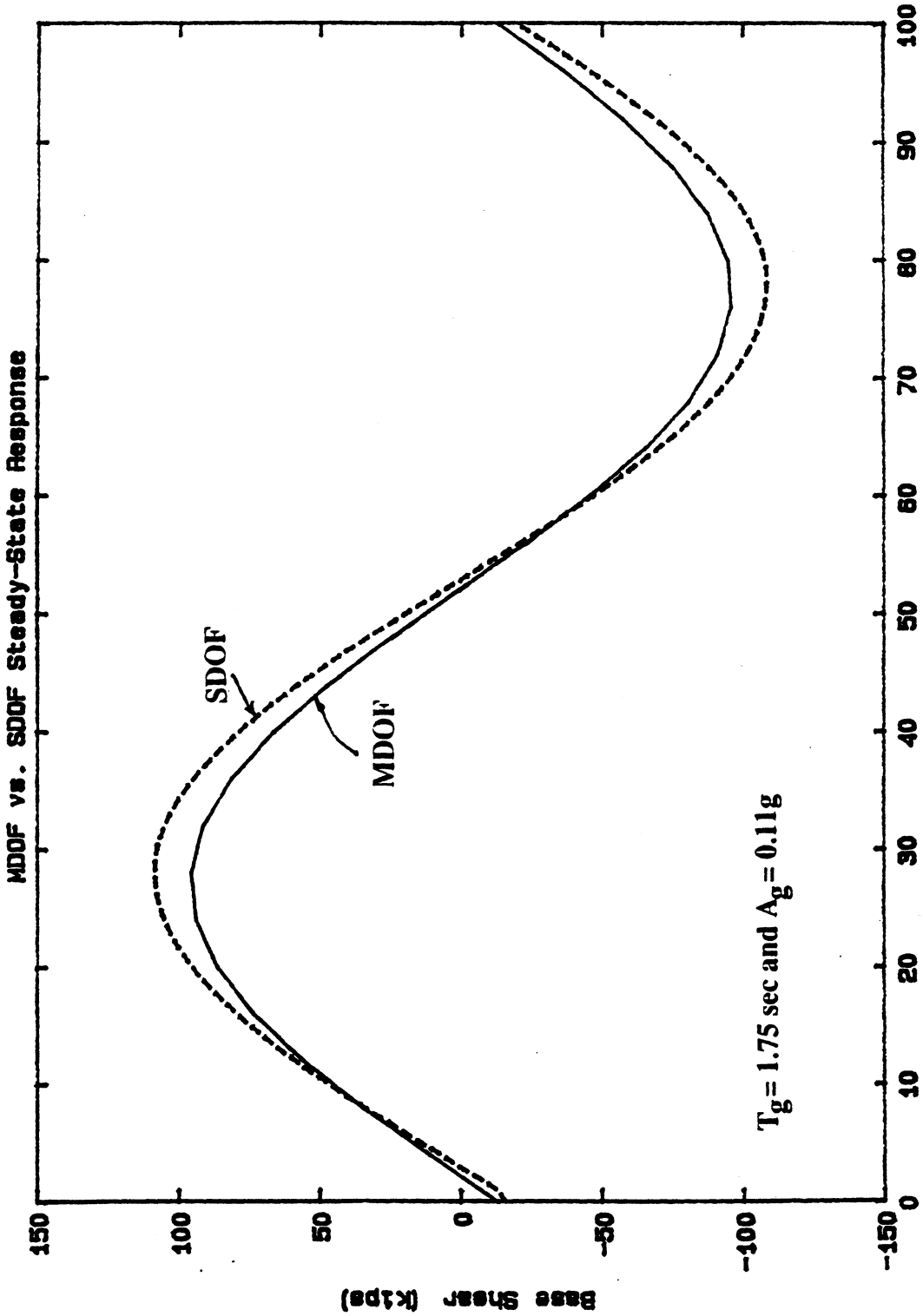

Figure 3.26 Response to Harmonic Earthquake

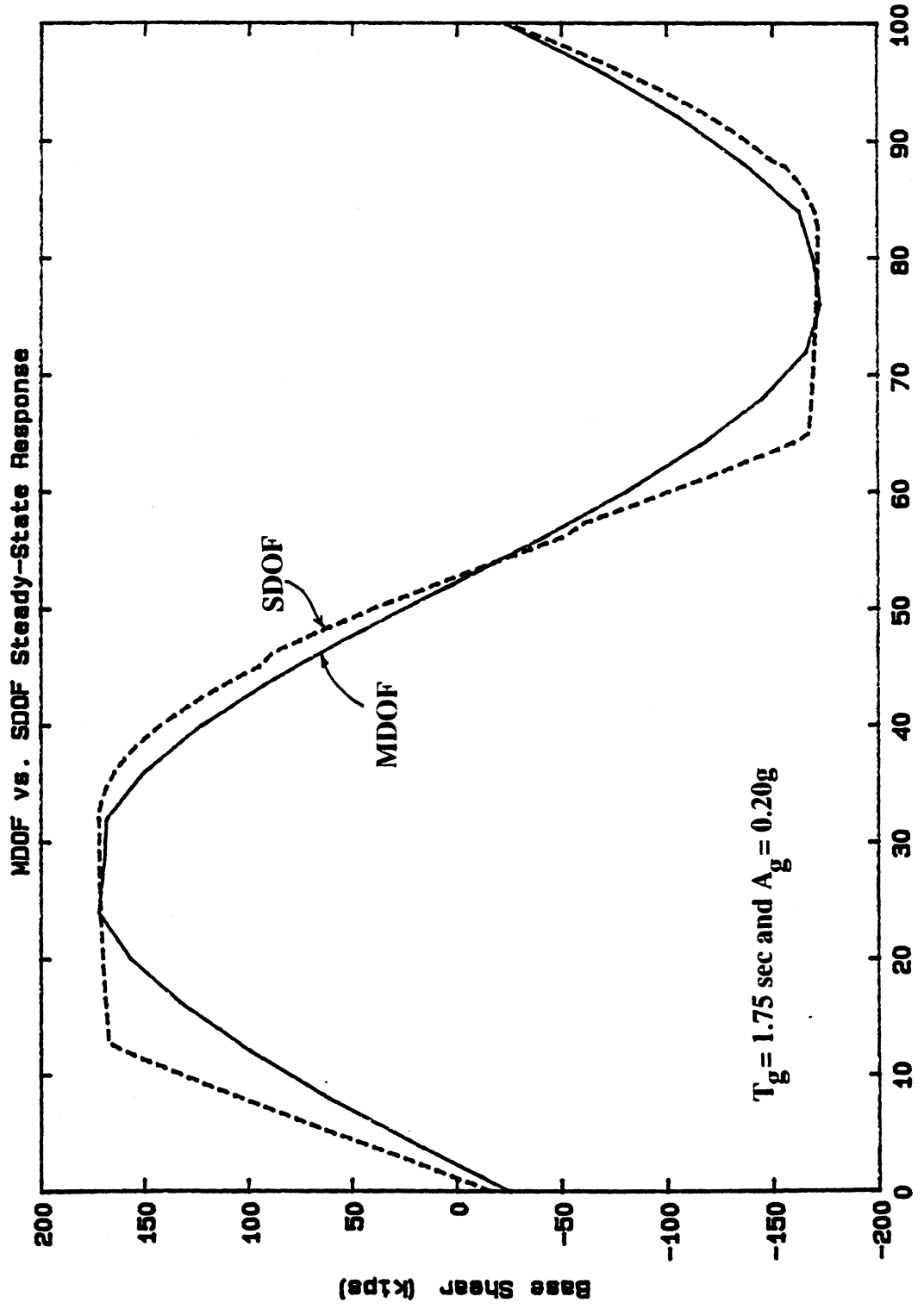

Figure 3.27 Response to Harmonic Earthquake

in this frequency range. Analyses of the MDOF and SDOF systems at T_g values between 0.75 and 1.25 seconds indicated that for $T_g < 1.125$ seconds, the influence of the second mode on the base shear response could not be neglected. The steady-state base shear response of the MDOF and SDOF systems at $T_g = 1.125$ seconds are shown in Figures 3.28 through 3.30. It should be noted that for this combination of T_g, T_1 and T_2 ($\beta_1 = 1.11$ and $\beta_2 = 0.412$), the amplitude of the dynamic base shear from the second mode is only about 13% of that of the first mode.

A general procedure for determining the T_g range between T_1 and T_2 over which SDOF harmonic analysis can be used to estimate the steady-state base shear response of a MDOF system is outlined as follows:

1) Obtain the vibration periods T_1 and T_2.

2) From T_g compute β_1 and β_2.

3) Use β_1 and β_2 to determine the dynamic amplification of the first and second modes and resolve the modal amplitudes to obtain modal base shear amplitudes V_1 and V_2.

4) If $V_1 >> V_2$, the second mode effect can be neglected.

5) If V_1 and V_2 are of the same order, the second mode effect cannot be neglected. It should be noted that for moment resisting frame systems, a general rule of thumb is that $T_2 \approx T_1/3$ while for braced frames or shear wall systems, $T_2 \approx T_1/5$ to $T_1/7$. This indicates that SDOF harmonic analyses may be applied over a wider β range for braced frame and shear wall systems than for moment resisting frame systems.

Once the range of applicability of the SDOF harmonic analysis is established, the dynamic structural response within this range can be reasonably estimated using SDOF procedures. Figure 3.31 illustrates how SDOF analysis can be used to assess the structural response of T_g - A_g grids that are much finer than the nine point grid shown in Figure 3.6.

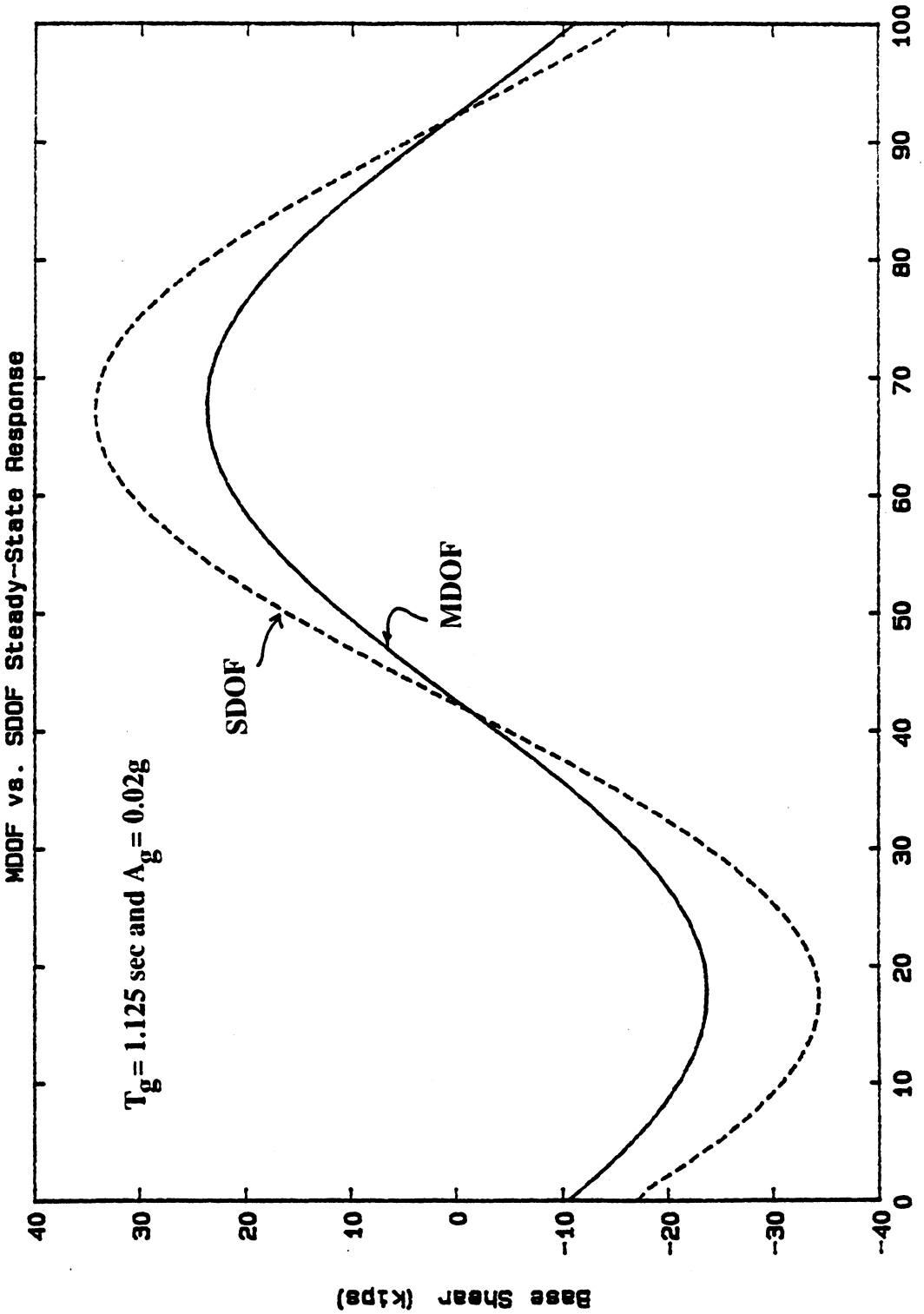

Figure 3.28 Response to Harmonic Earthquake

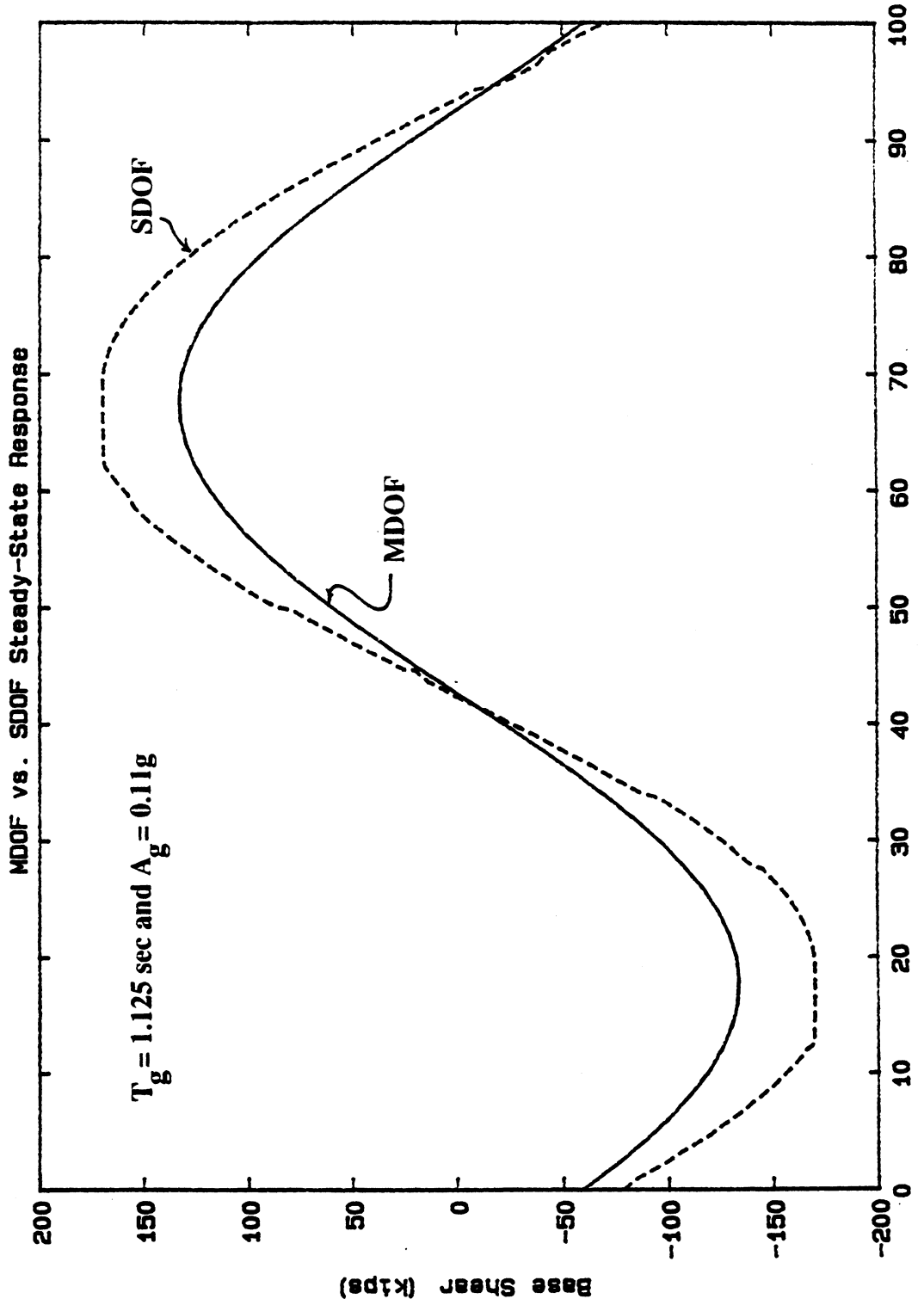

Figure 3.29 Response to Harmonic Earthquake

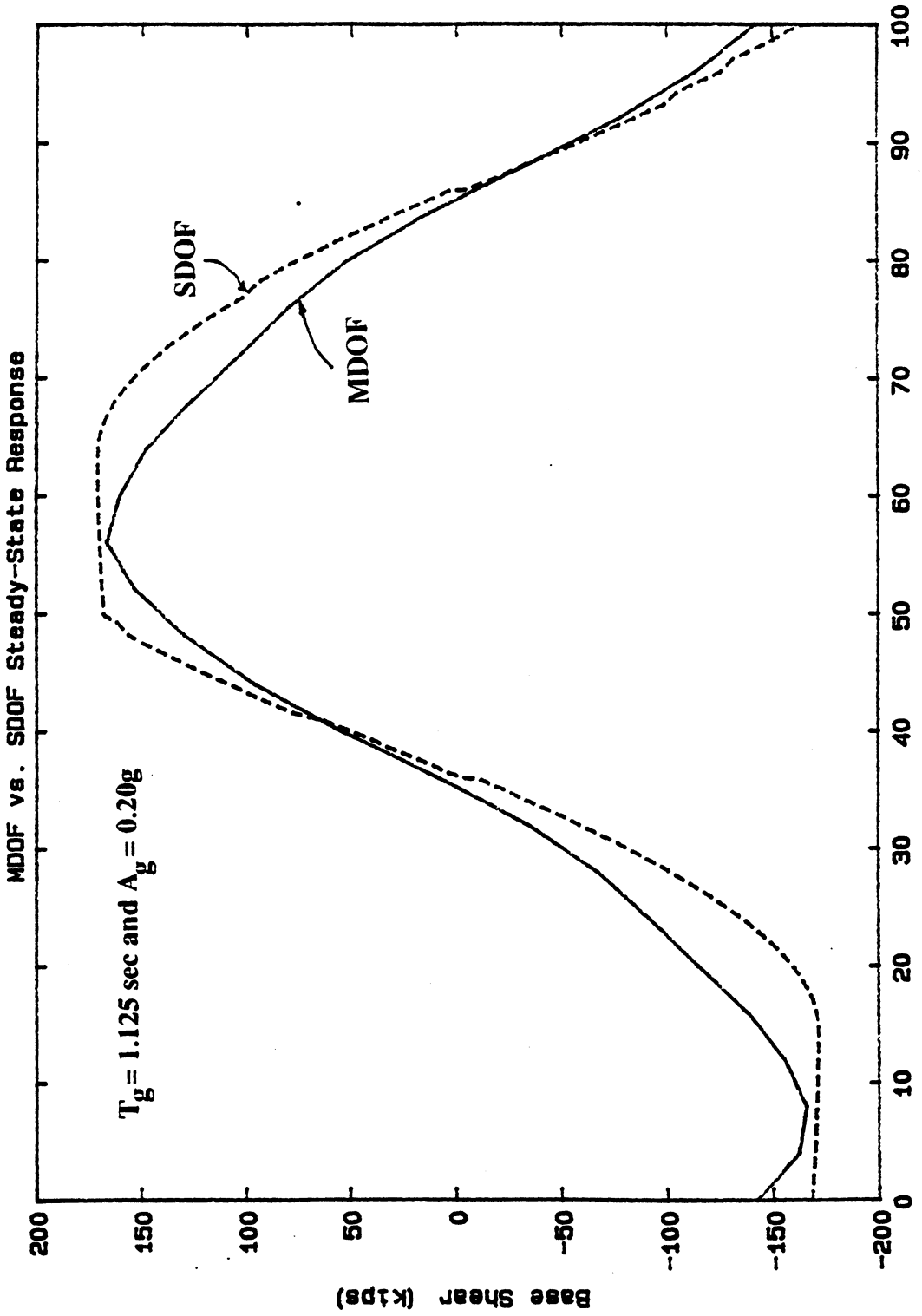

Figure 3.30 Response to Harmonic Earthquake

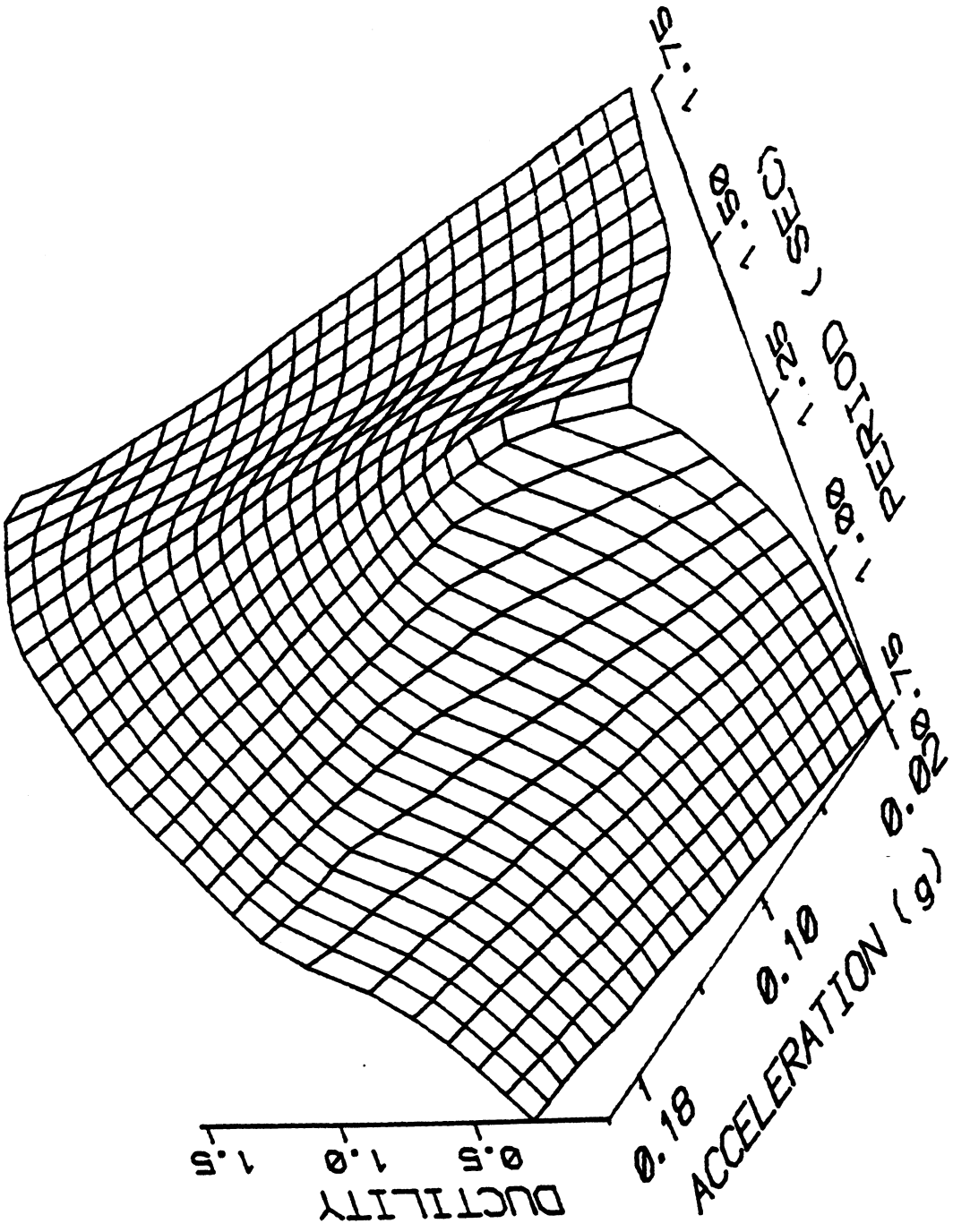

Figure 3.31 Spectral Surface of SDOF Ductility Response

3.2.3. Extension to Other Two-Dimensional Systems

The procedures used to obtain the vibration shapes for MDOF to SDOF reduction are based on physically reasonable assumptions regarding the distribution and amplitude of the inertia forces, and hence can also be applied to the analysis of more general two-dimensional building systems.

One fundamental difference between the analyses of different types of two-dimensional systems is that the vibration shapes used for MDOF to SDOF reduction are different for various systems. Figure 3.32 shows examples of qualitative vibration shapes obtained for moment resisting frame systems, shear wall systems and base isolated systems.

Another difference between the analyses of various two-dimensional systems is the manner in which the systems resist lateral forces. The essential requirement for the simplified SDOF analysis is that the resistance of the system can be represented using a bilinear model. Well designed lateral force resisting systems will resist moderate earthquakes without sustaining any damage and withstand major earthquakes undergoing controlled structural yielding without actually collapsing. This implies that the use of a bilinear resistance function, which qualitatively represents the damaged and undamaged states, is applicable for modeling well designed lateral force resisting systems.

3.2.4. Extension to Three-Dimensional Systems

Because the procedures to obtain the vibration shapes for simplified SDOF analysis are based on physical reasoning regarding the amplitude and distribution of the inertia forces, it is logical to extend the procedures to the analyses of general three-dimensional systems. Perhaps the most rational way to establish the vibration shapes for MDOF to SDOF reduction for three-dimensional systems is to observe that earthquake ground motions tend to excite the lowest modes of structural response, resulting in inertia forces oriented in directions associated with these modes. Hence, as a first step, it is rational to apply simplified analysis procedures in the principal directions of the three-dimensional

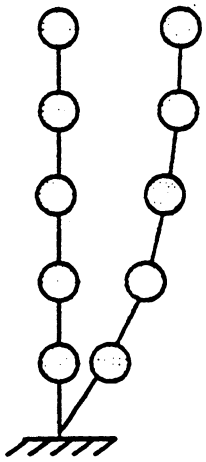

Moment Resisting Frame Systems

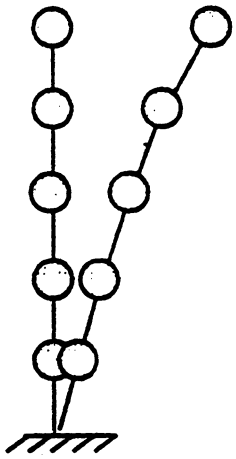

Shear Wall Systems

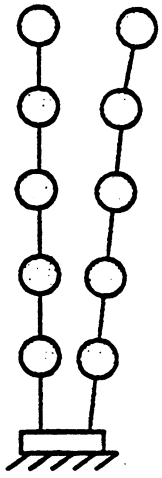

Base Isolated Systems

Figure 3.32 Qualitative Vibration Shapes for 2-D Systems

system. The principal directions are established by computing the elastic mode shapes of a simple elastic model of the structure. Three-dimensional building systems with several hundred displacement DOF can be investigated using a rigid diaphragm assumption and lumping three components of mass (two horizontal translational DOF and a rotational DOF about the vertical axis) at each story level. A simplified three-dimensional buiding model is illustrated in Figure 3.33 As discussed in [76], each mode shape of the elastic system can be considered to be the deflected shape due to a set of static loads. Hence, six base reaction forces (three base shears and three base moments) can be computed for each mode shape. Note that the six modal base reactions can be resolved to obtain an effective inertia force acting at an equivalent height and radial distance. Modes with a large radial distance have a large torsional component, while modes with a large effective height contribute to the overturning of the structure and modes which have a low effective height contribute mainly to the base shear. The orientation of the resultant horizontal base shear force provides a unique definition of the direction for each mode shape. Based on this observation, it is possible to define the principal directions of the structure in the directions of the base shear reactions for the two lowest modes of structural vibration [76]. These directions qualitatively represent the most flexible directions of the three-dimensional system.

Once the vibration shapes and structural resistance are established, the coordinate reduction and equivalent SDOF analysis procedures are identical to the procedures applied to two-dimensional systems. The only additional difficulty arises from the fact that the orthogonality conditions associated with the principal directions of the structure will be effected by the onset of nonlinear behavior. Therefore, the influence of loading in one principal direction on the inelastic displacement response in the other principal direction must also be examined.

The simple three-dimensional structure shown in Figure 3.34 can be used to demonstrate the application of the SDOF analysis procedure to three-dimensional systems. The

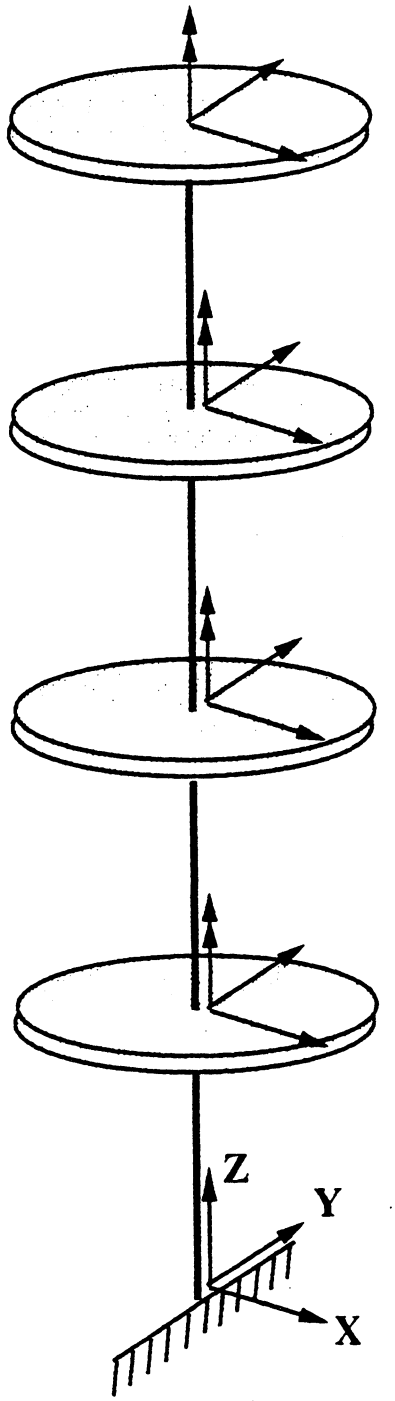

Figure 3.33 Rigid Diaphragm Model for 3-D Buildings

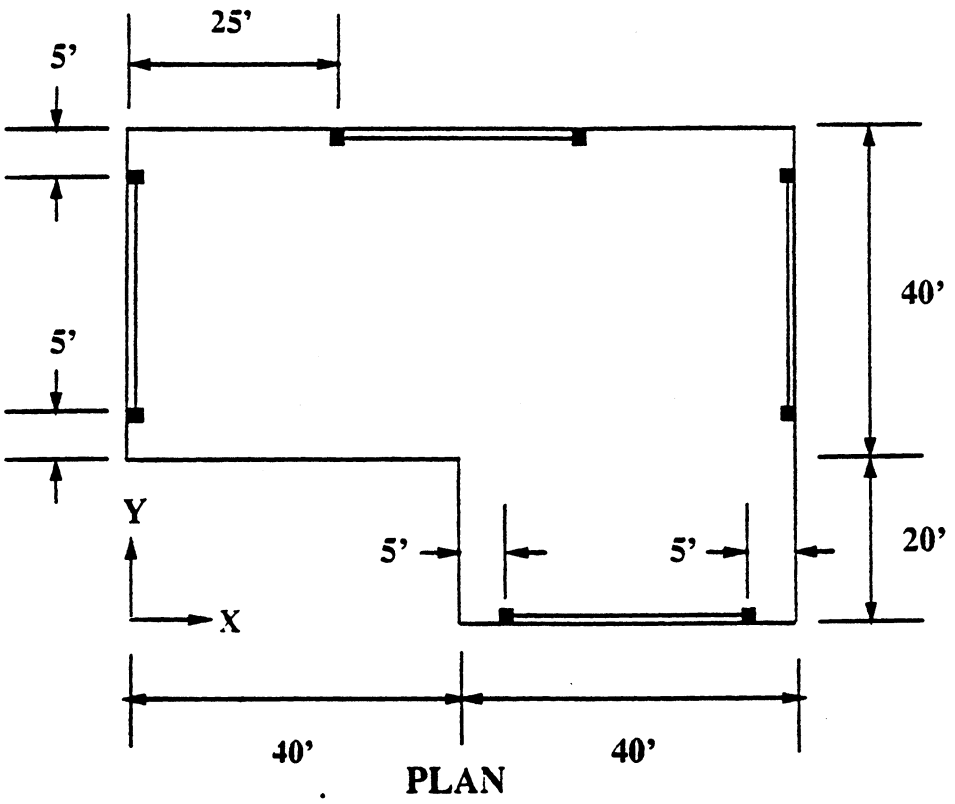

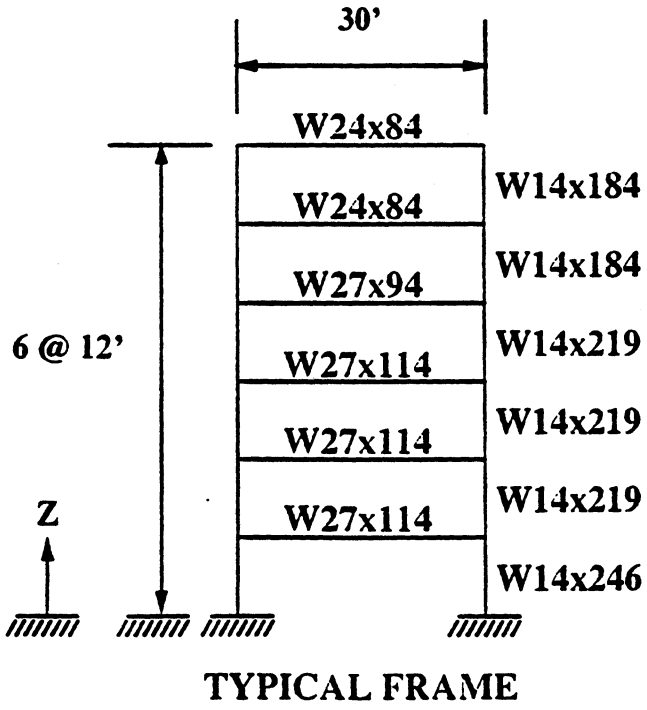

Figure 3.34 Simple 3-D Building System

building is a six story system consisting of four identical one bay frame substructures. The frames are arranged to provide equal lateral force resistance in the X and Y directions. Since the out-of-plane stiffness of the frames is negligible, each frame is capable of resisting only in-plane forces. Thus the structure is simplified to a three-dimensional system of two-dimensional frame substructures. The L shaped plan of the slab connecting the frames insures a dynamic eccentricity, resulting in the mode shapes of the building having a true three-dimensional character.

The building was first analyzed using the SAP89 [73] computer program for linear three-dimensional response analysis. The following assumptions were employed in the analysis:

a) The structure was idealized as an assemblage of three-dimensional elastic frame elements.

b) 190 kip story weights and a 110 kip roof weight were assumed.

c) All shear deformations were neglected.

d) All of the nodes at a story level were slaved to a master node, enforcing a rigid diaphragm assumption. This resulted in three dynamic DOF per story for a total of 18 dynamic DOF. Each master node was located eccentrically with respect to the story center of gravity (eight inches of eccentricity in the X and Y directions) to augment the three-dimensional behavior of the system.

The first six vibration mode shapes and frequencies of the structure were computed. The resulting modal vibration properties are presented in Table 3.2.

Once the elastic mode shapes of the frame system were established, static collapse analyses using rectangular and triangular lateral force patterns were conducted in the principal directions of the three-dimensional system. The computer program 3DSCAS [36] was implemented to conduct the inelastic static analyses. The following assumptions were applied in the analysis;

TABLE 3.2 MODAL RESULTS FOR 3-D SYSTEM

Mode	Period (sec)	Base Shear Reaction Factor (X)	Base Shear Reaction Factor (Y)	Angle (deg)	Height (inches)	Radius (inches)
1	0.878	0.568	-0.823	-55.4	600.0	287.6
2	0.871	-0.823	-0.568	34.6	599.8	576.9
3	0.488	0.574	-0.819	-55.0	580.3	3565.0
4	0.289	0.551	-0.835	-56.6	3.93	301.9
5	0.287	-0.835	-0.551	33.4	4.41	561.0
6	0.163	0.609	-0.793	-52.5	4.27	2963.7

a) The structure is idealized as a system of two-dimensional frames, each an assemblage of two-dimensional beam-column elements, capable of yielding only at plastic hinges at the element ends.

b) All shear deformations were neglected.

c) All of the nodes at a story level were slaved to the master node, enforcing a rigid diaphragm assumption.

d) Axial force - bending moment interaction was considered in all column members.

e) 190 kip story weights and a 110 kip roof weight were assumed.

f) P-Δ effects were accounted for by using the geometric stiffness associated with a two-dimensional truss element.

g) 1.0 % strain hardening in steel was assumed (E=30000 ksi).

h) Lumped static gravity loads were applied to the system to simulate the initial state of stress in the column elements prior to the application static lateral loads.

The base shear resistance versus lateral displacement relationships obtained from the analyses in the principal directions are shown in Figures 3.35 and 3.36. It should be noted that in general, the base shear versus lateral displacement relationship in a given principal direction may be unsymmetric, and hence must be established by analyses in both the positive and negative principal directions. Figure 3.37 illustrates the location of the roof master node in the X - Y plane for (positive and negative) rectangular loading in the principal directions. Figure 3.38 presents the absolute value of the response angle in the X - Y plane as a function of the base shear amplitude for rectangular loading in the principal directions. Both Figures 3.37 and 3.38 illustrate the range of displacements (or lateral forces) over which the response in one principal direction does not influence the response in the other principal direction (i.e., the range over which it is possible to estimate the MDOF response using a SDOF representation). The onset of effective yielding of the frames oriented in the X and Y directions is illustrated in these figures as a discontinuity in the displacement response path. It is possible that for more realistic three-dimensional systems

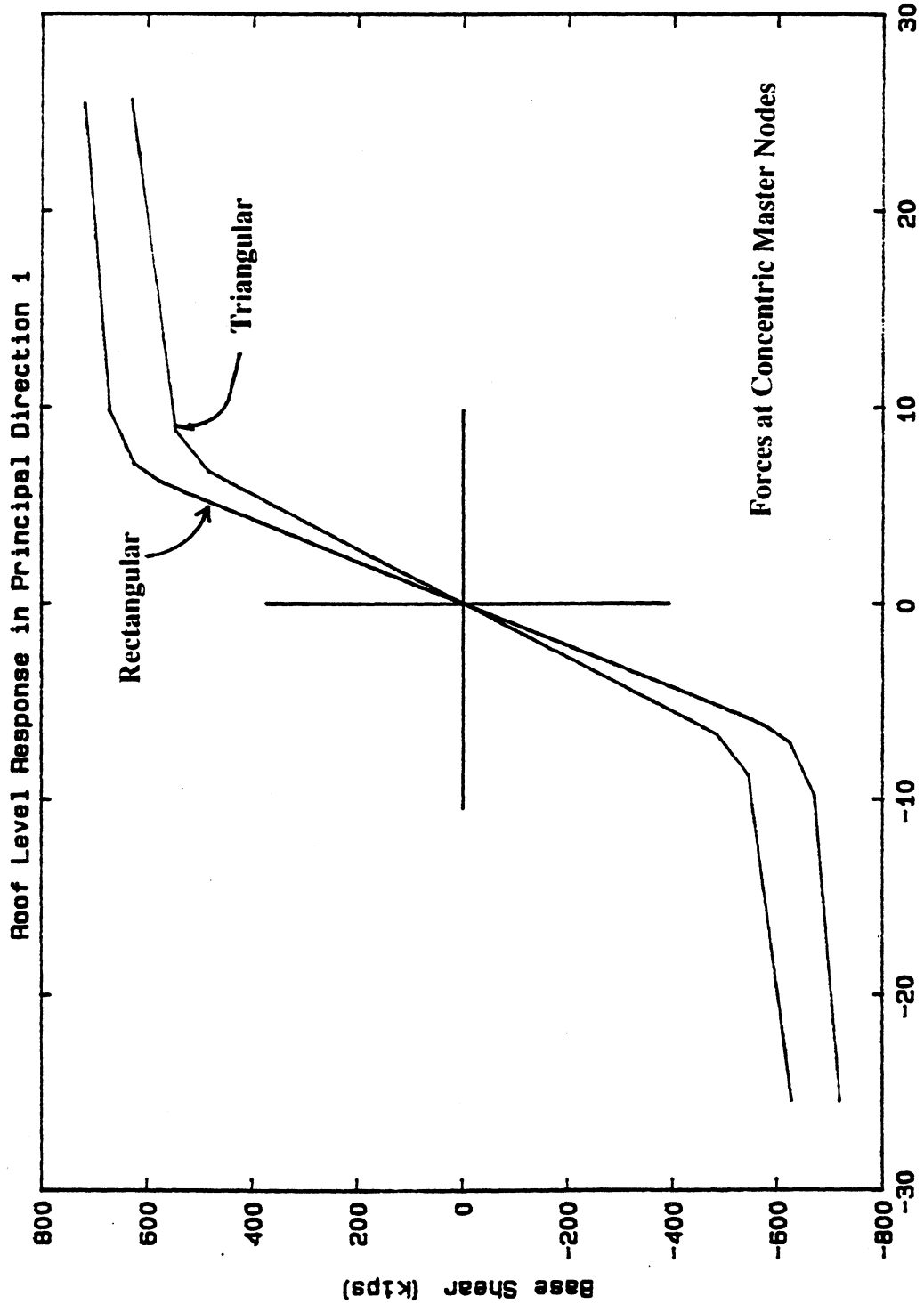

Figure 3.35 Response of 3-D System to Static Loading

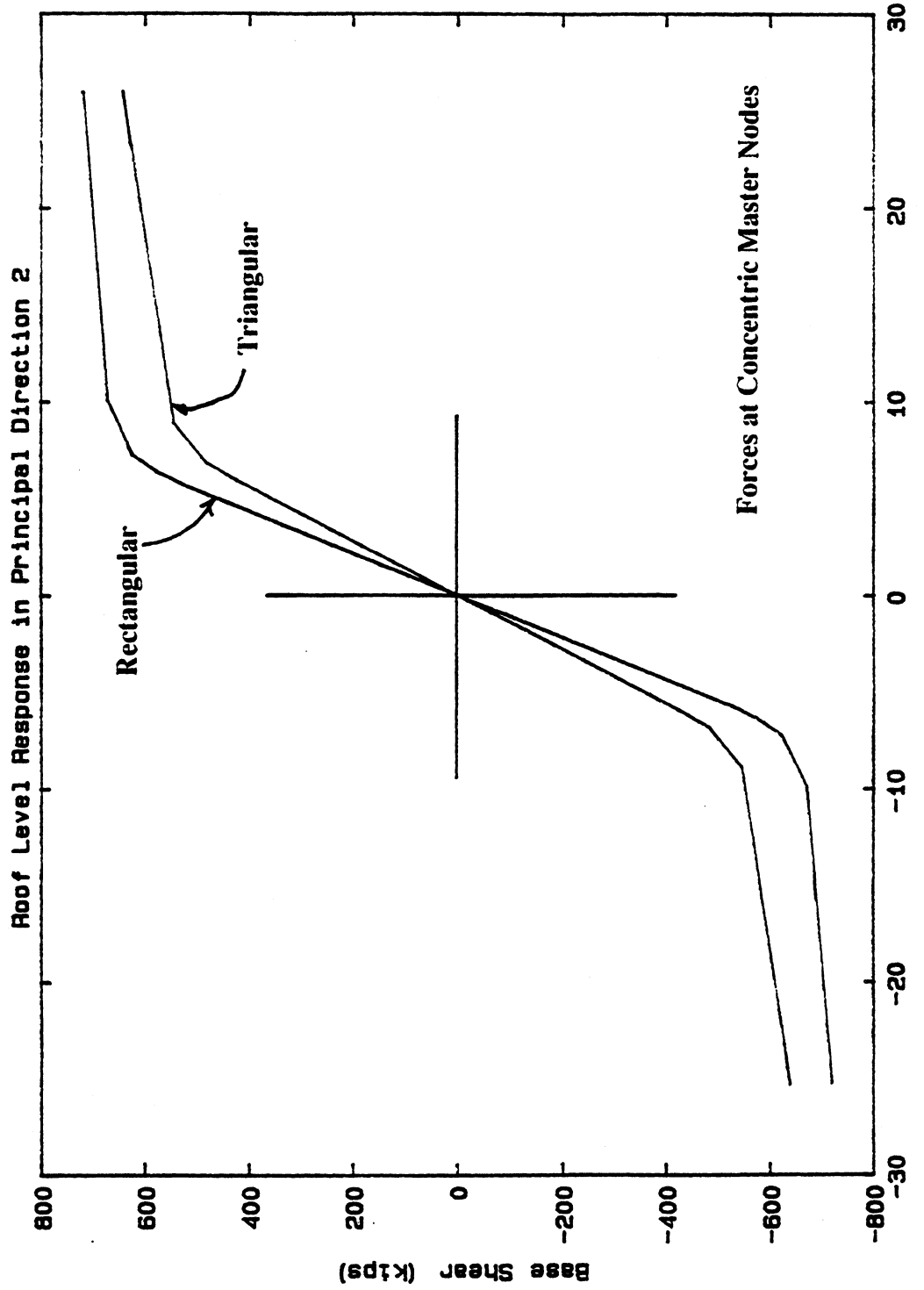

Figure 3.36 Response of 3-D System to Static Loading

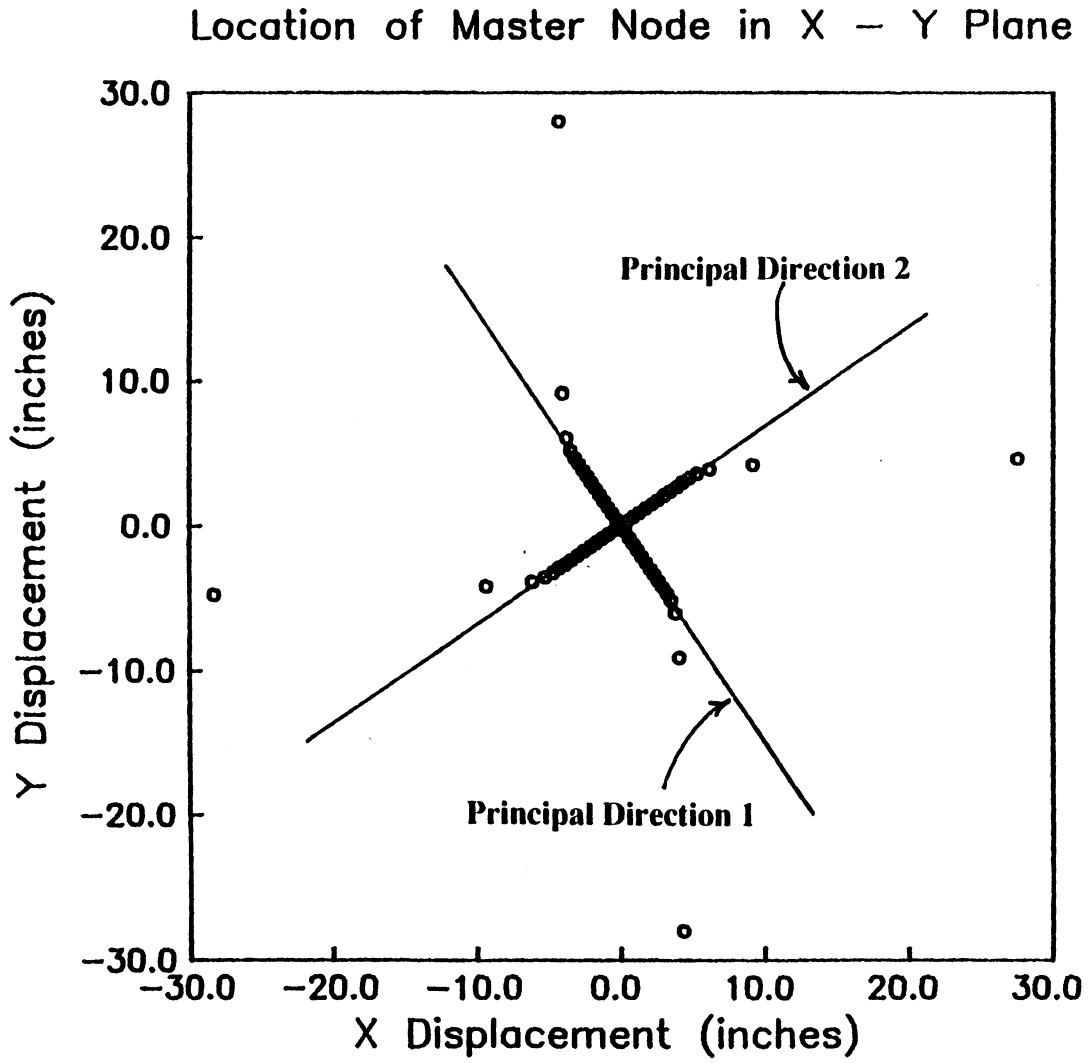

Figure 3.37 Roof Displacement Path for Loading in Principal Directions

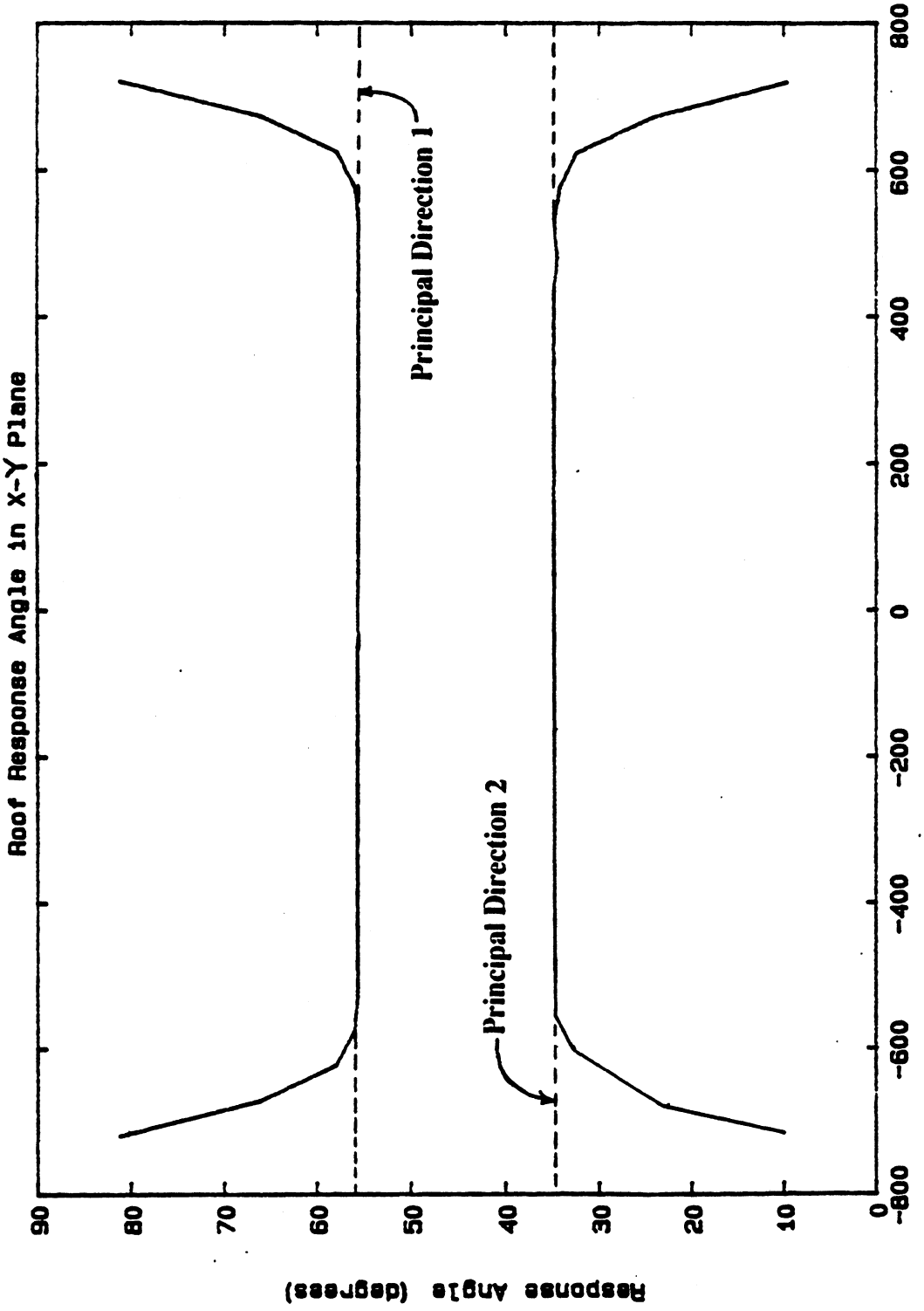

Figure 3.38 Roof Response Angle for Loading in Principal Directions

with a higher degree of redundancy, the effective yielding of frames with a given orientation would be less pronounced, which in turn would tend to increase the range over which the directions of the linear and nonlinear response are coincident.

It can also be argued that if the system were excited in uni-modal vibration in either of the first two modes, the inertial forces would provide a stabilizing or guiding influence, tending to maintain vibration in the principal direction, even after the onset of yielding in the frames oriented in the X and Y directions. The stabilizing influence of the inertial forces on the nonlinear vibration can be estimated by applying the static lateral loading with the constraint that the response of the structure remain oriented in the principal directions. This was accomplished by first relocating the story master nodes at a large radial distance (800 ft) away from the center of gravity of the stories along one of the principal directions. The master nodes were then restrained from translation in the X and Y directions. Triangular or rectangular moment patterns applied about the vertical (Z) axis at the master nodes located eccentrically along one principal direction produce the static equivalent of triangular or rectangular lateral force patterns oriented in the other principal direction. The rigid diaphragm between the master nodes and the structure constrain the system response to a circular arc tangent to either principal direction. Because the eccentricity is large with respect to the largest plan dimension of the building (a factor of ten was selected), the circular arc is essentially a straight line. Figures 3.39 through 3.42 provide a comparison of the base shear versus lateral displacement in the principal directions for triangular and rectangular load patterns induced by forces at concentric master nodes and by moments at eccentric master nodes. It is important to observe that the effective yielding strengths induced by the moment patterns applied at eccentric master nodes are roughly 10 to 15% larger than the corresponding effective yielding strengths induced by the force patterns applied at concentric master nodes. The post-yielding stiffness obtained with the moment induced loading are observed to be slightly larger than the post-yielding stiffness obtained with the translational force patterns. The strength and post-yielding stiffness increases observed when the lateral loads are induced by moments at eccentric master

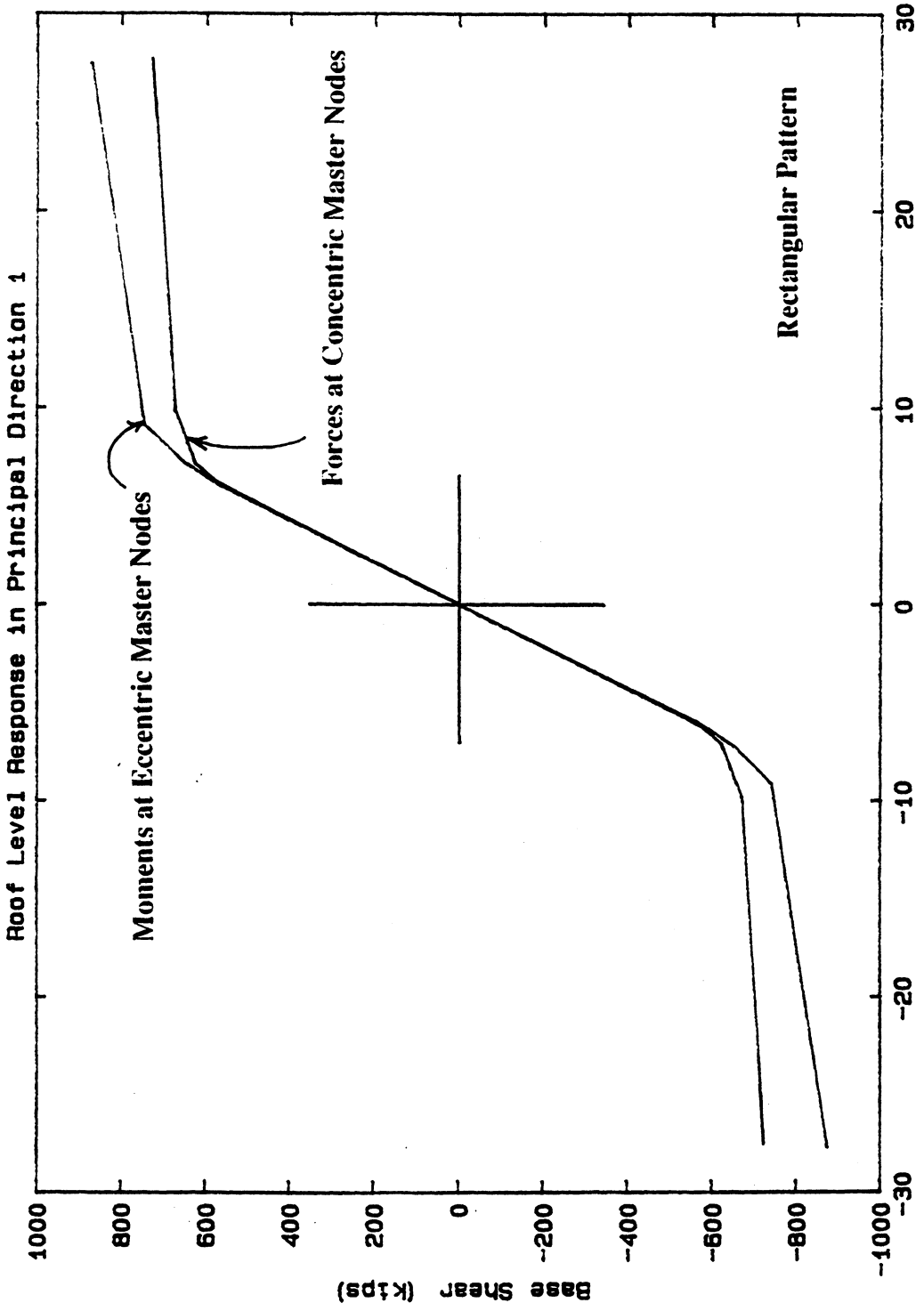

Figure 3.39 Response of 3-D System to Static Loading

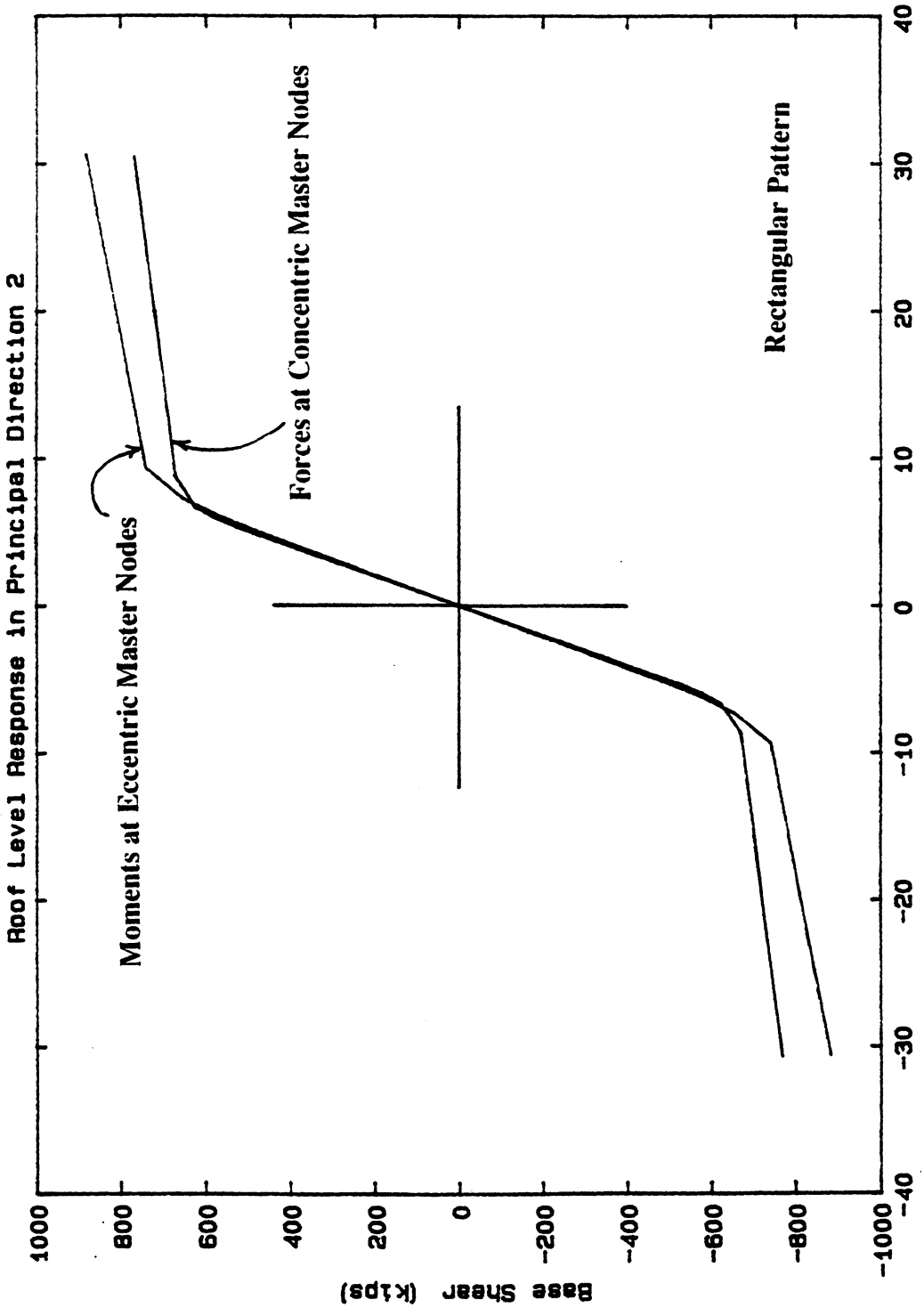

Figure 3.40 Response of 3-D System to Static Loading

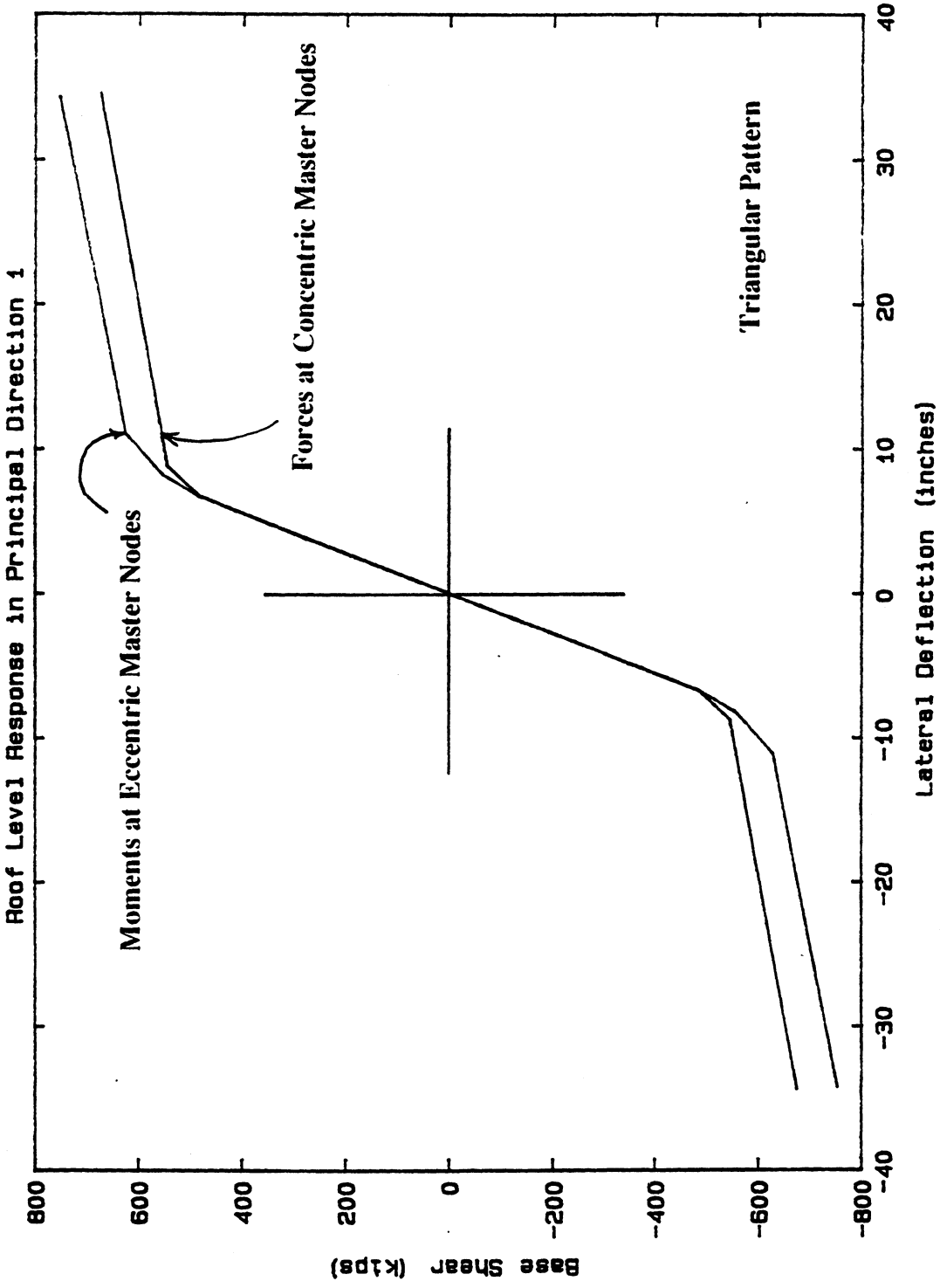

Figure 3.41 Response of 3-D System to Static Loading

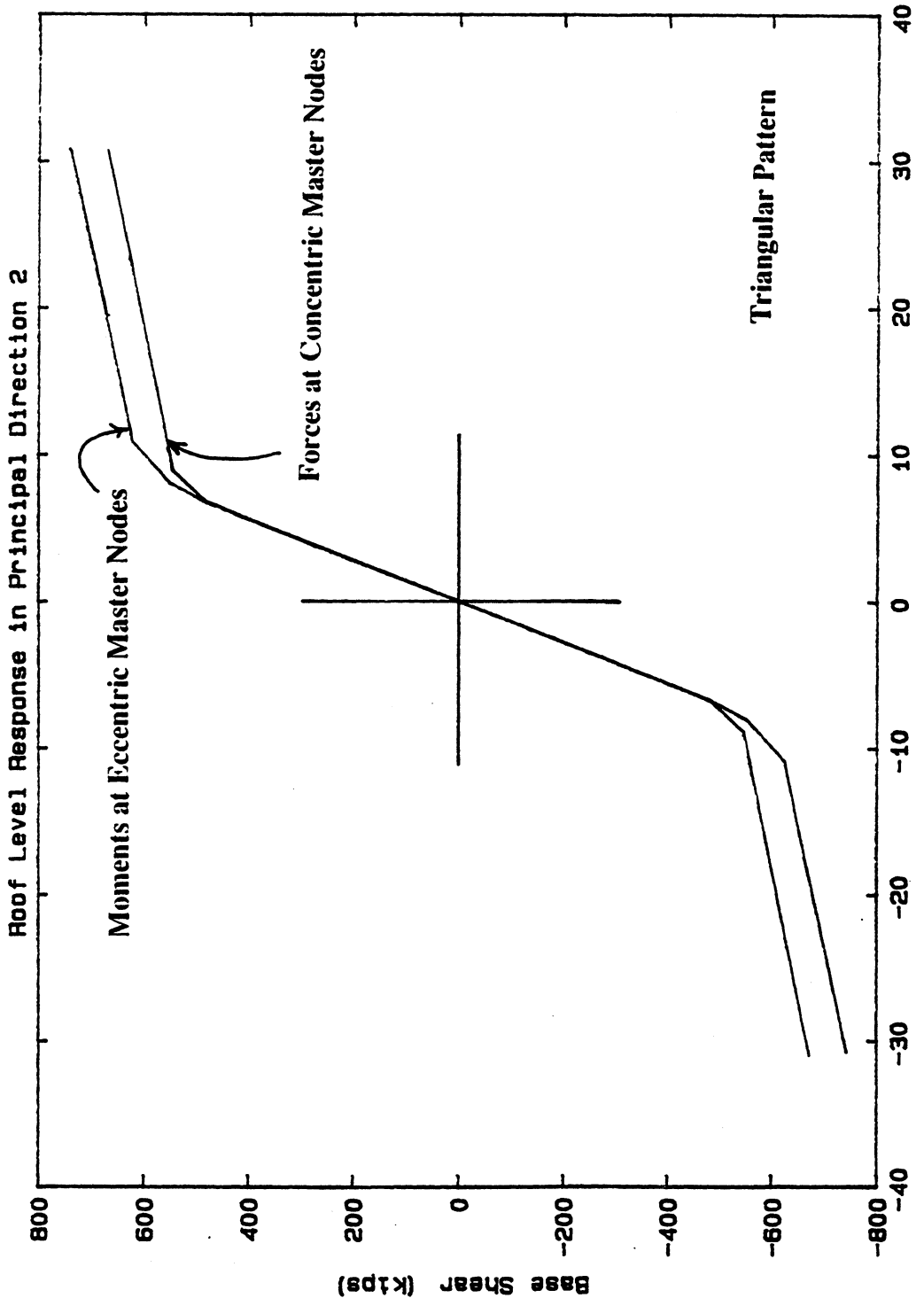

Figure 3.42 Response of 3-D System to Static Loading

nodes are the result of a more uniform distribution of yielding between the frames oriented in the X and Y directions.

Based on the discussions presented in Section 3.1.2.2 and in Appendix D, it is reasonable to assume that the MDOF response to the actual dynamic lateral force distributions acting on the system in the principal directions can be approximated by the static response to either triangular or rectangular lateral load patterns. It is aslo reasonable to assume that for a given lateral force pattern, the MDOF dynamic response would lie somewhere between the static response induced by moments at eccentric master nodes and that induced by concentric force patterns.

3.2.5. Design Evaluation Based on Harmonic Analyses

As previously discussed, a pure harmonic seismic loading can be used to obtain upper bounds on the cyclic response demands placed on structures subjected to "harmonic type" ground surface motions frequently observed at soft soil sites. The use of pure harmonic earthquake loading neglects the complex nature of earthquake loading but provides an attractive simplification wherein the earthquake is completely defined by the acceleration amplitude A_g and the vibration period T_g. For seismic design applications, it is important to establish measures of structural response which can be used to assess the performance of various designs. Typically, structural response is quantified by examining various peak response parameters [43,44] or the energy balance in the structural system [68]. The use of harmonic earthquake loading simplifies the assessment of the structural response since the response is entirely contained within a single cycle of steady-state vibration.

Conventional earthquake response spectra are plots of the maximum response (displacement, velocity, acceleration, ductility, etc.) of a SDOF structural representation subjected to a specific earthquake motion as a function of the elastic vibration frequency (or period) of the structure. As discussed in [13], it is common to subdivide earthquake response spectra into three distinct period regions; the short-period region where the maximum response is controlled by the maximum ground acceleration, the medium-period

region where the maximum response is controlled by the maximum ground velocity, and the long-period region where the maximum response is controlled by the maximum ground displacement.

In evaluating the response of a given structure to harmonic ground motions of a given amplitude, it is convenient to present plots of various response maxima as a function of the harmonic excitation frequency (or period). Harmonic spectra of this form differ from conventional earthquake response spectra in that they present the response maxima of one SDOF structure subjected to a range of harmonic earthquake motions as opposed to presenting the response maxima of a range of structures (defined by the elastic vibration period) excited by a single earthquake excitation. In situations where the predominant period (T_g) of the expected "harmonic type" site response is close to a natural period of structural vibration (T_s), a sweep of harmonic earthquake analyses at frequency ratios ($\beta = T_s/T_g$) in the vicinity of $\beta = 1.0$ can provide estimates of the structural response at or near resonant vibration conditions. Considering β values well above and below 1.0 can be useful in estimating structural response to relatively short and relatively long period ground motions.

The response maxima from a series of harmonic analyses over a range of T_g and A_g can be examined using two-dimensional spectra wherein the spectral ordinates are presented as a spectral surface above the $T_g - A_g$ plane. As an example, Figure 3.31 shows a three-dimensional perspective plot of the maximum ductilities obtained from harmonic analyses of a SDOF oscillator system at a grid of $T_g - A_g$ points. Alternately, a topographical plot of this spectral surface showing contours of equal ductility (as shown in Figure 3.43) can be used to determine the ductility demand corresponding to a given harmonic ground acceleration amplitude. Such plots can be useful in determining if the response demands associated with a given harmonic earthquake can be accommodated by the structure and the structural members.

Various procedures have been developed to evaluate seismic designs based on an

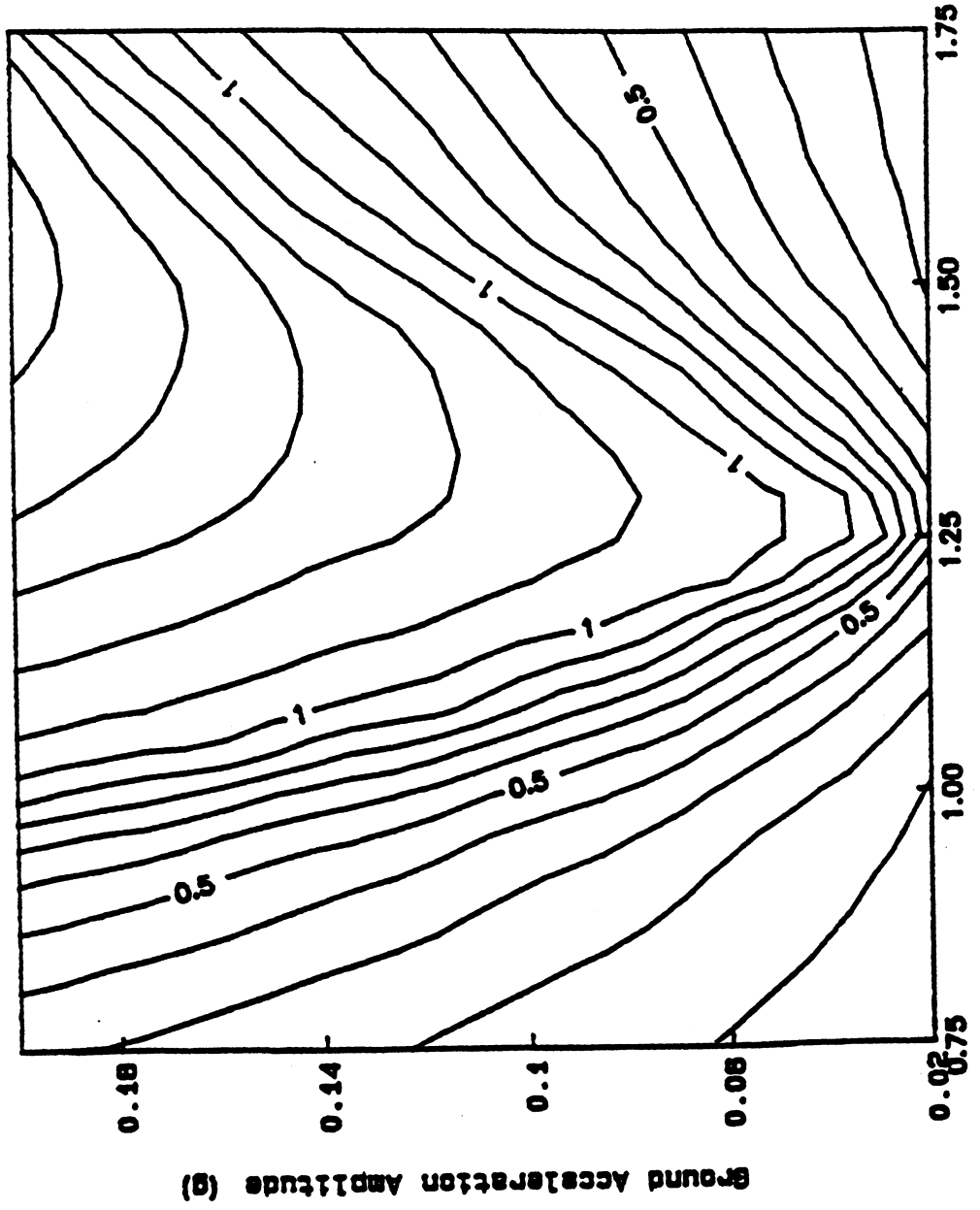

Figure 3.43 Topographical Plot of SDOF Spectral Ductility Surface

energy balance between the structure and the earthquake excitation. It is important to note that different expressions for earthquake input and kinetic energies result depending if the energy balance is developed using a relative or absolute formulation of the dynamic equilibrium equations [68]. The use of an absolute energy balance formulation is advantageous because it represents the earthquake input energy as the work done by the total shear at the base of the structure moving through the base displacement rather than as an equivalent lateral force moving through the relative structural displacements. In any case, the fundamental idea behind energy based procedures is that the energy dissipation and absorption supply of the structure must exceed the energy dissipation and absorption demands associated with the seismic loading. For the special case of steady-state vibration under harmonic earthquake excitation, the energy balance of the system can be evaluated on a "per cycle" basis. As an example, the area contained in a steady-state hysteresis loop represents the hysteretic energy dissipated during a steady-state vibration cycle. Moreover, normalizing the cyclic energy quantities by the vibration period T_g provides an estimate of the mean rate at which the energy quantities evolve. Examining the evolution of various energy quantities over a steady-state cycle can provide a means of assessing the energy balance as a function of the frequency ratio β.

CHAPTER 4

SOIL-STRUCTURE INTERACTION ANALYSIS

Soil-structure interaction (SSI) is one of the most widely studied phenomena in earthquake engineering. It is an important subject because the earthquake response of structures can be influenced significantly by the properties of the soil profile upon which they are founded and by the feedback mechanisms that can exist between the soil and the structure. The fundamental idea behind seismic SSI analysis techniques is that the structure and the soil site upon which it is founded form a combined dynamic system which responds to earthquake excitation. One of the most important considerations in SSI analysis is the potentially dangerous modifying effect of the site on the seismic waves as they propagate from the base rock to the ground surface (the bedrock motions in Mexico City were amplified by a factor of approximately five). Neglecting the seismic energy dissipated by the site can give rise to larger lateral forces, base shears and overturning moments which in turn could result in overly conservative elastic seismic designs. Another important consideration in SSI analysis is the interaction at and near the soil-structure interface which is influenced significantly by the foundation flexibility and the relative mass of the structure. Rocking behavior at the foundation level is known to increase the vibration period and frequently the damping in the structure's fundamental translational vibration mode(s) without greatly affecting the higher modes [48]. The increased vibration period is of particular concern for structures whose fixed base period is slightly below a large peak in the site response spectrum (for example, just below the peak near 2.0 seconds in the SCT pseudo acceleration spectrum shown in Figure 2.12). For such systems, an increased fundamental period could result in a dramatic increase in seismic excitation amplitude. Rocking behavior tends to magnify P-Δ effects and also tends to straighten the vibration shape of the fundamental translational mode(s) which results in a more triangular distribution of horizontal accelerations [48]. This observation may be important if simplified static analysis procedures are implemented to approximate seismic inertia force effects.

Many sophisticated SSI analysis procedures have been developed to account for numerous SSI phenomena; [6] provides an excellent overview of various SSI analysis procedures including general methods which consider structural embedment, arbitrary soil profile, foundation flexibility, spatial variation of the free-field motions and nonlinear behavior. It should be noted that rigorous SSI analysis procedures are typically only implemented for very important structures such as dams or nuclear power plants. The complex nature of the modeling and formulation of SSI analysis problems and the prohibitive costs associated with such analyses are the primary reasons why SSI analyses are not routinely utilized in seismic analysis for design of typical building structures.

In this chapter, the equations of dynamic equilibrium for soil-structure systems modeled using conventional SSI analysis procedures are presented. Simplified SSI analysis modeling procedures, which account for the effects of site response and foundation flexibility, are then discussed and illustrated for a simple soil-structure system.

4.1. General Equations of Motion

The dynamic equilibrium equations of interacting soil-structure systems depend on the modeling approach implemented. Various modeling approaches can be utilized to conduct SSI analysis, for example, the soil and the structure are modeled together as a dynamic system and the response of the combined system to base rock motions applied at the rock-soil boundary is computed. In another approach, the soil and the structure are modeled together and the response of the combined system to free-field motions (the motions which would result, in the absence of the structure, from the site response due to base rock motions) applied at the soil-structure interface is computed. Various substructure modeling approaches can also be employed.

A combined soil-structure system to be analyzed for base rock motions applied at the soil boundary is shown schematically in Figure 4.1. As shown in the figure, the structure is idealized using a lumped mass system of structural finite elements and the soil profile is discretized as a mesh of soil finite elements. Note that the soil mesh is selected so that

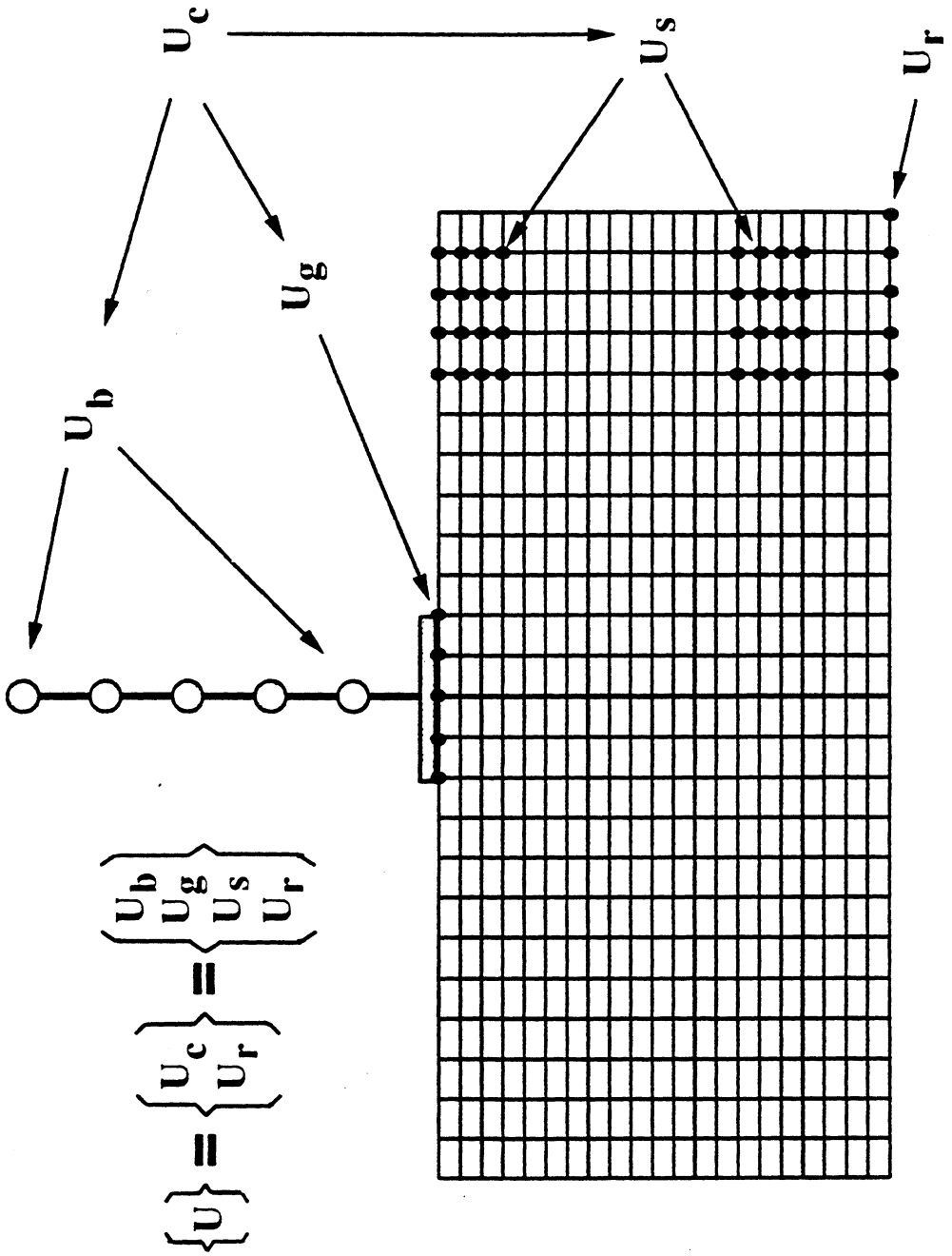

Figure 4.1 Schematic for Partitioning Combined Soil-Structure System

nodes are located coincident with the structural supports, forming the soil-structure interface. As developed in [11], the dynamic equilibrium for a discrete linear system which may have different support motions is:

$$\mathbf{M}\,\ddot{\mathbf{U}}(t) + \mathbf{C}\,\dot{\mathbf{U}}(t) + \mathbf{K}\,\mathbf{U}(t) = -(\mathbf{Mr} + \mathbf{M}_r)\,\ddot{\mathbf{U}}_r(t) \qquad (4.1)$$

The terms on the left hand side are the finite element property matrices and state vectors for the combined soil-structure system. The terms on the right hand side of the equation represent the earthquake load vector in which **M** is the MDOF lumped mass matrix, **r** is the static influence matrix, $\mathbf{M}_r$ is the mass coupling matrix which expresses the forces developed in the active DOF resulting from different base accelerations, and $\ddot{\mathbf{U}}_r(t)$ is the vector of base rock accelerations at the soil boundary. If the effect of different support motions is not considered, the base rock mass coupling matrix ($\mathbf{M}_r$) is dropped from the earthquake load vector. It should be noted that for nonlinear systems, the term $\mathbf{K}\,\mathbf{U}(t)$ on the left hand side can be replaced by the vector of static resisting forces, $\mathbf{R}_S(\mathbf{U})$.

In order to simplify subsequent derivations, the time dependence of the vectors, up to this point denoted by (t), will be implied (i.e., $\mathbf{U}(t) = \mathbf{U}$). As illustrated in Figure 4.1, the dynamic DOF's (**U**) of the combined soil-structure system can be partitioned into DOF associated with the base rock motions $\mathbf{U}_r$, and the combined soil-structure DOF, $\mathbf{U}_c$. The combined soil-structure DOF can be further partitioned into DOF associated with the building $\mathbf{U}_b$, the building-soil interface $\mathbf{U}_g$, and the soil $\mathbf{U}_s$. Following the free-field (or added motion) procedures outlined in [11], the equilibrium equations of the soil-structure system can be manipulated such that the effective earthquake load vector is a function of only the free-field motions of the contact DOF ($\mathbf{U}_g$) at the soil-structure interface. The following notation is employed:

$\tilde{\mathbf{M}}$, $\tilde{\mathbf{C}}$, and $\tilde{\mathbf{K}}$ are the property matrices of the soil system without the added structure

$\ddot{\tilde{\mathbf{U}}}_c$, $\dot{\tilde{\mathbf{U}}}_c$ and $\tilde{\mathbf{U}}_c$ are the total free-field motions which would result at the site in the absence of the structure

M_b, C_b, and K_b are the property matrices of the added structure

$\ddot{U}^t_c$, $\dot{U}^t_c$, and U^t_c are the total (absolute) added or interaction motions which reflect the difference between the total motion of the combined system and the free-field motion

The combined displacement vectors are partitioned as follows;

$$U^t_c = \begin{bmatrix} U^t_b \\ U^t_g \\ U^t_s \end{bmatrix} \qquad \tilde{U}_c = \begin{bmatrix} 0 \\ \tilde{U}_g \\ \tilde{U}_s \end{bmatrix} \tag{4.2}$$

while the combined mass, damping and stiffness matrices can be presented in the following form (presented here for the mass matrix only);

$$M_c = \begin{bmatrix} M_{bb} & M_{bg} & 0 \\ M_{gb} & M_{gg} & 0 \\ 0 & 0 & 0 \end{bmatrix} = \begin{bmatrix} M_b & 0 \\ 0 & 0 \end{bmatrix} \tag{4.3}$$

and

$$\tilde{M}_c = \begin{bmatrix} 0 & 0 & 0 \\ 0 & \tilde{M}_{gg} & \tilde{M}_{gs} \\ 0 & \tilde{M}_{sg} & \tilde{M}_{ss} \end{bmatrix} = \begin{bmatrix} 0 & 0 \\ 0 & \tilde{M}_s \end{bmatrix} \tag{4.4}$$

If the soil DOF are augmented to include the DOF at the boundary between the base rock and the soil system, the free-field equations of motion are;

$$\begin{bmatrix} \tilde{M}_{ss} & \tilde{M}_{sr} \\ \tilde{M}_{rs} & \tilde{M}_{rr} \end{bmatrix} \begin{bmatrix} \ddot{\tilde{U}}_s \\ \ddot{\tilde{U}}_r \end{bmatrix} + \begin{bmatrix} \tilde{C}_{ss} & \tilde{C}_{sr} \\ \tilde{C}_{rs} & \tilde{C}_{rr} \end{bmatrix} \begin{bmatrix} \dot{\tilde{U}}_s \\ \dot{\tilde{U}}_r \end{bmatrix} + \begin{bmatrix} \tilde{K}_{ss} & \tilde{K}_{sr} \\ \tilde{K}_{rs} & \tilde{K}_{rr} \end{bmatrix} \begin{bmatrix} \tilde{U}_s \\ \tilde{U}_r \end{bmatrix} = \begin{bmatrix} 0 \end{bmatrix} \tag{4.5}$$

The first matrix equation can be written as;

$$\tilde{M}_{ss} \ddot{\tilde{U}}_s + \tilde{C}_{ss} \dot{\tilde{U}}_s + \tilde{K}_{ss} \tilde{U}_s = -\tilde{M}_{sr} \ddot{\tilde{U}}_r - \tilde{C}_{sr} \dot{\tilde{U}}_r - \tilde{K}_{sr} \tilde{U}_r \tag{4.6}$$

where the right hand side is the earthquake load vector corresponding to the input motions at the rock-soil interface. When the building is superimposed on the soil, the properties and motion on the left hand side are modified by the added building motions while the input motions at the base rock level remain unchanged. The equilibrium equation of the combined soil-structure system subjected to rock motion input is:

$$\left[\tilde{M}_c + M_c\right]\left\{\ddot{\tilde{U}}_c + \ddot{U}_c^t\right\} + \left[\tilde{C}_c + C_c\right]\left\{\dot{\tilde{U}}_c + \dot{U}_c^t\right\} + \left[\tilde{K}_c + K_c\right]\left\{\tilde{U}_c + U_c^t\right\}$$

$$= -\tilde{M}_{sr}\ddot{\tilde{U}}_r - \tilde{C}_{sr}\dot{\tilde{U}}_r - \tilde{K}_{sr}\tilde{U}_r \qquad (4.7)$$

which can be manipulated into the following form;

$$\left[\tilde{M}_c + M_c\right]\ddot{U}_c^t + \left[\tilde{C}_c + C_c\right]\dot{U}_c^t + \left[\tilde{K}_c + K_c\right]U_c^t$$

$$= -M_c\ddot{\tilde{U}}_c - C_c\dot{\tilde{U}}_c - K_c\tilde{U}_c \qquad (4.8)$$

The right hand side of this expression can be reduced to;

$$= \begin{bmatrix} M_{bg} \\ M_{gg} \\ 0 \end{bmatrix}\ddot{\tilde{U}}_g + \begin{bmatrix} C_{bg} \\ C_{gg} \\ 0 \end{bmatrix}\dot{\tilde{U}}_g + \begin{bmatrix} K_{bg} \\ K_{gg} \\ 0 \end{bmatrix}\tilde{U}_g \qquad (4.9)$$

resulting in an earthquake load vector that is a function of only the free-field motions at the soil-structure interface. If the structure is embedded in the soil, different interface DOF will have different free-field motions, requiring the solution of a scattering problem [6]. Note that the earthquake load vector obtained with the formulation presented in Equation (4.9) requires the free-field velocities and displacements which must be obtained by integrating the free-field acceleration record. This inconvenience can be eliminated by expressing the added displacement response U_c^t as the sum of the relative and pseudo-static components [11];

$$U_c^t = U_c + r_c\tilde{U}_g \qquad (4.10)$$

where the influence matrix, r_c is defined as;

$$r_c = -\left[\tilde{K}_c + K_c\right]^{-1}\begin{bmatrix} K_{bg} \\ K_{gg} \\ 0 \end{bmatrix} \qquad (4.11)$$

The pseudo-static motion represents the motion of the combined system produced by the free-field displacements imposed at the contact DOF when dynamic effects are neglected. If the damping proportional part of the earthquake load vector (which is typically quite small relative to the mass proportional part) is neglected, the equilibrium equation can be expressed with the following simplified formulation;

$$\left[\tilde{M}_c + M_c\right]\ddot{U}_c + \left[\tilde{C}_c + C_c\right]\dot{U}_c + \left[\tilde{K}_c + K_c\right]U_c = -\left[\left[\tilde{M}_c + M_c\right]r_c + \begin{bmatrix} M_{bg} \\ M_{gg} \\ 0 \end{bmatrix}\right]\ddot{\bar{U}}_g \qquad (4.12)$$

If it is assumed that the free-field motions are the same at all contact DOF, the resulting pseudo-static displacements reduce to rigid body motions, and Equation (4.12) reduces to;

$$\left[\tilde{M}_c + M_c\right]\ddot{U}_c + \left[\tilde{C}_c + C_c\right]\dot{U}_c + \left[\tilde{K}_c + K_c\right]U_c = -\begin{bmatrix} M_{bg} \\ M_{gg} \\ 0 \end{bmatrix}\ddot{\bar{U}}_g \qquad (4.13)$$

4.2 Simplified Methods

As previously discussed, the complex nature of the modeling procedures and the problem formulation associated with SSI analysis has resulted in an extremely limited application of SSI analyses for seismic design of typical building structures. However, when the uncertainties associated with earthquake motions and the uncertainties associated with the material properties of the soil and the structure are considered, it can be argued that rigorous SSI analysis procedures are unduly complicated and the results of such analyses are of questionable value. With this in mind, it may be possible and desirable to implement simplified SSI analysis methods which attempt to capture the most important features of the response of soil-structure systems. The basic motivation behind the use of simplified SSI procedures is that the level of sophistication of the analysis should be compatible with the uncertainties of the input motion and the system material properties.

Because rigorous SSI analysis methods treat the building and the site as a combined dynamic system, they implicitly include; the site response, the structural response, the influence of the site on the structural response and the influence of the structure on the site response. The two most important characteristics of the earthquake response of soil-structure systems are, 1) the dynamic response of the soil profile, and 2) the effect of the soil (foundation) flexibility on the structural response. In this section, simplified

procedures which attempt to include the effects of site amplification and foundation flexibility are discussed.

For very massive structures, such as dams or nuclear power plants, the earthquake motions which develop at the soil-structure interface are likely to be significantly different from the motions which would develop in the absence of the structure. For typical building structures, which are far less massive then dams or nuclear power plants, the structure has a much smaller, more localized influence on the response of the site, which is typically assumed to be negligible. This is a reasonable assumption, since the volume (or mass) of the soil (which is essentially solid) far exceeds the volume (or mass) of the structure (which is mostly open space or "voids") in the combined soil-structure system. In fact, the net overburden effect of a building is often no greater than that of small soil berm at the ground surface. Based on this observation, and considering the stochastic nature of earthquake ground motions, it is reasonable to use the free-field motions directly as input to the structural model. With this approach, it is possible to obtain the seismic input for the structural model from separate site response analyses, from previously recorded accelerograms, or from artificial earthquake records compatible with a site specific response spectrum.

Perhaps the best simplified procedure to account for the effect of foundation flexibility on the structural response is the so called "massless foundation method" [10,25], which implements the free-field formulation. This method was developed based on the observation that although the property matrices and state vectors on the left hand side of Equation (4.13) involve the DOF of the combined soil-structure system, the earthquake load vector on the right hand side does not involve any of the mass associated with the soil DOF. The matrix formulation of the massless foundation method is illustrated in Figure 4.2 for an undamped soil-structure system. It is evident that this procedure neglects the effect of soil mass at the soil-structure interface (i.e., the terms in $\tilde{\mathbf{M}}_{gg}$ are negligible relative to the terms in $\mathbf{M}_{gg}$) but includes the effect of soil stiffness (or flexibility) at the soil-structure

$$\left[M_b\right] = \begin{bmatrix} M_{bb} & M_{bg} \\ M_{gb} & M_{gg} \end{bmatrix} \qquad \left[K_b\right] = \begin{bmatrix} K_{bb} & K_{bg} \\ K_{gb} & K_{gg} \end{bmatrix}$$

$$\left[\tilde{M}_s\right] = \begin{bmatrix} \tilde{M}_{gg} & \tilde{M}_{gs} \\ \tilde{M}_{sg} & \tilde{M}_{ss} \end{bmatrix} \qquad \left[\tilde{K}_s\right] = \begin{bmatrix} \tilde{K}_{gg} & \tilde{K}_{gs} \\ \tilde{K}_{sg} & \tilde{K}_{ss} \end{bmatrix}$$

Consistent Formulation:

$$\begin{bmatrix} \begin{bmatrix} M_b & \end{bmatrix} & 0 \\ 0 & \begin{bmatrix} & \tilde{M}_s \end{bmatrix} \end{bmatrix} \begin{bmatrix} \ddot{U}_b \\ \ddot{U}_g \\ \ddot{U}_s \end{bmatrix} + \begin{bmatrix} \begin{bmatrix} K_b & \end{bmatrix} & 0 \\ 0 & \begin{bmatrix} & \tilde{K}_s \end{bmatrix} \end{bmatrix} \begin{bmatrix} U_b \\ U_g \\ U_s \end{bmatrix} = - \begin{bmatrix} M_{bg} \\ M_{gg} \\ 0 \end{bmatrix} \ddot{\tilde{U}}_g$$

Massless Foundation Formulation:

$$\begin{bmatrix} M_b \end{bmatrix} \begin{bmatrix} \ddot{U}_b \\ \ddot{U}_g \end{bmatrix} + \begin{bmatrix} K_{bb} & K_{bg} \\ K_{gb} & \left[K_{gg} + \tilde{K}_{gg}\right] \end{bmatrix} \begin{bmatrix} U_b \\ U_g \end{bmatrix} = - \begin{bmatrix} M_{bg} \\ M_{gg} \end{bmatrix} \ddot{\tilde{U}}_g$$

Figure 4.2 Illustration of Massless Foundation Formulation

interface (i.e., the terms in $\bar{\mathbf{K}}_{gg}$ are significant relative to the terms in $\mathbf{K}_{gg}$). Thus, the method is physically analogous to including massless foundation springs at the interface DOF, as illustrated schematically in Figure 4.3.

An experimental and analytical investigation of a thirty story condominium building [66] indicated that a flexible foundation model did provide better correlation with experimental results. However, very little structure-foundation interaction was observed. Flexible foundation models were also shown to provide good agreement between analytical and measured vibration periods for both free-vibration and aftershock tests conducted on a multi-story building in Chile after the March 3, 1985 earthquake [71]. Analytical sensitivity studies [25] of a two-dimensional, ten story, one bay frame (similar to the frame investigated in Chapter 3) founded on soft soil compared the results of a fixed base system with systems which included various foundation extents. These studies indicated that, as expected, interaction effects were not significant and were mainly manifested by a slight increase in the vibration periods. Similar sensitivity studies [25] conducted on a gravity dam which was the subject of previous experimental and analytical investigations [10], compared the response spectrum analysis results obtained using a massless foundation formulation with those obtained using a consistent formulation. The study indicated that for this structure (where soil-structure interaction effects are significant) the massless foundation method provided an excellent approximation of the periods of the first and second modes of the system but tended to underestimate the periods of the higher modes. However, since soil-structure interaction effects are most significant in the low modes, the base shears and top displacements computed with the massless foundation method were essentially the same (within 4%) as those computed using the consistent formulation.

These results indicate that the massless foundation formulation can be used to account for the effect of foundation flexibility and provides an excellent approximation to the more rigorous, consistent formulation. For soils that can be idealized as a homogeneous elastic half-space, springs which represent resistance of the half-space to the transla-

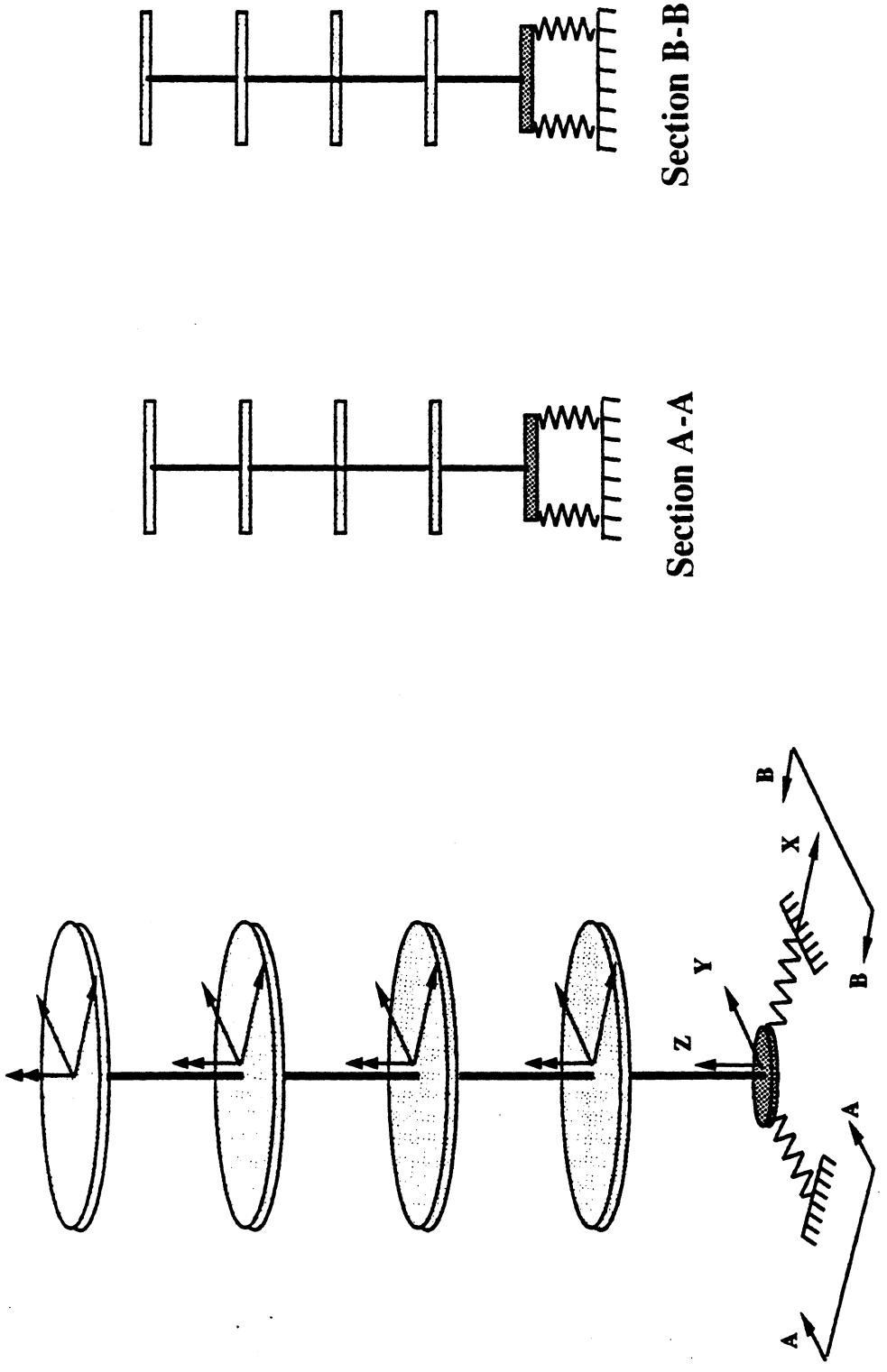

Figure 4.3 Schematic of 3-Dimensional Soil-Structure System

tional and rotational DOF of a rigid circular plate (foundation) supported at the surface [11,48] can be used to model the foundation resistance at the soil-structure interface. ATC-3-06 [3] provides guidelines for computing the increase in the vibration periods based on a knowledge of the foundation stiffness values. Approximate procedures can be used to estimate the flexibility of deep foundations or foundations on piles. Even order-of-magnitude estimates of the foundation flexibility of the structure, based on engineering judgement, are superior to assuming that the structure is fixed rigidly at the base.

4.3. Application to Simplified Soil-Structure System

As an illustration of simplified seismic analysis including site effects, analyses were conducted on a simple soil-structure system. The system consisted of the SCT soil profile model investigated in Chapter 2 (Figure 2.11) and the two-dimensional frame studied in Chapter 3 (Figure 3.5).

Linear site response analysis was conducted on the SCT site model subjected to the first 30.0 seconds of the CUMV EW base input. The computed SCT surface acceleration history, which has a peak ground acceleration of 0.16g, is shown in Figure 4.4, and the pseudo-acceleration spectrum is shown in Figure 2.16. It should be noted that, aside from some apparent higher frequency motions in the very beginning and near the end of the acceleration history, the response is nearly harmonic with a vibration period (T_g) of roughly 2.0 seconds and "steady-state" amplitude of slightly larger than 0.10g.

The two-dimensional frame system was assumed to be founded on a rigid, massless foundation disk with a 25 ft radius. The soil profile was idealized as a homogeneous elastic half-space with a shear modulus equal to the weighted average of the layer shear moduli shown in Figure 2.11. As presented in [11,48], the rotational stiffness of a circular disk on an elastic half-space is:

$$K_\theta = 2.7\, G\, r^3 \tag{4.14}$$

which for this system is K_θ = 38,475,000 kip-inches/radian. Adding this massless foundation spring to the base of the frame results in a 3% increase in the fundamental vibration

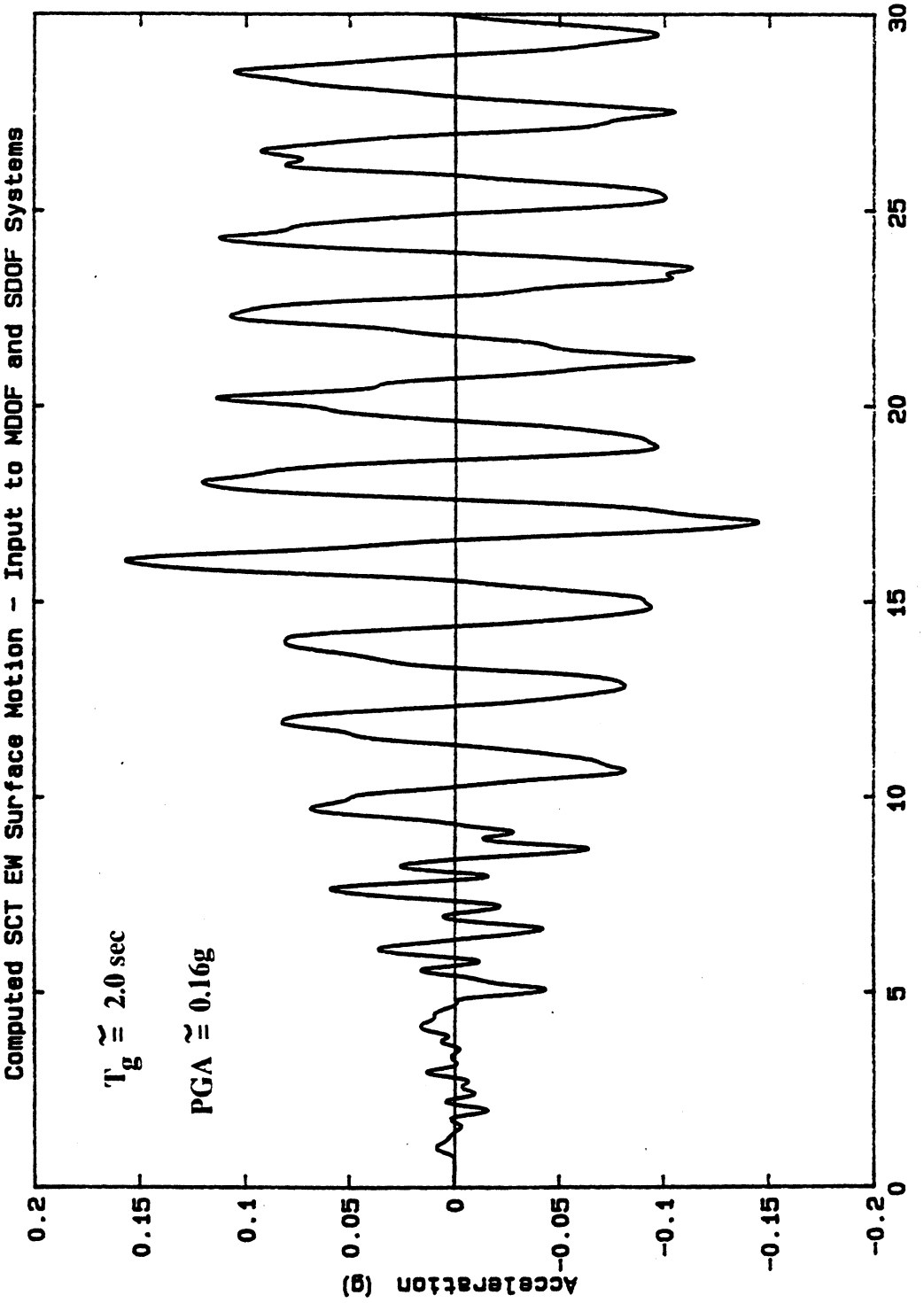

Figure 4.4 Surface Motion Input to 2-D Frame System

period T_1 from 1.25 to 1.29 seconds.

The computed SCT surface motion was used as free-field input to the MDOF and SDOF representations of the two-dimensional system. The analyses were conducted using DRAIN-2DX [1] employing step-by-step, event-to-event dynamic analysis [2] as discussed in Section 3.2.2.1. The time and amplitude axes of the near harmonic input motion were scaled to obtain four combinations of peak ground acceleration (PGA) and predominant site period T_g, namely; a) $T_g \approx 2.0$ seconds and PGA = 0.16g, b) $T_g \approx 2.0$ seconds and PGA = 0.32g, c) $T_g \approx 1.25$ seconds and PGA = 0.16g and d) $T_g \approx 1.25$ seconds and PGA = 0.32g. Combinations a) and b) reflect the site vibration conditions in downtown Mexico City, while combinations c) and d) were selected to represent resonant conditions between the site and the structure. Figures 4.5 through 4.8 present the roof displacement histories computed with the MDOF and SDOF models, while the base shear histories are shown in Figures 4.9 through 4.12. The following observations can be made regarding the correlation of the MDOF and SDOF analysis results:

1) The maximum roof displacements computed with the MDOF and SDOF representations are in good agreement. The worst agreement was obtained for $T_g \approx 2.0$ seconds and PGA = 0.32g where the SDOF maximum displacement exceeds that of the MDOF system by roughly 20%; for all other cases the maximum SDOF and MDOF roof displacements were within 10% agreement. The maximum base shears computed with the MDOF and SDOF representations are reasonably well correlated (all within 10% agreement).

2) For $T_g \approx 2.0$ seconds, the MDOF and SDOF roof displacement and base shear response histories are poorly correlated in the last 10.0 seconds of the record, possibly due to influence of higher frequencies in the MDOF response. For $T_g \approx 2.0$ seconds and PGA = 0.32g, the tilt in the SDOF oscillator response, which is the result of plastic base rotation induced by the large yielding excursion near 17.5 seconds, is not as pronounced in the MDOF system.

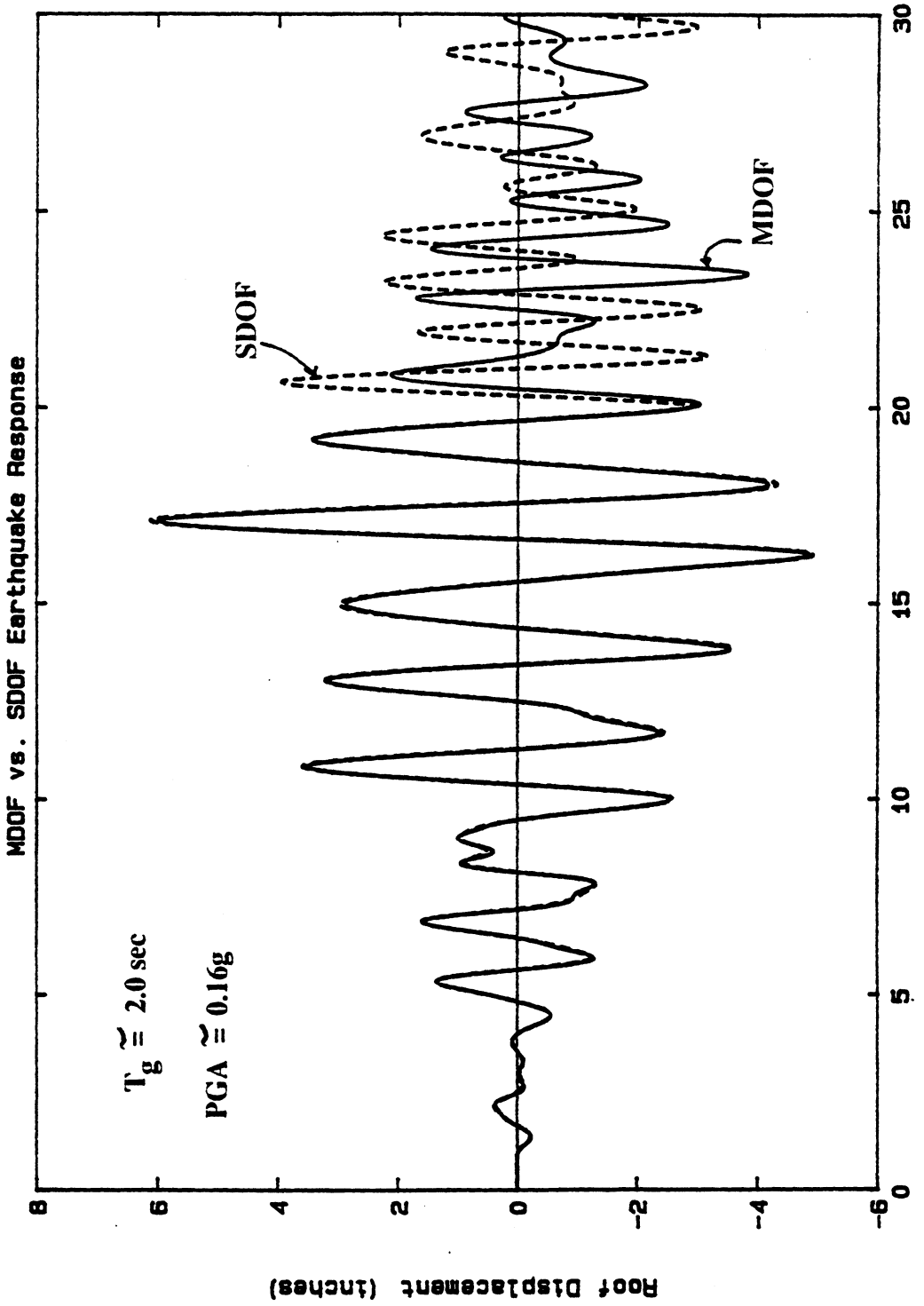

Figure 4.5 Response to Near Harmonic Earthquake

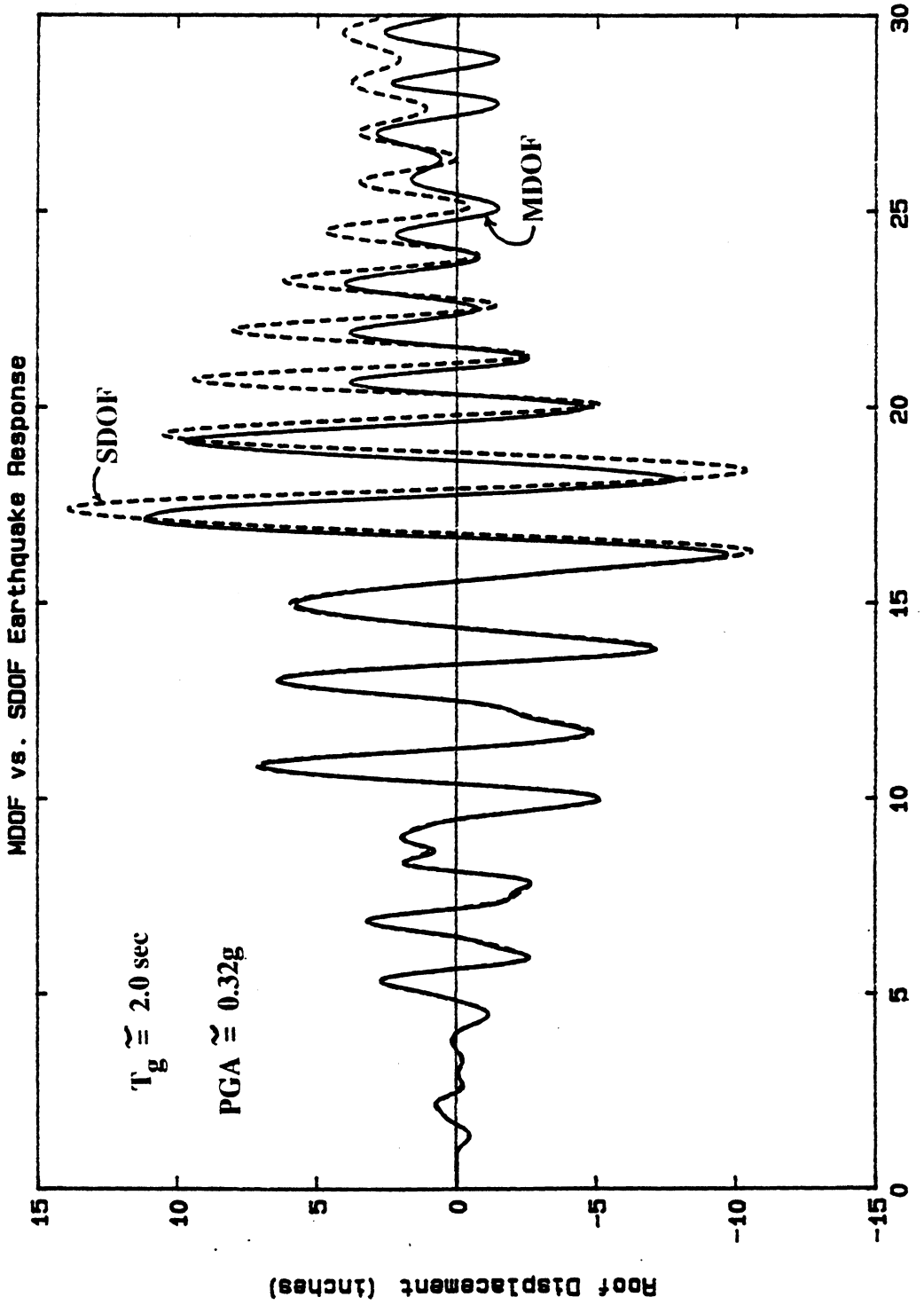

Figure 4.6 Response to Near Harmonic Earthquake

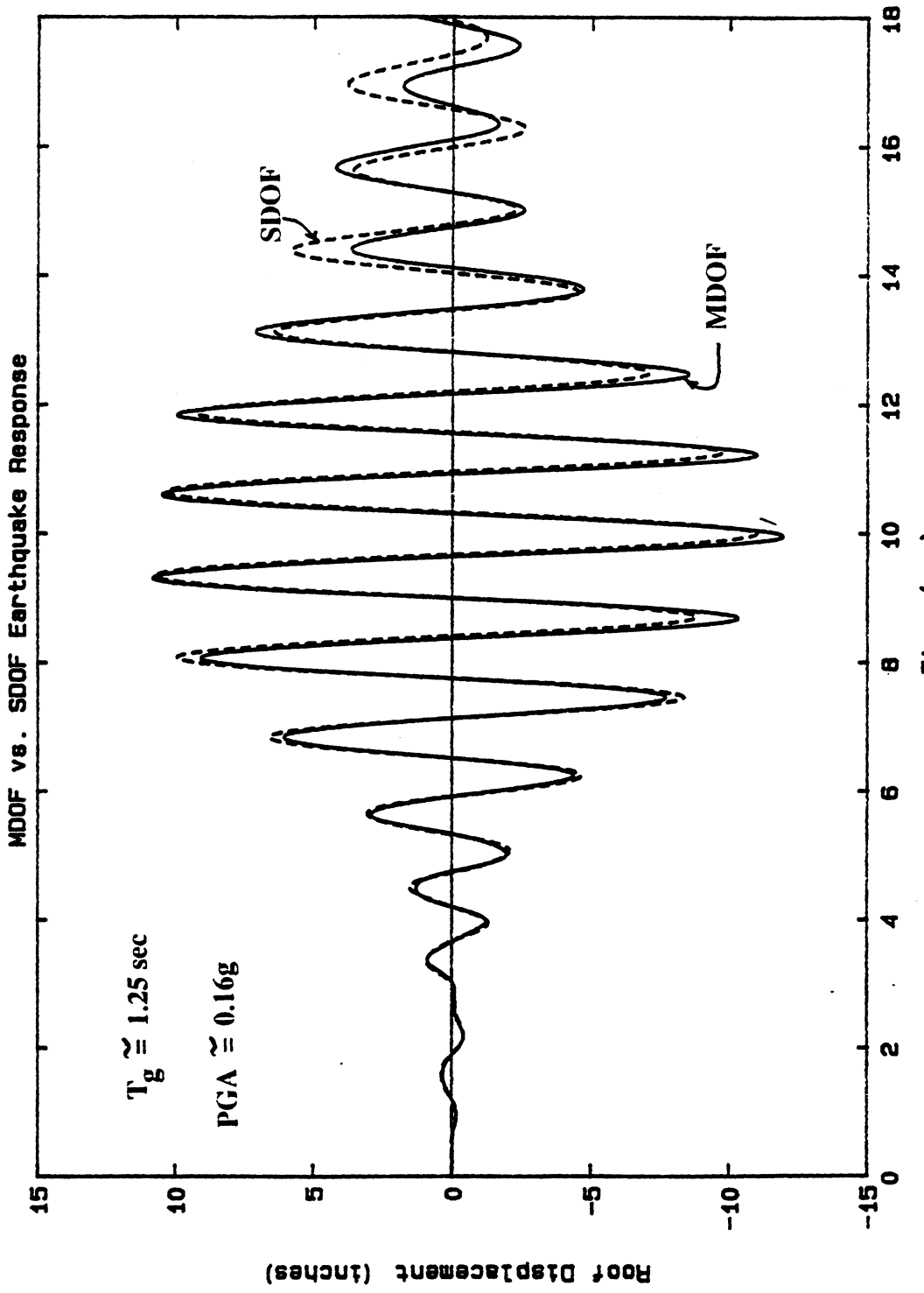

Figure 4.7 Response to Near Harmonic Earthquake

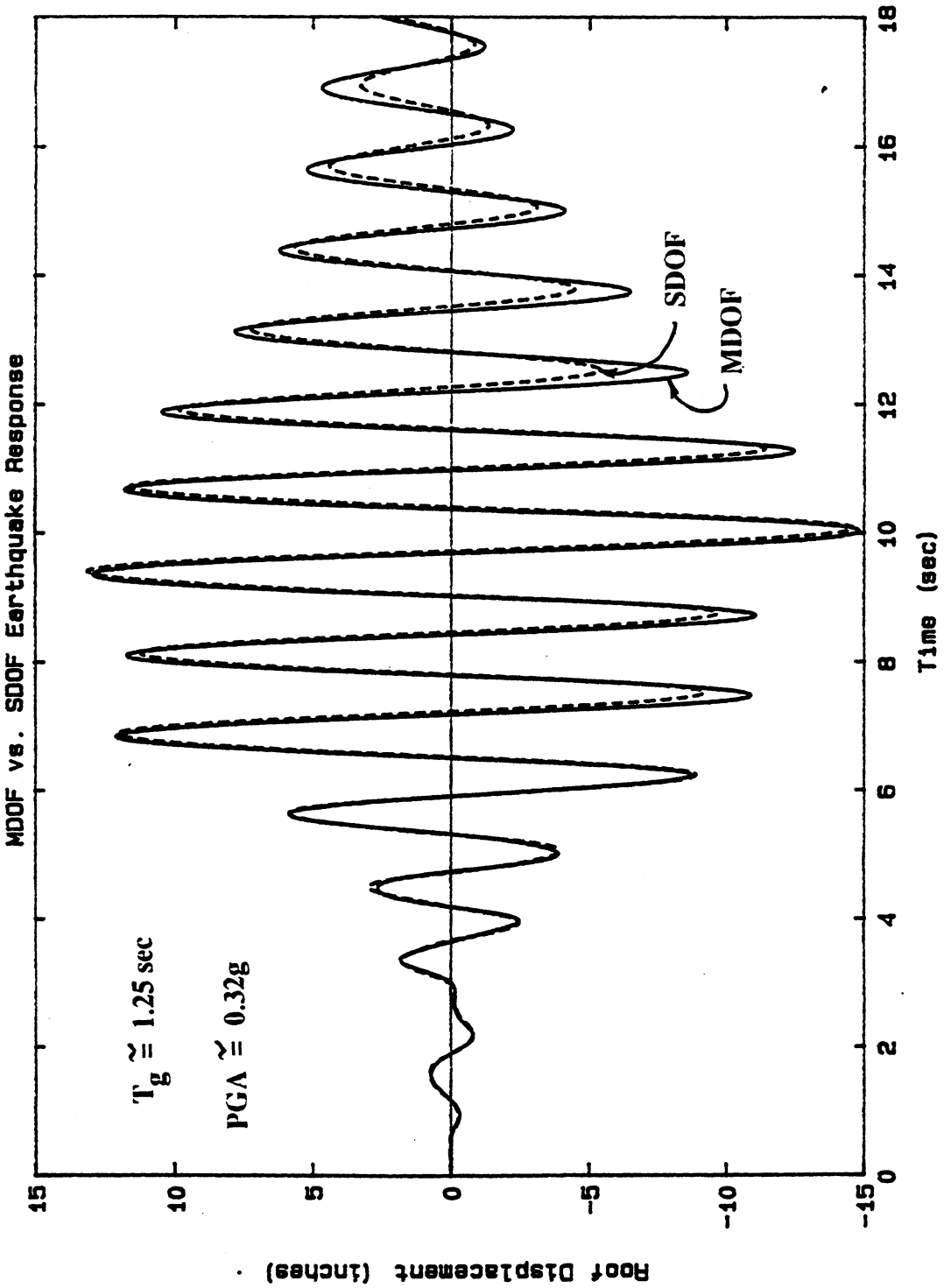

Figure 4.8 Response to Near Harmonic Earthquake

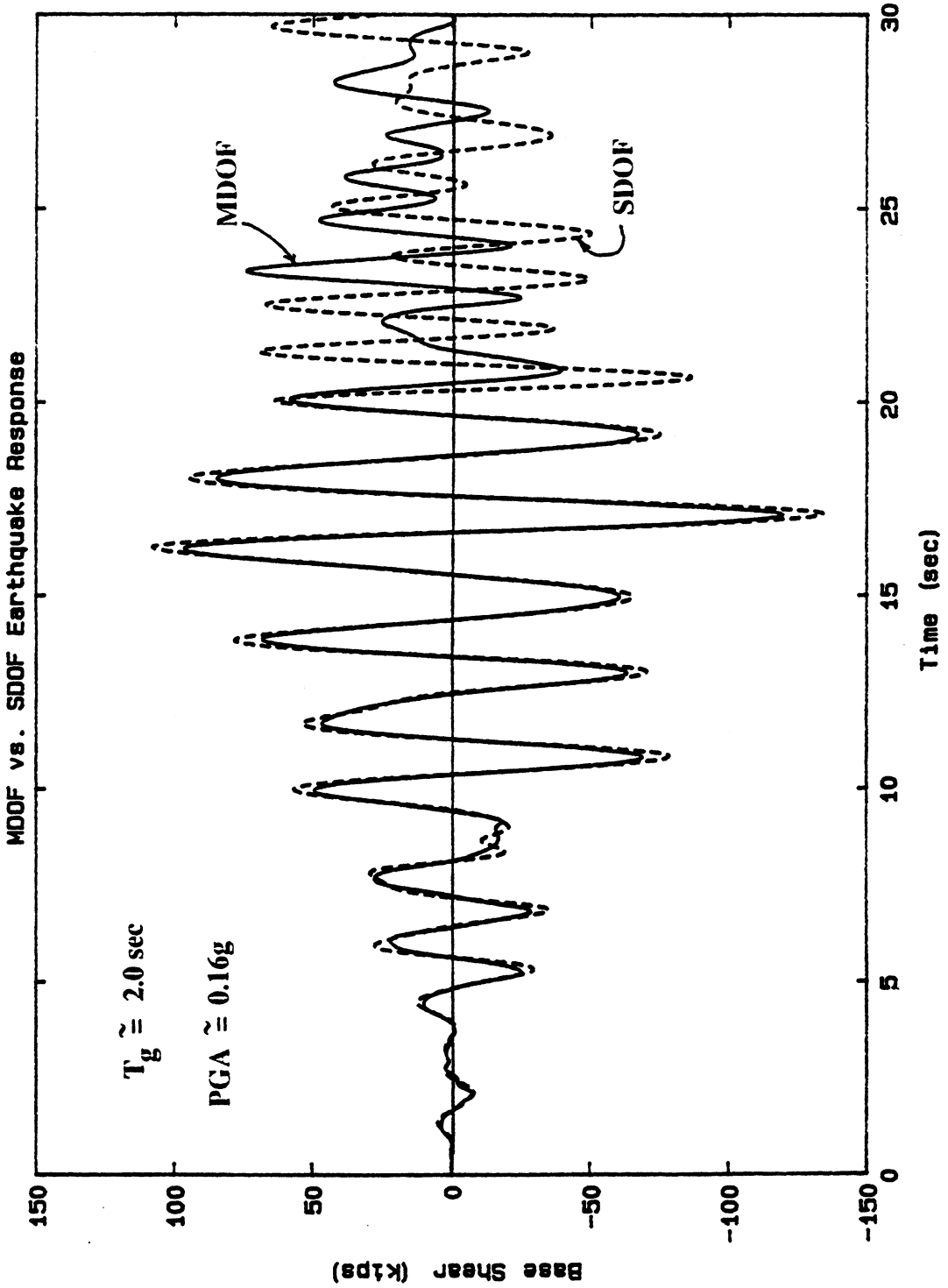

Figure 4.9 Response to Near Harmonic Earthquake

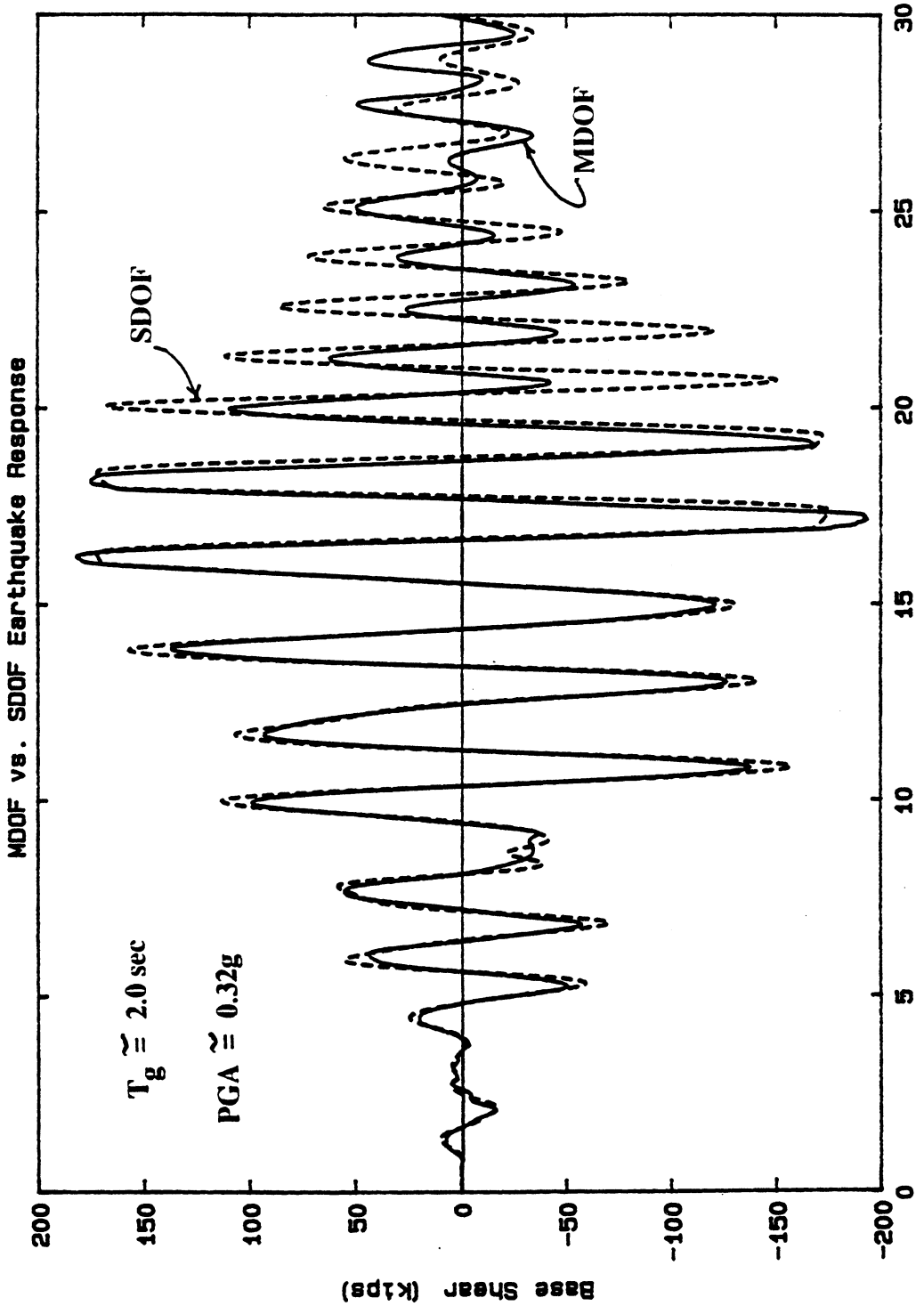

Figure 4.10 Response to Near Harmonic Earthquake

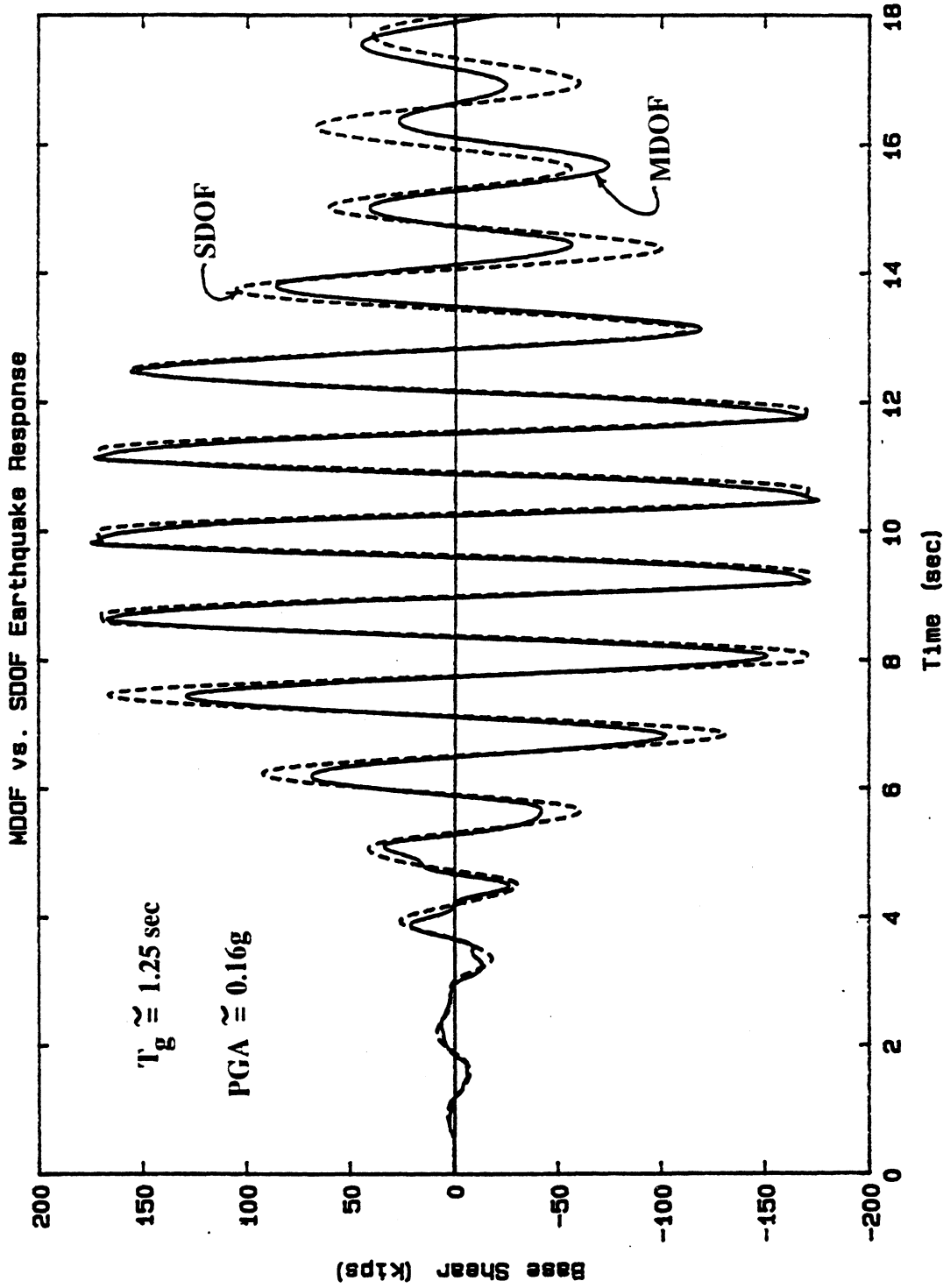

Figure 4.11 Response to Near Harmonic Earthquake

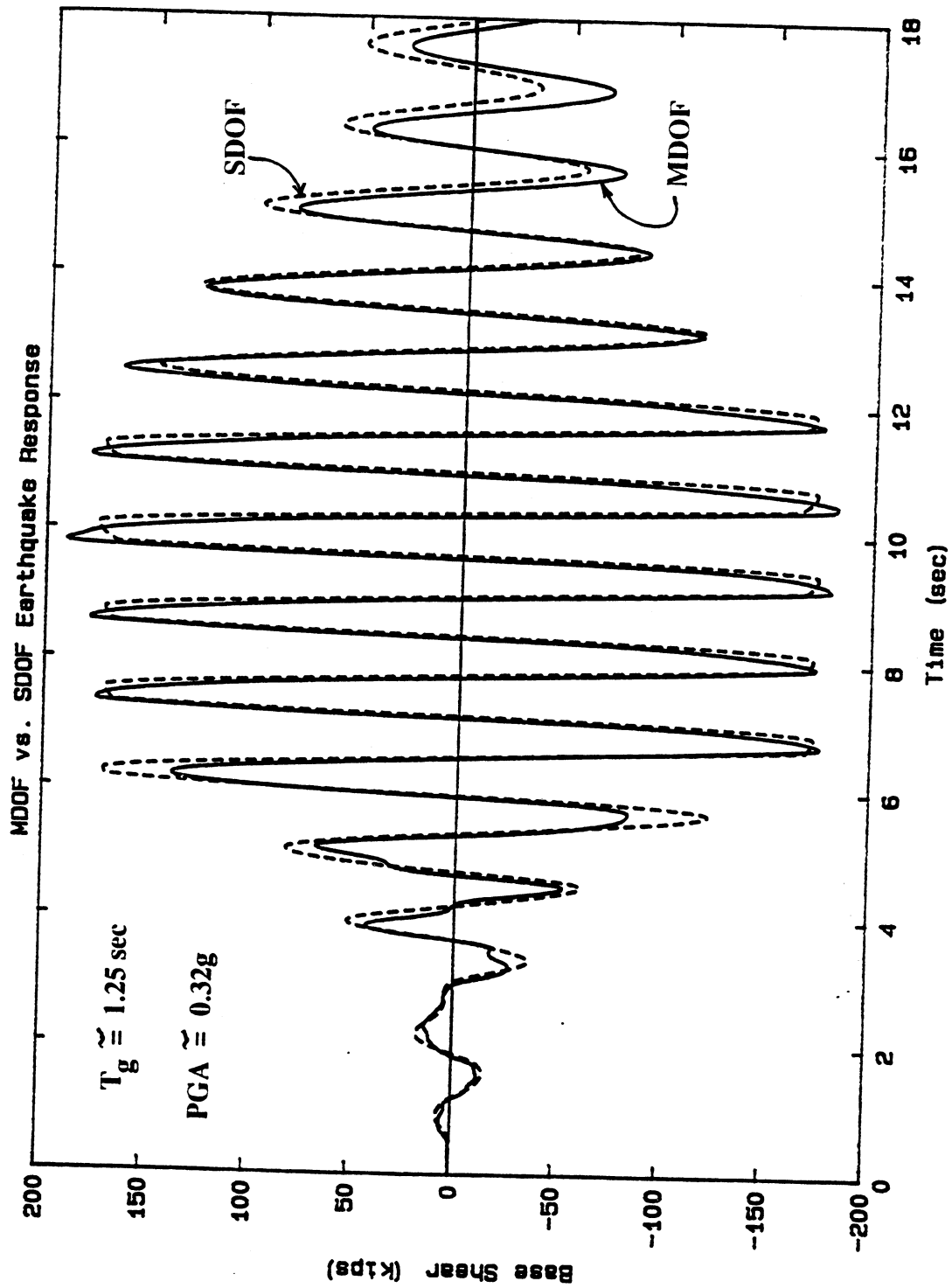

Figure 4.12 Response to Near Harmonic Earthquake

3) For the cases in which $T_g \approx 2.0$ seconds, the entire MDOF and SDOF roof displacement histories display a very good correlation. The corresponding base shear response histories are shown to be reasonably well correlated. It should be noted that significant nonlinear behavior was induced in both the MDOF and SDOF models.

It is very important to observe that for this particular structure, the computer execution time required to conduct the MDOF dynamic analyses was approximately 15 times greater than the time required to conduct the SDOF dynamic analyses. The fact that the SDOF representation provides a reasonable estimate of the MDOF response (particularly the response maxima) for harmonic and near harmonic ground motion input with a fraction of the computational effort illustrates the usefulness of simplified building response analysis.

CHAPTER 5

SUMMARY, CONCLUSIONS AND RECOMMENDATIONS

5.1 Summary

The work presented in this report was undertaken in consideration of the potentially dangerous modifying effect that flexible (soft) soil sites can have on earthquake motions as they propagate from the bedrock level to the ground surface, and the need to incorporate site response into the seismic analysis of buildings. A further motivation was that for structures founded on soft soil sites such as the Mexico City lake bed, it may be possible to represent the earthquake excitations as a harmonic motion and to estimate the structural response using simplified procedures. The emphasis of this work is on the introduction and use of simple, physical modeling and analysis procedures which can capture the important features of the response of soil profiles, buildings, and soil-structure systems.

The primary objectives of this report were to:

1) Present simple, efficient and easy-to-use procedures for evaluating the earthquake response of horizontally layered soil profiles.
2) Present simplified procedures for evaluating the seismic response and performance of building structures.
3) Review various methods of soil-structure interaction analysis and present simplified procedures for analyzing the earthquake response of building structures including site effects.

Chapter 1 provided an introduction to the motivation and objectives of this work and furnished a brief literature review on the topics of site response analysis, simplified building analysis and soil-structure interaction.

In Chapter 2, the topic of site response analysis was addressed including a basic review of frequency domain procedures and the development and implementation of various time domain analysis methods using a new one-dimensional site response analysis

program, WAVES.

The WAVES program implements a one-dimensional, lumped mass finite element formulation and takes advantage of the tri-diagonal nature of the one-dimensional equilibrium equations by implementing an extremely efficient Gauss elimination solution scheme. The program can compute the mode shapes and vibration periods of the finite element site model and can also conduct linear or iterative, equivalent linear site response analysis using direct step-by-step time domain procedures. Time domain procedures can result in slightly more efficient numerical solutions than similar frequency domain based procedures [23] with the added advantage of being able to perform true nonlinear site response analysis using various solution strategies. The input to the program consists of site information (number of layers, and the layer material properties) and earthquake input information (the user can select from a library of twenty earthquake records). Histories of any layer response quantity (including stress, strain, displacement, velocity or acceleration) can be requested as output. Earthquake response spectra, computed from the analytical acceleration response of any layer, can also be obtained.

The analysis results presented in Chapter 2, comparing the results of WAVES analyses with the results measured at the SCT site, indicated that simple procedures can capture the essential features of the dynamic response of soil profiles represented as one-dimensional systems. Both linear and nonlinear analyses predicted that the response of the SCT site was dominated by vibration at a period of approximately 2.0 seconds. The lack of correlation at vibration periods above 2.0 seconds may be the manifestation of two-dimensional behavior in the measured results. Clearly, the use of a one-dimensional site model is not applicable for the analysis of sites which exhibit two or three-dimensional behavior, but they may be used (with judgement) to obtain estimates of the important response characteristics of such sites.

Chapter 3 focused on building response analysis. An overview of conventional linear and nonlinear analysis methods was followed by a discussion of the use of harmonic earth-

quake motions to represent the "harmonic type" site motions frequently recorded at the surface of soft soil profiles. A correlation study, which related the harmonic response of a MDOF two-dimensional frame system with that of an equivalent SDOF representation was then presented. The extension of simplified harmonic analysis to other two and three-dimensional systems was then discussed followed by a section regarding seismic design evaluation based on the results of harmonic analyses.

As a step toward a better understanding and wider use of nonlinear analysis, it is prudent to begin with simple models. Approximate procedures, which are based on the transformation of a MDOF system to an equivalent SDOF bilinear oscillator using the results from MDOF static collapse analyses, provide a simple (and relatively inexpensive) starting point for predicting the global linear and nonlinear response of MDOF systems.

The ground motions at the SCT site in Mexico City during the 1985 earthquake illustrate a near harmonic wave form. Well over forty vibration cycles at a period of approximately 2.0 seconds can be observed in the record. For buildings founded on such soft soil sites, it may be argued that pure harmonic earthquake loading, at a frequency near the natural site period, can be used to estimate the cyclic response demands likely to be placed on the structure during "harmonic type" site response. The steady-state harmonic response of linear or (nondegrading) nonlinear structural models, which is often achieved after only a few vibration cycles, provides a condensed representation of the structural force, deformation, and energy response characteristics since they are entirely contained in a single vibration cycle.

The investigation of the steady state harmonic response of a MDOF two-dimensional frame model with that of an equivalent SDOF representation for a range of harmonic earthquakes indicated that the SDOF system provided a good estimate of the global displacement of the MDOF system for the full range of harmonic earthquakes considered. The steady state base shears computed with the SDOF system were accurate for all harmonic analyses for which $T_g \geq T_s$, but for T_g values less than T_s, the base shear contribu-

tion from the second mode provides a cancellation effect, reducing the MDOF base shear response amplitude relative to that of the SDOF system. It is most important to observe that when the response amplitudes af the MDOF and SDOF systems were relatively large, and in particular when nonlinear behavior was induced, the SDOF representation provided an excellent approximation to the MDOF results, reducing the need for extensive harmonic MDOF dynamic analyses.

The idea of simplified SDOF analysis procedures can be extended to the approximate analysis of three-dimensional MDOF systems by using MDOF to SDOF transformations on the results obtained from three-dimensional static collapse analyses in the principal directions of the structure. The relationships between the nonlinear resistance and the lateral displacement of the three-dimensional structure obtained from lateral loading induced by forces at concentric master nodes and moments at eccentric master nodes provide a rational starting point for estimating the MDOF dynamic response using SDOF procedures.

The assumption of harmonic earthquake excitation simplifies the task of evaluating the seismic performance of structural models. Harmonic spectra differ from conventional spectra in that they present the response maxima of one SDOF structure subjected to a range of harmonic earthquake motions, as opposed to presenting the response maxima of a range of structures (defined by the elastic vibration period) excited by a single earthquake excitation. Spectra from SDOF harmonic analysis can be used to rapidly assess the sensitivity of the structural response to parameters such as strength, stiffness or damping ratio, as well as the bilinear stiffness ratio of the oscillator.

In Chapter 4, a brief discussion of various methods of soil-structure interaction analysis procedures is followed by a presentation of the conventional, free-field formulation of the equations of motion for soil-structure systems. Simplified procedures, which attempt to capture the most important features of the seismic response of soil-structure systems are then suggested and applied to a simple soil-structure system.

The complex nature of the modeling and formulation of soil-structure analysis prob-

lems and the increased costs associated with such analyses are the primary reasons why SSI analyses are not routinely utilized in seismic analysis for design of typical building structures. However, when the uncertainty associated with the soil and structural properties and the uncertainties associated with the earthquake ground motions are considered, it can be argued that rigorous SSI analysis procedures are unduly complicated. The use of simple models is often justified by the idea that the level of sophistication of the analysis should be compatible with the uncertainty of the input and system material properties.

One of the most fundamental and commonly used simplifications is to neglect the influence of the building on the site response (i.e., the free-field motions can be used directly as input to the structural model). Hence, the input to structural models can be obtained from separate site response analyses, from previously recorded earthquake motions or from artificial earthquakes compatible with a site-specific response spectrum.

Elastic foundation deformations can be important and are typically manifested by an increased fundamental structural vibration period. Depending on the spectral properties of the structural input, an increased fundamental vibration period may increase the structural response (as in the case of structures located at the SCT site with a fixed base period slightly smaller than 2.0 seconds), or decrease the structural response (as in the case of structures located at the SCT site with a fixed base period slightly larger than 2.0 seconds). In either case, the flexibility effect can be accounted for in most building systems using the massless foundation formulation, where the structure DOF located at the soil-structure interface are restrained by zero mass foundation springs.

The investigation of a simple soil-structure system provided an illustration of simplified earthquake response analysis of a building including site effects. The surface response of the SCT site model subject to the CUMV EW base input was computed using WAVES and used as free-field input to MDOF and SDOF representations of a two-dimensional frame system. The fact that the SDOF representation provided a reasonable estimate of the MDOF response with a fraction of the computational effort illustrates the usefulness of sim-

plified building response analysis.

5.2 Conclusions

The research presented in this report spanned the topics of simplified site response analysis, building response analysis and soil-structure interaction analysis and attempted to briefly highlight the most important aspects of these subjects. The simplified procedures provided in this work can be easily understood and implemented by structural engineers and hence can provide a step toward a wider implementation of building response analysis including site effects. Numerous conclusions can be made regarding this study. The most important conclusions are:

Regarding site response analysis as presented in Chapter 2;

1) Site response analysis is extremely important and should be considered, especially for structures founded on soft soil profiles where the motions can be dramatically amplified between the bedrock and ground surface levels. As a minimum, estimates of the fundamental site period should be obtained to check for the potential of resonant vibration conditions between the site and the structure. The site period can be obtained from ambient vibration tests or using WAVES models based on site boring logs and/or measurements of the site shear wave velocity profile. WAVES can also be used to generate site-specific response spectra based on the analytical response of the site to an ensemble of base motion inputs.

2) The comparison of the results from WAVES analyses with the results measured at the SCT site, indicates that WAVES can be used to accurately model the essential features of the dynamic response of one-dimensional soil profiles. The program provides a simple and efficient site response analysis tool which can be of use to structural engineers and designers.

Regarding building response analysis as presented in Chapter 3;

1) Conventional linear structural analysis procedures are well established and numerous

computer codes are available an widely used by structural engineers in design practice. Linear analysis provides a rational starting point for evaluating the earthquake resistance of various seismic designs.

2) Nonlinear analysis can provide estimates of the distribution of damage throughout a structure and the ductility demands placed on a structure during severe seismic excitation. Unfortunately, the complexity of nonlinear analysis has generally resulted in only a very limited application of nonlinear procedures in conventional building design practice. Hence, the use of simple nonlinear models based on the results of MDOF static collapse analysis provides a sound starting point for predicting the nonlinear response of MDOF systems, especially for the evaluation of response of preliminary designs.

3) For buildings founded on soft soil sites such as the Mexico City lake bed, the use of pure harmonic earthquake loading, at a frequency near the natural site period, should be considered as one critical load case to estimate the cyclic response demands likely to be placed on the structure during "harmonic type" site response.

4) For the two-dimensional frame system investigated under harmonic earthquake loadings, the global displacement response computed with the SDOF system closely matched that of the MDOF system for the range of harmonic earthquakes considered. The steady state base shears computed with the SDOF system were accurate for all harmonic analyses in which the influence of the second mode was not significant. In cases where the response amplitudes af the MDOF and SDOF systems were relatively large, and in particular when nonlinear behavior was induced, the SDOF representation provided an excellent approximation to the MDOF displacements and base shears.

5) It is difficult to make conclusions regarding the applicability of approximate SDOF procedures for representing the response of general two and three-dimensional structural systems based on the limited investigation presented herein. However, for the

simple case of harmonic earthquake loading, it is reasonable to expect that trends similar to those observed in the correlation of the global MDOF and SDOF response (presented in Section 3.2.2.3) would also be observed in the response of other, similar structural systems.

Regarding soil-structure interaction analysis as presented in Chapter 4;

1) As discussed in Chapter 2, site response can be extremely important and should be considered, especially for structures founded on soft soil profiles. Simplified procedures can easily be implemented to model the response of soil profiles and to obtain estimates of the surface (free-field) motions likely to be developed at the base of the structure.

2) Elastic foundation deformations can be important and are typically manifested by an increased fundamental structural vibration period. The flexibility effect can be accounted for in most building systems using the massless foundation formulation.

3) For the "harmonic type" earthquake input motions considered in the analyses of the two-dimensional frame system, the maximum roof displacements and base shears computed using a simple SDOF representation were within 20%, and in most cases, within 10% of those computed using a MDOF representation.

4) The analysis of the soil-structure system presented in Chapter 4 illustrated the important ideas behind simplified earthquake analysis of buildings including site effects, namely; a) site response analysis, b) massless foundation springs and c) simplified building analysis. The efficiency and simplicity of these procedures make them useful tools for evaluating the seismic response of soil-structure systems.

5.3. Recommendations

In consideration of the work presented in this report, several recommendations regarding the earthquake analysis of buildings including site effects, as well as recommendations for future research can be made:

1) Structural engineers and designers should make every effort to obtain as much information as possible describing the properties of the site upon which a proposed structure is to be located. Useful site information includes site boring logs and soils test results, geophysical test results, and the results from ambient site vibration tests. The costs of obtaining this field data are easily justified when considered in light of the potentially devastating effect of site amplification.

2) The site properties should be used to build simple site models, which in turn can be used to provide a better definition of the input motions likely to develop at the base of the structure. The site properties should also be used to obtain the stiffness of massless foundation springs for modeling the foundation flexibility.

3) If the structure can be accurately represented as a two-dimensional system, then a linear two-dimensional structural model provides a reasonable starting point for evaluating the seismic design. However, since all structures really occupy three-dimensions, and since easy-to-use three-dimensional linear structural analysis programs are readily available, it is recommended that a linear three-dimensional structural model be developed in the early stages of the design. The mode shapes and vibration periods obtained from such a model give the engineer a good physical feeling for the dynamic behavior of the structure, which in turn can be used to improve the design.

4) A well designed structure should have a minimum amount of torsion in the three-dimensional mode shapes associated with the lower frequencies of the structure, which are most likely to be excited by earthquake loading [76]. As discussed in Chapter 3, the principal directions of the structure qualitatively represent its most flexible directions. It is intuitive that a well designed structure should have equal stiffness in all lateral directions so that there is no tendency for the structure to be excited in any one particular direction.

5) If an estimate of the ductility demands or the distribution of damage throughout a

structure are required, two or three-dimensional nonlinear dynamic analysis can be conducted. SDOF nonlinear dynamic analysis procedures, based on the results of two or three-dimensional static collapse analysis are recommended as a simplified alternative to MDOF dynamic analysis.

6) The idea that a well designed structure should have equal stiffness in all lateral directions can be extended to nonlinear response by recommending that the structure should also have equal strengths in all lateral directions, precluding the development of a "weak" direction when the structure is subject to severe seismic loading. Clearly, this design objective would be difficult to achieve in practice.

7) More work should be devoted to the implementation and verification of simplified nonlinear analysis methods. MDOF to SDOF transformation procedures should be evaluated for the approximate earthquake analyses of two and three-dimensional structures of various heights and configurations, designed using current seismic codes.

8) Existing structural analysis programs should be modified to include transformations that allow for the inclusion of additional translational and rotational DOF at the base of the structural model where massless foundation springs could be utilized.

REFERENCES

1) Allahabadi, R., and Powell, G. H., "DRAIN-2DX User Guide", Earthquake Engineering Research Center, Report No. EERC 88-06, University of California, Berkeley, March, 1988.

2) Allahabadi, R., "DRAIN-2DX Seismic Response and Damage Assessment for Two-Dimensional Structures", Ph. D. Dissertation, University of California, Berkeley, 1987.

3) ATC-03-06, "Tentative Provisions for the Development of Seismic Regulations for Buildings", Applied Technology Council, Palo Alto, California, 1971.

4) Apsel, R. J., and Luco, J. E., "Torsional Response of a Rigid Embedded Foundation", Journal of the Engineering Mechanics Division, ASCE, Vol. 102, No. EM6, 1976.

5) Bathe, K. J., and Wilson, E. L., "Numerical Methods in Finite Element Analysis", Prentice-Hall Inc., Englewood Cliffs, NJ, 1976.

6) Bayo, E. P., and Wilson, E.L. "Numerical Techniques for the Solution of Soil-Structure Interaction Problems in the Time Domain", Earthquake Engineering Research Center, Report No. EERC 83-04, University of California, Berkeley, 1983.

7) Beck, J.L and Dowling, M.J., "Quick Algorithms for Computing Either Displacement, Velocity or Acceleration of an Oscillator", Earthquake Engineering Research Laboratory, California Institute of Technology, Pasadena, California, 1986.

8) Biggs, J. M., "Introduction to Structural Dynamics", McGraw-Hill Book Company, New York, N.Y., 1964.

9) Borg, S.F., "The 19 September 1985 Mexican Earthquake - Rational Analysis of the Anomalous Central Mexico City Behavior", Technical Report COE-86-1, Stevens Institute of Technology, April 1, 1986.

10) Clough, R. W., Chang, K. T., Chen, H. Q., and Stephen, R. M., "Dynamic Response Behavior of Kiang Hong Dian Dam", Report No. UCB/EERC-84/02, University of California, Berkeley, April 1984.

11) Clough, R.W. and Penzien, J.P., "Dynamics of Structures", McGraw-Hill Book Company, New York, N.Y., 1975.

12) Cooley, J. W., and Tukey, J. W., "An Algorithm for the Machine Calculation of Complex Fourier Series", Mathematics of Computation, Vol. 19, No. 90, 1965.

13) Cruz, E. F., and Chopra, A. K., "Simplified Methods of Analysis for Earthquake Resistant Design of Buildings", Earthquake Engineering Research Center, Report No. EERC 85-01, University of California, Berkeley, February 1985.

14) "CSI-ETABS: A Computer Program for the Three-Dimensional Analysis of Building Systems", Computers and Structures, Inc., Berkeley, CA. 1989.

15) Dahlquist, G., Bjorck, A., and Anderson, N., "Numerical Methods", Prentice-Hall Inc., Englewood Cliffs, NJ, 1974.

16) Espinosa, A.F. and Algermissen, S.T., "A Study of Soil Amplification Factors in Earthquake Damage Areas - Caracas, Venezuela", NOAA Technical Report No. ERL280-ESL31, National Oceanic and Atmospheric Administration, Boulder, Colorado, 1972.

17) "FACTS: A Computer Program for Finite Element Analysis of Complicated Structures", SSD Inc., Berkeley CA, 1989.

18) Ghose, A., "Computational Procedures for Inelastic Dynamic Analysis", Ph. D. Dissertation, University of California, Berkeley, 1974.

19) Golafshani, A. A., "DRAIN-2D2 A Program for Inelastic Seismic Response Analysis", Ph. D. Dissertation, University of California, Berkeley, 1981.

20) Gupta, S., et al., "Hybrid Modeling of Soil-Structure Interaction", Report No. UCB/EERC-80/09, University of California, Berkeley, May 1980.

21) Gutierrez, J. A., and Chopra, A. K., "A Substructure Method for Earthquake Analysis of Structures Including Soil-Structure Interaction", Journal of Earthquake Engineering and Structural Dynamics, Vol. 6, 1978.

22) Hardin, B.O. and Drnevich, V.P., "Shear Modulus and Damping in Soils: Design Equations and Curves", Journal of Soil Mechanics and Foundations Division, ASCE, Vol. 98, No. SM7, July 1972.

23) Hart, J. D., "An Introduction to WAVES - A New Computer Program for Evaluating the Earthquake Response of Horizontally Layered Soil Deposits", Individual Research Report, Department of Civil Engineering, University of California, Berkeley, August, 1987.

24) Hughes, T. J. R., "Stability, Convergence and Growth and Decay of Energy of the Average Acceleration Method in Nonlinear Structural Dynamics", Computers and Structures, Vol. 6, pp. 313-324, 1976.

25) Ibrahimbegovic, A., "Dynamic Analysis of Large Linear Structure-Foundation Systems with Local Nonlinearities", Report No. UCB/SEMM 89/14, Department of Civil Engineering, University of California, Berkeley, June 1989.

26) Idriss, I.M., Lysmer, J., Hwang, R. and Seed, H.B., "QUAD4 - A Computer Program for Evaluating the Seismic Response of Soil Structures by Variable Damping Finite Element Procedures", Earthquake Engineering Research Center, Report No. EERC 73-16, University of California, Berkeley, July 1973.

27) Idriss, I. M., Dobry, R., and Singh, R. D., "Nonlinear Behavior of Soft Clays During Cyclic Loading", Journal of the Geotechnical Engineering Division, ASCE, No. GT12, Dec 1978.

28) Idriss, I. M., et al., "Behavior of Soft Clays Under Earthquake Loading Conditions", Proceedings, Offshore Technology Conference, OTC 2671, Dallas, TX, 1976.

29) Iwan, W. D., "On a Class of Model for the Yielding Behavior of Continuous and Composite Systems", Journal of Applied Mechanics, ASME, 1967.

30) Jaime, A. P., Romo, M. P., and Ovando, E. S., "Caracteristicas Del Suelo En El Sitio SCT" (In Spanish) Proy 6504, Elaborado para el Depatamento del Distrito Federal, Enero, 1987.

31) Jacobsen, L. S., "Steady Forced Vibrations as Influenced by Damping", Transactions, ASME, Vol. 51, 1960.

32) Jennings, P. C., "Response of Simple Yielding Structures to Earthquake Excitation", Ph. D. Dissertation, California Institute of Technology, Pasadena, CA, 1963.

33) Johnson, J.A., "Site and Source Effects on Ground Motion in Managua, Nicaragua", Report No. UCLA-Eng-7536, University of California, Los Angeles, May 1975.

34) Kamil, H., and Roesset, J. M., "Hysteretic Damping in Inelastic One Degree of Freedom Systems", Department of Civil Engineering, Report No. R69-52, Massachusetts Institute of Technology, Cambridge, Massachusetts, August, 1969.

35) Kan, C. L., and Chopra, A. K., "Linear and Nonlinear Earthquake Response of Simple Torsionally Coupled Systems", Earthquake Engineering Research Center, Report No. EERC 79/03, University of California, Berkeley, Feb, 1979.

36) Lee, K. L., and Aktan, A. E., "Microcomputer Program for Three Dimensional Static Collapse Analysis of Structures (3DSCAS)", Research Report 88-2, Department of Civil and Environmental Engineering, University of Cincinnati, Sept., 1988.

37) Leger, P., Wilson, E.L., Clough, R.W., "The Use of Load Dependent Vectors for Dynamic and Earthquake Analyses", Report No. UCB/EERC-86/04, University of California, Berkeley, March 1986.

38) Lysmer, J., Takekazu, U., Chang-Feng, T., and H. B. Seed,"FLUSH - A Computer Program for Approximate 3-D Analysis of Soil-Structure Interaction Problems", Report No. EERC 75-30, University of California, Berkeley, Nov. 1975.

39) Lysmer, J., Udaka, T., Seed, H.B., and Hwang, R., "LUSH - A Computer Program for Complex Response Analysis of Soil Structure Systems", Earthquake Engineering Research Center, Report No. EERC 74-4, University of California, Berkeley, April 1974.

40) Lysmer, J., et al., "SASSI, a System for Analysis of Soil Structure Interaction", UCB/GT/81-02, University of California, Berkeley, 1981.

41) Lysmer, J., "Analytical Procedures in Soil Dynamics", Earthquake Engineering Research Center, Report No. EERC 78-29, University of California, Berkeley, 1978.

42) Martin, P.P. and Seed, H.B., "MASH - A Computer Program for the Nonlinear Analysis of Vertically Propagating Shear Waves in Horizontally Layered Deposits", Earthquake Engineering Research Center, Report No. UCB/EERC-78/23, October 1978.

43) Mahin, S. A., and Bertero, V. V., "An Evaluation of Inelastic Seismic Design Spectra", Journal of the Structural Division, ASCE, Vol. 107, No. ST9, Sept., 1981.

44) Mahin, S., and Lin J., "Construction of Inelastic Response Spectra for Single-Degree-of-Freedom Systems", Report No. UCB/EERC-83/17, University of California, Berkeley, June, 1983.

45) Mondkar, D. P., and Powell, G. H., "Static and Dynamic Analysis of Nonlinear Structures", Report No. UCB/EERC-75/10, University of California, Berkeley, March 1975.

46) Neal, B. G., "The Plastic Methods of Structural Analysis", 3rd Edition, Chapman and Hall, New York, 1977.

47) Newmark, N. M., "A Method of Computation for Structural Dynamics", Journal of the Engineering Mechanics Division, ASCE, Vol. 85, No. EM3, 1959.

48) Newmark, N., and Rosenblueth, E., "Fundamentals of Earthquake Engineering", Prentice-Hall Inc., Englewood Cliffs, NJ, 1971.

49) Powell, G. H., and Simons, J., "Improved Iteration Strategies for Nonlinear Structures", International Journal for Numerical Methods in Engineering, Vol. 17, 1981.

50) Powell, G. H., and Row, D. G., "Influence of Analysis and Design Assumptions on Computed Inelastic Response of Moderately Tall Frames", Earthquake Engineering Research Center, Report No. EERC 76-11, University of California, Berkeley, April, 1976.

51) Ramberg, W., and Osgood, W. T., "Description of Stress-Strain Curves by Three Parameters", NACA Technical Note No. 902, 1943.

52) Richart, F. E., "Some Effects of Dynamic Soil Properties on Soil-Structure Interaction", Journal of the Geotechnical Engineering Division, ASCE, Vol. 101, No. GT12, Dec 1975.

53) Rukos, E.A., "Earthquake Analysis of Interacting Ground-Structure Systems", Report No. UCB/SESM 71-9, University of California, Berkeley, May 1971.

54) "SAP-90: A General Computer Program for the Three-Dimensional Analysis of Finite Element Systems ", Computers and Structures, Inc., Berkeley, CA. 1989.

55) Saiidi, M., and Hodson, K. E., "Analytical Study of Irregular Reinforced Concrete Structures Subjected to In-Plane Earthquake Loads", College of Engineering Report No. 59, University of Nevada, Reno, May, 1982.

56) Saiidi, M., and Sozen, M. A., "Simple and Complex Models for Nonlinear Seismic Response of Reinforced Concrete Structures", Structural Research Series No. 465, University of Illinois at Urbana-Champaign, Urbana, IL, Aug 1979.

57) Saiidi, M., "Simple Nonlinear Modeling of Earthquake Response in Torsionally Coupled Reinforced Concrete Structures", College of Engineering Report No. 60, University of Nevada, Reno, July 1982.

58) Saiidi, M., and Sozen, M. A., "Simple Nonlinear Seismic Analysis of Reinforced Concrete Structures", Journal of the Structural Division, ASCE, No. ST5, May, 1981.

59) Schnabel, P.B., Lysmer, J. and Seed, H.B., "SHAKE - A Computer Program for Earthquake Response Analysis of Horizontally Layered Sites", Earthquake Engineering Research Center, Report No. EERC 72-12, University of California, Berkeley, December 1972.

60) Schnabel, P.B., Seed, H.B. and Lysmer, J., "Modifications of Seismograph Records for Effects of Local Site Conditions", Earthquake Engineering Research Center, Report No. EERC 71-8, University of California, Berkeley, December 1971.

61) Seed, H.B., Idriss, I.M., Dezfulian H., "Relationships Between Soil Conditions and Building Damage in the Caracas Earthquake of July 29, 1967", Earthquake Engineering Research Center, Report No. EERC 70-2, University of California, Berkeley, February 1970.

62) Seed, H.B., and Idriss, I.M., "Soil Moduli and Damping Factors for Dynamic Response Analysis", Earthquake Engineering Research Center, Report No. EERC 70-10, University of California, Berkeley, December 1970.

63) Seed, H.B., M. P. Romo, J. Sun, ,A. Jaime, and J. Lysmer, "Relationships Between Soil Conditions and Earthquake Ground Motions in Mexico City in the Earthquake of Sept. 19, 1985" Earthquake Engineering Research Center, Report No. UCB/EERC-87/15, University of California, Berkeley, October 1987.

64) Simons, J. W., "Solution Strategies for Statically Loaded Nonlinear Structures", Ph. D. Dissertation, University of California, Berkeley, 1982.

65) Streeter, V.L., Wylie, E.B., Benjamin, E., and Richart, F.E., "Soil Motion Computations by Characteristics Method", Journal of the Geotechnical Engineering Division, ASCE, Vol. 100, No. GT3, March 1974.

66) Stephen, R.M., Wilson, E.L. and Stander, N.,"Dynamic Properties of a Thirty Story Condominium Tower Building", Earthquake Engineering Research Center, Report No. UCB/EERC-85/03, April 1985.

67) Thau, S. A., and Umek, A., "Coupled Rocking and Translational Vibrations of a Buried Foundation", Journal of the Applied Mechanics Division, ASCE, Vol. 1, No. EM3, 1974.

68) Uang, C. M. and Bertero V. V., "Use of Energy as a Design Criterion in Earthquake Resistant Design", Report No. UCB/EERC-88/18, University of California, Berkeley, November, 1988.

69) Veltsos, A. S., and Nair, V. V. D., "Torsional Vibrations of a Viscoelastic Foundations", Journal of the Geotechnical Engineering Division, ASCE, Vol. 100, 1974.

70) Veltsos, A. S., and Wei, T. Y., "Lateral and Rocking Vibration of Footings", Journal of the Soil Mechanics and Foundations Division, ASCE, Vol. 97, No. SM9, Sept, 1971.

71) Wallace, J. W., "The 1985 Chile Earthquake: An evaluation of Structural Requirements for Bearing Wall Buildings", Earthquake Engineering Research Center, Report No. EERC 89/05, University of California, Berkeley, January, 1989.

72) Wilson, E.L., "A Computer Program for the Dynamic Stress Analysis of Underground Structures", Report No. UC SESM 68-1, Department of Civil Engineering, University of California, Berkeley, January 1968.

73) Wilson, E.L., "SAP - 89, A Series of Computer Programs for the Static and Dynamic Finite Element Analysis of Structures - Users Manual", NISEE Computer Applications, Earthquake Engineering Research Center, Department of Civil Engineering, University of California, Berkeley, January 1989.

74) Wilson, E.L., "CAL86 - Computer Assisted Learning of Structural Analysis", Report No. UC SESM 86-05, Department of Civil Engineering, University of California, Berkeley, March 1986.

75) Wilson, E. L., Der Kiureghian, A., and Bayo, E. P., "A Replacement for the SRSS Method in Seismic Analysis", Short Communications, Journal of Earthquake Engineering and Structural Dynamics, Vol. 9., 1981.

76) Wilson, E. L., Suharwardy, M. I.,and Habibullah, A., "A Seismic Analysis Method Which Satisfies the 1988 Lateral Force Requirements", Computers and Structures, Inc., Berkeley, CA, Jan , 1989.

77) Wilson, E. L., and Dovey, H. H., "Three Dimensional Analysis of Building Systems"; Report No. UCB/EERC-72-08, University of California, Berkeley, 1972.

78) Wolf, J. P., "Dynamic Soil-Structure Interaction", Prentice-Hall Book Company, New York, N.Y., 1985.

79) Wylie, C. R., and Barrett, L. C., "Advanced Engineering Mathematics", McGraw-Hill Book Company, New York, N.Y., 1982.

APPENDIX A

RAMBERG-OSGOOD HYSTERESIS MODEL

The Ramberg-Osgood hysteresis model [51] was developed in 1943 to model the stress-strain relationships of steel using three control parameters. In 1963, Jennings [32] modified the relationship by adding a fourth control parameter. The model calculates strains or deformations as an explicit function of stress or forces. As shown in Figure A.1, the relationship is defined by two functions; one for loading on the primary curve and one for unloading:

Loading:

$$\frac{d}{d_c} = \frac{f}{f_c}\left(1 + \alpha \left|\frac{f}{f_c}\right|^{(\gamma-1)}\right) \tag{A.1}$$

Unloading:

$$\frac{d - d_o}{2\,d_c} = \frac{f - f_o}{2\,f_c}\left(1 + \alpha \left|\frac{f - f_o}{2\,f_c}\right|^{(\gamma-1)}\right) \tag{A.2}$$

where:

f = current force

d = current deformation

f_c = control force

d_c = control deformation

f_o = force at current unloading point

d_o = deformation at current unloading point

γ = exponential control parameter

α = control parameter introduced by Jennings

Figure A.1 shows the range of nonlinearity that can be obtained by varying the parameter γ; $\gamma=1$ will produce a linear-elastic primary curve while $\gamma=\infty$ will produce an elasto-plastic primary curve.

In the state determination phase of a nonlinear analysis, the function of the hysteresis model is to return the "state" of an element after an increment of strain or deformation is imposed. The element state essentially consists of the internal stress or resisting force and the tangent modulus. In order to implement the Ramberg-Osgood model into a displacement method of analysis, it must be modified to obtain the stress or force as a function of strain or deformation. This is accomplished by applying a Newton-Raphson iteration scheme to the one-to-one correspondence between force and deformation given by the Ramberg-Osgood functions.

The most important aspect of the practical use of the Ramberg-Osgood model is the proper selection of the four control parameters; f_c, d_c, α and γ. The control force and control deformation, f_c and d_c, should be selected based on a knowledge of the initial tangent modulus of the material. For shear deformations, the shear modulus at low strains can be expressed as a function of the mass density and shear wave velocity:

$$G_{max} = \rho V_s^2 \tag{A.3}$$

For $\gamma = 1$, the initial shear modulus is given by:

$$G_{max} = \frac{f_c}{d_c (1 + \alpha)} \tag{A.4}$$

For $\gamma > 1$, the initial shear modulus is given by:

$$G_{max} = \frac{f_c}{d_c} \tag{A.5}$$

Note that for relatively small values of γ, the tangent modulus is equal to f_c / d_c only for a very limited range of deformation, while for relatively large γ values, the tangent modulus is equal to f_c / d_c for a much larger range of deformations. Once a value of the control deformation d_c is selected, the control force f_c is computed based on the above relationships.

Techniques for determining the parameters α and γ for various materials have been presented in [27], [28], [52] and [65]. The basic approach to determine the parameters requires a knowledge of the force-deformation relationship of the material. A plot is made

of the log of the departure from linearity of the deformation versus the applied force. Examination of the primary loading curve relationship indicates that the departure from linearity is given by:

$$\log(\alpha) + \gamma \log\left(\frac{f_c}{d_c}\right) \tag{A.6}$$

Thus, α and γ are the intercept and the slope of the straight line which best fits the data of the semi-logarithmic plot. In one investigation [27] the hyperbolic modulus and damping curves proposed for soils by Hardin and Drenovich [22] were best fit by using:

$$f_c = 0.8\, f_{max} \tag{A.7}$$

$$\alpha = 1.0 \tag{A.8}$$

$$\gamma = 3.0 \tag{A.9}$$

When measured stress-strain data for a given material is unavailable, results from other investigations can be used. Experiments performed on various soil samples indicate that the approximate ranges:

$$1.0 < \gamma < 4.0 \qquad 0.3 < \alpha < 3.0 \tag{A.10}$$

may be appropriate [27,28,65]. In any case, the ideal selection of the Ramberg-Osgood parameters requires at least the basic information on the soil properties and the application of engineering judgement.

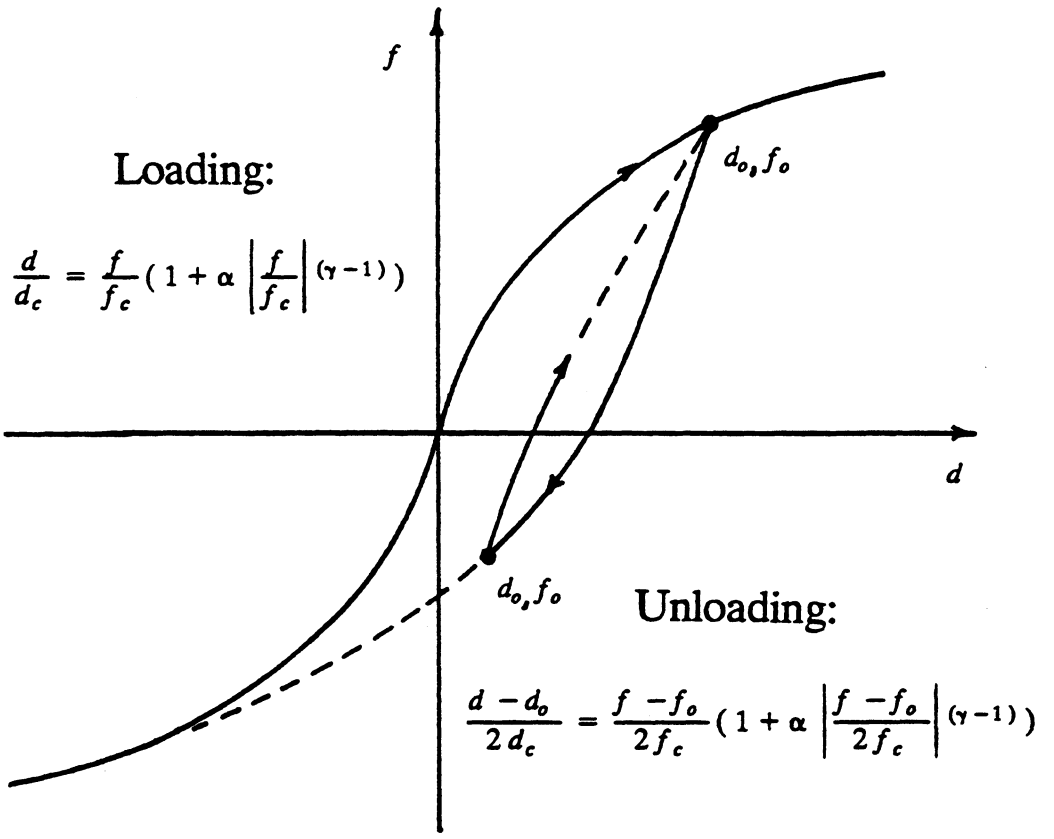

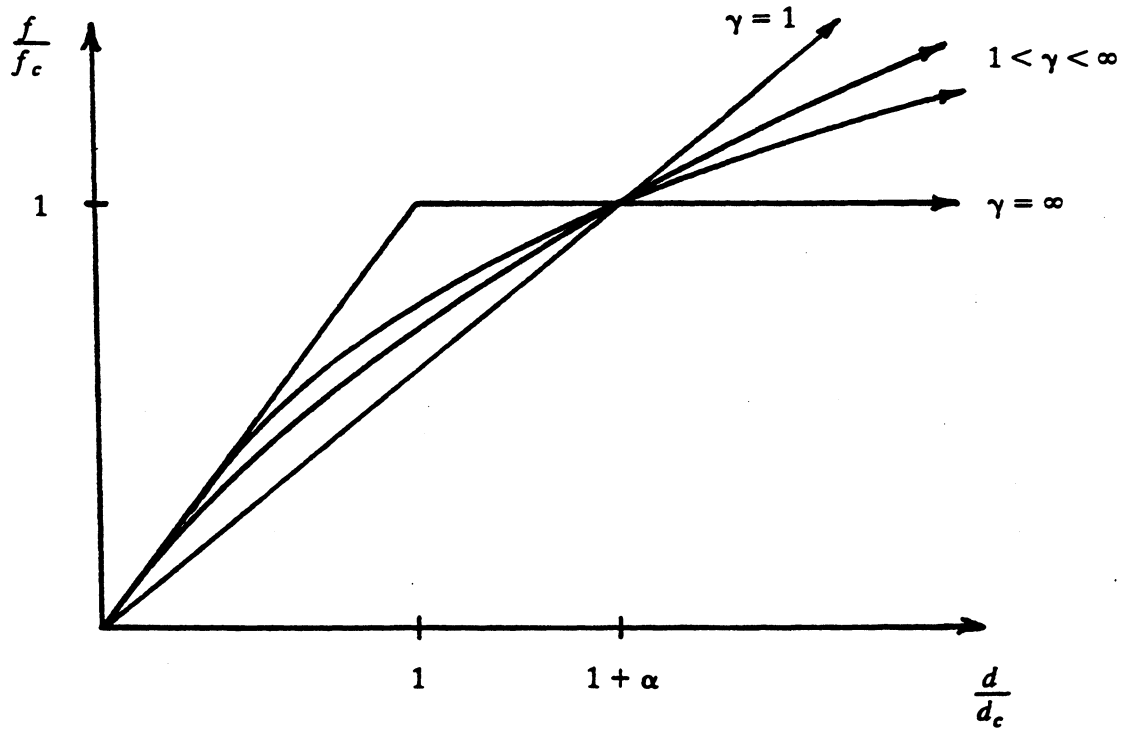

Figure A.1 Ramberg-Osgood Hysteresis Model

APPENDIX B

ENERGY BALANCE CALCULATIONS

Energy balance calculations performed on a finite element system subjected to dynamic loading can provide both a measure of the errors generated by numerical integration and an idea of the distribution of the different types of energy throughout the system. The energy balance can be developed by premultiplying the dynamic equilibrium equations by the transpose of the infinitesimal relative displacement vector **dU** yielding the following scalar equation:

$$[\mathbf{dU}]^T [\, \mathbf{M}\, \ddot{\mathbf{U}}_t + \mathbf{C}\, \dot{\mathbf{U}} + \mathbf{K}\, \mathbf{U}\,] = \mathbf{0} \qquad \text{(B.1)}$$

Where $\ddot{\mathbf{U}}_t$ is the vector of total nodal accelerations. Making the substitution $\mathbf{dU} = [\mathbf{dU}_t - \mathbf{1}du_g]$, into the first term of the above equation and rearranging terms results in the following differential energy expression:

$$dE_I + dE_D + dE_S = dE_E \qquad \text{(B.2)}$$

where:

$dE_I = [\mathbf{dU}_t]^T \mathbf{M}\, \ddot{\mathbf{U}}_t$ = kinetic energy differential

$dE_D = [\mathbf{dU}]^T \mathbf{C}\, \dot{\mathbf{U}}$ = damped energy differential

$dE_S = [\mathbf{dU}]^T \mathbf{K}\, \mathbf{U}$ = stiffness energy differential

$dE_E = du_g \mathbf{1}^T \mathbf{M}\, \ddot{\mathbf{U}}_t$ = earthquake energy differential

Each of these scalar differential energy terms can be expressed in the general form:

$$dE = [\mathbf{dU}]^T \mathbf{R} = \mathbf{R}^T \mathbf{dU} \qquad \text{(B.3)}$$

where **R** and **dU** are force and incremental displacement vectors, respectively. It follows that each energy term can be expressed as:

$$E = \int \mathbf{R}^T \mathbf{dU} \qquad \text{(B.4)}$$

Physically, this integral represents the area under the force-displacement curves for each component of the **R** and **U** vectors. Integrating each differential energy term would yield the energy balance for the system. Because the inertia forces are linear in acceleration, the

damping forces are linear in velocity and the static forces are linear in displacement (for linear systems), the external load required for equilibrium is obviously a complex function of displacement, velocity and acceleration. These observations indicate that the energy integrals as expressed above are, in general, quite difficult to evaluate.

As discussed in [2], step-by-step integration schemes do not, in general, satisfy energy balance, even for linear systems. However, for integration schemes which satisfy equilibrium at discrete time intervals, "pseudowork" expressions can be developed as approximations to the actual energy quantities. The incremental "pseudowork" or energy approximations are expressed in the general form:

$$\Delta E = [\Delta U]^T \mathbf{R}_{ave} = \mathbf{R}_{ave}^T \Delta U \tag{B.5}$$

where $\mathbf{R}_{ave}$ is a defined by the average values of $\mathbf{R}$ at the beginning and end of the time step:

$$\mathbf{R}_{ave} = \frac{1}{2} (\mathbf{R}_t + \mathbf{R}_{t+\Delta t}) \tag{B.6}$$

The "pseudowork" terms represent trapezoidal approximations to the area under the force-displacement curves for each component of the various $\mathbf{R}$ and $\mathbf{U}$ vectors. The evolution of the energy distribution in the finite element model is the approximated by the summation of the incremental "pseudowork" terms over all of the time steps:

$$E \approx \Sigma \Delta E \tag{B.7}$$

It should be noted that for numerical integration using small time steps, the "pseudowork" equations provide reasonable approximations to the actual energy balance equations.

An Fortran subroutine, ENERGY has been developed to compute the time history of the "pseudowork" approximations of the earthquake energy balance of soil profiles modeled as one-dimensional shear beam systems.

APPENDIX C

WAVES USER MANUAL

WAVES is a special purpose computer program for computing the dynamic characteristics and seismic response of horizontally layered soil deposits. The soil site is discretized into a finite element mesh of one-dimensional shear elements. The system is represented dynamically by a viscously damped, lumped mass system, as developed in Section 2.2. A collection of 20 earthquake records (Table C.1) accompany the program in earthquake library files and are available for use as base motion input to the soil profile model. Other ground motions can be used, provided that they are stored in a file labeled EQDATA using a standard format; a two line description of the motion followed by equally spaced acceleration values in a Fortran format of 8F9.5.

WAVES uses the CALSAP [74] free-field subroutines to obtain the input required to define the soil profile and activate various numerical solution strategies. Within the WAVES data file, "separator lines" are used to subdivide the data into logical groups or blocks. The data groups can be in any order with each group terminated with one or more blank lines. Data is defined using the following separators (which must begin in the first column of an input line);

1) **CONTROL** used to define the analysis control information
2) **SITE** used to define the one-dimensional soil profile
3) **OUTPUT** used to specify the required output information
4) **SPEC** used to specify the required spectral output

All lines of data are entered in the following free-field form:

A=A1,A2,A3--- B=B1,B2,B3---

where the input data is designated by Ai or Bi. Numerical data lists must be separated by a single comma or by one or more blanks. A data list of the form A=A1,A2,A3--- can be in any order or location on the line. A colon ":" indicates the end of information on a line. Information entered to the right of the colon is ignored by the program; therefore, it can be used to provide descriptive information (units, for example) within the data file. A semi-colon ";" in column 1 of any line will cause the line to be ignored by the program, allowing users to insert additional comments describing the input. A backslash "\" at the end of a line indicates that the next line is interpreted as a continuation of the previous line. This option allows a maximum of 160 characters to be entered as one line of data. Simple arithmetic statements are possible when entering floating point real numbers; the statement C=10+20/5-2 is evaluated as C=((10+20)/5)-2). It should also be noted that real numbers do not require decimal points and E formats with + or - exponents are accepted.

The input data required after each of the separator lines is described in the following sections. Program execution is accomplished by typing "WAVES" at which point the input and output file names are requested.

C.1. Analysis Control Information

The lines of data which follow the CONTROL separator define the mode of execution and provide additional information required to define the model and the analysis. A block of CONTROL data is illustrated below;

CONTROL
MODEX=? TITLE=?
NL=? M=? N=? NEQ=? GRAV=? DUR=? DTEQ=? DTINT=? ----

The first line of data following the CONTROL separator defines the mode of execution MODEX, and the problem description TITLE (which can have a maximum of 50 characters). The following modes of execution are available:

MODEX = 1 Eigenproblem solution implementing inverse iteration with Gram-Schmidt orthogonalization.

MODEX = 2 Linear earthquake response analysis using the TSTEPS subroutine described in Table 2.1.

MODEX = 3 Equivalent linear iterative earthquake response analysis using the ITERAT subroutine described in Table 2.2.

MODEX = 4 Nonlinear earthquake response analysis with a constant integration time step using the subroutine WALK described in Table 2.3.

MODEX = 5 Nonlinear earthquake response analysis with a variable integration time step using the subroutine AUTO described in Table 2.4.

The second line after CONTROL separator defines the additional problem control information required to conduct the analysis. The data required depends on the mode of execution MODEX as follows;

If MODEX = 1 (Eigenproblem Solution);

NL=? NMODES=? MAXI=? GRAV=? TOLF=?

where;

NL = Number of layer elements in site model

NMODES = Number of modes to extract (default=NL)

MAXI = Maximum number of iterations (default=20)

GRAV = Acceleration due to gravity (default=32.2 ft/sec^2)

TOLF = Convergence tolerance (in %) between the frequencies from subsequent iterations (default=0.1)

If MODEX = 2 (Linear Earthquake Response Analysis);

NL=? M=? N=? IE=? NEQ=? GRAV=? DUR=? DTEQ=? DTINT=? AFACT=? \
GAMMA=? BETA=? THETA=?

where;

NL = Number of layer elements in site model

M = Damping index (default=1);

1 Equivalent Modal Damping

2 Damping with control in modes 1 and N

N = Second control mode (nonzero only if M = 2)

IE = Energy balance computation index (default=0);

0 Skip energy balance computations

1 Energy balance history printed to file ENERGY.OUT

NEQ = Earthquake index (default=0);

0 Earthquake read from file

1-20 Earthquake read from earthquake library file

GRAV = Acceleration due to gravity (default=32.2 ft/sec^2)

DUR = Duration of earthquake input (Note - DUR/DTEQ acceleration values will be read from the earthquake record specified by NEQ)

DTEQ = Time step of earthquake data (Note - the frequency content of the original earthquake record can be modified by setting DTEQ to a value other than the actual time step)

DTINT = Integration time step (Note - DTINT must be selected such that DTEQ/DTINT is an integer value)

AFACT = Scale factor for input acceleration data (default=1.0)

GAMMA = Newmark-Wilson integration constant, γ (default=0.5)

BETA = Newmark-Wilson integration constant, β (default=0.25)

THETA = Newmark-Wilson integration constant, θ (default=1.0)

If MODEX = 3 (Equivalent Linear Iterative Earthquake Analysis);

NL=? M=? N=? IE=? NEQ=? MAXI=? NVC=? NVS=? GRAV=? DUR=? \
DTEQ=? DTINT=? AFACT=? GAMMA=? BETA=? THETA=? EFACT=? \
ERR=?

where;

NL = Number of layer elements in site model

M = Damping index (default=1);

1 Equivalent Modal Damping

2 Damping with control in modes 1 and N

N = Second control mode (nonzero only if M = 2)

IE = Energy balance computation index (default=0);

0 Skip energy balance computations

1 Energy balance history printed to file ENERGY.OUT

NEQ = Earthquake index (default=0);

0 Earthquake read from file EQDATA

1-20 Earthquake read from earthquake library file

MAXI = Maximum number of analysis iterations (default=5)

NVC = Number of strain points to define clay dynamic property curves

NVS = Number of strain points to define sand dynamic property curves

GRAV = Acceleration due to gravity (default=32.2 ft/sec^2)

DUR = Duration of earthquake input (Note - DUR/DTEQ acceleration values will be read from the earthquake record specified by NEQ)

DTEQ = Time step of earthquake data (Note - the frequency content of the original earthquake record can be modified by setting DTEQ to a value other than the actual time step)

DTINT = Integration time step (Note - DTINT must be selected such that DTEQ/DTINT is an integer value)

AFACT = Scale factor for input acceleration data (default=1.0)

GAMMA = Newmark-Wilson integration constant, γ (default=0.5)

BETA = Newmark-Wilson integration constant, β (default=0.25)

THETA = Newmark-Wilson integration constant, θ (default=1.0)

EFACT = Effective strain factor, γ (default=0.65)

ERR = Convergence tolerance (in %) for dynamic soil properties. A solution is converged when the difference between the current dynamic properties and the strain compatible dynamic properties for each level are below this level (default=5.0)

If MODEX = 4 (Nonlinear Earthquake Analysis, constant time step);

NL=? M=? N=? IE=? NEQ=? NUNL=? GRAV=? DUR=? DTEQ=? DTINT=? \
TOLE=? AFACT=?

where;

NL = Number of layer elements in site model

M = Damping index (default=1);

1 Equivalent Modal Damping

2 Damping with control in modes 1 and N

N = Second control mode (nonzero only if M = 2)

IE = Energy balance computation index (default=0);

0 Skip energy balance computations

1 Energy balance history printed to file ENERGY.OUT

NEQ = Earthquake index (default=0);

0 Earthquake read from file EQDATA

1-20 Earthquake read from earthquake library file

NUNL = Maximum number of unloadings in Ramberg-Osgood soil elements (default=20) (Note - Because the unloading function of the Ramberg-Osgood model (see Appendix A) requires the current unloading coordinates, an array of NUNL of these values is stored in order to properly model hysteretic memory. If NUNL is exceeded, a warning is printed by the program).

GRAV = Acceleration due to gravity (default=32.2 ft/sec^2)

DUR = Duration of earthquake input (Note - DUR/DTEQ acceleration values will be read from the earthquake record specified by NEQ)

DTEQ = Time step of earthquake data (Note - the frequency content of the original earthquake record can be modified by setting DTEQ to a value other than the actual time step)

DTINT = Integration time step (Note - DTINT must be selected such that DTEQ/DTINT is an integer value)

TOLE = Equilibrium tolerance (Note - TOLE x (total weight of site model) is compared to the absolute sum of the unbalance vector computed using Equation 2.37) (default=0.001)

AFACT = Scale factor for input acceleration data (default=1.0)

If MODEX = 5 (Nonlinear Earthquake Analysis, variable time step);

NL=? M=? N=? IE=? NEQ=? NUNL=? NMAX=? GRAV=? DUR=? DTEQ=? \
TOLE=? TOLA=? AFACT=?

where;

NL = Number of layer elements in site model

M = Damping index (default=1);

1 Equivalent Modal Damping

2 Damping with control in modes 1 and N

N = Second control mode (nonzero only if M = 2)

IE = Energy balance computation index (default=0);

0 Skip energy balance computations

1 Energy balance history printed to file ENERGY.OUT

NEQ = Earthquake index (default=0);

0 Earthquake read from file EQDATA

1-20 Earthquake read from earthquake library file

NUNL = Maximum number of unloadings in Ramberg-Osgood soil elements (default=20) (Note - Because the unloading function of the Ramberg-Osgood model (see Appendix A) requires the current unloading coordinates, an array of NUNL of these values is stored in order to properly model hysteretic memory. If NUNL is exceeded, a warning is printed by the program).

NMAX = Maximum number of steps with a given time step before time step is increased (default=4)

GRAV = Acceleration due to gravity (default=32.2 ft/sec^2)

DUR = Duration of earthquake input (Note - DUR/DTEQ acceleration values will be read from the earthquake record specified by NEQ)

DTEQ = Time step of earthquake data (Note - the frequency content of the original earthquake record can be modified by setting DTEQ to a value other than the actual time step)

DTINT = Integration time step (Note - DTINT must be selected such that DTEQ/DTINT is an integer value)

TOLE = Equilibrium tolerance (Note - TOLE x (total weight of site model) is compared to the absolute sum of the unbalance vector computed using Equation 2.37) (default=0.001)

TOLA = Accuracy tolerance (Note - TOLA x (total weight of site model) is compared to the maximum norm of the mean equilibrium error vector computed using Equation 2.40) (default=0.0001)

AFACT = Scale factor for input acceleration data (default=1.0)

C.2. Site Information

The data which follows the SITE separator defines the site by specifying the geometry of the soil profile model and the dynamic properties of the soil layer elements. The site

information block depends on MODEX as follows;

If MODEX = 1 or 2;

SITE
SITEHED=?
L=1 H=? G=? ZETA=? GAM=?
L=2 H=? G=? ZETA=? GAM=?
(one line, in any order, for each layer element)

where;

L =	Layer number (top layer=1, bottom layer=NL)
H =	Thickness of soil layer element
GAM =	Unit weight of soil layer element
G =	Elastic shear modulus of soil layer element
ZETA =	Elastic damping ratio of soil layer element (in %) required only if MODEX=2)

If MODEX = 3;

SITE
SITEHED=?
LW=? WWAT=? CEP=?
L=1 H=? G=? ZETA=? GAM=? FACTG=? FACTZ=? LTYPE=?
L=2 H=? G=? ZETA=? GAM=? FACTG=? FACTZ=? LTYPE=?
(one line, in any order, for each layer element)

CLAY
CLAYE=E_1,E_2,...,E_{NVC}
CLAYG=G_1,G_2,...,G_{NVC}
CLAYZ=Z_1,Z_2,...,Z_{NVC}

SAND
SANDE=E_1,E_2,...,E_{NVS}
SANDG=G_1,G_2,...,G_{NVS}
SANDZ=Z_1,Z_2,...,Z_{NVS}

where;

LW =	Number of first submerged layer (default=base)
WWAT =	Unit weight of water (default=0.0624 kips/ft^3)
CEP =	Coefficient of lateral earth pressure (default=0.45)

L = Layer number (top layer=1, bottom layer=NL)

H = Thickness of soil layer element

GAM = Unit weight of soil layer element

G = Elastic shear modulus of soil layer element

ZETA = Elastic damping ratio of soil layer element (in %)

FACTG = Shear modulus scale factor for soil layer (Note - For clay layers, the discrete strain dependent shear modulus curve is obtained from the relationship:

$$G(i) = FACTG \times CLAYG(i)$$

For sand layers, the discrete strain dependent shear modulus curve is obtained from the relationship developed in [62]:

$$G(i) = FACTG \times SANDG(i) \times (1000 \times SMEAN)^{1/2}$$

where SMEAN is the effective mean principal stress. WAVES includes the principal stress effect automatically, hence FACTG need only include a relative density correction).

FACTZ = Damping ratio scale factor for soil layer (Note - The discrete strain dependent damping ratio is obtained by scaling the appropriate damping curve (CLAYZ or SANDZ) by the factor FACTZ).

LTYPE = Layer type;

1	Clay
10	Clay (dynamic properties not updated with iteration)
2	Sand
20	Sand (dynamic properties not updated with iteration)

If NVC > 0, a CLAY separator line must be followed by three lines of data used to specify the strain dependent property curves for clay (Omit if NVC=0). As indicated above, the strain dependent clay curves are stored in the vectors CLAYE, CLAYG and CLAYZ where;

E_i = the NVC effective strain coordinates (in %)

G_i = the shear moduli corresponding to the NVC effective strains

Z_i = the damping ratios (in %) corresponding to the NVC effective strains

If NVS > 0, a SAND separator line must be followed by three lines of data used to specify the strain dependent property curves for sand (Omit if NVS=0). As indicated above, the strain dependent sand curves are stored in the vectors SANDE, SANDG and SANDZ where;

E_i = the NVS effective strain coordinates (in %)

G_i = the shear moduli corresponding to the NVS effective strains

Z_i = the damping ratios (in %) corresponding to the NVS effective strains

If MODEX = 4 or 5;

SITE
SITEHED=?
L=1 H=? ZETA=? GAM=? DC=? FC=? A=? GAMMA=?
L=2 H=? ZETA=? GAM=? DC=? FC=? A=? GAMMA=?
(one line, in any order, for each layer element)

where;

L =	Layer number (top layer=1, bottom layer=NL)
H =	Thickness of soil layer element
GAM =	Unit weight of soil layer element
ZETA =	Elastic damping ratio of soil layer element
DC =	Control shear strain (in %) for Ramberg-Osgood constitutive model (see Appendix A)
FC =	Control shear stress for Ramberg-Osgood constitutive model (see Appendix A)
A =	Ramberg-Osgood control parameter, α (see Appendix A)
GAMMA =	Ramberg-Osgood control parameter, γ (see Appendix A)

C.3. Output Control Information

The data which follows the OUTPUT separator defines the output control variables. Response histories and their maxima can be requested for any of the layers in the site model. The response histories are printed columnwise to various output files for plotting or postprocessing. The first column of a history file contains the time value while the remaining columns contain the corresponding response values for the layers of interest. The following quantities can be requested; relative displacement, relative velocity, total acceleration, stress, strain, as well as base displacement, velocity and acceleration and integration time step (if MODEX = 5). A block of OUTPUT information is illustrated as follows;

OUTPUT
NDIS=? NVEL=? NACC=? NSPEC=? NHYS=? IBASE=? IDT=?
LAYD=L_1,..,L_{NDIS} LAYV=L_1,..,L_{NVEL} LAYA=L_1,..,L_{NACC} LAYS=L_1,..,L_{NSPEC} \
LAYH=L_1,..,L_{NHYS}

The first line after the OUTPUT separator defines the number of layers for which various output quantities are requested and the second line after the OUTPUT separator defines the specific layers (LAYi for i=D,V,A,S,H) for which the (displacement, velocity, acceleration, spectral or hysteretic, respectively) response quantities are requested. The output control variables are defined as follows;

NDIS = Number of layers for which displacement response is requested (displacement histories printed column-wise to file DIS.OUT)

NVEL = Number of layers for which velocity response is requested (velocity histories printed column-wise to file VEL.OUT)

NACC = Number of layers for which acceleration response is requested (acceleration histories printed column-wise to file ACC.OUT)

NSPEC = Number of layers for which spectral calculations are requested (output files specified in spectral analysis section)

NHYS = Number of layers for which hysteretic response is requested (applicable if MODEX = 4 or 5, stress and strain histories printed column-wise to file HYS.OUT)

IBASE = Base output (displacement, velocity and acceleration histories) flag;

0 Base output not requested

1 Base output printed column-wise to file BASE.OUT

IDT = Time step output flag (only applicable if MODEX = 5);

0 Time step history not requested

1 Time step history printed to file DT.OUT

$L_1,\ldots,L_{NDIS}$ are the NDIS layers for which the displacement response is requested

$L_1,\ldots,L_{NVEL}$ are the NVEL layers for which the velocity response is requested

$L_1,\ldots,L_{NACC}$ are the NACC layers for which the acceleration response is requested

$L_1,\ldots,L_{NSPEC}$ are the NSPEC layers for which spectral computations are requested (Note - a layer can be specified more than once if spectral computations at different damping ratios are required)

$L_1,\ldots,L_{NHYS}$ are the NHYS layers for which the hysteretic response is requested

C.4. Spectral Analysis Information (Omit if NSPEC = 0)

Response spectrum analysis can be performed on the total acceleration response of any of the layers in the soil profile model. The computations are performed using an extremely efficient algorithm described in [7]. The spectral output files contain a column of spectral periods and additional columns containing the requested spectral coordinates. A block of SPEC information is illustrated as follows;

SPEC
M=? T=T_1,T_2,T_3 C=? SPECOUT=?
M=? T=T_1,T_2,T_3 C=? SPECOUT=?
(one line for each of the NSPEC layers)

The data following the SPEC separator provides information required to generate the various response spectra for each of the NSPEC layers. The variables are described as;

M = Spectral ordinate index;

1 True relative displacement (TRD)
2 True relative velocity (TRV)
3 True absolute acceleration (TAA)
4 Pseudo-Velocity (PsV)
5 Pseudo-Acceleration (PsA)
6 TRD, TRV, TAA
7 TRD, PsV, PsA
8 TRD, TRV, TAA, PsV, PsA

T_1 = First period value in response spectrum (default=0.05 sec)

T_2 = Last period value in response spectrum (default=4.0 sec)

T_3 = Period increment between T_1 and T_2 (default=0.05 sec)

C = Damping ratio (in %) for spectral computations (default=0.0)

SPECOUT = Output file name for spectra computed for this layer (up to 13 characters)

TABLE C.1 EARTHQUAKE LIBRARY

EQN	Date	Location	Earthquake Component	PGA	Time of PGA	Number of Points	Δt
1	2/9/71	Castaic	N21E	0.315g	2.6s	3089	0.02s
2	2/9/71	Castaic	N69W	0.270g	1.9s	3094	0.02s
3	5/18/40	El Centro	S00E	0.348g	2.12s	2688	0.02s
4	5/18/40	El Centro	S90W	0.214g	11.44s	2674	0.02s
5	3/22/57	Golden Gate	N10E	0.083g	1.34s	1994	0.02s
6	3/22/57	Golden Gate	S80W	0.105g	1.44s	1994	0.02s
7	2/9/71	Pacoima Dam	S16E	1.170g	7.74s	2024	0.02s
8	2/9/71	Pacoima Dam	S74W	1.075g	8.5s	2086	0.02s
9	6/27/66	Parkfield	N65W	0.270g	4.0s	1518	0.02s
10	6/27/66	Parkfield	S25W	0.347g	4.3s	1520	0.02s
11	7/21/52	Taft	N21E	0.156g	9.1s	2719	0.02s
12	7/21/52	Taft	S69E	0.179g	3.7s	2720	0.02s
13	9/19/85	CUMV	S90W	0.040g	15.5s	3000	0.02s
14	9/19/85	CUMV	S00E	0.039g	17.9s	3000	0.02s
15	9/19/85	SCT	S90W	0.172g	58.08s	8956	0.02s
16	9/19/85	SCT	S00E	0.100g	54.14s	9000	0.02s
17	9/19/85	Tacubaya	S90W	0.034g	55.23s	5000	0.03s
18	9/19/85	Tacubaya	S00E	0.035g	38.58s	5207	0.03s
19	9/19/85	Viveros	S90W	0.043g	17.48s	6000	0.01s
20	9/19/85	Viveros	S00E	0.045g	23.65s	6000	0.01s

APPENDIX D

VIBRATION SHAPES FOR NONLINEAR SDOF RESPONSE ANALYSIS

The primary requirement for estimating the dynamic response of a MDOF structural system using a SDOF representation is that the vibration of the structure can be represented using one vibration shape. For linear systems, sufficient accuracy can often be obtained using the fundamental mode shape or Ritz vector of the structure to estimate the MDOF response. The first Ritz vector provides a successful representation of the structural response because it takes into account the spatial distribution of the dynamic loading [37]. The concept of capturing the spatial distribution of the dynamic loading can be extended to the solution of nonlinear problems with the physical reasoning that up to the point of collapse, the dynamic forces acting on a structure must be balanced by the internal structural resistance. Therefore, the shapes used for SDOF analysis are typically obtained from inelastic MDOF analyses in which the assumed distribution of the dynamic loading is applied statically.

The motivation for using a SDOF representation of a MDOF system is that the solution of a SDOF system can be obtained with a fraction of the computational effort required for a MDOF system. Thus SDOF procedures provide a rapid and inexpensive analysis tool which can reduce (or eliminate) the number of MDOF dynamic analyses required for the evaluation of structural response. It is important to note that because SDOF modeling methods are simple and approximate, the static methods used to obtain the equivalent SDOF properties should not be unduly complicated. In some cases, the use of more sophisticated static analysis procedures which result in more realistic and accurate SDOF representations may be justified.

Several methods can be used to estimate the structural vibration shape and characteristics of the structural resistance. The method implemented depends largely on how much is known about the structure and the earthquake loading. The simplest methods may be useful for obtaining estimates of the structural response demands in the initial

design stages while more sophisticated procedures may be applicable as the design progresses. Several methods are presented below.

Mechanism Method

This simple method requires a basic knowledge of the structural dimensions, element strengths and the approximate mass distribution and fundamental vibration period. The SDOF properties are obtained as follows;

1) Assume a lateral force distribution (a triangular distribution is commonly assumed for seismic loading).

2) Use the mechanism method of analysis [46] to obtain;

   a) the appropriate mechanism for use as an estimate of the vibration shape Φ

   b) the ultimate lateral load (or base moment)

3) A bilinear approximation to the structural resistance can be established by;

   a) using the estimates of the elastic vibration period and the structural mass to compute the elastic stiffness

   b) computing the lateral displacement (or rotation) level associated with the ultimate force (or base moment) based on the assumed elastic stiffness

   c) estimating the secondary stiffness based on judgement and/or some knowledge about the strain hardening ratios in the structural elements

Q-Model Method [56]

The Q-Model method was developed for the earthquake response of reinforced concrete structures. It is a simple method for establishing the approximate vibration shape and structural resistance characteristics based on inelastic static analyses. The method is outlined as follows;

1) Apply a monotonically increasing triangular lateral force distribution to the MDOF structure to the point of effective structural collapse. This portion of the analysis

results in relationships between base moment and lateral displacements of the story levels.

2) The initial loading base moment versus lateral displacement curve is idealized as a bilinear function using the following graphical procedure;

   a) a tangent to the initial loading portion of the curve is drawn

   b) from the horizontal axis, at points corresponding to lateral displacements of 0.2% and 0.3% of the equivalent height, two lines are drawn parallel to the initial loading tangent

   c) the yield point of the bilinear system is assumed to be between the intersections of these lines with the calculated curve

   d) the secondary stiffness is established by joining the yield point to a point on the calculated curve at an abscissa of five times the abscissa of the yield point

One uncertainty associated with the Q-Model method is the use of a triangular force distribution. The actual distribution of the seismic inertia forces depends on the absolute acceleration. Hence the actual inertia force distribution can be better represented using some combination of triangular (relative) and rectangular (rigid body) inertia force patterns. It is important to note that the sequence of plastic hinge formation, the collapse mechanism, and the ultimate load level obtained using triangular and rectangular lateral force patterns can be significantly different.

The Iterative Shape Improvement Method

As previously discussed, the concept of capturing the spatial distribution of the dynamic loading can be extended to the solution of nonlinear problems by physical reasoning that up to the point of collapse, the dynamic forces acting on the structure must be balanced by the internal resistance of the structure. Assuming that inertial forces due to ground motion can be applied as equivalent static loads on the structure, and that the structural responds harmonically in one vibration shape, results in the following system of equilibrium equa-

tions:

$$\mathbf{R_S} = \mathbf{R_I} \tag{D.1}$$

where $\mathbf{R_S}$ is the restoring force vector and $\mathbf{R_I}$ ($= \mathbf{M\ddot{U}}$) is the inertia force vector. Since the response of the system is assumed to be harmonic, the vector of structural accelerations is proportional to the vector of structural displacements:

$$\ddot{\mathbf{U}} = \lambda \mathbf{U} \tag{D.2}$$

and hence, for undamped linear elastic systems, the equilibrium equations reduce exactly to the eigenproblem;

$$\mathbf{M}\,\lambda\mathbf{U} = \mathbf{K}\,\mathbf{U} \tag{D.3}$$

The problem is somewhat more complicated for nonlinear structural systems since the structural resistance is a nonlinear function of the structural displacements, $\mathbf{R_S}$ ($=\mathbf{R_S}(\mathbf{U})$), and changes in the deflected shape directly influence the idealized distribution of inertial forces, $\mathbf{R_I} = \mathbf{M}\,\lambda\mathbf{U}$. A procedure to obtain the vibration shape, which is based on iterative nonlinear static analyses, is outlined as follows:

1) An estimate of the distribution of lateral inertial forces is obtained by premultiplying an arbitrary (triangular, rectangular or other) assumed shape pattern Φ_o, by the lumped mass matrix of the MDOF structure:

$$\mathbf{R_I} = \mathbf{M}\Phi_o \tag{D.4}$$

2) The inertial force pattern is applied as a monotonically increasing static force vector to an MDOF structural model which accounts for nonlinear material behavior and P-Δ effects. Loading is initiated with the structure in the undeformed equilibrium configuration:

$$\mathbf{R_S}(\mathbf{U}) = \mathbf{R_I} \tag{D.5}$$

3) The load amplitude is increased and equilibrium is maintained to the point of effective structural collapse which is defined as the mechanism condition or the point of geometric instability. If estimates of the displacement demands are available (from spectra or other means), the analyses can be conducted up to the estimated displace-

ment levels.

4) The shape corresponding to effective collapse Φ_i, is obtained and is assumed to be an improved vibration shape.

5) The improved shape Φ_i, is then premultiplied by the lumped mass matrix to obtain an improved estimate of the inertial force distribution:

$$\mathbf{R_I} = \mathbf{M}\Phi_i \qquad \text{(D.6)}$$

6) Steps 2 through 5 are repeated until the shape at effective collapse is unchanged by additional iteration, i.e., the solution has converged.

7) The converged shape is denoted as Φ and the equilibrium path (base moment versus lateral deflection of story levels) from the final nonlinear analysis is approximated using a bilinear function.